ADDIS ABABA UNIVERSITY

COLLEGE OF NATURAL AND COMPUTATIONAL SCIENCES

SCHOOL OF EARTH SCIENCES

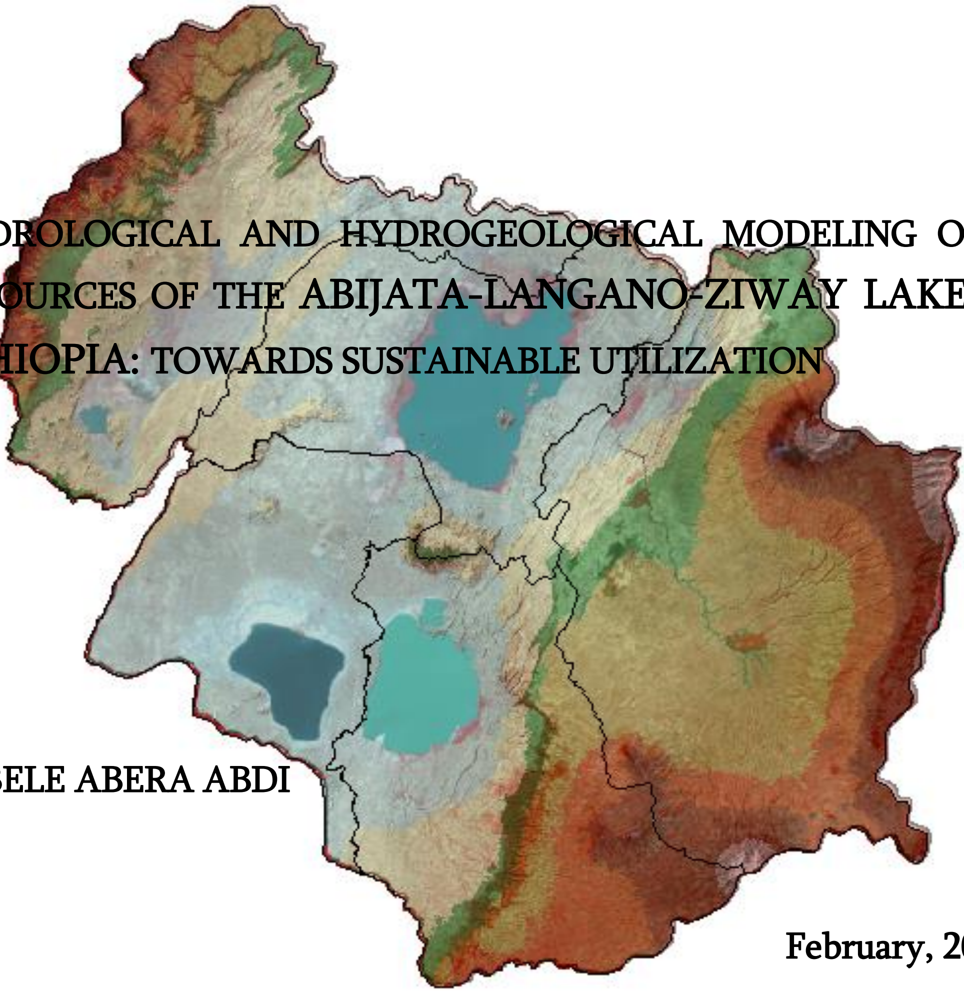

HYDROLOGICAL AND HYDROGEOLOGICAL MODELING OF WATER RESOURCES OF THE ABIJATA-LANGANO-ZIWAY LAKES BASIN, ETHIOPIA: TOWARDS SUSTAINABLE UTILIZATION

DEBELE ABERA ABDI

February, 2023

Addis Ababa, Ethiopia

ADDIS ABABA UNIVERSITY

COLLEGE OF NATURAL AND COMPUTATIONAL SCIENCES

SCHOOL OF EARTH SCIENCES

HYDROLOGICAL AND HYDROGEOLOGICAL MODELING OF WATER RESOURCES OF THE ABIJATA-LANGANO-ZIWAY LAKES BASIN, ETHIOPIA: TOWARDS SUSTAINABLE UTILIZATION

DEBELE ABERA ABDI

A thesis submitted to the School of Earth Sciences, Addis Ababa University. In Partial Fulfillment of the Requirement for the Degree of Doctor of Philosophy in Earth Sciences (Hydrogeology)

Advisor: Prof. Tenalem Ayenew

February, 2023

Addis Ababa, Ethiopia

ADDIS ABABA UNIVERSITY

COLLEGE OF NATURAL AND COMPUTATIONAL SCIENCES

SCHOOL OF EARTH SCIENCES

This is to certify that the thesis prepared by Debele Abera Abdi, entitled: **"Hydrological and Hydrogeological Modeling of Water Resources of the Abijata-Langano-Ziway Lakes Basin, Ethiopia: Towards Sustainable Utilization"**, and submitted in partial fulfillment of the requirements for the Degree of Doctor of Philosophy in Earth Sciences (Hydrogeology) complies with the regulations of the University and meets the accepted standards with respect to originality and quality.

Approved by Examining Committee:

Name		Signature	Date
1. Prof. Tenalem Ayenew	(Advisor)	____________	____________
2. Prof. Seifu Kebede	(External)	____________	____________
3. Dr. Dessie Nedaw	(Internal)	____________	____________

____

Chair of Department or Graduate Programme Coordinator

Abstract

The Abijata-Langano-Ziway Lakes Basin (ALZLB) is situated in the Central part of the Main Ethiopian Rift. Understanding the complex hydrologic and hydrogeologic systems is the critical to assessing the water resources system and their management practices. This study was aimed at implementing an integrated water resources model to assess the effects of stresses on water resources of the basin by setting plausible scenarios. WEAP-hydrology modeling was used that consists of a lumped, one dimensional; two-buckets soil water recording that applies empirical functions to separate water to evapotranspiration, surface runoff, interflow, and deep percolation for a subbasin-unit at the root zone. MODFLOW model was used to characterize the qualitative hydrogeological conceptual model into numerical representation and thereby describe the groundwater system. The Link Kitchen tool is used to link the surface-groundwater models. Coupling was accomplished through a GIS shapefile, which map MODFLOW grid cells to WEAP catchments, groundwater node, and river elements. This shapefile linkage enables the dynamic transfer of data between WEAP and MODFLOW models. Later, the linked model was used to investigate the consequences of variable scenarios (supply, demand, and management alternatives) on water resources. The outputs of the WEAP-based hydrologic model demonstrated that the comparison of monthly measured and simulated streamflow statistics (For the Ketar: R^2= 0.82, NSE = 0.80, and IA =0.95; and for Meki: R^2 =0.79, NSE = 0.79, and IA =0.94) for the calibration period. While for the validation period (Ketar: R^2 of 0.91, NSE of 0.91, and IA of 0.98; and Meki: R^2 = 0.74, NSE =0.62, and IA = 0.91). The steady-state calibrated statistics between the observed and simulated groundwater head showed that R^2=0.98, NSE=0.97, and ME=-8.3, for groundwater modeling. The model output shows that the balance between inflow and outflow was fit to the steady-state modeling condition at a discrepancy of -0.75. The monthly based performance index for the linked WEAP-MODFLOW model indicated that (Ketar R^2=0.81, NSE=0.95, IA=0.95) and (Meki subbasin R^2=0.75, NSE=0.74, and IA=0.93). The result of coupled WEAP-MODFLOW model revealed that there would be a change by about -5 to +5m (the Rift floor basin); -41 to +39m (the Ketar subbasin); -13 to +12m (Meki subbasin) in groundwater level for ±20% annual precipitation over the study period. Water extraction for projected irrigation expansion will impact the groundwater head. For instance, in the Rift floor subbasin (C=38, R=43), (under IES-1: -7m (2020), -11.9m (2030), -14.9m (2040), and -21m (2055) ; IES-2: -7.3m (2020), -12.8m (2030), -16.9m (2040), and -27.9m (2055); IES-3: -7.6m (2020), -14.5m (2030), -21.1m (2040), and -39.1m (2055) compared to baseline scenario. Predominantly, the model efficiency showed a very good fit among measured and simulated data. The linked model was able to simulate the supply, demand, and management scenarios of water resources. These findings suggest that the implementation of effective management scenarios should be targeted with enhancing irrigation efficiency. The demand and supply side management is of paramount importance in the reduction of water scarcity and subsequent environmental and socio-economic impacts.

Keywords: Hydrologic modeling, Groundwater flow modeling, Soil moisture method, link kitchen, climate change

Acknowledgments

I would like to acknowledge Addis Ababa University, School of Earth Sciences for giving me the opportunity to continue my PhD studies. My deepest gratitude goes to Arsi University for sponsoring me to follow this PhD program. I am very much indebtedness for my supervisor, Professor Tenalem Ayenew, for his unreserved support during my study. A special thank goes to, Dr. Behailu Berhanu, who invested his time, knowledge, and support for the successful completion of this PhD thesis. This thesis wouldn't have been completed in this way without his keen contribution.

I would like to extend my gratitude to: Dr. Bayisa Regassa (Graduate program coordinator) and Dr. Balemwal Atnafu, Head of School of Earth Sciences and Dr.seifu Kebede , Dr. Dessie Nadew and Biniam GISlab. I also appreciate the support I got from Mr. Worku and other members of the school.

Ministry of Water and Energy of Ethiopia (MoWE), National Meteorology Agency, Geological Survey of Ethiopia and Oromia Water and Energy Bureau are highly appreciated for providing me with the necessary data. My friends and professionals who directly or indirectly contributed to the successful completion of this research work (benezer Kefene, Ali Aman, and Abebayehu Tadesse) are all acknowledged.

Table of Contents

Figures

Table

Publications

Debele Abera, A., & Tenalem, A. (2021). Evaluation of the WEAP model in simulating subbasin hydrology in the Central Rift Valley basin, Ethiopia. *Ecological Processes*, *10* (1), 1–14. https://doi.org/10.1186/s13717-021-00305-5

Debele Abera, A., & Tenalem, A. (2021). A scenario-based modeling of climate change impact on the hydrology of Ketar watershed, Central Rift Valley Basin, Ethiopia. *Modeling Earth Systems and Environment*, *7*(4). https://doi.org/https://doi.org/10.1007/s40808-021-01314-1

1. General Introduction

1.1. Background

Water is of the most essential natural resources that support the existence of life on the earth. Water resources are come to be a crucial gift for socio-economic advance, particularly in water stressed regions. In several nations, along with fast population advance and economic progress, water resources are in intense stress from anthropogenic and natural factors, further initiating water inadequacy issues (Li, Deng, Wu, & Hasan, 2015). Water inadequacy hinders growth, increases food deficiencies and conflicts that could cause adversarial impacts human and ecosystem health; thus, disrupt ecosystem service provision, which is a vital subject in the water resource governance to balance water supply and requirement (Notter et al., 2012).

Similarly to the other parts of the world, the study basin has also been facing the challenges in satisfying demands for irrigation, domestic and minimum water flows to sustain ecological health of the basin (Alemayehu et al., 2006; Ayenew, 2007; Legesse & Ayenew, 2006; Pascual-ferrer et al., 2013). Hence, the continuity of water resources is severely challenged in the phases of stressors such as population growth, increased demand for agricultural and urban uses, the need to maintain adequate environmental flows to sustain healthy ecology, and potential impacts of mankind-induced modifications such as land use change and climate change.

Effective water resources management depends on a in-depth knowing of the amount and quality characteristics of accessible water (Lorenz & Ziegeweid, 2015). This, in turn, requires knowledge of the surface water and groundwater system of the area at the subbasin level, to quantify Spatio-temporal water availability that plays a significant role not only inequitable allocation but also to address the impacts of the present and forthcoming water demand plan and its management issues.

The hydrological model was used to represent land surface hydrological parameters (infiltration, recharge, river flow, and surface runoff etc.). The numerical groundwater model was prepared to characterize groundwater conditions. Nevertheless, the standalone models do not give comprehensive answers to questions regarding water resources management. Hence, to evaluate the effects of future conditions (climate change, irrigation expansion, water abstraction, and management strategies) on water resources a sort of coupling must exist (Holman et al., 2012; Pulido-Velazquez et al., 2015) that link the two inseparable water resource systems (i.e. surface water and groundwater).

An integrated method is required for determining the amount of water entering and exiting the basin, combining both surface water and groundwater systems. Many inputs and outputs are considered in the mass balance relationship for groundwater-surface water systems. Inputs deep percolation, returns flow recharge, and seepage from streams and lakes while outputs include evapotranspiration, pumping, and outflow to a stream (SEI, 2015). Among various approaches to improve integrated water resources management, the implementation of scenarios are an effective technique to forecast the response of physical hydrological processes to climate change and growing irrigation water demand effects on water resources (Li et al., 2015). Effective water resource management demands a thorough understanding of the past, the state of the present, and the creation of plausible scenarios for the future.

Therefore, the main focus of this investigation is to evaluate water resources system by coupling two well-known modeling tools i.e., for surface water, Water Evaluation and planning system Tool (WEAP, www.weap21.org) and for groundwater, a numerical model groundwater flow, MODFLOW models (McDonald & Harbaugh, 1988; SEI, 2007).

Prior to this study, it has been tested and applied in different part of the world as a Decision Support System tool by (Droubi et al., 2008) and proven its strength in addressing the impacts of demand-supply, climate change, sewage reclaim, and non-natural recharge scenarios on water supply. The water resource models are a successful tool in predicting the consequences of climate change, irrigation expansion, and water resources management strategies in the basin.

This topic is identified as being important to assess the impacts of the current and plausible upcoming conditions of anthropogenic and natural events on water systems that potentially impact water resources at the extent of sub-basin.

1.2. Statement of Problem

Agricultural and associated practices constitute the key pillar in supporting the economy in the basin. As of 2007 the basin's economy earns about 67% of the gross domestic product (GDP) (MOWR, 2007) from a population of 2.5millions, 1.9millions are rural residents who earn their livelihood from agriculture (OWWDSE, 2016). Currently, irrigation-based agriculture-related investments are increasing more than ever in the ALZLB though the introduction of large-scale irrigation has been dated back to 1970s, in the past five years, irrigated land escalates to about 70% around Ziway lake (Legesse & Ayenew, 2006). For instance, the irrigated area has been drastically increasing from

10,303ha in 2006/07 and reached 87,235ha 2015/06 using water sources(OWWDSE, 2016). Despite the high rate of irrigation expansion, it accounts for only about 1.3% of lands under agricultural practices in the basin as of 2007 (Jansen et al., 2007). Nevertheless, over exploitation of water resources has been mentioned as one of the emerging challenges in basin, particularly the problem that has been associated with lake water resources. Recent studies indicated that over the past decade irrigated area has increased to over 29000ha in the vicinity closer to Lake Ziway (OWWDSE, 2016). Moreover, increased uncontrolled flooded irrigation is leading to soil salinization (Chernet et al., 2001). Consequently, converting forest land to farm land has been on the increasing as farmers leave the salt-affected lands and seek for new lands (Shimelis, 2008).

On the other hand, a lack of proper management of water resources (water allocation and priority) problems emerged in 1980s, which was noted in a decrease in lake level recorded, while there has been rising industrial water use from the Lake Abijata (Alemayehu et al., 2006). Moreover, a proper environmental flow has not been allotted to downstream flows yet. For instance, from 2002 to 2007, as the mean level of lake Ziway decreased by 0.5m and this subsequently caused in 40% reduction the Lake Abijata size (Jansen et al., 2007). This reduction in the Lake Abijata is attributed to water abstraction from upstream rivers and lakes that is intensified regularly by climate change and land development(Abraham et al., 2018; Desta & Lemma, 2017). Consequently, the Lake Abijata area coverage has declined from 179.2km^2 in 1972 to 131.8km^2 in 2015 (Hailu & Girma. 2019). This brought about a loss of freshwater ecosystems biodiversity degradation because of human impacts (Ayenew, 2007). Water abstraction is commonly practiced without a basic familiarity of the complex hydrological and hydrogeological system and the sensitive nature of the rift ecology (Ayenew, 2007). On contrary to this, rainfall has not significantly lessened over the past 50 years (Ayenew, 2004).

ALZLB is the endorheic basin that consists of a series of interconnected lakes (Ziway, Langano, and Abiyata) located in arid and semi-arid rift floor region. Consequently, any conditions that bring an imbalance between inflow from rivers emanating from both eastern and western humid highlands and evaporation to the atmosphere and water abstraction will cause water resources degradation. For instance, the study by (Zeray et al., 2007) speculates that Lake Ziway will be shrunk by 19% to 27% because of global climate alteration in the coming 50 years.

The investigation carried out by Pascual-ferrer et al.(2014) summarizes the major water-related problems that need sound water resource management comprising (1) the overexploitation of water, currently endangering the area's ecosystem and severe contests of water use and its undifferentiating use. (2) water quality deterioration both for irrigation and domestic uses. (3) the excessive reliance of the population on water resources to endure their livings.

Furthermore, there are problems to be addresses by further studies Pascual-ferrer et al.(2014): (1) to establish a monitoring plan which enables to address the effects of the actions realized and if the intended aims are attained; (2) Information on water amount and quality to evaluate water system behavior and to investigate the association among water systems and environmental services; (3) to support the viable use of water resources by giving due concern for the local hydrology, the impacts of water abstractions and the subsequences of ecological deterioration; (4) to adopt to mid-term scenarios that may improve water management, enhancing water efficiency in agriculture, efficiently safe-guarding the environment and to realize various tasks related to natural resource management that improve water availability. Since ALZLB valley is found in two regions water use priority allocation and implementation actions to justify water abstraction based on accountability criteria and ensure both equitability and efficiency of water use and (5) awareness-raising of people to develop a sense of shared accountability for water and environmental protection among the residents.

If not, the accessible water is not used in a well-adjusted manner between supply and requirement and with careful deliberation of its continuity, without compromising environmental water requirements, fulfilling the requirements of the coming generation will remain be unanswered.

1.3. Objectives

The core aim of this research is to understand and provide the scientific basis of the surface and groundwater system behaviors and its response to natural processes and human-induced stresses in the Abijata-Langano-Ziway Lakes Basin.

The specific objectives:

- Prepare a hydrological model using WEAP model to assess model capability in simulating hydrological conditions of the ALZLB.
- Prepare a numerical groundwater flow model to understand occurrence, movement and localization of groundwater conditions in the basin
- Couple of surface water and groundwater models
- Simulate and evaluate the effect of projected climate change on water resources
- Simulate the impact of irrigation expansion and management strategies on water resource system

1.4. Research approach & Methodology

Integrated surface water and groundwater model was applied to the basin, Water Evaluation and Assessment Tool (WEAP) was prepared to characterize surface hydrologic conditions and scenario analysis. The numerical groundwater flow model (MODFLOW) was prepared to characterize groundwater conditions. Stand-alone models were prepared for surface water and groundwater and were calibrated. Then linking of the two models was done using appropriate procedures. Later, the coupled model was used to address the situation in water resources in an integrated manner. Finally, the most plausible scenarios pertaining to water resources management, development, and adaptation measures were adapted and evaluated. Scenario analyses were made to address anthropogenic activities and natural processes on water system and the detailed methodology is addressed in the respective chapters.

1.5. Significance of the study

1.5.1. Scientific and environmental significances

The ALZLB is characterized by high water resources potential, a fast-growing development corridor (intensification of irrigation), high population density, and a potentially productive area with good access to the central market. The basin is characterized by fast dynamics both on water supply and demand sides. Hence, the modeling will help to understand the capability of computer-based models in capturing the hydrologic and hydrogeological behaviors of the basin at reasonable extent. So that the output of the research will improve knowledge concerning the present and future change in the basin. Moreover, the effects of climate change, land development, and adaptation strategies are predicted to utilize the water resources sustainably under different scenarios.

It contributes to water governance aspects in understanding the behaviors of groundwater and surface water conditions of the basin. Optimum use of water helps to maintain the energy balance and food chain (wetlands, lakes and riverine) of basin ecosystems and lake water quality (salinity) influenced by inflow and outflow of water from upstream rivers and the climatic condition (evaporation). It also helps to understand the impacts on going land development (irrigation) and climate change which influence the water availability by altering the hydrologic system of the basin.

1.5.2. Socio-economic Significance

In the basin, several towns are dependent on surface and groundwater resources for drinking water supply and livestock. Currently, there is high competition for irrigation, fishing, tourism, and industries water demand, particularly on the rift floor, where its climate is arid and semi-arid besides the fast-growing population. In the highland plateau region, a number of springs or rivers (Ketar and Meki) feed the low-lying lakes (Ziway, Langano, and Abijata) from which irrigation schemes, tourism activities, and industries rely on their water requirement.

These indicate the vital significance of the water of the basin in the socio-economic activities of the region. To sustain its contribution to the socio-economic of the basin in particular and to the country at large, an integrated water resources management approach should be applied under different sets of development and management scenarios that target to climate variability and irrigation expansion. Therefore, the output of this research finding will play an important role in addressing matters associated to water resources management to maximize its benefits.

1.6. Previous studies

Previous studies that contributed a lot to setup geological framework of the Main Ethiopian Rift, during the past many decades (Abebe et al., 2010; Benvenuti et al., 2002; Dainelli et al,, 2001; Di Paola, 1972; Kazmin, Seife et al., 1980; Le Turdu et al., 1999; P. A. Mohr, 1967; P. Mohr et al., 1980; Mohr, 1987; Woldegabriel et al., 1990) (Mohr, 1960, 1962,). The geological map extensively used for this study was produced by (Dainelli et al., 2001) at the scale of 1:250000.

In relation to a water resources, the study by the Ethiopian Institute of Geological Survey Tesfaye Chernet (1982) laid the cornerstone for the characterization of the hydrogeology of the lakes region and produced a basic hydrogeological report and map.

A study by Ayenew (1998) analyzed the general hydrology and hydrogeological system of the Ethiopian Rift Valley basin using a numerical groundwater flow model and isotope methods aimed to address water exchanges between the lakes and the aquifers; the roles of Rift floor faults and fractures on the occurrence and movement of groundwater; boundary conditions with adjacent basin; the impacts of water use plan on lakes level and groundwater contribution to the lakes; and estimate lakes water balance.

It is well known that basin hydrologic processes can be altered by changing land development and climate conditions. In a related study, the effects of climate and landuse change on streamflow and lakes level fluctuation in the Main Ethiopia Rift valley basin was investigated with a physically-based, distributed Precipitation Runoff Modelling System (PRMS) model (Legesse et al., 2003, 2004; Legesse et al., 2010). They have investigated the basin's hydrologic processes (Evapotranspiration, surface runoff, interflow, Baseflow components, and evaporation of lakes).

There is the study for accessing the water system of the basin using WEAP model by (Halcrow, 2009) and the water balance model output suggests that a decrease by about 20% of the Ketar and Meki Rivers inflows to Lake Ziway would be enough to reduce the lake levels below the sill height for the Bulbula River (1635.5masl) which would, in turn, causes a hardly empting the Bulbula River which significant impact on the Lake Abiyata existence. Lakes Ziway and Langano are open lakes and feed Lake Abiyata to the south via the Bulbula and Horakelo Rivers, respectively.

Since Lake Abiyata is a closed lake and fed chiefly by overflow of Ziway and Langano lakes, and as of its terminal location in the drainage basin, and it is shallow in depth, and is more responsive to any variations in the basin and is principally susceptible to any alteration of feeder rivers for irrigation schemes connected to the Meki and Ketar Rivers, as well as water pumped directly from Lake Ziway for different purposes.

Another study, still worth mentioning is the study by (JICA, 2012) that investigated the groundwater potential of Rift Valley Lakes Basin. To alleviate scarcity and uncertainty of data, test boreholes have been drilled and identified three potential aquifers: Alluvium and Lacustrine deposit; Pleistocene tuff, tuff breccia, and basaltic units; and Plio-Pleistocene tuff and basalt. This study developed a groundwater model to assess its potential and impacts on future groundwater development for water supply to selected towns in the region.

The above-mentioned and other previous studies in the Central Rift Valley basin gave consideration only to groundwater or surface water resources in an isolated manner and also do not promote integrating both demand and supply sides in water resource management. However, coupled surface and groundwater model that is the most critical to water resources management for different scenario analyses has not been done yet. Since surface water bodies (i.e. the rivers: Meki, Ketar, Bulbula, Horakelo, Gedemso, Lepsi and Huluka ; and the lakes: Ziway, Langano, and Abijata) and groundwater reservoirs (aquifers) are closely tied to each other in Central Main Ethiopian Rift Valley Basin (Ayenew, 1998).

1.7. Thesis Structure

The thesis is organized in nine (9) Chapters. A brief overview of the structure is as follows:

Chapter one provides a general introduction about water resources management, emerging challenges, application modeling surface water and groundwater, coupling tools theoretical aspects. In addition to organizing the aims of the study, significance and overall research methodology of the thesis are indicated briefly.

Chapter two presents physical location of the basin, physiographic and drainage characteristics, climatic condition, data on hydro-meteorological characteristics (precipitation, temperature, evaporation & evapotranspiration, relative humidity, wind speed and sun shine hour). It also characterizes the surface water hydrology (rivers and lakes), baseflow separation analysis, and water balance analysis. It also describes the landuse dynamics, socio-economic aspects, and water demands of different sectors.

Chapter three is dedicated to present literature review on geological and hydrogeological description of major units. The regional and local geology of the basin have been incorporated. It also describes the major lithological units and aquifers properties that have a significant in controlling effect on the basin water dynamics and water resources distribution in spatio-temporal dimensions. The objective of this chapter is to understand the hydrological and hydrogeological conceptual model of the basin. The conceptual model provides insight on the water system of the basin and is required as input for modeling basin characteristics.

Chapter four is devoted in presenting of hydrological modeling using WEAP. This chapter includes the introduction, literature review, method, result and discussion. The introduction section describes hydrological modeling principles and presents literature review on WEAP hydrological modeling. It also presents detailed methodology with governing equation and the model setup units and catchment parameters. Besides, it also describes calibration and validation steps and performance evaluation. Finally, the chapter ends up with illustrating the results and discussions.

Chapter five is dedicated to the developing numerical groundwater flow model of the study basin using the MODFLOW model. This chapter includes the introduction, literature review, method, result and discussion. The introduction section describes the principle numerical groundwater flow modeling and presents literature review on MODFLOW modeling. It also presents detailed methodology with governing equation and the model boundaries and cell input parameters. Besides, it also describes calibration and validation steps and performance evaluation. Finally, the chapter ends up with illustrating the results and discussions.

Chapter six presents the coupling of the surface water model (WEAP) and the groundwater model (MODFLOW) using the Link kitchen tool that is intended to exchange data among the models (Output of one model services as input for the other model, or vice-versa). This chapter is also organized in to introduction and literature review, method, results and discussion sections.

Chapter seven begins with global climate challenges and its effects on hydrology and water resources concepts as background. Literatures are reviewed on climate change projection under representative concentration pathways (RCP). It also presents previous studies on climate change projection of down scaled from different GCMs under different RCPs. It presents the basin based future climate change parameters (precipitation and temperature) projection and scenarios are made. Uses coupled model to simulate the future climate variation parameters on hydrology and groundwater level and recharge. It describes impact of future projected climate change on water resources based on alternative scenarios.

Chapter eight presents with irrigation expansion trends and Irrigation water use efficiencies in the basin. The calibrated coupled surface and groundwater model is prepared examine the impacts of irrigation water demand on water supply under different irrigation expansion and water use efficiency scenarios. It also describes management or adaptation strategies based on scenarios and discussing their impacts on water resources.

Chapter nine describes a conclusions and recommendations on the results found in this research.

2. Description of the Study Basin

2.1. Geographic Location and Accessibility

The Abijata-Langano-Ziway Lakes Basin (ALZLB) is located in the Central Section of the Central Main Ethiopian Rift valley, which encompasses part of Oromia and Southern Nations and Nationalities and Peoples' Administrative Regions. It is a part of the Ethiopian Rift Valley Basin and it is bounded by geographic coordinates of 414500-545180mE longitude and 797930- 93592mN latitude (Fig. 2.1).

It is a part of the Great East African Rift Valley, which splits the Ethiopian highland into northern and southern parts, creating a rift floor inhabited with a rows of lakes with different size, hydrological and hydrogeological settings (Ayenew, 2003). The basin contains: Ziway, Langano and Abiyata lakes and the highlands on both sides of the basin deliver numerous persistent streams (Meki, Ketar, Gedemso, Lepsi, and Huluka) that feed the lakes lodging in the axis of the rift. The basin supports a population of approximately to 2million whose livelihoods mainly rely on subsistent farming (CSA, 2013) with the annual growth rate of 3% and a family size ranging from 4-to 8 persons (CSA, 2006) and inhabit about a 1.8million of livestock (Meshesha et al., 2012). The basin covers an area of more than 10, 000km^2

2.2. Climate characteristics

The climatic conditions characterizing the highlands, the escarpment, and the Rift valley differ greatly. Mean yearly precipitation over the entire basin is around 900mm, showing high spatial variations as no more than 700mm/year and as high as 1200mm/year in the rift flour and highlands respectively. There is also temporal variability of total rainfall around 59% occurs during the summer season (June - September), the remaining 28%, and 13% fall during the months of (Match, April, and May) and (October-February) respectively (Pascual-ferrer et al., 2014).

The average annual temperature is about 15^{0}C in the plateaus and around 20^{0}C in the rift and actual evapotranspiration ranges from about 900mm/year in the plateaus to 650mm/year in the rift (Ayenew, 2003). While actual evaporation of Lake Ziway was valued at about 1800mm/year for the data collected in 1994 and 1996 (Vallet-coulomb, Legesse, Gasse, Travi, & Chernet, 2001). The basin is characterized by humid to sub-humid in the plateaus and semi-arid in the rift floor.

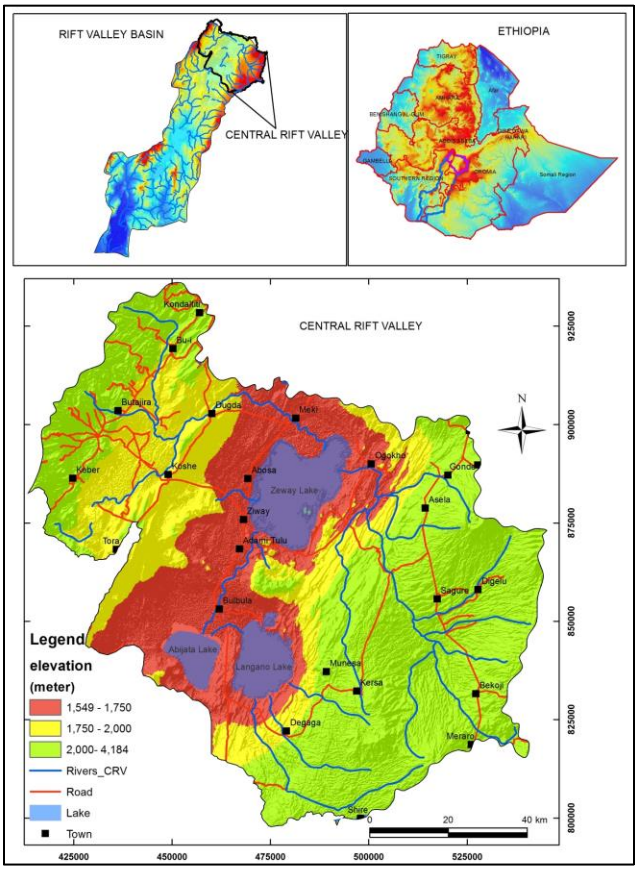

Fig. 2.1 Location map of study area

2.3. Physiography and Drainage

The physiographic and drainage of the region is attributed to the intensive faulting has caused in disruption of the volcanic rocks and creation of stair faults and horst and graben landscape. The ALZLB can be divided into three physiographic regions: the rift floor (< 1750m above mean sea level (a.s.l.), the intermediate escarpment (1750-2000m a.s.l.) and the plateau (>2000m a.s.l.). Their aerial coverage and percentage of each subbasin can be seen in Table 2.1.

The central elongation of the basin is the rift floor lying in between the east and west by the southeastern plateau and shewan plateau respectively. Its altitude varies from 1550–1750m a.s.l.). There is a big landscape difference between the rift floor and the plateau and the topographic cross-section is shown in Fig. 2.2 aligned along NW-SE on Fig. 2.1. The elevation varies from a slight over 2700m asl in large portions of the watershed in the plateau to 1600m a.s.l. around the fat rift lakes. The large Pliocene trachytic shield volcanoes of Mount Chilalo (4006m), Mount Kaka (4245m), Mount Badda (4170m), and Mount Kubsa (3760m) are the very elevated areas and aid as the surface water divide of the ALZLB system from the east. Numerous inactive silicic caldera volcanoes elevated above the rift floor such as Mount Bora (2293 m), the Alutu Caldera (2328m), the O'a Caldera (1960m), and the Corbetti Caldera (2320m). The eastern rift boundary is manifested by deep gorges and canyons owing to the existence of big regional peripheral fault system.

Table 2.1 Subbasin area coverage based on physiographic regions

Subbasin	Ketar Area (ha)	%	Meki Area (ha)	%	Rift floor Area (ha)	%	Langano Area (ha)	%	Bulbula Area (ha)	%
Rift plateau	292599	90	109075	48	4846	3	113921	57	596	0
Escarpment	23391	7	91938	41	51492	30	30429	15	26666	20
Rift floor	10369	3	24988	11	115627	67	56798	28	108100	80
Sum	326359	100	226001	100	171964	100	201148	100	135362	100

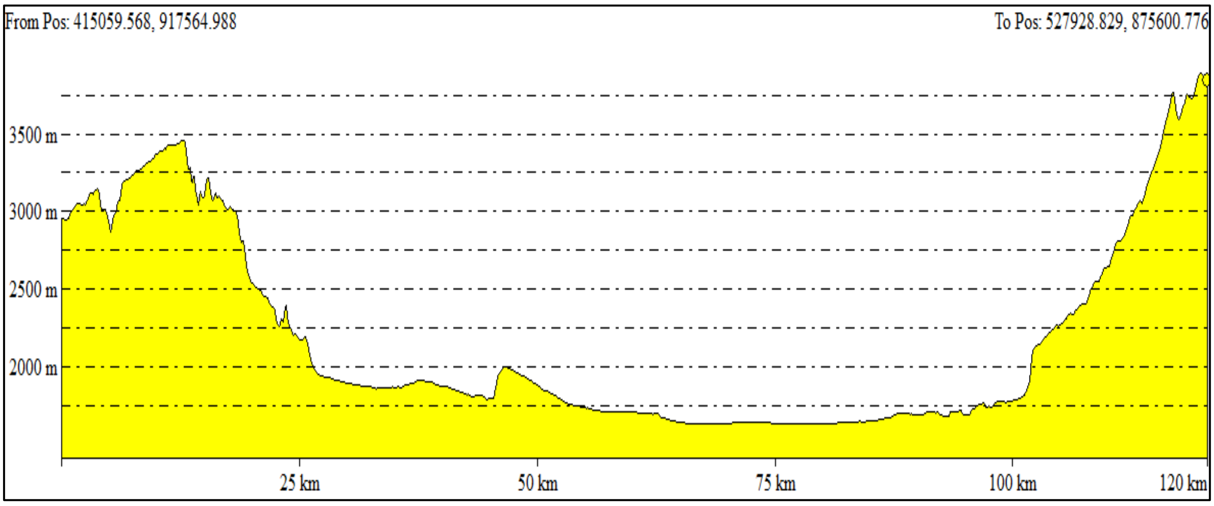

Fig. 2.2 Topographic cross-section

2.4. Hydrometeorology

2.4.1. Precipitation

Rainfall is the single input source of water that is available for evapotranspiration, surface runoff, groundwater recharge, and interflow; in turn, it determines streamflow that mostly feeds the lakes. The basin is considered by three main seasons. The seasonal variations of precipitation over the basin is controlled by the location of the Inter-Tropical Convergence Zone, ITCZ (Ayenew, 1998);(Legesse et al., 2003).

Accordingly, the extended rainy season in the summer (June–September; locally known as kiremt) is principally governed by the seasonal relocation of the Inter-Tropical

Convergence Zone (ITCZ), that lies on the north of Ethiopia at that time. Consequently, the basin under study captures most of the monsoon precipitation from the Atlantic and Indian oceans. On the contrary, when ITCZ moves to the South of Ethiopia between October and February (known as bega) characterized by the dry period, with little rainfall. From March to May, the ITCZ is moving toward north from south, as a result of high pressure occurs over the Indian Ocean and Gulf of Eden and contrasting low pressure occurs in the Arabian region. For this reason, this high pressure produces a moist easterly air movement over the Southeastern part of Ethiopia and produces spring (belg) rainfall, which is much less in amount as compared to summer.

The local spatial distribution of rainfall amount seems to be controlled by topographic variation (1550-4184masl). Consequently, the rainfall amount is also ranging from 650mm/yr on the rift floor to as high as 1420mm/yr in the highland area (Fig. 2.5). There are 14 meteorological stations widely dispersed in the basin and the Thiessen polygon method (Fig. 2.3) was used to determine the percentage weight of each station (appendix 1) to estimate subbasin long term rainfall average depth (Table 2.2) and (Fig. 2.4) as shown below.

Table 2.2 Subbasin Mean Monthly precipitation (mm) using Thiessen polygon

Subbasin	Jan	Feb	Mar	Apr	May	Jun	Jul	Aug	Sep	Oct	Nov	Dec	Annual
Ketar	23.7	40.6	68.7	86.1	96.7	110	151	142	97.1	49.9	15	9.5	889.7
Meki	33.2	52	81.8	93.7	88.2	114	183	161	101	51.2	21.7	17.2	998.2
Rift Floor	28.1	39.3	56.4	69.1	69.1	83.1	163	145	85.2	39.8	14.2	8	800.4
Langano	21.4	37.3	60.1	75.7	89.4	113	165	153	118	55.6	17.8	12.4	918.6
Bulbula	30.9	35	46.9	72.1	75	94.4	133	113	82.9	47.7	17.6	12.7	761.1

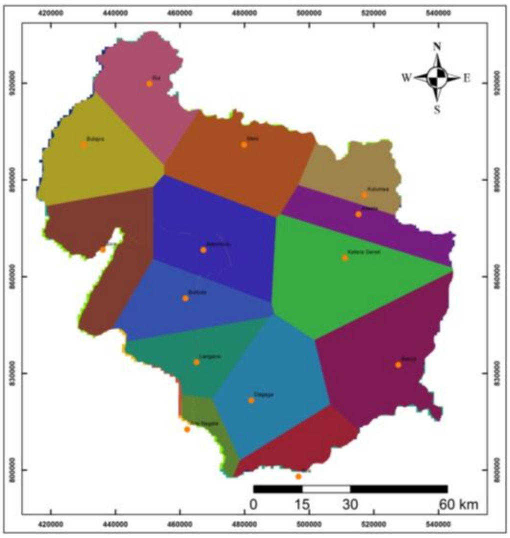

Fig. 2.3 Thiessen polygon method of meteorological stations

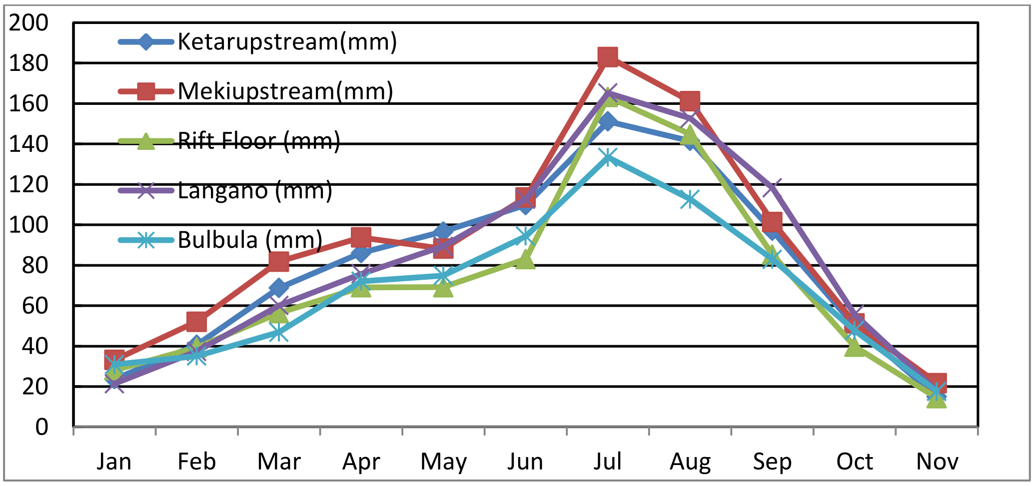

Fig. 2.4 Mean monthly precipitations of subbasins

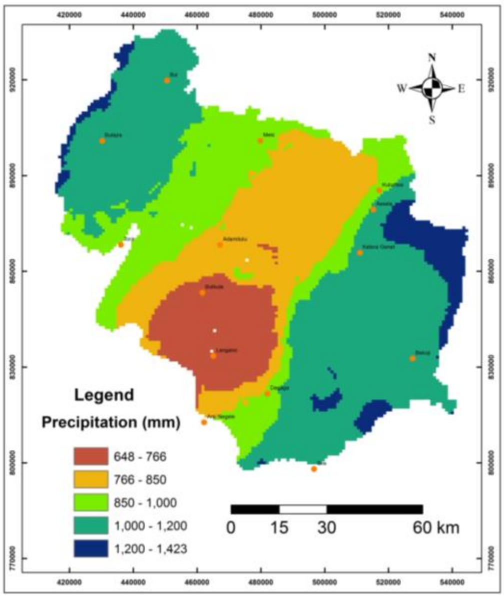

Fig. 2.5 Isohyets Map of the study area (values in mm/yr)

2.4.2. Evapotranspiration

Open water evaporation and wet surfaces and evapotranspiration from vegetation are one of the main variables in the hydrologic cycle. The biggest portion of rainfall is gone in the form of evaporation and evapotranspiration with the amount fluctuating from region to region globally. For instance, in the United States, evapotranspiration (ET) is the highest consumer of the water budget, recording for an average of 70 percent of annual precipitation in the United States, and up to 95 percent in arid climate (Melesse et al., 2009).

It is one of the key components of the hydrologic cycle influencing water resource supply and is important in water resource development and management (Abtew & Melesse, 2013). Various models are used estimating of evapotranspiration from the complex as Penman-Monteith method to the simple Pan method and usually provide different results (Melesse et al., 2009).

2.4.2.1. Common hydro-meteorological factors affecting evapotranspiration

2.4.2.1.1. Temperature

In the study area, there are stations that record maximum and minimum daily temperatures. Five of the stations: Asella, Sagure, Meraro, Degaga and Bui are found in the highlands while Kulumsa and Butajira, are situated at the escarpments; and Ziway, langano, and Adamitulu at the rift floor and these towns are shown in Fig. 2.1. Temperature varies with altitude; and they exhibit a strong inverse correlation with a coefficient of -0.89 (Dribsa, 2006) and some of the representative stations mean monthly temperature is presented in Table 2.3.

Table 2.3 Mean monthly temperature of the stations in the catchment (°C)

No	Station	Jan	Feb	Mar	Apr	May	Jun	Jul	Aug	Sep	Oct	Nov	Dec
1	Adamitulu	19.7	20.8	22.0	22.1	22.3	21.5	20.0	20.1	20.3	20.0	19.5	19.1
2	Asella	14.3	15.6	15.9	16.4	16.5	15.8	14.9	14.7	15.9	14.9	14.1	14
3	Bui	16.6	17.3	18.4	18.6	19.5	17.5	16.2	16.3	16.7	16.4	15.8	15.7
4	Butajira	18.2	18.6	19.2	19.2	19.1	18.5	17.6	17.7	18.4	18.4	18.1	17.8
5	Degaga	16.1	16.9	17.9	18.3	17.9	17.2	16.4	16.3	15.9	16.4	15.9	15.4
6	Kulumsa	15.7	16.7	17.8	18.2	18.1	17.2	16.1	15.8	16	16.6	15.9	15.4
7	Meraro	14.3	14.9	15.8	15.9	16.1	15.2	14.5	14	14.2	14.7	14.1	13.5
8	Langano	20.6	21.4	22.3	22.6	22.5	21.9	20.7	20.8	21.2	21.1	20.6	20.2
9	Sagure	14	15.1	15.9	15.8	15.7	14.9	14.3	14.3	14.3	14.1	13.6	13.5
10	Ziway	19.3	20.4	21.4	21.5	21.8	21	19.9	19.7	19.9	19.7	18.9	18.7

2.4.2.1.2. Relative humidity

It is the percent fraction of the grams of water per cubic meter of air to the capacity of air to embrace the maximum level of air, for the temperature of air mass (Shaw et al., 2011). It articulates the degree of saturation of the air as a fraction of the actual to the saturation vapor pressure at the same temperature. Four stations in the study area (Meraro, Kulumsa, Ziway and Bui), have monthly records of mean relative humidity (Table 2.4).

Table 2.4 Mean monthly relative humidity of the selected meteorological stations (%)

No	Station	Jan	Feb	Mar	Apr	May	Jun	Jul	Aug	Sep	Oct	Nov	Dec
1	Bui	63	61	64	64	63	72	80	80	74	65	63	63
2	Kulumsa	58	54	58	61	61	68	78	81	78	62	54	58
3	Meraro	62	57	58	69	67	73	82	82	78	73	65	62
4	Ziway	67	66	66	68	68	69	76	77	74	66	64	66

2.4.2.1.3. Wind speed

The existence of atmospheric turmoil can significantly upsurge the amount of evaporation by eliminating vapor from evaporating surfaces and giving space for fresh air capable of holding the extra vapor in the air. Four stations located in the study area have records of wind speed at 2m above the ground surface (Table 2.5).

Table 2.5 Monthly average wind speed of meteorological stations in the basin (m/s)

No	Station	Jan	Feb	Mar	Apr	May	Jun	Jul	Aug	Sep	Oct	Nov	Dec
1	Bui	2.1	2.1	2.1	1.8	2.1	1.6	1.5	1.4	1.4	1.9	2.1	2.1
2	Kulumsa	2.6	2.5	2.2	2.1	2.2	1.9	2.1	1.7	1.3	2.7	3	2.8
3	Meraro	2.5	2.6	2.9	3	2.8	1.9	1.5	1.5	2	2.8	2.8	2.6
4	Ziway	1.4	1.4	1.3	1.3	1.5	1.9	1.8	1.6	1.1	1.2	1.5	1.5

2.4.2.1.4. Sunshine hour

Since loss of water in the atmosphere needs a continuous source of energy which is derived mostly from solar radiation, the radiation will be a factor of considerable importance. There are four sunshine hour recording stations available in the study area (Table 2.6).

Table 2.6 Average sunshine hours of meteorological stations in the catchment (hours/day)

No	Station	Jan	Feb	Mar	Apr	May	Jun	Jul	Aug	Sep	Oct	Nov	Dec
1	Ziway	9.5	9.4	8.3	8.4	9.2	8.4	6.4	6.6	7	9.1	10.2	10.1
2	Meraro	8.5	7.5	7.9	6.7	7.6	6.3	4.6	5.5	6.1	6.3	8.6	8.8
3	Bui	8.9	8.4	8.2	8.1	8.2	6.8	5	5	6.8	8.7	9.9	9
4	Kulumsa	8.1	7.8	7.3	6.7	7.2	7	5.3	5.3	5.6	7.5	8.7	8.7

2.4.7. Estimation of Evapotranspiration

2.4.7.1 Thornthwaite Method

Thornthwaite formed a method for computing PET based on temperature as the index of energy offered for evapotranspiration with a correction being done for the latitude, location and number of daytime sunshine hours and detail can be seen in (Table 2.7). However, the previous study Ayenew (2003) reported the Thornthwaite method to under estimate evapotranspiration in the basin, particularly in the rift plateau region. In addition to the limitation to capture high spatial variation of climatic parameters exist in the rift.

Table 2.7 PET Thornthwaite method in (mm)

Station	Jan	Feb	Mar	Apr	May	Jun	Jul	Aug	Sep	Oct	Nov	Dec	Annual
Asella	51.6	59.3	62.1	66.8	68.5	64.7	58.7	57.0	63.2	55.8	50.5	49.5	**707.8**
Bui	58.5	63.3	71.7	74.9	82.6	69.1	60.0	60.1	61.7	58.3	53.7	52.6	**766.4**
Butajira	64.3	67.6	73.0	74.9	75.4	71.5	64.5	64.7	68.5	66.8	63.6	61.1	**815.9**
Kulumsa	54.7	61.2	69.2	73.7	74.2	68.7	61.0	58.7	58.9	61.1	55.9	52.5	**749.9**
Meraro	53.2	57.0	63.2	65.4	67.8	62.8	58.1	54.7	55.0	56.4	52.1	48.8	**694.6**
Sagure	52.1	58.6	64.3	65.3	65.8	61.5	57.5	57.0	56.1	53.5	49.9	49.0	**690.6**
Ziway	66.0	75.1	84.8	87.9	92.1	85.6	75.5	73.3	73.7	70.3	63.1	61.1	**908.4**

2.4.7.2. Penman-Monteith Method

Potential evapotranspiration can be computed with help of FAO Penman-Monteith equation. It requires regular meteorological data of air temperature, humidity, wind speed, and solar radiation. To confirm the reliability of calculations, the weather measurements should be prepared at 2m (or converted to that height) above a wide-ranging surface of green grass, shading the ground and not short of water (Allen, Pereira, Raes, & Smith, 1998).

The FAO Penman-Monteith method to estimate ETo is expressed as:

$$ET_o = \frac{0.408\Delta(R_{n-}G) + \gamma\frac{900}{T+273}U_2(e_s - e_a)}{\Delta + \gamma(1 + 0.34u_2)}$$

Where:

ET_o Reference evapotranspiration (mm/day),

R_n Net radiation at the crop surface (MJ/m^{2}day),

G Soil heat flux density (MJ/m^{2}day),

T Mean daily air temperature at 2 m height (°C),

U2 Wind speed at 2 m height (m/s),

e_s Saturation vapour pressure (KPa),

e_a Actual vapour pressure (KPa),

$e_s - e_a$ Saturation vapour pressure deficit (KPa),

Δ Slope vapour pressure curve (Kpa /°C),

γ Psychrometric constant (Kpa/°C),

There are only four meteorological stations that have records of relative humidity, wind speed, and sunshine hour and thus were used to estimate potential evapotranspiration with the FAO-CROPWAT model and the result is shown in Table 2.8.

Table 2.8 Evapotranspiration by Penman Monteith method (in mm)

Station	Jan	Feb	Mar	Apr	May	Jun	Jul	Aug	Sep	Oct	Nov	Dec	Total
Ziway	131	130	146	141	153	141	120	120	119	138	134	131	**1603**
Bui	129	130	144	138	149	128	110	112	115	135	131	129	**1549**
Meraro	114	118	127	119	125	110	96	100	101	117	115	114	**1356**
Kulumsa	136	127	136	126	128	113	103	103	102	132	140	137	**1484**

2.4.7.3. Actual Evapotranspiration

Actual evapotranspiration was assessed by means of the Soil-water balance method founded on data records of average monthly precipitation and average monthly temperature and soil water holding capacity of 100mm. The results of the sub-basin are shown in Table 2.9. However, the Soil-water balance approach method does not consider the channel loss in discrete features or focused recharge mechanism.

Table 2.9 Actual Evapotranspiration estimation (mm)

Subbasin	Jan	Feb	Mar	Apr	May	Jun	Jul	Aug	Sep	Oct	Nov	Dec	Annual
Ketar	33	45	70	81	82	78	73	71	70	69	48	30	750
Meki	42	56	82	86	87	84	80	79	81	76	54	36	842
Rift floor	35	43	58	70	70	83	91	89	89	75	44	24	771
Langano	33	43	62	76	81	78	74	73	70	69	51	34	744
Bulbula	38	38	48	73	75	94	92	91	88	67	37	23	764

2.4.7.4. Lake Evaporation

Various methods have been employed to estimate lakes' evaporation (Vallet-coulomb et al., 2001) and (Ayenew, 2003) and the outcomes are presented in Table 2.10 and Table 2.11.

Table 2.10 Lake Ziway evaporation estimations with various methods

Month	Evaporation					
	Energy balance[1]	Penman[1]	CRLE[1]	Penman[2]	Radiation[2]	Pan[2]
	(mm)	(mm)	(mm)	(mm)	(mm)	(mm)
Jan.	143	154	132	150	135	159
Feb.	149	162	135	128	120	144
Mar.	152	166	149	148	142	192
Apr.	156	166	155	188	138	142
May	163	170	160	188	138	156
Jun.	147	168	155	135	107	137
Jul.	128	136	146	139	115	126
Aug.	136	137	136	135	115	123
Sep.	141	136	137	164	124	112
Oct.	159	162	141	200	151	170
Nov.	160	161	144	223	157	178
Dec.	143	157	139	225	157	130
Annual	**1777**	**1875**	**1728**	**2023**	**1599**	**1769**

Source: from [1] (Vallet-coulomb et al., 2001) and [2] (Ayenew, 2003); complementary relationship lake evaporation (CRLE) method

Table 2.11 Lake Abiyata and Langano evaporation estimations with various methods (mm)

Lake	Abiyata		Langano		
Method	Penman	Radiation	Penman	Radiation	Pan
Jan	173	178	177	166	115
Feb	141	155	159	146	117
Mar	159	177	185	179	139
Apr	207	171	176	154	139
May	181	164	170	151	151
Jun	132	128	149	128	131
Jul	127	133	150	129	138
Aug	128	133	147	132	129
Sep	149	142	178	133	118
Oct	212	171	183	166	112
Nov	257	185	188	168	113
Dec	193	185	147	145	124
Annual	**2060**	**1922**	**2010**	**1651**	**1526**

Source: Ayenew, 2003

2.5. Discharge Analysis and Baseflow separation

2.5.1. Rivers

Numerous persistent rivers originate from the plateaus on both sides of the basin and they enter into a series of lakes that lodge the in the rift floor. The main rivers are Ketar, Meki, Bulbula, Horakelo, Gedemso and Lepsi (shown in the location map).

2.5.1.1. Ketar River

The sub-basin of the Ketar River arises to over 4,000m a.s.l. on the peaks of Mounts Badda and Kaka towards the lowland (1534m a.s.l.). The slope of the river is mostly steep through its course to Lake Ziway, and it is often extended up to 50m below the neighboring land. Arising from its topography only limited extents of area are suitable for irrigation. Therefore, the prime importance of the Ketar River is its contribution to the lake. The overall subbasin's area of the river at the Abura is 3,264 km^2. According to the streamflow data recorded at the Abura town (1990–2000), the mean annual runoff volume of the river is 406MCM. The monthly average discharge is concised in Table 2.12.

Table 2.12 Mean monthly flow (in m3/s) of Ketar River at Abura

Month	Jan	Feb	Mar	Apr	May	Jun	Jul	Aug	Sep	Oct	Nov	Dec	Av.
Discharge (m^3/s)	2.0	3.1	4.5	5.4	4.6	5.4	16.2	50.2	35.9	16.9	5.0	2.6	12.6

2.5.1.2. Meki River

Meki River emanates from the Gurage highlands and travels a distance of about 100 Km to lose its head from 3,600m to 1,636m altitude before draining into Lake Ziway. The river rapidly descends from the rift valley escarpment to below 2,000m asl before being joined by several major tributaries, including the Lebu, the Akamuja, and the Weja rivers. The entire subbasin area of the river at Meki town is 2, 260km^2. According to the streamflow data recorded at Meki town (1990 - 2000), the mean annual runoff volume of the river is 339MCM. The average monthly discharge of the river at Meki Town is given in Table 2.13.

Table 2.13 Mean monthly flow (in m3/s) of Meki River at Meki Town

Month	Jan	Feb	Mar	Apr	May	Jun	Jul	Aug	Sep	Oct	Nov	Dec	Av.
Discharge (m^3/s)	0.82	2.14	5.72	6.54	6.34	7.31	20.86	40.06	23.81	12.14	4.00	1.16	10.91

2.5.1.3. Bulbula River

The Lake Ziway water level is checked by the natural basalt bar at some 6m downstream from the discharge of the lake and it controls the amount of inflows to the Bulbula River. The average annually discharges of Bulbula river is about 176 MCM of water from Lake

Ziway into Lake Abijata. Table 2.14 depicts the average monthly discharge of the river recorded at the station near Adami Tulu Town which was being abandoned since 1983.

Table 2.14 Mean monthly flow (in m/s) of Bulbula River

Month	Jan	Feb	Mar	Apr	May	Jun	Jul	Aug	Sep	Oct	Nov	Dec	Av.
Discharge (m^3/s)	4.1	2.6	1.2	1.3	1.3	1.4	2	6.2	14	15	12	7.5	5.7

2.5.1.4. Horakelo River

It originates from Lake Langano and feeds Lake Abiyata. The annual contribution of Horakelo to Lake Abiyata is 24MCM and the average monthly flow is shown in Table 2.15.

Table 2.15 Mean monthly flow (in m3/s) of Horakelo river

Month	Jan	Feb	Mar	Apr	May	Jun	Jul	Aug	Sep	Oct	Nov	Dec	Av.
Discharge (m^3/s)	0.55	0.33	0.18	0.13	0.11	0.14	0.26	0.79	1.61	2.22	1.7	1	0.75

2.5.1.5. Gedemso River

It is one of the several rivers that emanate from the eastern highland and drain into Lake Langano. Data recorded from 1997 to 2000 indicate that its average annual volume is about 65MCM and the average monthly contribution to the Langano is shown in Table 2.16. Besides these, many rivers start from the eastern highland and feed Lake Langano without gauging stations.

Table 2.16 Mean monthly flow (in m3/s) of Gedemso River

Month	Jan	Feb	Mar	Apr	May	Jun	Jul	Aug	Sep	Oct	Nov	Dec	Av.
Discharge (m^3/s)	0.36	0.22	0.43	0.37	0.85	0.6	3.05	8.03	4.59	4.39	1.26	0.48	2.05

2.5.2. Baseflow Separation

Streamflow is commonly thought of as comprising three components: Surface runoff, sub-surface runoff, and deep percolation to groundwater. The stream baseflow has been described as flow from groundwater aquifers (Eckhardt, 2008). It is always the slowest responding and longest lasting component of Streamflow (Duncan, 2019; Eckhardt, 2008). Yet another authors (Wittenberg & Sivapalan, 1999) also describe the streamflow of many rivers, in many different hydrological and climatic settings, as the outflow emanating from the shallow groundwater reservoirs of the associated catchments.

Understanding baseflow characteristics is a critical issue in water development and utilization. Since baseflow is not only a function of rainfall amount but also about the geological settings and hydrogeological properties of the region. These may include the geological materials, aquifer properties (permeability and storage), Geomorphic features (graben, horst, depositional surfaces, ridge, hills, flat, sloppy, etc.), and Geological structures (fault, fracture, lineament).

These have paramount importance in controlling the recharge mechanisms, rates and groundwater dynamics in a particular region. For the study area, the historical daily streamflow records are available for Ketar (from 1990 to 2000) at Abura gauging station; and Meki River (1968-1991) at Meki gauging station and River Package Analysis (RAP) program was used to separate Baseflow from streamflow. The result depicts that the ratio of Baseflow to Surface runoff is about 0.34: 0.66 and 0.32: 0.68 for Ketar and Meki rivers respectively. During dry periods the streamflow is sustained by the baseflow component and in (Table 2.17), Fig. 2.6 and Fig. 2.7. Hence, the annual baseflow contributions (groundwater discharges) of Ketar and Meki sub-basins are 138MCM (42.4mm) and 88.7MCM (39.25mm), respectively.

Table 2.17 Mean monthly streamflow, baseflow and surface runoff for Ketar and Meki Rivers.

	FC	Jan	Feb	Mar	Apr	May	Jun	Jul	Aug	Sep	Oct	Nov	Dec	Sum
Ketar	TSF	5.8	5.8	7.1	11.1	11.6	14.7	39.8	138.7	99.4	47.0	13.9	6.7	402
	BF	5.3	5.0	4.6	5.8	6.9	8.1	11.3	25.0	34.3	18.3	8.0	5.8	138
	SF	0.5	0.9	2.4	5.3	4.7	6.6	28.5	113.7	65.2	28.7	6.0	1.0	263
Meki	TSF	1.6	7.0	18.1	19.4	14.8	14.9	52.3	66.3	51.4	19.4	7.4	1.8	274.3
	BF	0.8	1.3	3.5	5.7	5.9	6.8	11.8	22.4	19.1	7.1	2.9	1.3	88.7
	SF	0.8	5.7	14.6	13.7	8.8	8.1	40.5	43.9	32.3	12.3	4.4	0.4	185.5

FC- flow component; TSF-Total Streamflow (MCM); BF-Baseflow (MCM); and SF-Surface flow (MCM)

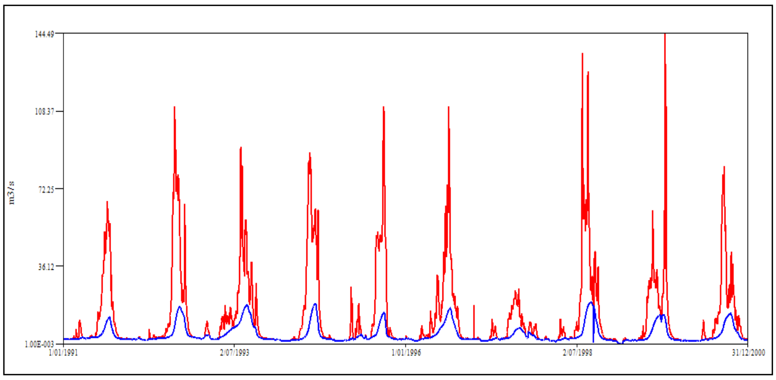

Fig. 2.6 Ketar river hydrograph and Baseflow component at α*=0.975

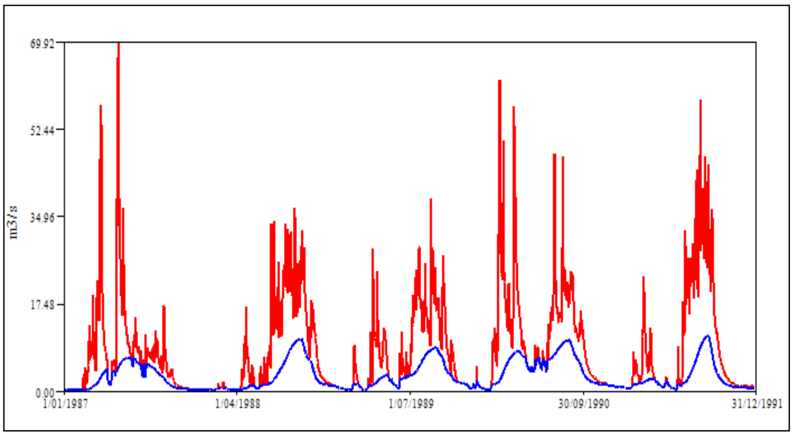

Fig. 2.7 Meki river hydrograph and Baseflow component at α*=0.975

* (α or Alpha): filter parameter in Lyne-Hollick recursive digital filters algorithm

2.6. Water balance Analysis

A simple water recording method is applied to calculate various components in a subbasin. Rainfall in a sub-basin partially converts to runoff; some portion is lost by evapotranspiration and the residual goes to deep percolation to groundwater via recharge. When there is no water abstraction from the basin, water balance is denoted by a simple equation as follows.

$\boldsymbol{P - R_n - ET - G_{wr} - G_{out} = \Delta S}$ ………………….. Eqn 2 .1 (Han, 2010)

Where, P is precipitation; R_n is surface runoff; ET is evapotranspiration; G_{wr} is Groundwater recharge; G_{out} is groundwater outflow from the basin and $\Delta \boldsymbol{S}$ change in storage.

Groundwater recharge, in natural long-term conditions (steady-state, $\Delta \boldsymbol{S} = \boldsymbol{0}$), i.e., where the groundwater withdrawal is negligible, is equivalent to the percentage of groundwater discharge. Provided that all groundwater outflows into the rivers, either directly or via springs, in the long term the river baseflow become equivalent to the groundwater recharge in a given basin (Kresic, 2007). In the same way, Surface runoff and groundwater recharge is equal to stream discharges (D) i.e., (R_n +G_{wr}=D). The water balance for the Ketar and Meki upstream sub-basins have been estimated from Table 2.2 and Table 2.9 and given in Table 2.18.

Table 2.18 Ketar and Meki upstream sub-basint water balance (in mm)

		Jan	Feb	Mar	Apr	May	Jun	Jul	Aug	Sep	Oct	Nov	Dec	Annual
Ketar upstream	P	24	41	69	86	97	110	151	142	97	50	15	10	890
	ET	-33	-45	-70	-81	-82	-78	-73	-71	-70	-69	-48	-30	-750
	D	-2	-2	-4	-4	-4	-4	-13	-41	-29	-14	-4	-2	-123
														17
Meki upstream	P	33	52	82	94	88	114	183	161	101	51	22	17	998
	ET	-42	-56	-82	-86	-87	-84	-80	-79	-81	-76	-54	-36	-843
	D	-0.7	-3.1	-8.0	-8.6	-6.5	-6.6	-23	-29.3	-22.7	-8.6	-3.3	-0.8	-121.4
														34

Abstractions of 17mm (55.5MCM) and 34mm (77MCM) in Ketar and Meki upstream sub-catchments respectively. This could be water abstracted for Wetland consumption and domestic uses.

2.7. Lakes and Lakes water balance

2.7.1. Lakes

The Rift floor region of the central rift valley basin is occupied by a row of lakes: Ziway, Langano, and the terminal lake Abijata (shown in the location map) while their areal extension, depth and volume in the 1ate 1990s' (Table 2.19). However, the current size the Lake Abijata modified to the large extent. Over the past 30 years, the lake Abijata area has been declining from a maximum of 225 km^2 in 1970-72 to 166km^2 in 2000. However, according to Hailu & Girma (2019) the lake's area coverage has estimated to 179.2km^2 in 1972 and 131.8km^2 in 2015. As of 2020 the estimated area of the lake from the image of Google Earth was 166km^2. This variation may be associated to temporal change of the lake area coverage. Lake Abiyata has highly saline alkaline-sodic water and cannot be used for irrigation (Halcrow, 2009).

Table 2.19 The basic lakes data

Lake	Altitude (masl)	Lake area (km^2)	Maximum Depth(m)	Mean Depth (m)	Volume (MCM)
Abijata	1580	180	14.2	7.6	954
Langano	1585	230	47.9	17	3800
Ziway	1635	440	8.9	2.5	1466

Source: (Ayenew, 1998)

2.7.2. Lakes water balance

The Lake water balance equation is given by

$$\boldsymbol{Inflow - Outflow = 0}$$

$$P + R_i + G_i + Sr - Evap - R_o - G_o - Abs = 0$$

Table 2.20 Water balance of lakes in the central rift valley basin (in Million cubic meter)

Lake	Inflow				Outflow			Diff
	P	R_i	G_i*	Sr*	Evap	Ro	Abs *	
Ziway	323	392 264.5	-	48	890	184	28	-74
Langano	186	212	63	-	463	46	-	-48
Abijata	113	184 46		15	372	-	13	-27

Source: (Ayenew, 1998)

P-precipitation; Ri-Runoff; Ro-Runoff outflow; Gi-groundwater inflow; Go-Groundwater inflow; Sr-surface runoff from ungauged sub-catchment; Eva-Evaporation; Abs-Abstraction.

2.8. Land use and Land cover

Understanding of land-use/land-cover (LULC) change is crucial in a number of fields based on land surface processes such as quantitative inventory of land use land dynamics, environmental and hydrological. Consequently, assessment in LULC change is inevitably required for a different of objectives for the welfare of human beings in the context of rapid and uncontrolled population growth along with economic and industrial development, especially in developing countries with intensified LULC changes (Dutta et al., 2019). LULC changes may have a series of impacts on both human society and environment in many ways (by increasing flood and drought vulnerability, environmental degradation, loss of ecosystem services, groundwater depletion, landslide hazards, soil erosion and others.

For this study, relatively cloud-free Landsat 8 Operational Land Imagery (OLI) image was used for the acquisition period of dry season of 2020 with Path 168 and Row 054/055 acquired from the United States Geological Survey (USGS), earth explorer website (https://earthexplorer.usgs.gov). The recent landuse land cover the basin is dominated by cultivated land accounts for about 49% and followed by shrub land and forest with 12.5%, and 8.77%, respectively. Grassland covers about 7.36% of the basin. While, the woodland, water bodies and wetlands are mainly found in the rift floor covers about 5.4%, and 8.5%, respectively. The detailed area coverage and distribution across the basin is shown in the Table 2.21 and Fig. 2.8.

Table 2.21 Landuse/land covers of the subbasin

S/N	Landuse type	Area in Hectare (ha)	Percentage
1	Cultivated	521,373	49
2	Shrubland	133,445	12.5
3	Forest	93,281	8.77
4	Grassland	78,255	7.36
5	Woodland	57,263	5.4
6	Water bodies	80,418	7.5
7	Barren/Built-up area	90,086	8.45
8	Wetland	11,215	1
	Area (ha)	1,063,593	100

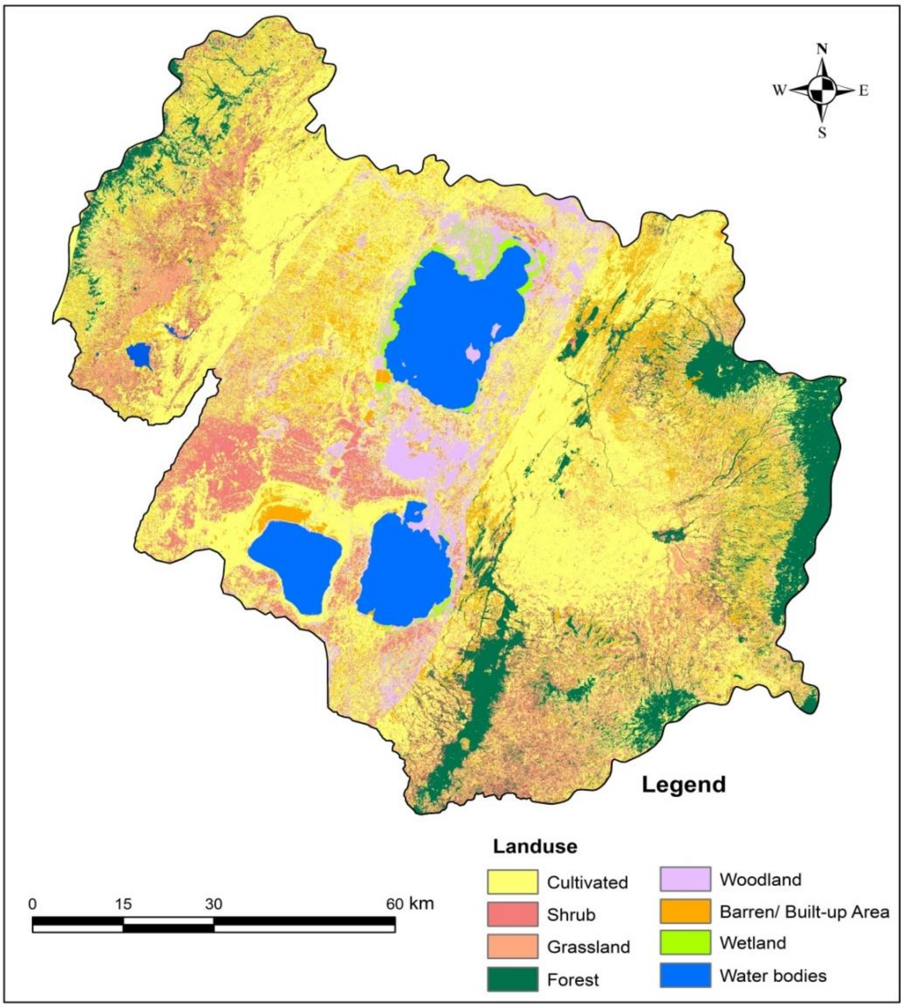

Fig. 2.8 Landuse/land cover map of 2020

2.9. Socio-economic aspects

2.9.1. Population

The population in the basin is growing rapidly in the last decades due to birth rate and migration to the areas from other places. Subsequently, burden on the natural resource has been increasing extremely. The population growth rate in the basin about 3%. A long-term population projection for 30 years (2015/2016 – 2037 E.C.) is prepared based on the census count of population data of 2007 E.C.as a benchmark for the projection. To project future population, the geometric formula $P = P_i[1 + r]^t$ is used to manipulate the calculation by assuming the natural consistent of each series. The total population is estimated to be more than 2.5millions in 2015/2016 (Table 2.22).

Table 2.22 Population of the subbasin estimated at 2015/2016

Subbasin	Rural	Urban	Total
Ketar Upstream	545,399	62,426	607,825
Meki upstream	876,191	94,281	970,472
Rift floor	225,014	61,681	286,695
Langano	447,780	82,154	529,934
Bulbula	120,482	20,923	141,405
Total	2,214,866	321,465	2,536,331

2.9.2. Economic activities

Agriculture is the core pillar of the source of the economy for the most of people living in the basin. In this regard, the two major agricultural production activities are crop and livestock production are the major ones. Both rainfed and irrigation crop production are commonly practiced in the subbasin. The furthermost vital source of income for smallholders is still rain-fed agriculture and cattle keeping. The major crops grown by rain-fed agriculture include maize, wheat, barley, teff, haricot bean, and different types of vegetable crops such as tomatoes, potatoes, onions, etc.

During the last two decades, irrigation-based cultivation has been increasing rapidly in the study areas, mostly focusing on the availability of water resources (Surface water and groundwater). This was mainly for the purpose of ensuring food security conditions of the areas through necessary supports of Governmental and NGOs to private investors and smallholder farmers are able to practice effective irrigation development activities. Table 2.23 shows the current status of irrigation in the woredas in the subbasin.

The second major most important agriculture production activities following crop production is livestock rearing. Rearing livestock is practiced amongst the majority of the farmers; and hence, in these areas, there is numerous livestock production as a means of livelihoods for large number of people. Major livestock reared in the areas include: cattle, goat, sheep, horse, mule, donkey and poultry; and there are some highland areas where bee-keeping is practiced as a supplementary means of livelihoods. According to the data obtained from zones in the subbasin: East Shewa, Arsi, Gurage, and Silte zones and the livestock data are presented in table 2.23

In addition to the above-mentioned economic activities, fisheries, charcoal production (forest product selling), petty trades and wage workers on the others farms are common means of earning in the region.

Table 2.23 Amount of irrigated land in the woredas in the basin

Woreda	**Existing Irrigated Area(ha)**
Ziway-Dugda	10892
Dugda	13288
ATJK	5136
Tiyo	4348
Munessa	1850
Lemmu -Bilbilo	6761
Hetosa	140
Digalu-Tijo	9142
Masken	8268
Mareko	4711
Silte	14154
Lanfro	338
Sodo	4080
Total	83,108

Source: OWWDSE 2015/2016 report

Livestock: the number of livestock resources has to be standardized using conversion factors to Tropical Livestock Unit (TLU) and is estimated at 2.3Million TLU and the table is shown appendix 2. TLU is a standard unit used to relate various animal species, which uses the following conversion factors: Cattle=0.7 TLU, sheep/goat = 0.1 TLU, horse 0.8 TLU, donkey = 0.65 TLU, mule = 0.7 TLU, pig = 0.2 TLU, chicken = 0.01 TLU as stated in (Pascual-ferrer & Candela, 2015)

2.9.3. Water demands of different sectors

Irrigation is the furthermost water demanding sector in the basin according to the inventory made by (OWWDSE, 2016) and its outcomes indicated that the water demand for irrigation purposes including both surface water and groundwater sources is estimated to 1045MCM annually. The mean annual water demand for the domestic purpose of the rural population is 25L/person/day and 40L/person/day for urban dwellers according to (Halcrow, 2009). Whereas, the average yearly consumption of water livestock by TLU is 25L/TLU/day)(Pascual-Ferrer & Candela, 2015). Industrial water demand is estimated based on the consideration of 5% of domestic water demand(OWWDSE, 2016). The annual water demand for different sectors for the year 2015/2016 is given in Table 2.24.

Table 2.24 Summary of annual water demand for different sectors in the basin

S/No.	Sector	Unit	Quantity	Water demand, MCM
1	Domestic	Number	2.5Millions	25
2	Livestock	TLU	2.3Millions	21.2
3	Industry	LS	-	1.3
4	Irrigation	Hectare	83,108	1,045
			Total	1,092.5

LS =lump sum

3. Geology and Hydrogeology

3.1. Introduction

The study basin is located in the Main Ethiopian Rift (MER) which the northern portion of the East African Rift System (EARS). It oriented proximately NNE–SSW dissecting Ethiopia landmass (Williams et al.,2004) (Fig. 3.1). It had been impacted by tectonic and volcanic events during the periods the Late Holocene and Quaternary. Though its width reached about 80km, the tectonically and volcanically active region was bounded with a 10-20km along sub-axial zone named the Wonji Fault Belt (WFB), which is found along the eastern rift margin (Mohr, 1960, 1967; Mohr et al., 1978) (Paul Mohr, 1987) and in western margin its equivalent is marked as the Silti-Debre Zeit Fault Zone (SDZFZ).

The WFB was perhaps originated about 1.6 Ma ago and a main volcanism and tectonic processes happened within it at 0.25 Ma (Berhe, 1986). The geologic setups and its geomorphic features are the key issues that affect the hydrologic and hydrogeologic parameters of the basin in general.

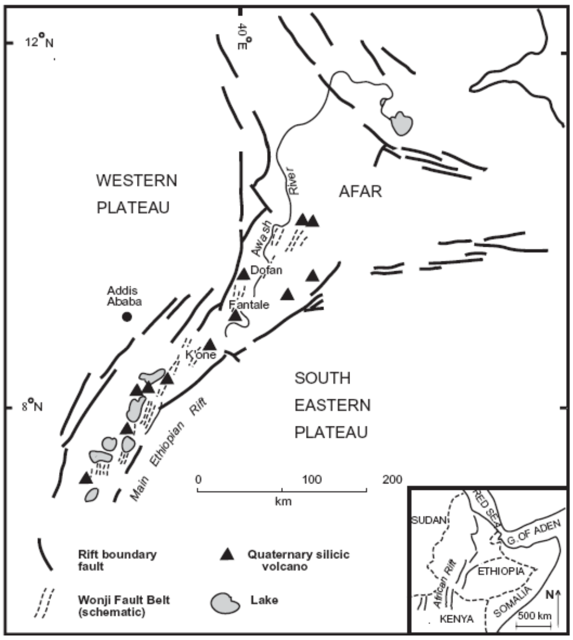

Fig. 3.1 The Main Ethiopian Rift and Afar (Adapted from Williams et al., 2004)

3.2. Geology of the study basin

There are three major rocks categories in the study basin: (i) Basement and Mesozoic Sedimentary rocks; (ii) Volcanite and pyroclastic rocks and older lacustrine deposits; and (iii) Quaternary Sedimentary Deposits. The area was investigated by (Benvenuti et al., 2002; Chernet et al., 1998; Dainelli et al., 2001) and produced a geological map of the Ziway-Shalla basin at the scale of 1:250,000 and units were identified and mapped and the detail can be seen (Fig. 3.2). Later (OWWDSE, 2016) described the various lithologic units and their role in influencing the basin's hydrologic and hydrogeologic as below.

3.4.1. Basement and Mesozoic Sedimentary Rocks (Bm)

These rocks are exposed at limited localities in western highlands - rift shoulders at Kela horst (Arno et al., 1993; Woldegabriel et al., 1990). It is explained as a crustal block closely linked to rifting processes (Arno et al., 1993). These rocks are strongly weathered basement rocks (dark gray, medium to coarse-grained biotite and hornblende gneiss, covered by sheets of Mesozoic sedimentary series comprised of sandstones, shales, marls and limestone (OWWDSE, 2016). This unit has substantial significance form the perspective of groundwater.

3.4.2. Volcanites, Volcanoclastic and Older Lacustrine Deposits

These groups of rocks comprise seven units and covering about 71% of the basin and they range in age from Oligocene to Middle Pleistocene. It comprises of volcanic rocks in the both sides of the highlands and ignimbrite of the rift floor with the exception to areas covered by lacustrine deposit (Fig. 3.2). These groups of rocks have great significance in determining the hydrological and hydrogeological flow regimes of the basin. A detailed description of each unit was given in (OWWDSE, 2016) report.

3.4.2.1. Volcanites of the Plateau (Tt)

These Oligocene to Early Pliocene volcanites unit is made of basalts and rhyolitic ignimbrites and tuffs. Although there are some Oligocene to Miocene basaltic layers, especially in the western part of the basin where the Meki River is originated, the flat-lying plateau and the strongly faulted major plateau – rift escarpment in the basin are dominantly constituted by Pliocene age ignimbrites and tuffs which belong to the older units of what is regionally considered as the "Nazareth Group".

Where they occur, especially at the western plateau, the Oligocene - Miocene volcanics form thick beds of flood basalts, with rare beds of basic tuffs, agglomerates, and volcanic breccia, associated with some interlayered silicic volcanic rocks. The upper unit is dominantly rhyolite and trachyte flows with minor basalts, while flood basalts with minor silicic flows constitute the lower parts. The flood basalts exposed have undergone moderate to high intensity of weathering forming a relatively thick weathered material on undulating, relatively flat topography.

The Pliocene volcanic rocks, which are dominantly silicic, are exposed on the plateau close to the plateau-rift transition zones and within the rift. They form three prominent landforms: vast flat terrains constituted by extensive pyroclastic deposits, strongly affected by NE-SW oriented rift margin faults forming stepped ridges, and dotted by rhyolitic and trachytic central volcanic massifs and domes. The western highlands and the eastern (Arsi plateau) and their shoulders are covered by the Pliocene rhyolitic-ignimbrites and tuffs rocks.

The lower sections of the Pliocene volcanics are composed of thick successions of welded pyroclastic flows, ash-flow tuffs, and pantelleritic ignimbrites, forming wide, slightly undulating plains, mostly with the hardly weathered bedrock close to the surface, except in a few places where secondary alluvial deposits cover narrow and shallow valleys developed over this unit. The Lower "Nazareth Group" is also underlying the narrow, alluvium filled NE-SW oriented linear grabens, and adjoining low horsts at the western rift margin. The Meki and Ketar Rivers and the numerous normal faults bounding the rift expose this unit forming steep cliffs beneath the pyroclastic sequences of the Middle Nazareth Group. The Middle Nazareth Group is composed of hardly welded to unwelded pyroclastic flows, which form vast sheet plains on the eastern plateau. The pyroclastic rocks are strongly weathered and reworked at the top to form a typical soil layer called "paleosol", which is a mixture of devitrified glass, pumice and ash, mixed with clay minerals (smectite and kaolinite). As deduced from some deep well logs, and some exposures at vertical faults, the thickness of the Lower and Middle Nazareth Group reaches up to 200m. This unit has a great influence in controlling river flow direction and groundwater flow regime.

3.4.2.2. Arsi Shield Volcanoes (Mt)

The Late Miocene to Pliocene age forms shield volcanoes that largely contains basalts, mugearites and minor trachytes, and phonolites, but they also contain inter-bedded basaltic breccia (agglomerates). The shield form of reaching up to 4000masl.) for instance, origin of Ketar river in the highland. They form prominent topographies above the generally flat-lying Volcanites of the Plateaux. Although most are of mid-Pliocene age, e.g., ages from Chilalo range between 2.31 and 1.74 Ma, the Mount Chike phonolite center, close to the rift margin, has an age of 11.6 and 12 Ma (Woldegabriel et al., 1990). The summit caldera of Mount Chike is dissected and breached along the northern side forming a 60m deep gorge cut by the Ketar River in the flat region between Chilalo and Chike exposing a stratigraphic succession of welded tuff and unconsolidated ash flows of Quaternary age. This unit has a significant influence on meteorological and hydrological parameters, because of its occurrences at the highly elevated Easter part of the basin.

3.4.2.3. Rift Floor Ignimbrites (Pp)

These early to middle Pliocene pyroclastic materials are composed of peralkaline-rhyolitic- ignimbrites and loosely fused ignimbrites and pumice with subordinate lava flow of basaltic composition. This group of rocks found abundantly in low lying rift floor region. (Di Paola, 1972; Woldegabriel et al., 1990), however, they are partially underlain by the recent formations and the lakes. They also occupy the WFB and the SDZFZ faulting zones. These pyroclastic units mainly form part of what is regionally called the “Dino Formation”, though the lower parts could also be associated with the “Nazareth Group” rocks, especially at the WFB (OWWDSE, 2016). As it was mentioned in the same study, the Lower units are constituted by coarse, unwelded pumaceous pyroclastics, forming elongated ridges, while the upper units are composed of ignimbrites, tuffs, surges, and occasional lacustrine beds intercalated within the pyroclastics. The upper units form generally flat terrain exposed by NE-SW oriented normal faults, and overlain by lacustrine deposits in places, especially close to the margins of the modern lakes. The thickness of these units, as deducted from borehole data (Gianelli & Teklemariam, 1993; OWWDSE, 2016) and from outcrop observation(Di Paola, 1972; Woldegabriel et al., 1990) suggests it is in the range of 500-600m. This unit could be a zone of high groundwater potential that have significant control over the groundwater flow regime. In addition, it significantly influences the hydrochemistry of the basin because of rhyolitic composition of rocks.

3.4.3. Gademotta – Balci Alkaline and Peralkaline-rhyolitic lavas (Pa)

The Late Pliocene to Middle Pleistocene lava flows constituted of alkaline-peralkaline-rhyolitic lava flows with subordinate of pumice, tuff and obsidian. They are exposed only in a few separate localities in the Basin, at Gademotta and Wulbareg and Dalocha, forming domal landscape. From a groundwater perspective, this unit has little influence, since it occupies a small area in the basin. It acts as a local barrier to groundwater to the lake basin because it is an impermeable unit.

3.4.4. Alutu - Bericcio Rhyolitic Lava Flows (Pw)

This Early Pleistocene to Holocene rocks is constituted of rhyolitic-lava-flows and forms domes with tuffs, pumice, and volcanic-ashes. These young, axial volcanic centers are found at the Bora, Moye, Alutu volcano and a silicic dome at Adami Tulu and the small southwestern islands of Lake Ziway in the central part, and the northern rim of the Corbetti volcano in the south (Di Paola, 1972; P. Mohr et al., 1980). It has great significances on hydrology and hydrogeology regime of the basin, and subsequently influences the outflow of water from Lake Ziway.

3.4.5. Wonji – Butajira Basaltic Lava Flows (Qb) and Scoria Cones (Qb1)

The Early Pleistocene to Holocene basaltic lavas and associated scoria cones are exposed in two distinct areas following major tectonic lines, at the WFB and the SDZFZ, east and west of Lake Ziway, respectively. The basaltic lava flows are relatively thin sheet flow lavas while the scoria cones usually form on top of the lava flows as hyaloclastites and scoria deposits or as isolated spatter cones. These flows are associated with the active, axial volcano-tectonic process of the WFB and the SDZFZ (Woldegabriel et al., 1990) and by slightly inclined lava flows (Di Paola, 1972); (Arno et al., 1993). These units are mainly occurred at (i) northeast of Lake Ziway where a nearly 10 km zone across the rift (the WFB) is enclosed by fresh basaltic-lava-flows (***Qb***) with rare scoria cones, almost entirely covering older units for a length of about 20 km along the rift axis; (ii) east and south of Lake Ziway and at the Tulu Gudo island of Lake Ziway, where a field of numerous isolated scoria cones (***Qb1***) form following a general NNE-SSW orientation parallel to the major fault direction and in many instances on top of faults which in turn are sealed by very thin but extended basaltic lava flows; there are also some basaltic flows overlain by younger lacustrine and fluvio-lacustrine deposits and exposed by river sections like the Bublula River basalt flow and (iii) associated lava flows and scoria cones covering significantly big areas (about 20 km long along the rift and 5 km across) in three localities oriented NE-SW in the western margin at the SDZFZ; there are also some isolated scoria cones with some crater lakes in this area. Hence, this unit is highly affected by faults and therefore faults act as barrier to surface water and groundwater flow.

3.4.6. Fluvio-Lacustrine Deposits Inter-bedded with Volcanites (Qfl)

These groups of rocks are inter-bedded sediments composed of clay, silt, and sand of the middle Pleistocene. They are exposed only in a few localities, mainly within the Alutu volcanic complex and at the base of a faulted rim southwest of the shore of Lake Langano.

3.4.7. Quaternary Sedimentary Units

These Late Pleistocene to Late Holocene a intricate sequence of lacustrine and fluvial deposits, and recent colluvial and fluvial deposits exposed at the foot of ridges (alluvial fans) and at paleo-river channels outcropped at the lake margin. These groups of rocks have limited exposure but where they occur, they can influence groundwater flow regimes and strongly determine the hydrochemistry

Various sedimentary rock units are formed in association to lake level fluctuations. These variations were largely enforced by climatic change and controlled by volcano– tectonic activities, subsequent in variation in the type and degree of depositional and erosional processes (Benvenuti et al., 2002; Le Turdu et al., 1999). The Lacustrine deposits of late Pleistocene (***Ql1***) and Early-Mid Holocene (***Qt2, Ql2,*** and ***Qs2***) sediments. The colluvial, fluvial, lacustrine and volcaniclastic deposits referred to the end of Pleistocene (***Qcg, Qu/Qu1, Qc***), and to the late Holocene (***Qt3, Qbs, Qs3, Qp*** and ***Qf, Qdm, Qd***) phases. These rocks significantly influence on the hydrochemistry of the basin as a result of the presence of diatomaceous and carbonaceous layers and some impermeable layers that could influence the hydrologic and hydrogeologic conditions.

3.4.7.1. Colluvial – Alluvial Deposits

These Middle Pleistocene (***Qcg***) and Middle Pleistocene to Holocene (***Qu/Qu1*** and ***Qc***) colluvial and alluvial gravel, sand, silt, reworked pyroclastic and agglomerate deposits are exposed in a few localities in the basin, mostly at the base of the western escarpment, along the bottom of long faulted ridges (horsts) mostly close to the western margin of the rift, and at the foot of major domes and caldera remnants. These colluvial - alluvial deposits (***Qcg*** and ***Qu/Qu1***) pre-date the Megalake phase lacustrine deposits (***Ql1***) or they represent the shrinking phase of the lakes (***Qc***). One major exposure of this unit is at the Gademotta caldera. The ***Qc*** is characterized by basal delta front sands with age of 39,000-year-old.

3.4.7.2. The Megalake Phase Lacustrine Deposit (Ql1)

This unit is characterized by lacustrine-fluvio-deltaic, and volcaniclastic sediments made up of a succession of clay, diatomite, sand, shell beds and reworked pumice, resting uncomfortably over Plio-Pleistocene volcanic rocks and older hill deposits (i.e., the colluvial-alluvial gravel, sand, silt and reworked pyroclastics, ***Qu*** and ***Qcg***) (Benvenuti et al., 2002; Laury & Albritton, 1975; Le Turdu et al., 1999). This unit is mostly and extensively exposed west and east of Lake Ziway forming a generally subdued, but faulted topography. This unit also outcrops on the east coast of Lake Ziway, and the eastern foot of the Gademotta ridge and the Bulbula River gorge.

3.4.7.3. The Macrolake Phase Lacustrine and Fluvial and Fluvio-deltaic Deposits

These Early to Middle Holocene (*Qt2* and *Ql2*) and Middle Holocene (*Qs2*) deposits represent the single macro lake "Ziway – Shala" during the Early Holocene wet phase where the lake levels reached nearly 120m above the present Ziway Lake Level (Benvenuti et al., 2002; Le Turdu et al., 1999). The older terraced deposits of the Ziway Lake (*Qt2*) represented by a succession of clay, reworked pumice and shell beds are extensively exposed immediately surrounding Lake Ziway, exposed at prominent lake terraces and strand lines. The Central Lacustrine Deposits (*Ql2*) composed of clay, marls, diatomite, sand, shell beds and reworked pyroclastic deposits, are prominently exposed at the eastern shore of Lake Ziway; along the Bulbula River defining the Bulbula plain, and in patches north of Lake Shala, and east and southeast of Lake Langano. In the Bulbula Plain the lacustrine deposits (*Ql2*) unconformably overlie *Ql1,* and are frequently open and containing deep lake diatomites and marls to sandy deposits, and bearing shell beds implying shallower lake margin settings. The Late Holocene shore sands and reworked pumice deposits (*Qs2*) are exclusively exposed on the nearly flat terrain north of Lakes Langano and Abijata lakeshores.

These units are found generally intercalated with colluvial and volcaniclastic sediments (*Qc*), fluvial (*Qf*) and fluvio-deltaic (*Qdm*) sediments, and intervening buried soils. The fluvial silt, sand and clay are locally terraced and are exposed in small patches in different parts of the basin, particularly northwest of Lake Shala. These deposits also mark old paleo-river channels at the eastern side of Lake Ziway and northern part of Lake Meki. The fluvio-deltaic deposits (*Qdm*) are exclusively formed north of Lake Ziway representing nearly 8km diameter silt and clay-filled delta formed by the prograding activity of the Meki River.

3.4.7.4. The Separated Lakes Lacustrine and Fluvio-Deltaic Deposits

These Late Holocene deposits were formed after the four lakes separated and nearly achieved their present form. These units are represented by clay, reworked pumice and shell beds of the younger terraced deposits of the Ziway Lake (*Qt3*) which is exposed surrounding the outline of the Lake Ziway shoreline; the shore sand and reworked pumice (*Qbs*) and the shore sand and reworked pumice with well-preserved strandlines (*Qs3*) which are exclusively exposed surrounding the Lakes Abijata, Shala and Langano; and the lacustrine clay, organic clay and peat (*Qp*) exposed under shallow water covered by reeds and organic accumulates surrounding the nearly flat shores of Lake Ziway, particularly at its western shore, and at some isolated swamps and wetlands, particularly in the structural grabens east of Lake Ziway. The lacustrine deposits in places are covered by patches of fluvio-deltaic sand, silt and clay (*Qd*), which currently are heavily exploited for construction purposes in many localities in the basin.

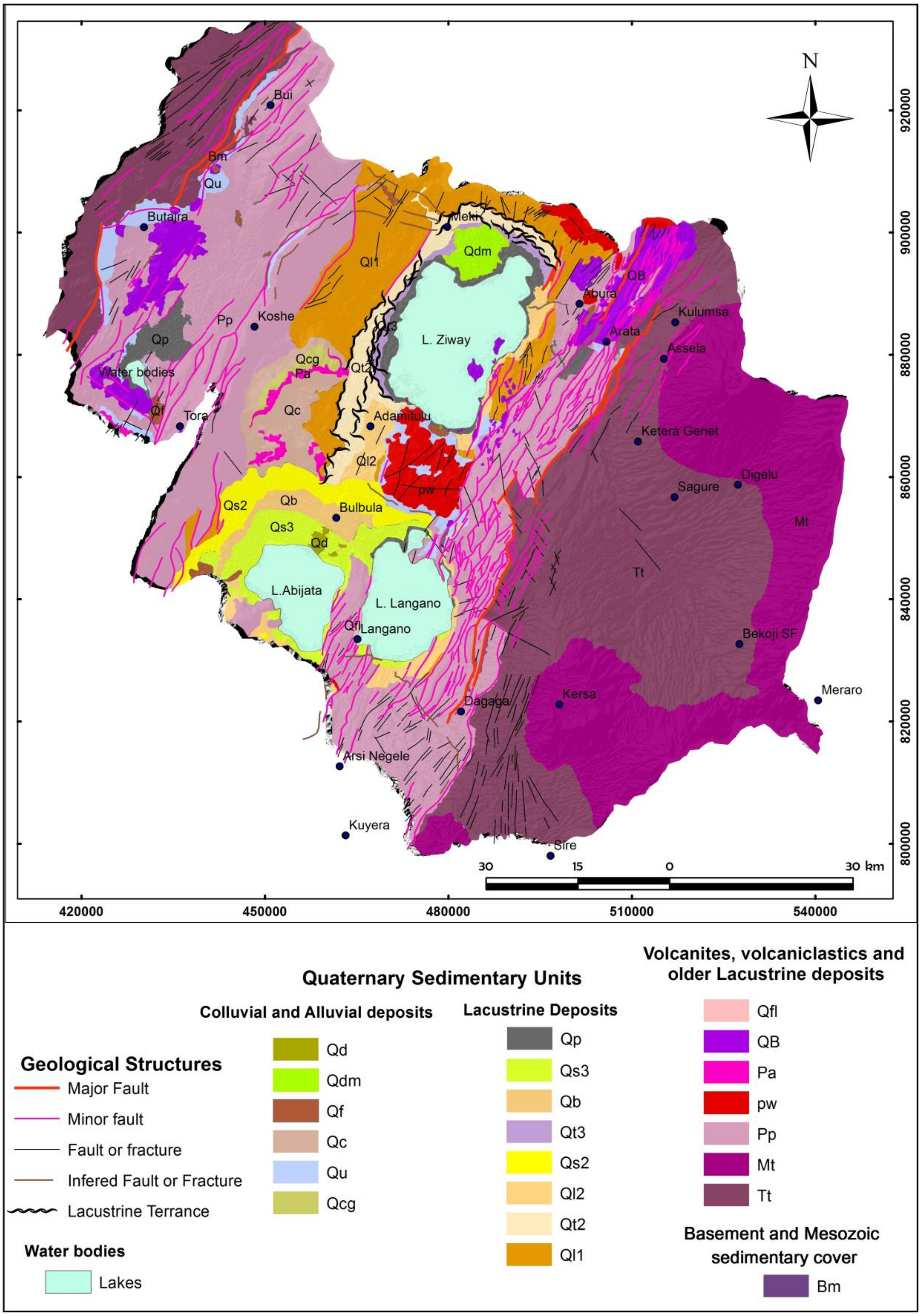

Fig. 3.2 Geological map the Ziway-Shalla Lakes Basin (Adapted from Dainelli et al., 2001 with 1:250,000 scale).

3.5. Litho-Stratigraphy

The litho-Stratigraphic setting of the Main Ethiopian Rift has been developed by various investigators (Dainelli et al., 2001; EWTEC, 2008; JICA, 2012) and shown in (Fig.3.3).

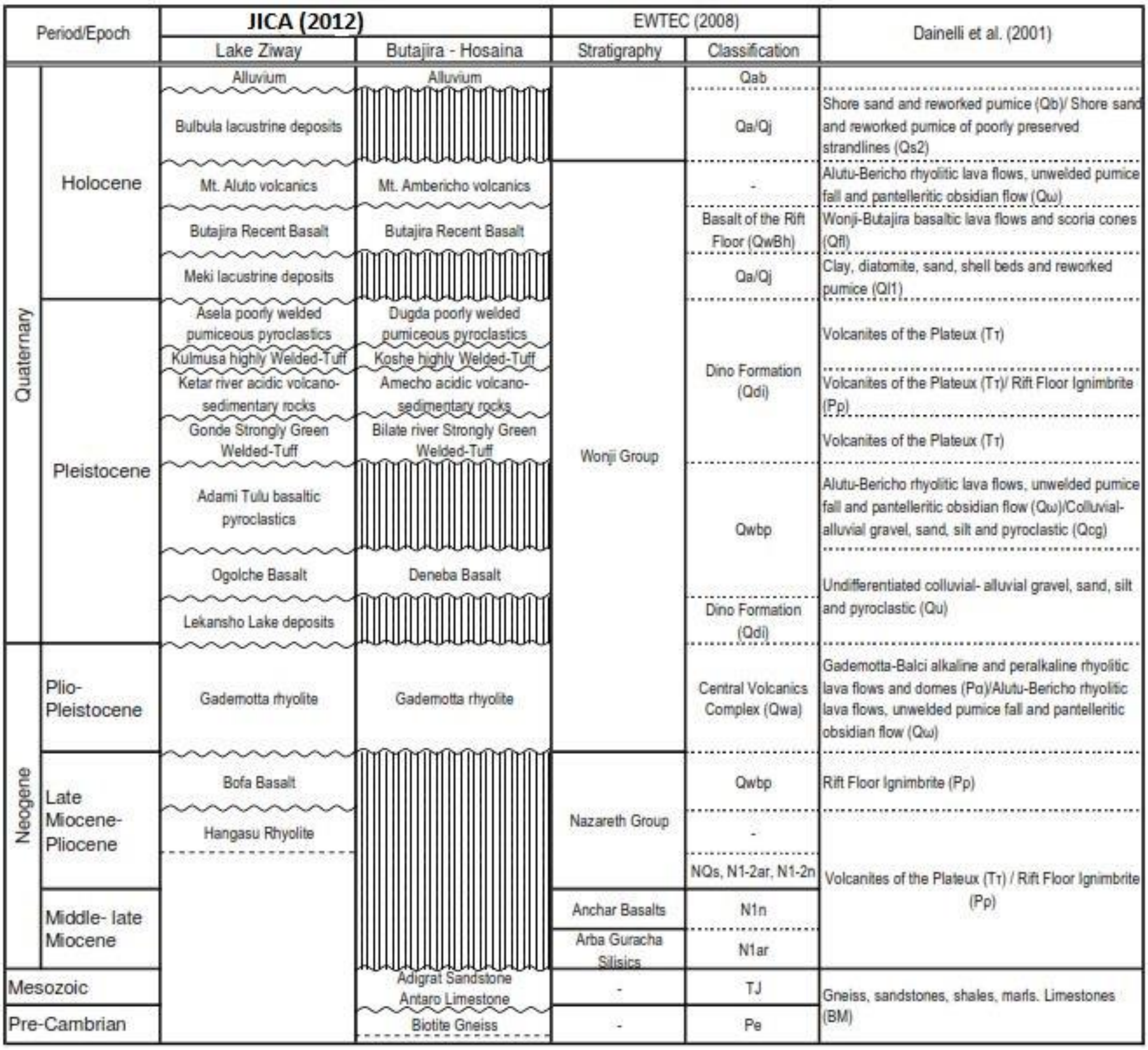

Fig.3.3 Litho-Stratigraphic setting of Main Ethiopian Rift Valley basin

3.6.Geomorphologic Setting

The Lakes Basin is a structurally controlled system with NNE-SSW running, generally active faults of the WFB bounding the eastern shore of the Ziway Lake. The geomorphology of the basin and its landscapes is largely influenced by volcano-tectonic activities, with some surface processes. The major tectonic features are the WFB and SDZFZ: The WFB is an 8km wide belt of NNE oriented normal fault that lies at the east of Lake Ziway and extends along the whole section of the MER (Le Turdu et al., 1999) and the SDZFZ, at the western part of rift, that has paramount importance influence on the landscape and hydrological and hydrogeological processes.

The most important geomorphologic feature is the formation of the Oligocene to Pliocene volcanic plateaus to the east and west of the rift margin form generally flat but elevated highland plateaus spotted by prominent shield volcanoes, particularly in the eastern plateau, where headwaters of the Ketar River are located (OWWDSE, 2016).

The WFB form the graben and horst forming eastern margin of Lake Ziway, as well as the western margin of the basin at the SDZFZ, where the headwaters of the Meki River start (OWWDSE, 2016). In addition to that landform associated to basaltic lava flow and scoria cones (e.g the group islands of Tulu Gudo of Ziway lake) and the Late Pliocene to Late Pleistocene acidic volcanic centers of Alutu and Gademotta form prominent topographic hills in the southern and southwestern shores of the Ziway Lake over the flat terrain underlain by the lacustrine sediments (Fig. 3.4).

Since Middle Pliestocene, fluvio-lacustrine depressions were formed along with the WFB, under volcano-tectonic control (Le Turdu et al., 1999) at the foot of some prominent ridges, Ketar and Meki Rivers and also the flat-lying wide plain to the immediate west of Lake Ziway.

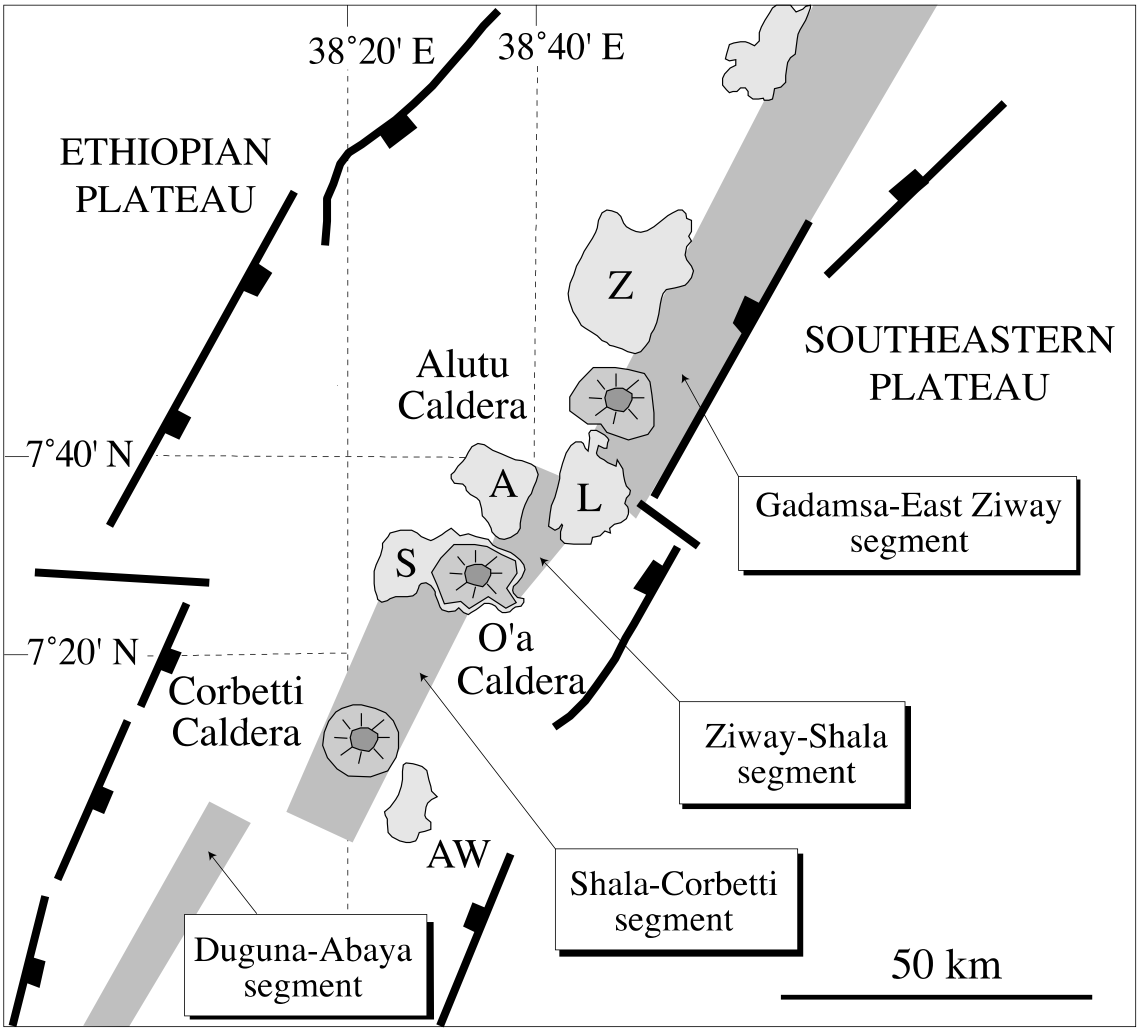

Fig. 3.4 The Wonji Fault Belt showing the NNE-trending segments within the ALZLB system (Modified and cited in (Le Turdu et al., 1999))

3.7. Hydrogeology

From the hydrogeological perspective, geological formations are generally grouped into three hydrogeological units as aquifer, aquitard, and aquiclude based on transmission and storage properties (Sen, 2015). Furthermore, the aquifer is defined as (Freeze & Cherry, 1979) “an aquifer is saturated geologic formation that is adequately porous to yield water in substantial amounts to a well or spring, whereas a limiting unit has low porousness that limits the movement of groundwater and restrictions the usefulness of the unit as a source of water supply”.

In Ethiopia, there are four major aquifer forming categories of rocks that hold groundwater at different capacities (Kebede, 2013). These are (1) volcanic aquifers: groundwater formed in fractures and joints and is mostly found in central Ethiopia and they cover 2/3 of Ethiopian landmass (2) Alluvial lacustrine sediments and volcaniclastic aquifers: abundantly found in the basin and occupying inter-mountain-grabens, local depressions, river valleys and lake margins. Groundwater occurs in the primary porosity and is mostly known for the shallow water table. (3) Sedimentary aquifers: groundwater occurs in opening spaces, cracks or cavities. They are found in Blue Nile gorge, Mekele outlier in Tigray, and in the southeastern plateaus reaching Ogaden. (4) Metamorphic aquifers are characterized by the limited potential for groundwater, because of their low storage and transmission properties, and largely found at the peripheral lowlands.

Likewise, in the ALZLB, the lithological units have a significant influence on the hydrologic and hydrogeologic regimes. Though, there is a complex groundwater circulation in the lithological units that were widely affected by geological structures. In such a complex terrain, groundwater flow may not only directly flow from the high to the low potential area, rather flow in through fractures and conduits and then form a localized of the groundwater flow system. The dominant and vast aquifer-forming groups of rocks are volcanics and volcanoclastic and Quaternary sedimentary units. These volcanics and volcanoclastic rocks comprise rocks of alkali trachytes, rhyolites, ignimbrite, tuffs and basalts are found at the eastern and western escarpment and plateau of the basin. These groups rocks cover the dominant portion of the basin and were affected by rift faulting. They are intensively fractured and jointed and these structural features facilitate fast infiltration into the groundwater system.

Quaternary sedimentary units occur in the central (lakes region) and low-lying part of the basin and it is the second largest unit in surface area coverage. They comprise rocks such alluvial, fluvial and colluvial deposits. Rocks of these units, in places where, have secondary porosity and have an enormous capacity to store and transmit the groundwater. In contrast to these, they may have an impermeable layer that affects the region's hydrologic and hydrogeologic characteristics in some places.

Similarly, the study basin, based on the lithologic units described in section 3.2(geology of the basin) and borehole data records, five main hydrogeologic units or permeability zones were identified (Ayenew, 1998). These are: high to very high permeability zone; medium to high permeability zone; medium permeability zone; low to medium permeability zone and very low permeability zone and their lithologic composition, and properties have been given below with spatial distribution and areal extents are shown in (Fig. 3.5).

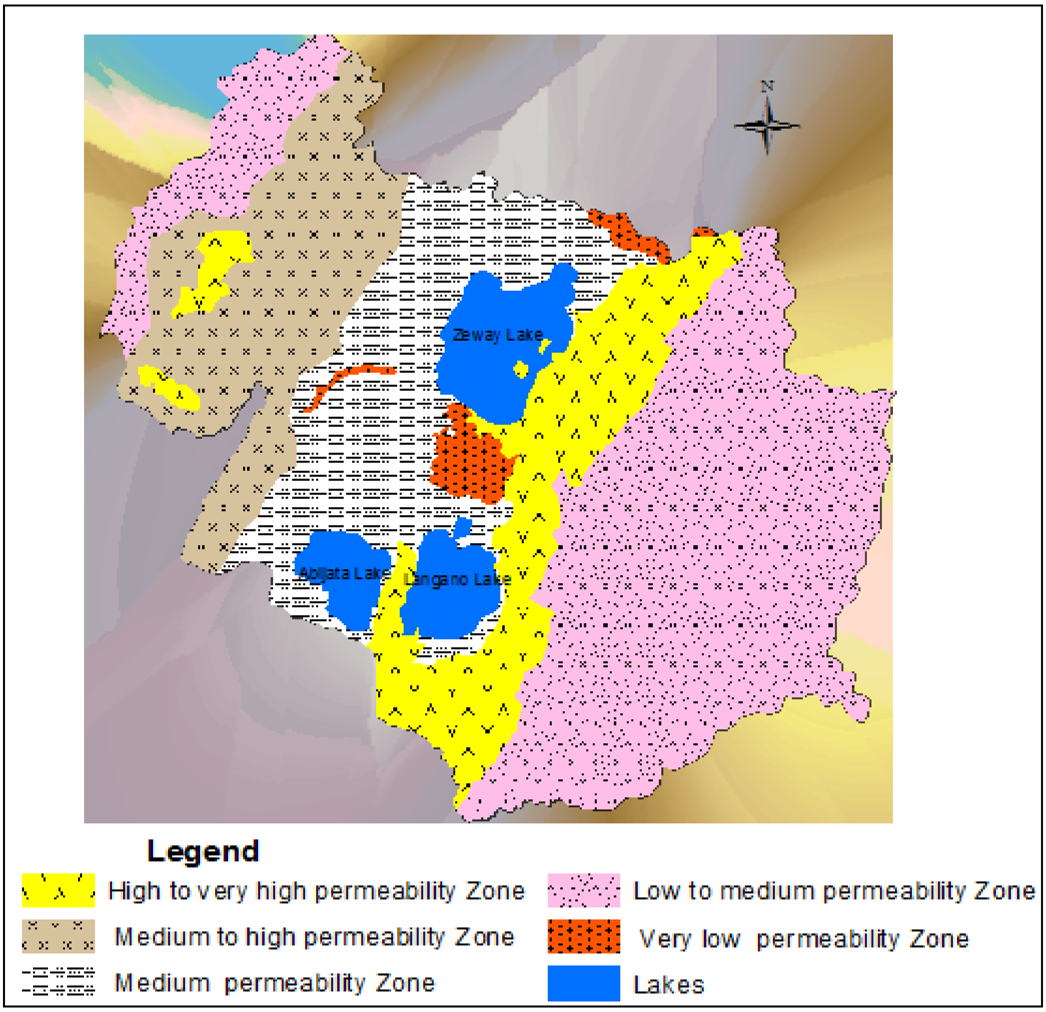

Fig. 3.5 Simplified permeability map adapted from (Ayenew, 1998)

High to very high permeability zone

This zone is composed of Early to Middle Pliocene pyroclastic materials: poorly welded rhyolitic ignimbrite, pumice fall, unwelded pumiceous and fresh basalts, and highly fractured ignimbrites in the eastern faulted escarpment; and scoria cones along the major fault east of Butajira. Permeability of these rocks are principally associated to joints, faults, vesicles and fragment size of scoria. It is an unconfined aquifer and its permeability value is estimated ranging from 10-20m/day. The thickness of this unit is not exactly known yet; the existing borehole records show that the unit has a thickness of more than

210m. However, (OWWDSE, 2016) estimates its thickness to be 500m from borehole records.

Medium to high permeability zone

This zone is also mainly composed of loosely welded ignimbrites interbedding with pumice fragments, slightly fractured basalts, alluvial and colluvial deposits occurred at the foot of volcanic mountains. The units have medium to high permeability owing to property of ignimbrite and extent of fracturing and weathering. It is the unconfined aquifer with estimated permeability values ranging from 5-10m/day that located at the western part of the basin. Its thickness is estimated to be more than 3000m.

Medium permeability zone

This zone covers a large portion of the rift floor (lakes region). This zone is constituted of ignimbrites overlain by lacustrine sediments: clay, diatomite, shale beds and reworked pumice. In addition to these, rhyolite, pumice, tuff and ignimbrite with low secondary permeability (1-5m/day); and is overlain dominantly by silty soil, black-cotton soils and sporadically lacustrine sediment. It is unconfined aquifer with the average thickness of this unit is estimated to 250m.

Low to medium permeability zone

The main group rocks constitute this zone are Oligocene to Early Pliocene volcanites: very welded ignimbrites, tuff, basalt, rhyolite-trachyte flow without large faults. The top weathered rocks and soils are permeable; nevertheless, the underlying volcanic sequences are massive with low to medium permeability values (0.1-1m/day). It is the most extensive zone covering a large part of the eastern highland mountainous regions of Chilallo, Kaka, Galama and western plateaus of Guraghe Mountain. It is unconfined aquifer and the average thickness of unit is estimated to be 350m from drilled bore data records. However, there was no bore drilled that fully penetrate to impermeable aquifer boundary.

Very low permeability zone

The unit consists of acidic-volcanic that forms plugs and caldera rims dominated by alkaline-peralkaline-rhyolitic-lava flow and domes with pyroclastic rocks: pumice, tuff and ash with subordinate obsidian lava flows. It is unconfined aquifer with very low permeability (0.01-0.1m/day). This zone covers the smallest portion mainly occupy the rift floor in addition to, along basin boundaries serving as hydrogeological divides.

3.7.1. Groundwater dynamics

The groundwater flow direction is evaluated by generating contour lines from available data. Generally, groundwater flows from both from the Arsi and Guraghe highland plateaus towards the rift floor the lakes region following the topography of the basin. Then after, reaching Lake Ziway, it turns towards the South direction to Lake Shalla (Fig. 3.6). The groundwater level is general flat in the rift floor. However, the groundwater flows from Lake Ziway to south direction (Lake Abijata and Lake Langano) in the rift floor (EWTC, 2008). This indicates that the highland plateaus and the escarpments can be considered as a potential recharge zone. On the other hand, the rift floor is a groundwater discharge zone, since groundwater flows from the recharge area to the discharge region.

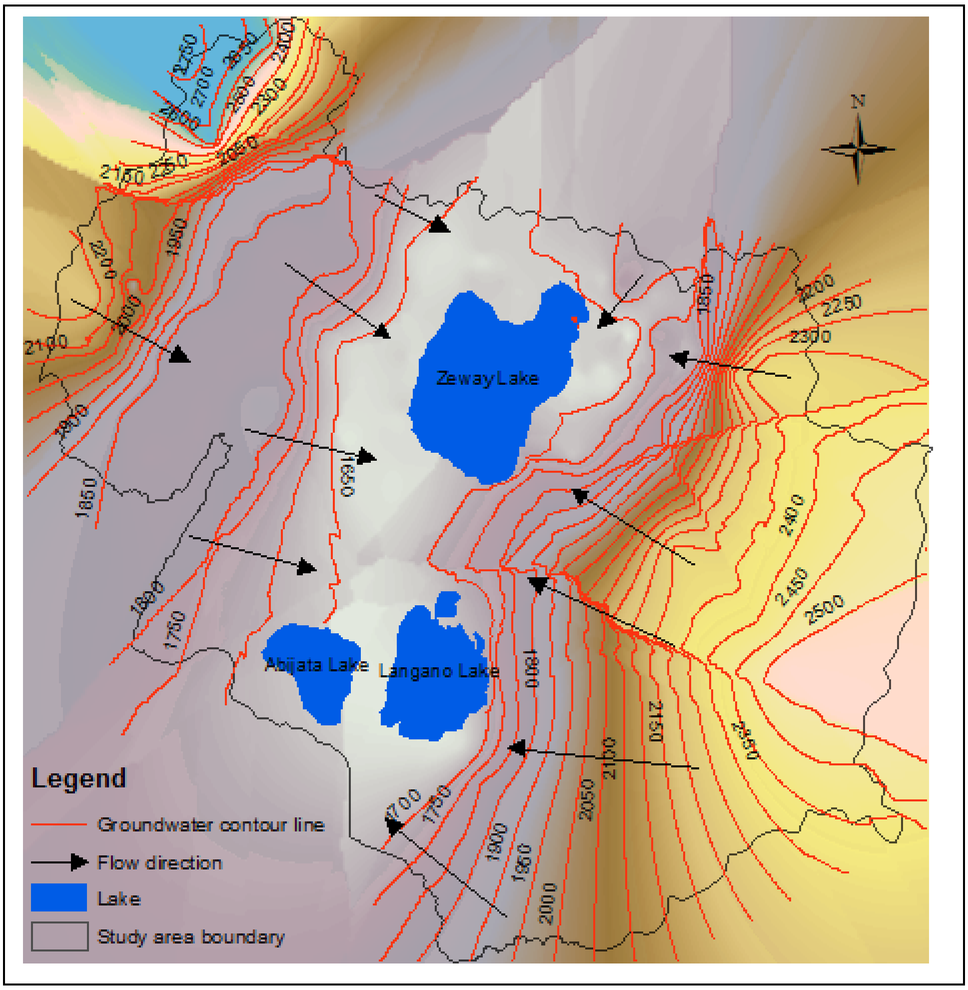

Fig. 3.6 Groundwater contour line map

3.7.2. Groundwater Recharge and Recharge mechanism

Groundwater recharge is processes of downward movement of water to the saturated zone with influence of gravity or guided by hydraulic conditions (Balek, Simmers, 1987). It is the most imperative part of water budget component. Understanding and quantifying rate are the fundamentals for any water resource study, although being it is most tough to quantify (Kresic, 2009; Wheater, Mathias, & Li., 2010) as it cannot be measured directly (Bakker & Bartholomeus, 2013).

Because it commonly takes place over large areas with varying conditions that affect the rates of recharge. These factors are climate; land use and land cover; porosity and permeability of soil cover; geologic and geomorphic properties and heads of groundwater (Kresic, 2009).

This groundwater recharge may take place in different recharge mechanisms. Regarding recharge mechanisms in the rift valley basin, previous studies by (Kebede, 2013) has identified the major recharge mechanisms in Ethiopia and this study showed that more than ¾ of aquifers in Ethiopia receive localized and indirect recharges. Accordingly, the main recharge mechanisms identified in this study basin are (a) fast selective recharge from heavy rain, (b) mountain block and mountain front recharges, (c) indirect recharge arise associated to flood water, and (d) direct diffuse recharge at small areas.

The increase in rainfall will enhance the groundwater recharge rate for the above-mentioned recharge mechanisms except (d) the direct diffuse recharge areas. The direct diffuse recharge occurs where there is a dense soil layer in humid and semi-humid areas, high rainfall exceeds the soil water retention capacity thus reducing recharge levels (Bates et al,.2008). On the contrary, in the semi-arid and arid region (e.g., Ethiopian Rift Valley) the expected rise in precipitation will increase groundwater recharge due to high-intensity rainfall would penetrate quickly adequate prior to evaporating to atmosphere. However, the central part of the basin get primarily recharge by inundation of flooding because alluvial aquifers are occupied the rift valley (Kebede, 2013).

Large areas of escarpment and adjacent mountain obtain recharge from mountain block and mountain front recharge (Fig. 3.7). The groundwater connected to mountain block and mountain front recharges indicate less susceptibility to seasonal climatic shocks. Similarly, isotopic evidence over the plateaus of Ethiopia suggests that the dominant recharge takes place via fractures from heavy rainfall rather than recharging from excess soil moisture (Kebede et al,.2005; Kebede et al., 2007).

In the ALZLB, the direct recharge is supposed to occur large areas with exception to where low permeable lacustrine soils exist (diatomite) in the rift floor, around Lake Ziway (OWWDSE, 2016). Numerous studies have been conducted in the study basin to estimate the rate of recharge by using different methods. According to Ayenew(2003) the mean annual recharge estimated using catchment soil-water balance mode with 50mm soil moisture-holding capacity is about 10% and 13% of precipitation for Ketar and Meki subbasins respectively. In another study by (EWTC, 2008) the mean annual recharge estimated using the chloride mass balance method at Butajira (Meki subbasin) and Ziway area were about 10% and 0.068% of the precipitation respectively).

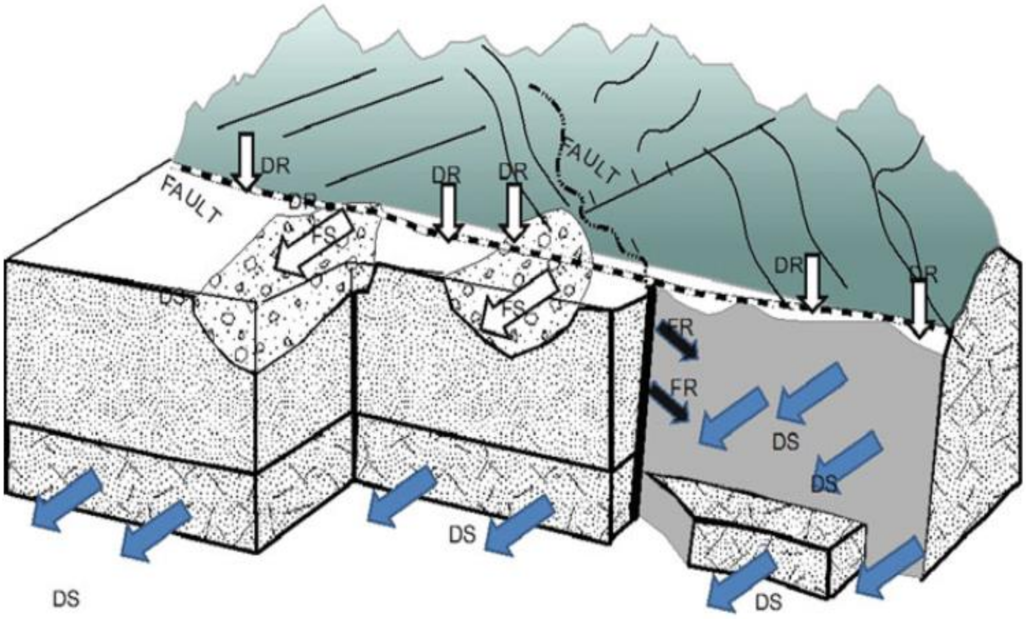

Fig. 3.7 The diagram illustrated various recharge mechanism: diffuse mountain block recharge (DS), direct recharge from surface (DR), focused recharge from surface (FS), focused recharge from mountains (FR) (adapted from Kebede, 2013)

3.7.3. Groundwater discharge

Groundwater discharge can be described as the withdrawal of water from the saturated zone of aquifer across the water table along with the related flows towards the water table within the saturated zone (Freeze & Cherry, 1979). The discharge of groundwater may be exhibited as rivers, springs, swamps, wetlands and seepages and developed wells for multi-purpose uses. In the rift valley basin, the low-lying lakes regions are considered as the main discharge zone, in addition to springs originating from high lands (Ketar, Meki, Bulbula, Horakelo, Gedemso and Lepsi Rivers) that drain into the lakes and wetlands. Likewise, groundwater withdrawal for different purposes is also considered as groundwater discharge (the detailed presented in section 2.5).

4. Hydrological Modeling Using WEAP

4.1. Introduction

An appropriate understanding of the basin hydrological processes is a basic to estimate the basin dynamics of hydrologic system in spatio-temporal dimensions. Natural and human-induced factors may alter the hydrologic system of the basin. Since the earth's hydrological system encompasses the physical hydrological processes as rainfall, evapotranspiration (ET), surface runoff, interflow, deep percolation or discharge, and groundwater flow and their interactions in the atmosphere, land surface, and sub-surface that controls water dynamics, distribution, and transformation from one system to the other (Delfs et al,. 2013; and Niu et al., 2014).

These could be largely influenced by meteorological parameters, land surface properties, and soil parameters. To estimate hydrologic parameters, models are widely used. Hydrological models are simplified mathematical representation of the actual world system that is executed to enhance the realizing, and prediction of hydrologic processes (Pacheco, 2015; Santos et al., 2014). In the recent decade, hydrologic models play a very crucial role in properly characterizing subbasin properties by predicting target parameters based on input data. They provide a chance to estimate some input parameters that are difficult to measure in the field because of their inherent nature (which may vary in a spatio-temporal scale) (Wheater et al., 2010). Moreover, well-developed, calibrated, and validated models can be used for various impact evaluation of change in some of the input variables (e.g., land-use change, climate change, and development activities are a few among others), and are suitable for setting scenarios and analysis.

Generally, the physical-based models and artificial intelligence (AI) models are intensively used to estimate time series hydrologic parameters (Mohammadi et al., 2020). Recently, the applications of artificial intelligence models have been widely and effectively used to predict hydrologic and meteorological parameters (Mohammadi et al., 2020; Mohammadi et al., 2020; Mohammadi et al., 2020). The artificial intelligence models can estimate required parameters based on a series of input predictors without understanding the physical processes (Mohammadi et al., 2020). In contrast to the artificial intelligence model, the physically-based models are used to simulate time series hydrologic parameters through modeling the potential interactions among various factors (Fang et al., 2019; Wang et al., 2016). These groups of models have been widely practiced across the world, for instance: SWAT (Arnold et al., 1998) and the WEAP (SEI, 2007) are a few among others.

In recent years, the study basin (in Ethiopia) is also facing a challenge in satisfying demands owing fast growing demands for irrigation, domestic and ecosystem services. Consequently, accelerate struggles to access to water in the basin. In addition to this, the

Therefore, a model-based assessment is required to understand the basin's hydrologic components; and to predict future hydrologic dynamics, and evaluate the impact of various development and management strategies on water resources (Dougherty et al., 2007; Lerner, 2002; Scanlon et al., 2007). In recent years, model-based scenario analysis is widely implemented to explore different alternatives.

Water resources modeling is a requirement to, and an essential portion of, scenario analysis in water governance and various generic software platforms can be applied based on the purpose they intended to serve (Ahmadi et al., 2018). In Ethiopia, numerous hydrological investigations have been carried out using physically-based models (Desta & Lemma, 2017; Legesse et al., 2003; Zeray et al., 2007).

It is well known that basin hydrologic processes can be altered by changing land development and climate conditions. For instance, the hydrological response of the Main Ethiopia Rift valley basin to Landuse and climate change on streamflow, as well as lakes level fluctuation was studied with a physically-based, distributed Precipitation Runoff Modeling System (PRMS) model (Legesse et al., 2010; Legesse et al.,2003; Legesse et al., 2004). They have investigated the basin's hydrologic processes (Evapotranspiration, surface runoff, interflow, baseflow components and evaporation of lakes). A Soil Water Assessment Tool (SWAT) model was used by (Zerayet al., 2007) to assess the impact of climate change on Ziway lake water level. The same model was developed to assess the hydrologic processes and distributed water balance of the Ketar subbasin (Desta & Lemma, 2017).

However, integrated hydrological and water resource models have been not done to date. In this effect, Water Evaluation and Planning (WEAP) model was selected to be implemented in the ALZLB. The WEAP modeling software, developed by the Stockholm Environment Institute, was used as a basis for building the hydrology component. It is water resources modeling system that comprises choices to simulate both the natural and anthropogenic hydrological processes and the adaption strategies implemented to the water system (Yates et al., 2005). WEAP has earlier been effectively used to simulate climate, land use, and population growth in agricultural and urban catchments in a variety of locations worldwide (Höllermann et al., 2010; Joyce et al., 2006; Mehta et al., 2013; Purkey et al., 2008).

Therefore, this study aimed to evaluate the applicability of the WEAP model in the ALZLB subbasin and simulate hydrological parameters of the subbasin using the WEAP model

4.2. Hydrologic Model Development

The WEAP hydrologic model was applied to evaluate the hydrologic behavior at the subbasin or land-use level. It is a lumped continuous model that is based on Rainfall-Runoff Method (Soil Moisture Method). This takes into account a one-dimensional, 2-layers (or "bucket") soil moisture dynamic recording system that uses empirical functions to partition water into ET, surface runoff, sub-surface runoff (i.e., interflow), and deep percolation for a subbasin unit at the root zone Equation(4.1) and shown in (Fig. 4.1) (SEI), 2007). One of the most important input data is the climate data set as precipitation, temperature, relative humidity, and wind speed. Each subbasin has a unique climate data set that is uniformly distributed across the subbasins.

The soil moisture method permits the description of various land use classes climate, and soil properties in estimation hydrological processes. The subbasin is fractionally divided into a sole set of independent land use/land cover classes (j) which sums up 100% of the subbasin's area. To reflect the lumped hydrologic response, LULC values from each fractional area within the subbasin are then added, with the over land flow, interflow, and baseflow being connected to a river node and ET being lost from the system. For each fractional area, j of N, a water balance is computed. When proper linking is made among the subbasin unit node and a groundwater node, the deep infiltration within the subbasin unit can be conveyed to a surface water body as baseflow or subsequently tied to groundwater storage, and finally, the water balance empirical equation was computed as follow (SEI, 2007).

$$Rd_j \frac{dz_{1,j}}{dt} = P_e(t) - ET_0(t)K_{c,j}(t)\left(\frac{5Z_{1,j} - 2Z_{1,j}^2}{3}\right) - P_e(t)Z_{1,j}^{RRF_j} - f_j k_{s,j} Z_{1,j}^2 - \left(1 - f_j\right)K_{s,j}Z_{1,j}^2 \qquad (4.1)$$

Where, $Z_{1,j}\ \epsilon[0,1]$ is Relative soil water storage, a fraction of the total effective water storage in the root zone layer land use j [dimensionless], j is Landuse and land cover unit (e.g. cultivated land, forest land, shrub, etc.) and each subbasin has N fraction of land use and land cover units, Rd_j is soil water holding capacity of land use j [mm], P_e is effective precipitation [mm], $ET_O(t)$ is reference evapotranspiration [mm/day], $K_{c,j}$ is crop coefficient landuse j; RRF_j is runoff resistance factor of landuse and land cover j, $P_e(t)Z_{1,j}^{RRF_j}$ is the surface runoff, $f_j k_{z,j} Z_{1,j}^2$ is interflow from the first layer land use j, f_j is segregating coefficient related to the land cover type, soil, and topography for the area j, that divides flow into horizontal f_j and vertical ($1-f_j$) flows, and $K_{s,j}$ is saturated hydraulic conductivity of the root zone layer of land use j [mm/time].

In Equation (1) the second term represents the reference ET; it is estimated using the Penman-Monteith equation modified for a standardized crop of grass, 0.12 m in height and with a surface resistance of 69 s/m. Continuing with Equation (4.1), the $k_{c,j}$ is the crop/plant coefficient for each fractional land cover. The third term represents surface runoff, where RRF_j is the Runoff Resistance Factor of the land cover. Larger values of RRF_j cause to less surface runoff. The fourth and fifth terms are the interflow and deep percolation terms, respectively, where the parameter ks,j is an estimate of the root zone saturated conductivity (mm/time) and fj is a partitioning coefficient related to soil, land cover type, and topography that fractionally separates water both horizontally and vertically.

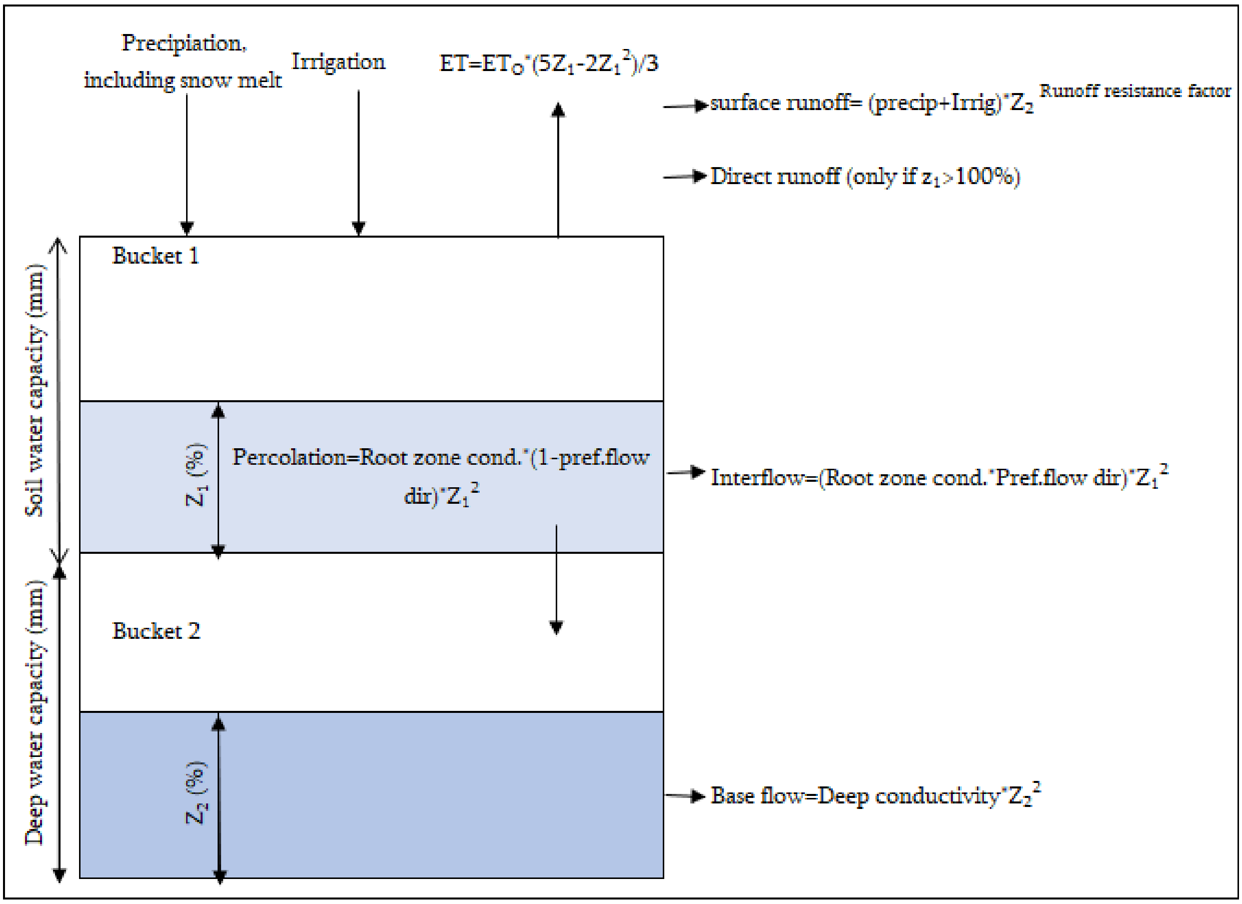

Fig. 4.1 Conceptual diagram and equations incorporated in the Soil moisture Model after (Seiber & Purkey, 2015)

Thus, total surface runoff (RT) and interflow, from each sub-catchment at time t is given as Equation (4.2).

$$RT(t) = \sum_{j=1}^{N} A_j \, P_e(t) Z_{1,j}^{RRF_j} \tag{4.2}$$

The total interflow (IF), for each sub-catchment at time t, is given as Equation (4.3).

$$\text{IF}(t) = \sum_{j=1}^{N} A_j \, f_j k_{s,j} Z_{1,j}^2 \tag{4.3}$$

When an alluvial aquifer is replaced into the model and a runoff/infiltration connection is made between the subbasin node and the groundwater node and groundwater recharge (R) (volume/time) to the aquifer is computed as follow:

$$R = \sum_{j=1}^{N} A_j \left(1 - f_j\right) K_{s,j} Z_{1,j}^2 \tag{4.4}$$

For applications where no return flow link is created from a catchment to a groundwater node base flow emanating from the second bucket will be computed as

$$S_{max} \frac{dz_2}{dt} = \left(\sum_{j=1}^{N} \left(1 - f_j\right) K_{s,j} Z_{1,j}^2 \right) - K_{s,2} Z_{2,j}^2 \tag{4.5}$$

Where the inflow to this storage, S_{max} is the deep percolation from the upper storage given in Equation (1) and $K_{s,2}$ is the saturated conductivity of the lower storage (mm/time), which is given as a single value for the subbasin, and therefore, does not include a subscript, *j*.

Actual Evapotranspiration (ET) is also computed using reference ET, crop coefficient (K_c), and soil water level in the modeling unit root zone is given by Equation (4.6).

$$ET = ET_0 * K_c \left(5Z_1 - 2{Z_1}^2\right)/3 \tag{4.6}$$

ETo is normally recognized to be the volume of water from a land surface that would be lost to the atmosphere where water is satisfactory to meet the demand for atmospheric evaporation from the reference surface. ETo estimation uses standard climatological records of solar radiation (sunshine), air temperature, humidity, and wind speed above an extensive surface of green grass, shading the ground and not short of water (Allen, Pereira, Raes, & Smith, 1998). The Penman-Monteith method to estimate ETo is expressed as:

$$ET_0 = \frac{0.408\Delta(R_n - G) + \gamma \frac{900}{T + 273} u_2(e_s - e_a)}{\Delta + \gamma(1 + 0.34u_2)} \quad (4.7)$$

Where, ET_0 is reference evapotranspiration (mm/day), R_n *is* net radiation at the crop surface (MJ/m^{2}day), G is soil heat flux density (MJ/m^{2}day), T is mean daily air temperature at 2 m height (^{o}C), u_2 is wind speed at 2 m height (m/s), e_s is saturation vapor pressure (KPa), e_a is actual vapor pressure (KPa), $e_s - e_a$ is saturation vapor pressure deficit (KPa), Δ is slope vapour pressure curve (Kpa /^{o}C), and γ *is* Psychrometric constant (Kpa/^{o}C).

4.2.1. WEAP Model Calibration and Validation

Model calibration (parameter estimation) is primarily aimed at obtaining a set of parameters applicable to the subbasin to reasonably represent the hydrology of the Ketar and Meki River at Abura and Meki towns gauging stations respectively. It comprises the automatic (Doherty, 2010) and/or manual tuning of model parameters to lessen the variation among observed and simulated data by tuning the model parameter values (Ingol-Blanco & McKinney, 2013). In this study, the manual approach (trial-and-error) was used to fit, as closely as possible, the simulated and measured streamflow data. It also accounts for abstractions/diversion of water for different uses. The WEAP embedded soil moisture method involves seven soil and land use-related parameters (Ingol-Blanco & McKinney, 2013; Sieber & Purkey, 2015) that can be used to re-calibrate the hydrologic model. These are crop coefficient (Kc), soil water capacity (Sw), deep water capacity (Dw), runoff resistance factor (RRF), the conductivity of root zone (Ks), conductivity of deep zone (Kd), preferred flow direction (f) and initial storage fraction at the beginning of simulation of upper soil layer (Z_1) and initial storage fraction at the beginning of simulation of lower soil layer (Z_2).

On the other hand, the main importance implementing of hydrologic models is to model subbasin hydrologic conditions. In this effect, the model validation process is essential to assess the validity of a model to simulate the hydrologic behavior of the subbasin for circumstances unalike to that applied throughout the calibration period (Legesse et al., 2003).

4.2.2. WEAP Model Performance Evaluation measures

The performance efficiency of the model was calculated through analysis using various methods: (1) joint plots of the monthly and mean monthly simulated and observed hydrographs, (2) Commonly used a statistical method to measure the goodness-of-fit of a model are: the Coefficient of determination (R^2); Nash-Sutcliffe coefficient of efficiency (NSE); Index of Agreement (IA); Root mean square error (RMSE) and RSR (Barbaro & Zarriello, 2006; Ingol-Blanco & McKinney, 2013; Mccabe & Legates, 1999) for measured and simulated streamflow over the calibration and validation periods.

Coefficient of Determination (R^2)

It was given by (Krause et al.,2005)(Krause and Boyle 2005) as shown in Eqn. 4.8

$$R^2 = \frac{(\sum[X_i - \bar{X}][Y_i - \bar{Y}])^2}{\sum(X_i - \bar{X})^2 \sum(Y_i - \bar{Y})^2} \quad (4.8)$$

Where X_i is measured monthly values, $\bar{X}$ is measured average value Y_i is simulated monthly values, and $\bar{Y}$ is aveage simulated value at time/place, i.

Nash-Sutcliffe coefficient (NSE)

It was given by (Nash & Sutcliff, 1970) as shown in Eqn. 4.9

$$NSE = 1 - \frac{\sum_{i=1}^{n}(X_i - Y_i)^2}{\sum_{i=1}^{n}(X_i - \bar{X})^2} \quad (4.9)$$

Where X_i is measured monthly values, $\bar{X}$ is measured average value Y_i is simulated monthly values, and $\bar{Y}$ is aveage simulated value at time /place, i.

Index of agreement (IA)

It was established by (Willmott, 1981) to offset the susceptible of NSE and R^2 to changes in measured and simulated means and variances. It is also a broadly used pointer of goodness-of-fit of hydrological models (Harmel & Smith, 2007) and is defined by Eqn 4.10.

$$IA = 1 - \frac{\sum_{i=1}^{n}(X_i - Y_i)^2}{\sum_{i=1}^{n}(|Y_i - \bar{X}| - |X_i - \bar{X}|)^2} \quad (4.10)$$

Where X_i is measured monthly values, $\bar{X}$ is measured average value Y_i is simulated monthly values at time/ place, i.

Root Mean Square Error (RMSE)

It was given by (Singh et al., 2005) as shown in eqn.4. 12

$$\mathrm{RMSE} = \sqrt{\frac{\sum_{i=1}^{n}(X_i - Y_i)^2}{n}} \qquad (4.12)$$

Where, X_i is measured monthly values, Y_i is simulated monthly values at time /place, i, and n is number of observations.

RMSE-observations standard deviation ratio (RSR)

RSR standardizes RMSE applying the observations standard deviation, and it combines both an error index and the additional information developed by (Singh et al.,2005). RSR is computed as the fraction of the RMSE and standard deviation of measured data, as shown in eqn. 4.11.

$$\mathrm{RSR} = \frac{\sqrt{\sum_{i=1}^{n}(X_i - Y_i)^2}}{\sqrt{\sum_{i=1}^{n}(X_i - \overline{Y})^2}} = \frac{\mathrm{RMSE}}{\mathrm{STDEV}_{X_i}} \qquad (4.11)$$

Where X_i is measured monthly values, Y_i is simulated monthly values, and $\overline{Y}$ is aveage simulated value at time / place, i.

4.2.3. WEAP Model Input data

To simulate the subbasin monthly hydrological processes with the WEAP hydrological model, meteorological data including Monthly precipitation, temperature, wind speed and relative humidity are required in addition to landuse, and soil layer depth and geographic latitude data. Monthly precipitation data for Fifteen years (1991–2005) were collected from meteorological stations and used both model calibration and validation periods (the detailed stations are described in chapter-2). To estimate average areal precipitation (depth) across the subbasin, the Theisen polygon method was used. Whereas, the average monthly temperature, relative humidity, and wind velocity data were obtained for the years 1991–2005 from National Meteorological Agency (NMA) and used as input.

In addition to climate data, the Landuse and land cover (LULC) have also a significant role in determining the hydrologic processes of the subbasins. The landuse and land cover data was developed and the LULC types and their percentage is described in chapter 2. The daily discharge data were obtained from the MOWIE for the Ketar and Meki rivers at Abura and Meki town for the period of (1991–2005) respectively and later summed to monthly time steps and pictorially presented with precipitation in Fig. 4.2 and Fig. 4.3. Of which, the monthly data from (1991 to 2000) and (2001 to 2005) were used for calibration and validation respectively. The missing data were filled by the linear interpolation method. Another important data input is the soil layer depth and hence the soil depth considered is 500mm and 250mm for the top and bottom layers respectively.

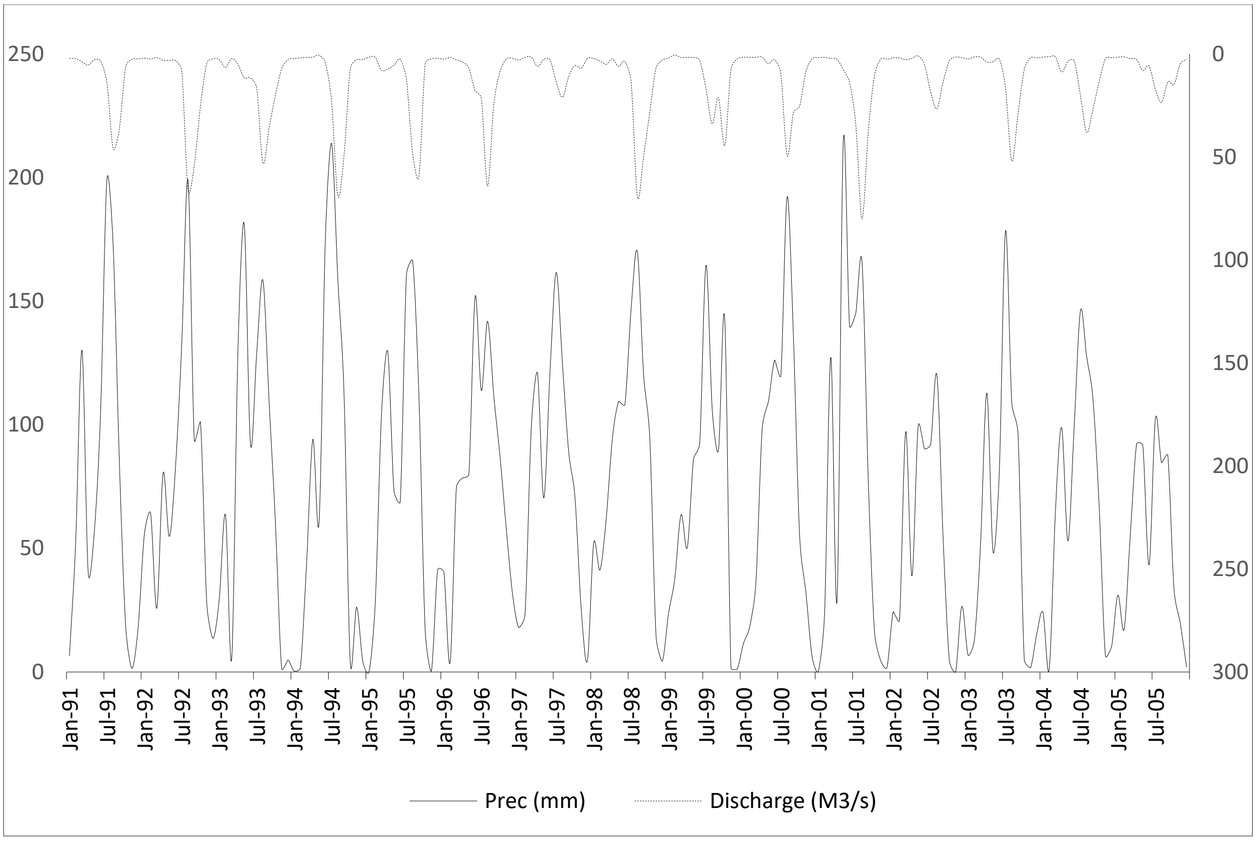

Fig. 4.2 Monthly precipitation and Ketar River discharge at Abura gauging station

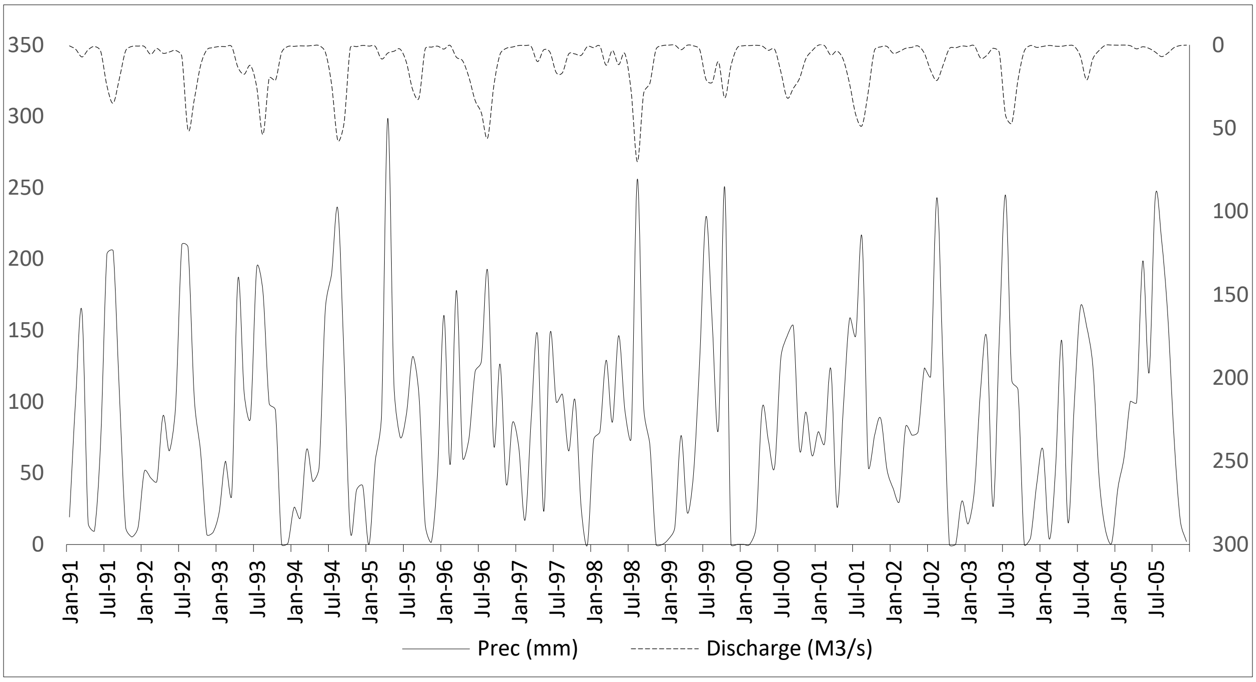

Fig. 4.3 Monthly precipitation and Meki River discharge at Meki town gauging station

4.2.4. Building WEAP model for the ALZLB

The study basin was divided into five neighboring catchments to maintain spatial continuity and these units are used to estimate several water balance components using the soil moisture method in WEAP at a monthly time step. The model mechanisms are defined using different spatial elements in WEAP, i.e., “nodes” and “links”. Fig. 4.4 shows the spatial arrangement of these elements in WEAP. Each subbasin node was further divided into categories of land use and land cover classes and with a unique climate dataset.

In WEAP, all rivers and tributaries were executed as “River” elements; and “Demand sites” are used to account for irrigation, domestic, industrial, and livestock water requirements in each catchment with a preference for the sources of supply. The lakes were described as a “Reservoir node” with important data inputs (storage capacity, initial storage, volume-elevation curve, monthly net-evaporation rate, and abstraction data) entered into WEAP. A “groundwater node” in WEAP model was also allocated for each catchment to represent groundwater storage and flows for that catchment, along with storage capacity, maximum extraction, and groundwater recharge.

Finally, all nodes are tied using “links” in the WEAP that outline the movement of water between spatial elements (model components). There are two types of links are available in WEAP: "Transmission links" and "Runoff and infiltration links". Runoff and infiltration links are made to (i) connect the subbasin node to the river element (river reach) that receives its irrigation return flows (surface runoff and interflow), and (ii) link subbasin nodes and groundwater nodes to allow groundwater recharging from the root zone to the aquifer element of the model.

On the other hand, transmission links are used to join river elements, reservoirs and groundwater nodes to "demand sites" from the lower part of the subbasins. Finally, the demand site's water allocation procedure (D. Yates et al., 2005) available in WEAP is used to prioritize the "Demand sites" and also define preferences ranks for sources of supply i.e., Surface water and groundwater abstractions.

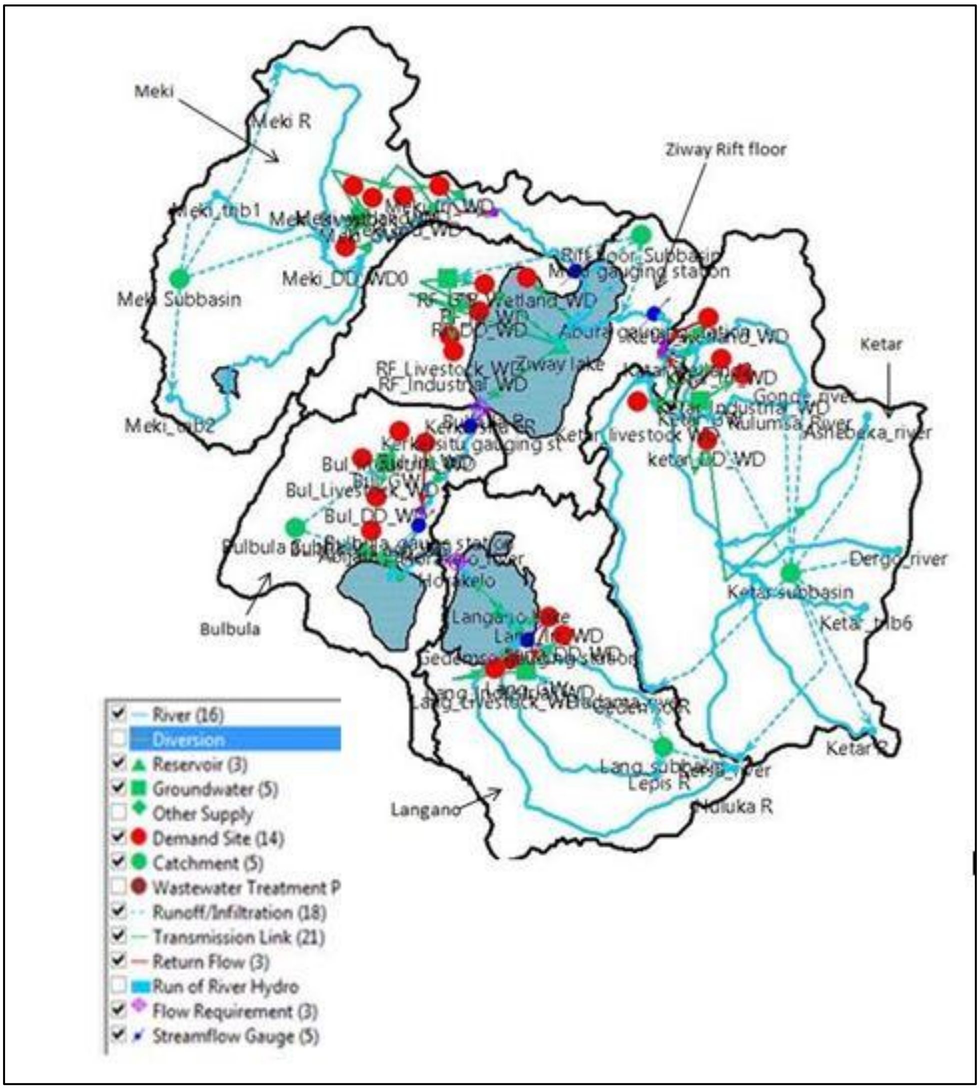

Fig. 4.4 The schematic representation of the ALZLB WEAP model

4.3. Results

4.3.1. Model: Calibration and Validation

The model was calibrated to compute land use and soil-related parameters using the manual (trial-and-error) method until a good fit is observed between the measured and simulated streamflow. It was carried out against ten hydrologic years (1991-2000) for the calibration and five years (2001-2005) for the validation periods with monthly periods of measured streamflow (runoff) at the outlets.

The outputs of calibrated WEAP model were presented in Table 4.1 and Table 4.3 for the Ketar and Meki subbasins, respectively. Model performance evaluation was explained using graphical comparison and statistical methods such as Coefficient of determination (R^2), Nash-Sutcliffe Coefficient (NSE), Index of Agreement (IA), Root Mean Square Error (RMSE), and RMSE-observations standard deviation ratio (RSR).

4.3.1.1. The Ketar upstream subbasin

The average measured and simulated the Ketar streamflow were $13m^3/s$ and $12.5m^3/s$ for the model calibration period while it was $10.4m^3/s$ and $9.6m^3/s$ in the validation period. The monthly hydrographs of measured and simulated streamflow statistics results were presented in (with values of R^2 = 0.82, NSE = 0.80 and IA = 0.95 for the calibration period. Likewise, for the validation period, the statistical values of the measured and simulated streamflow during this period were R^2 =0.91, NSE = 0.91 and IA = 0.98.

The comparison between the measured and simulated monthly runoff for the Ketar river basin for the calibration and validation periods were illustrated pictorially in Fig. 4.5

Monthly hydrograph of measured and simulated streamflow of Ketar River at Abura outlet and monthly precipitation of the subbasin: (a) the calibration and (b) the validation period

(a) and (b), respectively. On the other hand, the mean monthly measured and simulated streamflow shown in Fig. 4.6 (a) and with R^2 = 0.99, NSE = 0.97 and IA = 0.99 for the calibration period. Whereas, Fig. 4.6(b) shows the mean monthly measured and simulated streamflow for the validation period with values of R^2 = 0.94, NSE = 0.93 and IA = 0.93 for the mean monthly period.

Table 4.1 *Range of values for the estimated parameters used in the WEAP model for Ketar River Subbasin*

parameters	Definition	Range in Values
Kc	Crop coefficient	0.34 - 1.05
SWC	Effective Soil water capacity of upper layer(mm)	500
DWC	Effective Soil water capacity of lower layer(mm)	250
RRF	Runoff Resistance factor	2.5 - 405
RZC	Root Zone rate of conductivity at full saturation (mm/Month)	0.8 - 179
DC	Rate of conductivity of deep layer at full saturation (mm/month)	4-24
PF	Preferred Flow direction	0.65
Z1	Initial storage fraction of upper layer at the beginning of the simulation (%)	28 -50
Z2	Initial storage fraction of lower layer at the beginning of the simulation (%)	70

Table 4.2 Summary of model performance statistics for measured and simulated of Ketar streamflow

statistics	Monthly	Mean monthly
Calibration period	1991-2000	
Drainage Area (ha)	327,161	
Number of months	120	
Mean measured flow (m^3/s)	13	12.52
Mean simulated flow (m^3/s)	12.5	12.98
STDEV measured	17.8	16
STDEV simulated	17.2	18.2
Coefficient of determination (R^2)	0.82	0.99
Nash-Sutcliffe coefficient (NSE)	0.8	0.97
Index of Agreement (IA)	0.95	0.99
Root Mean Square Error (RMSE)	7.62	6.56
RMSE-observations standard deviation ratio (RSR)	0.44	0.15
Validation period	2001-2005	
Number of months	60	
Mean measured flow (m^3/s)	10.4	10.4
Mean simulated flow (m^3/s)	9.6	9.6
STDEV measured	14.5	13.1
STDEV simulated	14.4	13.3
Coefficient of determination (R^2)	0.914	0.94
Nash-Sutcliffe coefficient (NSE)	0.91	0.93
Index of Agreement (IA)	0.98	0.98
Root Mean Square Error (RMSE)	4.3	3.3
RMSE-observations standard deviation ratio (RSR)	0.3	0.25

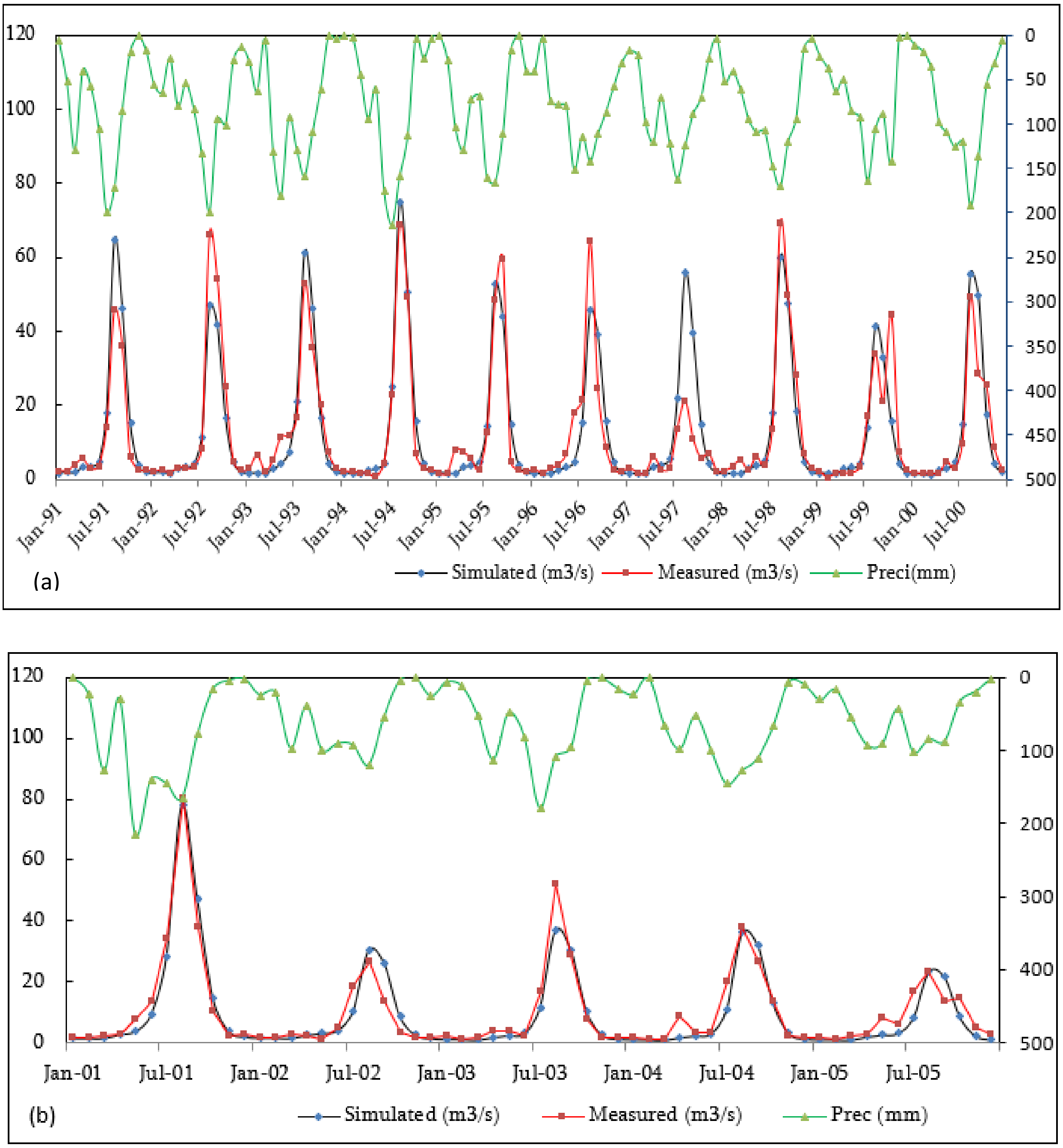

Fig. 4.5 Monthly hydrograph of measured and simulated streamflow of Ketar River at Abura outlet and monthly precipitation of the subbasin: (a) the calibration and (b) the validation period

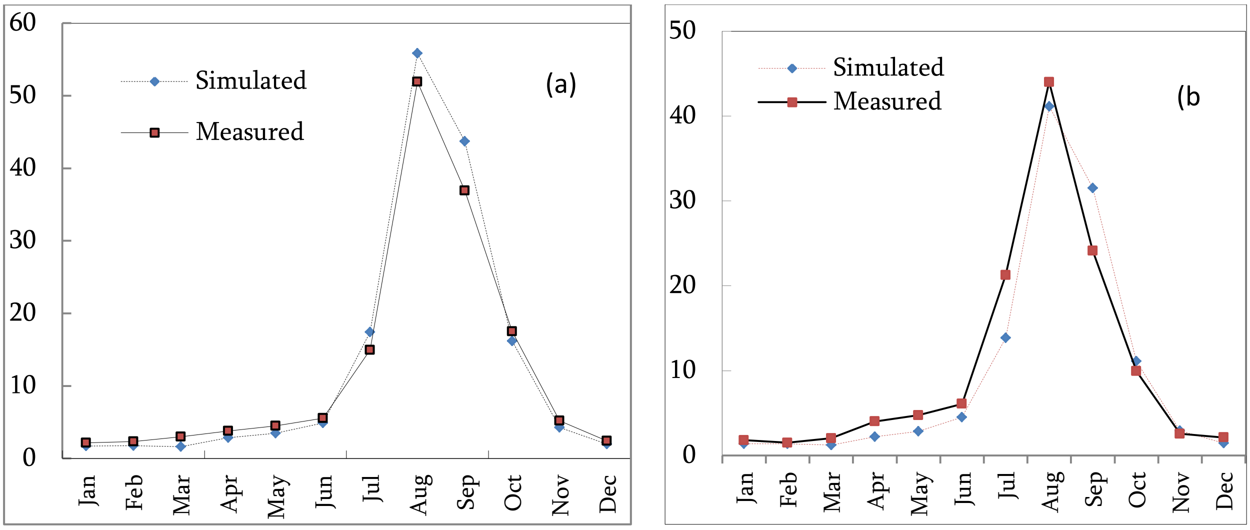

Fig. 4.6 Mean monthly measured and simulated flow of Ketar River at Abura gauging station for (a) the calibration and (b) the validation period.

4.3.1.2. The Meki upstream subbasin

The mean measured and simulated Meki streamflow were 11.1m³/s and 10.6m³/s for the model calibration period while it was 8.8m³/s and 10m³/s in the validation period, respectively. The graphical comparison between the measured and simulated monthly runoff for the Meki River at the Meki town outlet for the calibration (1991-1999) and validation (2000-2004) periods were shown in Fig. 4.7 (a), and (b). The monthly measured and simulated streamflow statistics were presented in (Table 4.4) with statistical values of R^2 = 0.79, NSE = 0.79 and IA= 0.94 for the calibration period. Likewise, for the validation period, the statistical values of the measured and simulated streamflow during this period were R^2 = 0.74, NSE = 0.62 and IA = 0.91.

On the other hand, the mean monthly measured and simulated streamflow in Table 4.4 showed a statistical value of R^2 = 0.99, NSE = 0.98 and IA= 0.99 for the calibration period. Whiles, the performance measurement indices were given as R^2 =0.99 NSE = 0.93 and IA

= 0.98 for the mean monthly flow for the validation period. The graphical comparison between mean monthly measured and simulated was presented in Fig. 4.8 (a) and (b).

Table 4.3 Range of values for the estimated parameters used in the WEAP model for Meki River Subbasin.

parameters	Definition	Range in Values
Kc	Crop coefficient	0.15 - 1.05
SWC	Effective Soil water capacity of upper layer(mm)	500
DWC	Effective Soil water capacity of lower layer(mm)	250
RRF	Runoff Resistance factor	3.5 - 650
RZC	Root Zone rate of conductivity at full saturation (mm/Month)	0.5 – 75.25
DC	Rate of conductivity of deep layer at full saturation (mm/month)	42-145
PF	Preferred Flow direction	0.55
Z1	Initial storage fraction of upper layer at the beginning of the simulation (%)	15 -85
Z2	Initial storage fraction of lower layer at the beginning of the simulation (%)	22

Table 4.4 Summary of model performance statistics for measured and simulated of Meki streamflow

statistics	Monthly	Mean monthly
Calibration period	1991-1999	
Drainage Area (ha)	221,175	
Number of months	108	
Mean measured flow (m^3/s)	11.1	11.2
Mean simulated flow (m^3/s)	10.6	10.7
STDEV measured	14.8	12.7
STDEV simulated	13.8	13.0
Coefficient of determination (R^2)	0.79	0.99
Nash-Sutcliffe coefficient (NSE)	0.79	0.98
Index of Agreement (IA)	0.94	0.99
Root Mean Square Error (RMSE)	17.9	3.66
RMSE-observations standard deviation ratio (RSR)	0.45	0.1
Validation period	2000-2004	
Number of months	60	
Mean measured flow (m^3/s)	8.8	8.8
Mean simulated flow (m^3/s)	10	10
STDEV measured	12.6	10.9
STDEV simulated	14.7	12.9
Coefficient of determination (R^2)	0.74	0.99
Nash-Sutcliffe coefficient (NSE)	0.62	0.93
Index of Agreement (IA)	0.91	0.98
Root Mean Square Error (RMSE)	20.6	7.47
RMSE-observations standard deviation ratio (RSR)	0.6	0.25

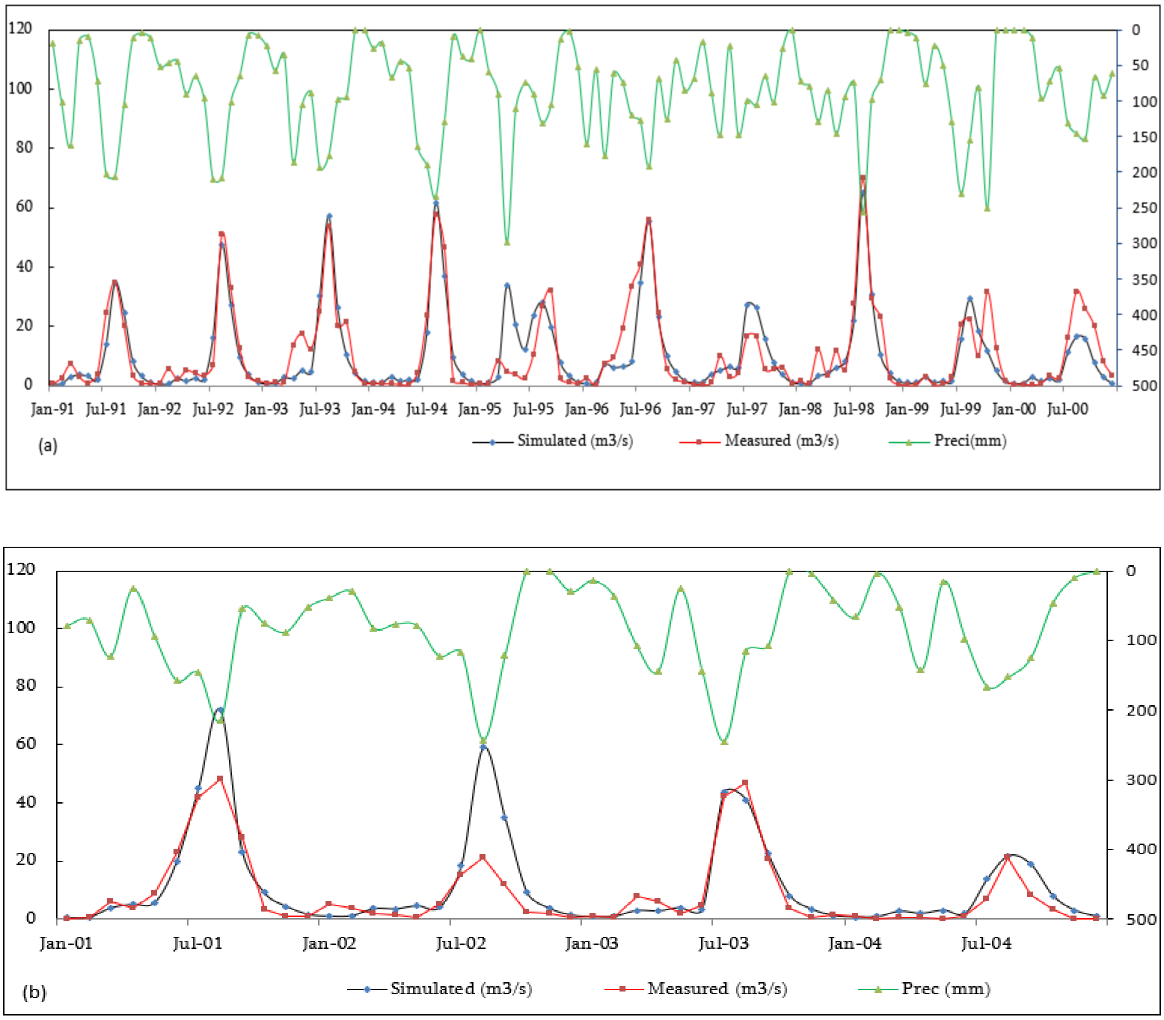

Fig. 4.7 Monthly measured and simulated streamflow (m3/s) of Meki River at Meki town gauging station for (a) the calibration and (b) the validation period.

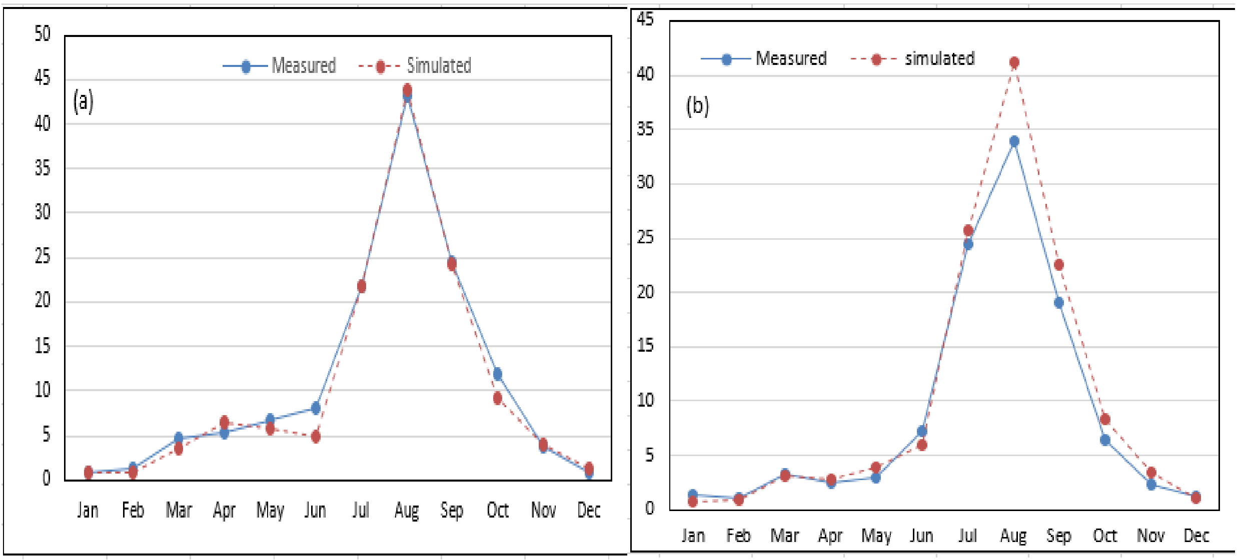

Fig. 4.8 Mean monthly measured and simulated flow (m3/s) of Meki River at Meki gauging station for (a) the calibration and (b) the validation period.

4.3.2. Hydrological processes /components/

Precipitation is the only source of water input and plays critical role in estimating of water balance the basin that significantly influences other hydrologic components of the subbasins. On the contrary to this, one of the major hydrologic components that is critical to be estimated using the WEAP model was actual evapotranspiration. Since it is the main component of the hydrologic cycle altering water supply and is important in water resource development and management (Abtew & Melesse, 2013). The long-term monthly values of hydrological components of Ketar and Meki subbasins are presented in Table 4.4 and Table 4.5 and graphically, the long-term monthly proportion of the hydrologic components were presented in Fig. 4.9 and Fig. 4.10 Evapotranspiration loss takes the lion share of precipitation input and estimated to 799mm and 853mm annually for Ketar and Meki subbasins respectively. The remaining share is attributed to the streamflow (runoff) components are the interflow, baseflow and surface runoff accounts for 9.3mm/year, and 4.5mm/year annually in the Ketar subbasin respectively. Whereas, the streamflow (runoff) components are in order of their contribution; the surface runoff and baseflow accounts 11mm/year, and 5mm/year for the Meki subbasin, respectively.

Evapotranspiration loss accounts for 84-86% of overall precipitation available water in the subbasin. The evapotranspiration significantly exceeded the amount of precipitation in (October, November, and December). On the contrary, in months ranging from March to August evapotranspiration was less than precipitation amount and nearly closer in the months of February and September. On the other hand, the remaining 14% of precipitation was the Ketar streamflow (runoff) which is comprised of 4.5%, and 9.3%

baseflow, and surface runoff respectively. Likewise, similarly, 16% of precipitation goes to streamflow and in turn, it is composed of 11%, and 5% surface runoff and baseflow in the Meki catchment respectively.

Table 4.5 Long-term estimated of hydrologic components of Ketar river subbasin (mm/year)

	Prec	ET	Baseflow	Surface Runoff
Jan	23.7	29.7	1.7	0.1
Feb	33.5	30.0	1.6	0.1
Mar	64.5	39.4	1.4	0.3
Apr	91.7	57.8	1.8	0.9
May	88.3	72.4	2.2	1.0
Jun	112.6	83.9	2.5	1.8
Jul	154.3	83.9	3.4	8.9
Aug	159.0	99.6	7.5	38.4
Sep	105.8	96.8	10.2	24.5
Oct	65.0	105.1	5.4	8.2
Nov	18.9	66.0	2.6	1.1
Dec	12.9	34.6	1.8	0.1
Sum	930.2	799.3	42.2	87.2
Min	12.9	29.7	1.4	0.1
Max	105.1	105.1	10.2	38.4
Mean	77.5	66.6	3.5	7.2
Median	76.7	69.2	2.4	1.1
SD	50.1	28.0	2.8	12.1
Share (%)	100.0	86	4.5	9.3

Table 4.6 Long-term estimated of hydrologic components of Meki river subbasin (mm/year

	Prec	ET	Baseflow	Surface runoff
Jan	44.52	30.10	2.32	0.08
Feb	42.27	43.28	2.62	0.14
Mar	89.20	55.56	4.65	1.36
Apr	102.48	64.50	1.82	6.47
May	66.28	67.67	1.89	5.78
Jun	112.02	71.52	2.08	6.18
Jul	159.08	87.84	7.50	20.56
Aug	181.23	107.50	9.16	42.69
Sep	101.30	105.98	7.50	20.24
Oct	66.49	118.84	4.47	7.77
Nov	22.55	69.39	4.66	1.24
Dec	27.68	31.34	2.82	0.22
Sum	1015.0	853.51	51.49	112.7
Min	22.55	30.10	1.82	0.08
Max	181.23	118.84	9.16	42.69
Mean	84.59	71.13	4.29	9.39
Median	77.85	68.53	3.64	4.65
SD	49.92	29.29	2.53	7.72
Share (%)	100	84	5	11

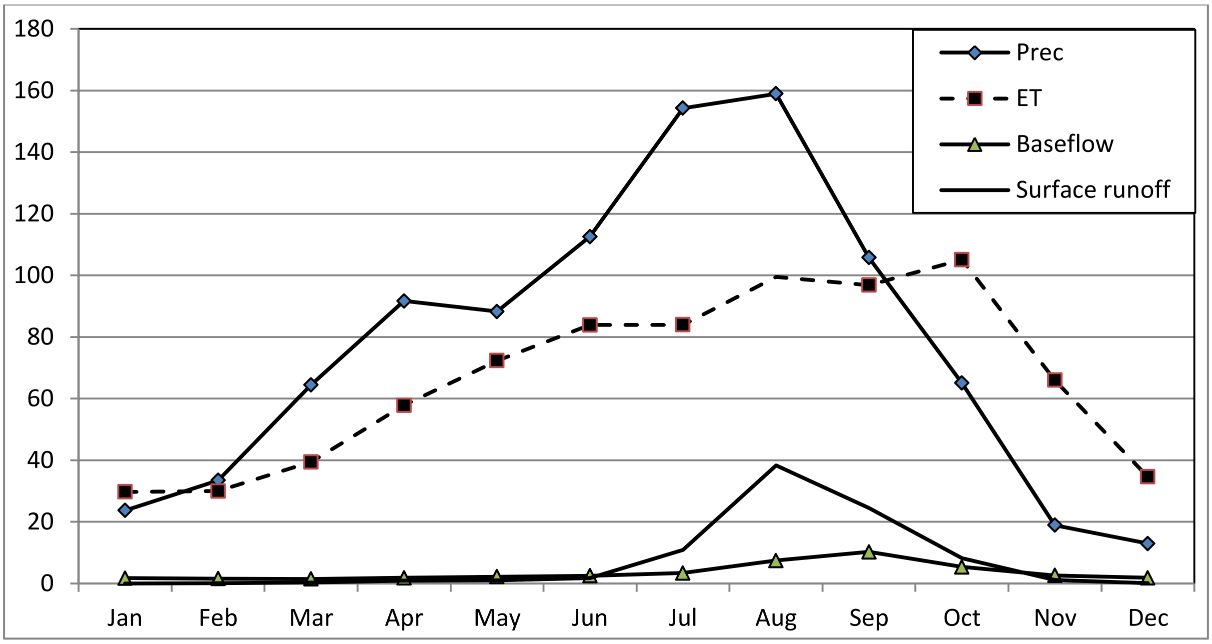

Fig. 4.9 Long-term monthly relative proportion of hydrologic components in Ketar subbasin

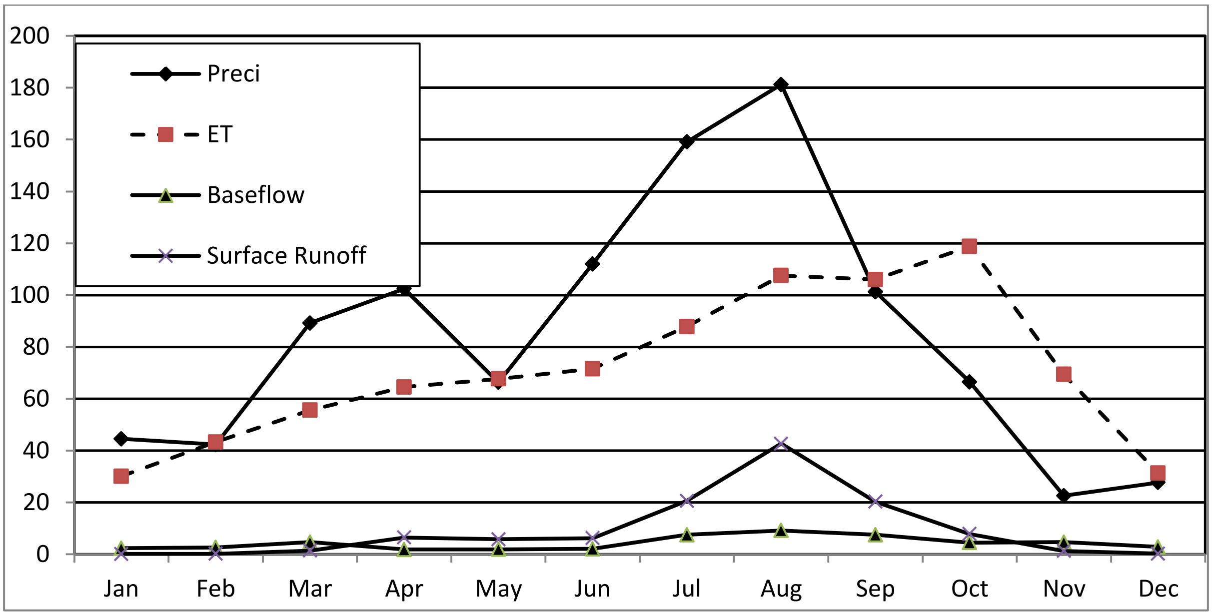

Fig. 4.10 Long-term monthly relative proportion of hydrologic components in Meki subbasin

4.3.3. Streamflow analysis

4.3.3.1. The Ketar and the Meki River sub-basins

The WEAP model average monthly simulated and measured of Ketar streamflow was 31.38MCM and 31.22MCM respectively. The minimum and maximum simulated values were 3.95MCM in February and 136.45MCM in August respectively. Their corresponding values in measured streamflow were 5.66MCM and 132MCM in the same months respectively. Table 4.7 shows the long-term average monthly values of Ketar streamflow at the outlet. Similarly, Table 4.8 indicates the model simulated average monthly Meki streamflow was 27.5MCM against the measured average value was 27.3MCM. The minimum and maximum simulated values were 2.0MCM in January and 114.7MCM in August against measured values of 2.8MCM in December and 106.9 MCM in August respectively.

Table 4.7 shows the long-term mean monthly values of Ketar stream at the outlet (MCM)

	Jan	Feb	Mar	Apr	May	Jun	Jul	Aug	Sep	Oct	Nov	Dec	Sum
Simulated	4.3	3.9	4.0	6.9	8.8	12.4	43.5	136.4	102.7	38.8	9.9	4.8	376.5
Measured	5.5	5.1	7.2	10.0	12.3	14.8	45.7	132.0	84.6	40.1	11.2	6.2	374.6

Table 4.8 shows the long-term mean monthly values of Meki stream at the outlet (MCM)

	Jan	Feb	Mar	Apr	May	Jun	Jul	Aug	Sep	Oct	Nov	Dec	Sum
Simulated	3.0	3.0	11.3	11.5	14.5	20.0	61.0	106.9	58.5	26.7	8.4	2.8	327.6
Measured	2.0	2.2	9.0	13.6	13.9	13.8	62.1	114.7	61.3	23.9	9.7	3.4	329.7

4.3.3.2. Ungauged subbasin

Out of five subbasins, only two have gauging stations at the outlet. Since there have no measured data to calibrate the model. For the purpose of guessing hydrologic parameters, model calibration parameters were taken from the neighboring gauged sub-basins. For this work, these ungauged sub-basins are estimated to contribute about 19MCM, 24MCM and 283.5MCM of water (runoff) to Lake Ziway, Abijata and Langano annually respectively.

4.3.4. Evaporation

There are important lakes for which monthly evaporation have been estimated using the WEAP model. The results are presented in Table 4.9. The open water evaporation consumes about 1755mm, 1754mm and 1774mm of water flux a year from Lake Ziway, Langano, and Abiyata respectively.

Table 4.9 Lakes evaporation (mm)

Month	Ziway	Langano	Abijata
Jan	109	136	143
Feb	145	168	176
Mar	152	160	162
Apr	158	159	161
May	169	164	164
Jun	157	150	148
Jul	125	131	122
Aug	117	118	110
Sep	116	115	111
Oct	198	153	158
Nov	198	157	165
Dec	111	145	153
Sum	1755	1754	1774

From the water resource perspective, the large amount of water lost through lake evaporation is presented in Table 4.10. MCM. For instance, 772MCM, 403MCM and 271MCM from Lake Ziway, Langano and Abijata respectively. The monthly WEAP output of evaporation is presented in Fig. 4.11.

Table 4.10 Evaporation of lakes (MCM)

Month	Ziway	Langano	Abijata
Jan	48	31	22
Feb	64	39	27
Mar	67	37	25
Apr	69	36	25
May	75	38	25
Jun	69	34	23
Jul	55	30	19
Aug	51	27	17
Sep	51	26	17
Oct	87	35	24
Nov	87	36	25
Dec	49	33	23
Sum	772	403	271

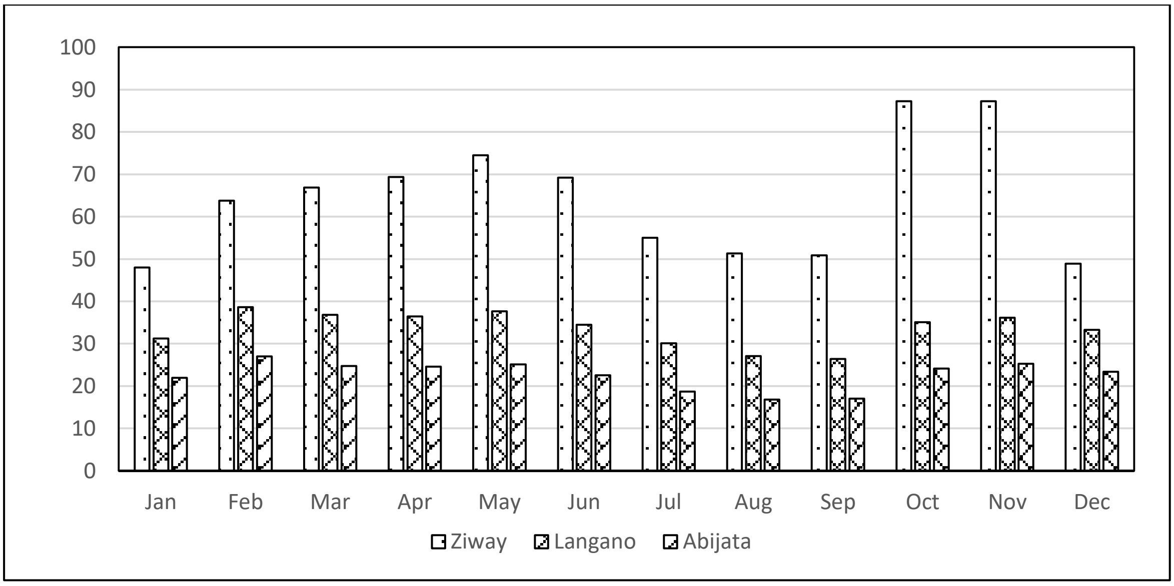

Fig. 4.11 Evaporation of lakes (in MCM)

4.4. Discussion

4.4.1. Model performance Evaluation

4.4.1.1. Streamflow

The efficiency of model performance is tested using statistics such as Coefficient of determination (R^2), Nash-Sutcliffe coefficient (NSE), Index of agreement (IA), Root mean square error (RMSE) and RSR. As stated in (Santhi et al., 2001; Van Liew et al., 2007) the values of $R^2 > 0.5$ are considered adequate with higher values indicating less error variance. For monthly data NSE values range between $-\infty$ and 1.0 and values between $0.75<NSE\leq1$ and $0<=RSR\leq0.5$ are rated as very good; $0.65<NSE\leq0.75$ and $0.5<=RSR\leq0.6$ as good; $0.5<NSE\leq0.65$ and $0.6<RSR\leq0.7$ as satisfactory; and $NSE\leq0.5$ and $RSR>0.7$ rated as unsatisfactory (Moriasi et al., 2007). The other the model performance evaluation is the IA which can be used as a standardized measure of the degree of model prediction error and with values ranges from 0 to 1; the value of 1 indicates a perfect agreement and 0 indicates no agreement at all between the measured and simulated values (Willmott, 1981).

According to (Moriasi et al., 2007) the result shows there has been a very good and good agreement between monthly observed and simulated streamflow for both the Ketar and the Meki subbasins, respectively.

Similarly, previous studies have confirmed that the capability of the WEAP hydrologic model in reproducing catchment hydrology processes in different parts of the world (Table 4.11). Among these, (Asghar et al., 2019) reported the WEAP hydrologic model to attain the NSE and R^2 values of 0.85, 0.86, 0.89, and 0.87 for the monthly calibration and validation periods between the measured and simulated streamflow in the central Indus basin, respectively. From five gauging stations in the Western Algeria watersheds, ranging values of NSE=0.23-0.88, and R^2=0.74-1.0 were achieved between measured and simulated average monthly flows (Hamlat, Errih, & Guidoum, 2013). To balance future water availability and demand, the WEAP model was applied in Benin, (Höllermann et al., 2010) and obtained values NSE=0.91, R^2=0.92, and NSE=0.78 and R^2=0.83 for calibration and validation periods, respectively. To assess the potential impacts of climate and land-use change on irrigation water supply in the USA, the WEAP hydrologic model was developed by (Mehta et al., 2013) and the model has demonstrated the capability with values of NSE=0.91, R^2=0.92, and NSE=0.78 and R^2=0.83 at calibration and validation periods between measured and simulated flows data respectively.

Finally, (Ingol-Blanco & McKinney, 2013) developed the WEAP model to assess the hydrologic processes in Rio Conchos Basin, Mexico. Six gauging stations were used in the basin for model performance evaluation. Values of NSE=0.65-0.87; R^2=0.92-0.97, and NSE=0.60-0.88 and R^2=0.92-0.97 pertinence between measured and simulated flows were found respectively. As compared to these studies, the present study shows modest R^2 and NSE agreement between measured and simulated discharges.

Table 4.11 Comparison of WEAP hydrologic model performance evaluation with other similar studies elsewhere

Country	Model accuracy statistics R^2	Model accuracy statistics NSE	Modeling Periods	Reference
Ethiopia (Ketar)	0.82	0.8	calibration	Present study
	0.91	0.91	validation	
Ethiopia (Meki)	0.79	0.79	calibration	
	0.72	0.62	validation	
Pakistan	0.96	0.85	calibration	(Asghar et al., 2019)
	0.87	0.89	validation	
Algeria	0.74-1.0	0.23-0.88		(Hamlat et al., 2013)
Benin	0.92	0.91	calibration	(Höllermann et al., 2010)
	0.83	0.78	validation	
USA	0.92	0.91	calibration	(Mehta et al., 2013)
	0.83	0.78	validation	
Mexico	0.92-0.97	0.65-0.87	calibration	(Ingol-Blanco & McKinney, 2013)
	0.92-0.97	0.60-0.88	validation	

4.4.2. Hydrologic characteristics of the subbasin

4.4.2.1. Evapotranspiration

One of the major hydrologic components that sought to be estimated using the WEAP model is actual evapotranspiration. Since it is one of the main components of the hydrologic cycle influencing water existence and vital in water resource use and governance (Abtew & Melesse, 2013). The result revealed that ET loss accounted for about 84-86% of available water in the basin. A similar investigation by (Jansen et al., 2007) indicated that 88% of precipitation is consumed by evapotranspiration in the ALZLB of Ethiopia. Results of the SWAT model by (Desta & Lemma, 2017) showed lower values as compared to the current study that ranging from 64%-69%, and 69%-72% of precipitation lost to the atmosphere through evapotranspiration for Ketar and Meki subbasins respectively.

The current study revealed that 799mm and 854mm of available water was lost via evapotranspiration annually from Ketar and Meki subbasins respectively. Both subbasins with similar months (September, August, and October) recorded higher values 96mm, 100mm, and 105mm for Ketar and 106mm, 107mm and 119mm for Meki sub-catchments respectively. While the minimum and maximum values were 30mm and 105mm for Ketar and 30mm and 119mm for the Meki subbasin in January and October respectively. The previous study, using the soil water balance approach for the same catchments by (Ayenew, 2003) indicated that the annual actual evapotranspiration was estimated to 866mm and 766mm for Ketar and Meki subbasins respectively. These slight variations among the two studies could be the difference in climate data (temporal), landuse and methods applied.

With monthly minimum and maximum values were 11.5mm and 138.6mm for the Ketar subbasin in December and August respectively and 8.2mm and 111mm for the Meki subbasin in the months of December and August respectively and detailed monthly values are available in Table 4.12. Yet another study by (Desta & Lemma, 2017) revealed that the annual evapotranspiration simulated using SWAT model results were 662mm, and 675mm for the Ketar subbasin and 654mm and 693mm for the Meki subbasin during the model calibration period (1988-2000) and validation period (2001-2013) respectively.

Table 4.12 Comparison of evapotranspiration estimation

Month	Ketar subbasin		Meki subbasin	
	(Ayenew,2003)	WEAP	Ayenew,2003	WEAP
Jan	24.2	29.7	22.6	30.1
Feb	55.7	30.0	53.2	43.3
Mar	73.9	39.4	79.8	55.6
Apr	97.7	57.8	80.4	64.5
May	80	72.4	86.8	67.7
Jun	101.2	83.9	82.2	71.5
July	123.8	83.9	116.7	87.8
Aug	138.6	99.6	111	107.5
Sep	104	96.8	89.8	106
Oct	38.2	105.1	25.6	119
Nov	16.9	66.0	9.9	69.4
Dec	11.5	34.6	8.2	31.3
Sum	866	799	766	854

4.4.2.2. Evaporation from different methods

The comparisons of lake evaporation from different methods were presented in Table 4.13 and Table 4.14. There are various models ranging from the complex as Penman-Monteith method to the simple Pan method used to estimate evaporation and usually produce different results (Melesse et al., 2009). Hence, the result obtained from WEAP reasonably agrees with previous studies finding (Vallet-coulomb et al., 2001) and (Ayenew, 2003).

Table 4.13 Comparison of Lake Ziway evaporation estimations with various methods

Month	Evaporation						
	Energy[1] (mm)	Penman[1] (mm)	CRLE[1] (mm)	Penman[2] (mm)	Radiation[2] (mm)	Pan[2] (mm)	WEAP (mm)
Jan.	143	154	132	150	135	159	109
Feb.	149	162	135	128	120	144	145
Mar.	152	166	149	148	142	192	152
Apr.	156	166	155	188	138	142	158
May	163	170	160	188	138	156	169
Jun.	147	168	155	135	107	137	157
Jul.	128	136	146	139	115	126	125
Aug.	136	137	136	135	115	123	117
Sep.	141	136	137	164	124	112	116
Oct.	159	162	141	200	151	170	198
Nov.	160	161	144	223	157	178	198
Dec.	143	157	139	225	157	130	111
Annual	**1777**	**1875**	**1728**	**2023**	**1599**	**1769**	**1755**

Source: from [1] (Vallet-coulomb et al., 2001) and [2] (Ayenew, 2003); complementary relationship lake evaporation (CRLE) method

Table 4.14 Comparison of Lake Abiyata and Langano evaporation estimations (in mm)

Lake	Abiyata			Langano			
Method	Penman[1]	Radiation[1]	WEAP	Penman[1]	Radiation[1]	Pan[1]	WEAP
Jan	173	178	143	177	166	115	136
Feb	141	155	176	159	146	117	168
Mar	159	177	162	185	179	139	160
Apr	207	171	161	176	154	139	159
May	181	164	164	170	151	151	164
Jun	132	128	148	149	128	131	150
Jul	127	133	122	150	129	138	131
Aug	128	133	110	147	132	129	118
Sep	149	142	111	178	133	118	115
Oct	212	171	158	183	166	112	153
Nov	257	185	165	188	168	113	157
Dec	193	185	153	147	145	124	145
Annual	**2060**	**1922**	**1774**	**2010**	**1651**	**1526**	**1754**

Source: [1]Ayenew, 2003

4.4.2.3. Streamflow proportion and baseflow analysis

The relative proportion of the three components of the runoff (baseflow, interflow, and surface runoff) relies on the physical properties of the subbasin, the land use, soil, topography, geomorphology, and geology characteristics. The annual discharges of Ketar and Meki rivers were estimated to 14%, and 16% of the annual precipitation of the subbasins respectively. The Ketar streamflow was comprised of (68% surface runoff and predominantly exceeded the other components in the months June to October and followed by 32% baseflow which was sustained throughout the year and the monthly relative comparison was presented in Fig. 4.5.

These results are consistent with the study by (Legesse et al., 2003) using the PRSM model in the same catchment. The PRSM revealed that of the total annual flow, the interflow was about 60% and the highest significant constituent during the rainy seasons, while the baseflow was 30% that sustains the river flow during the dry season. The same study explains for abundance of interflow and baseflow as compared to surface runoff is associated to a huge proportion of cultivated/grazing land in the subbasins that support penetration in the soil zone and thus lateral subsurface flow along subsurface channels, macro pores, and fractures. Contrary to this, the less contribution of surface runoff to the streamflow is explained by the absence of significant impervious surfaces in the catchment.

On the other hand, the Meki streamflow is comprised of 68.5%, and 31% of surface runoff, and baseflow. The study by (Legesse et al., 2010) using PRSM in the same catchment showed that 43.4%, 32.1% and 24.5% of interflow, baseflow and surface runoff respectively. This result indicated that the relative annual contribution of subsurface flow is the highest as compared other two components of stream runoff which exists throughout the year. However, in the month of August the surface runoff largely dominated over the baseflow and interflow and the monthly proportion was presented in (Fig. 4.13). Moreover, the SWAT model outputs by (Desta & Lemma, 2017) where the streamflow was composed of only the baseflow and surface runoff components constitute 55-57% and 43-45% of Ketar streamflow and 45-55% to 55-58% of Meki streamflow during the periods of model calibration (1988-2000) and validation (2001-2013) respectively.

The comparison between monthly baseflow estimation using the WEAP model and Simple baseflow separation are presented in (Table 4.15 and Table 4.16) for Ketar and Meki rivers respectively. The RAP result revealed that the baseflow contribution to Ketar streamflow was about 34% of the annual discharge. While the relationship between the WEAP model and RAP method outputs have shown a very good agreement for Ketar with a correlation coefficient determination (R^2) of 0.99 shown (Fig. 4.14). In the case of Meki River, the RAP baseflow component was smaller as compared to the WEAP baseflow amount and the coefficient of determination (R^2) was 0.70 shown in (Fig. 4.6).

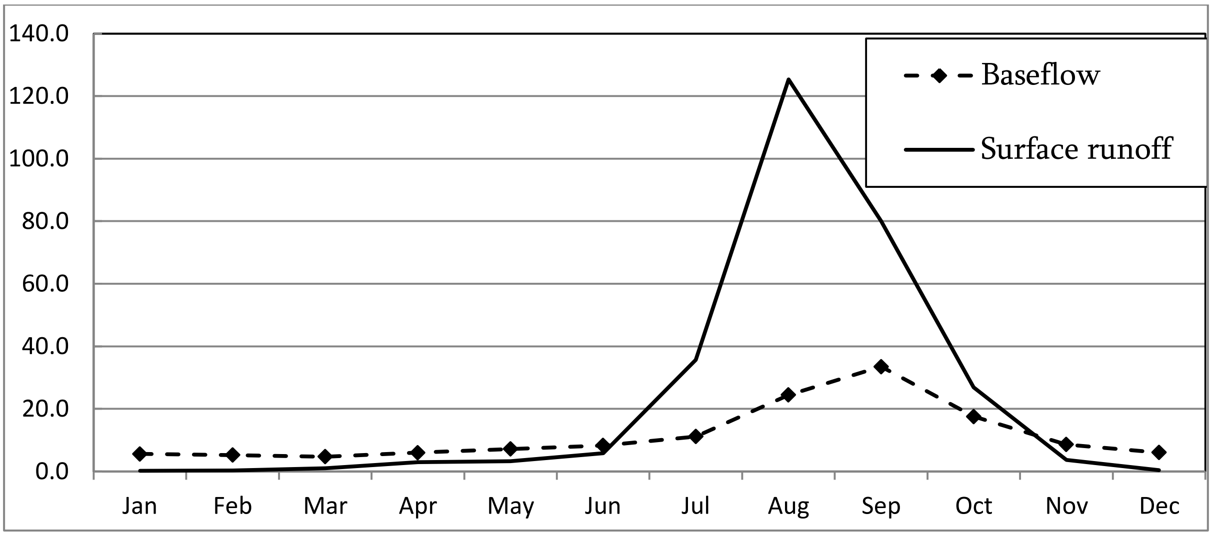

Fig. 4.5 Monthly simulated discharge of Ketar stream flow components (in MCM)

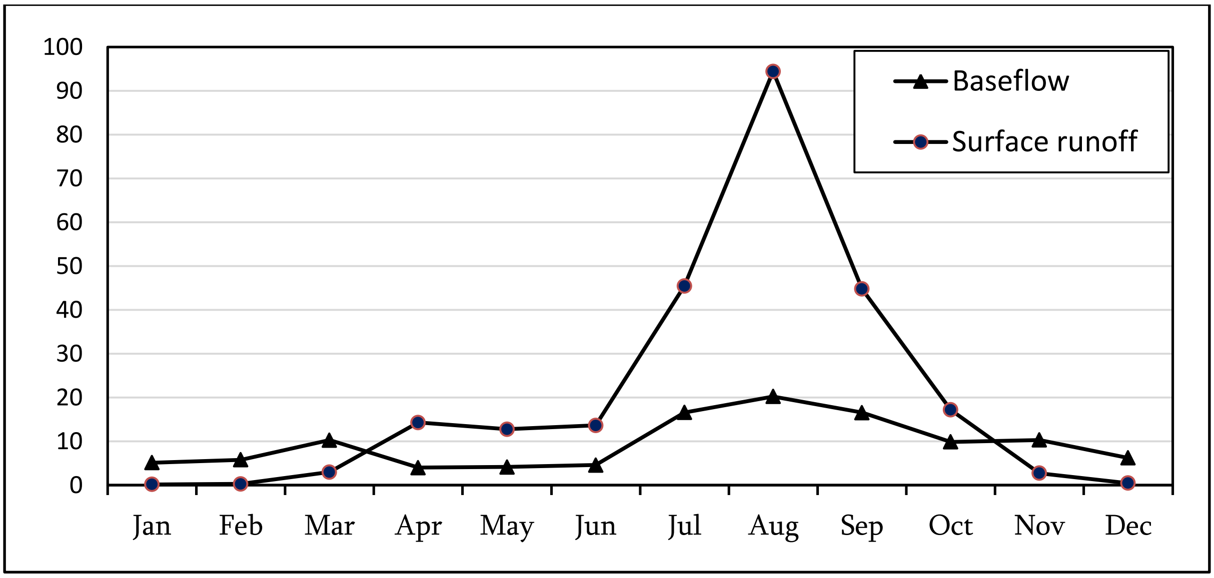

Fig. 4.13 Monthly simulated discharge of Meki streamflow components (in MCM)

Table 4.15 Baseflow estimation using WEAP and RAP for Ketar River (in MCM)

	Jan	Feb	Mar	Apr	May	Jun	Jul	Aug	Sep	Oct	Nov	Dec	Sum	Min	Max	Mean
WEAP	5.6	5.2	4.7	6.0	7.2	8.3	11.2	24.4	33.5	17.5	8.6	6.0	138.2	4.7	33.5	11.5
RAP	5.3	5.0	4.6	5.8	6.9	8.1	11.3	25.0	34.3	18.3	8.0	5.8	138.4	4.6	34.3	11.5

RAP (River Analysis Package)

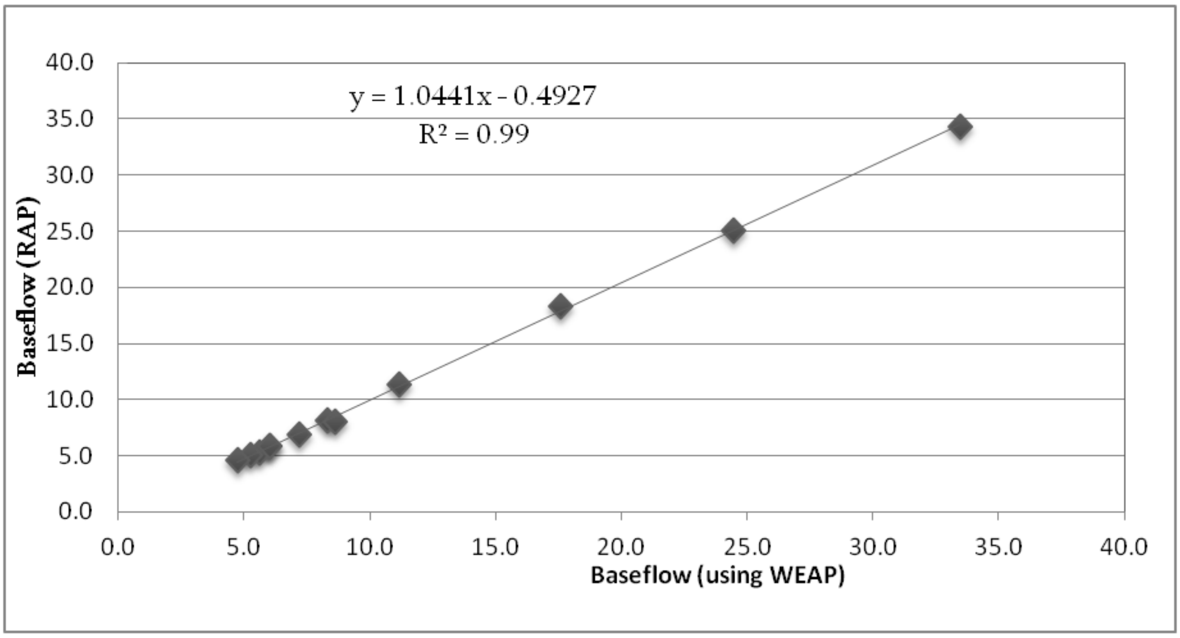

Fig. 4.14 Relationship between monthly baseflow (RAP) and Baseflow (WEAP) for Ketar River

Table 4.16 Baseflow estimation using WEAP and RAP for Meki River (in MCM)

	Jan	Feb	Mar	Apr	May	Jun	Jul	Aug	Sep	Oct	Nov	Dec	Sum	Min	Max	Mean
WEAP	5.1	5.8	10.3	4.0	4.2	4.6	16.6	20.3	16.6	9.9	10.3	6.2	113.9	4.0	20.3	9.5
RAP	0.8	1.3	3.5	5.7	5.9	6.8	11.8	22.4	19.1	7.1	2.9	1.3	88.7	0.8	22.4	7.4

(RAP = River Analysis Package)

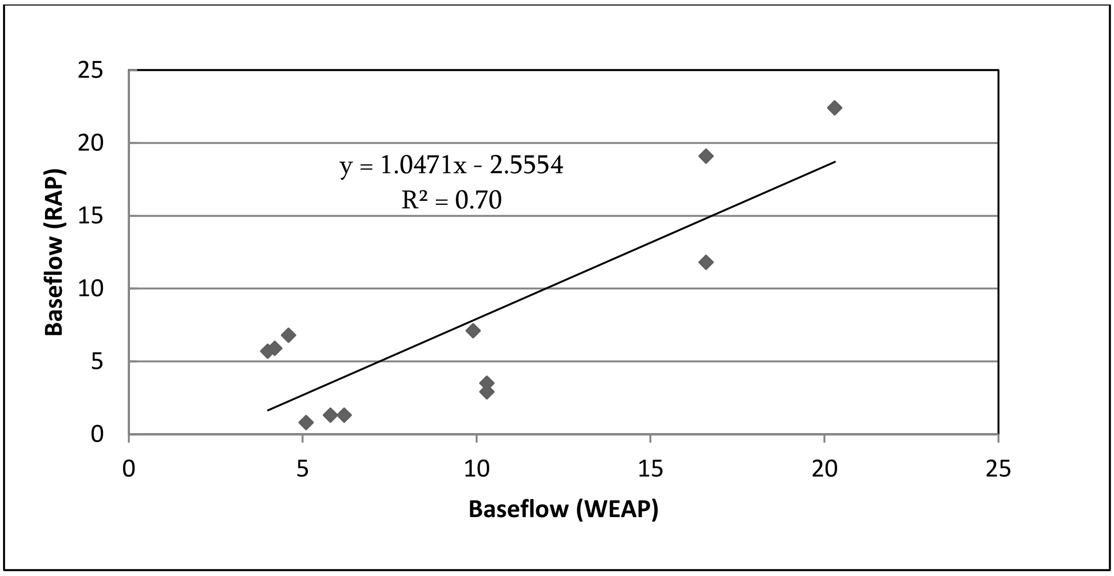

Fig. 4.6 Relationship between monthly baseflow (RAP) and Baseflow (WEAP) for Meki River

4.5. Model Limitations and uncertainties

WEAP model has been implemented in this study. The WEAP embedded soil-moisture modeling process which contains sophisticated model settings and unique value for entire subbasin are likely to bring uncertainties to the results. The soil-moisture method uses two soil layer compartments and that partitioning water into different hydrologic components based on empirical equation may have limitations for aquifers with different recharge mechanisms than diffused recharge. For instance, in the ALZLB, the dominant types of recharge mechanisms are Selective, mountain block, and mountain front with a small proportion of direct recharge since the study area was originated by volcano-tectonic activities that modified its geology, geomorphology, and topographic settings. Moreover, axial flow through faults in Ziway basin that may affect the baseflow amount measured at gauging stations; Lack of soil development in escarpment areas; and Limited in well distributed gauging stations across the basin.

5. Numerical Groundwater Flow Modeling

5.1. Introduction

Groundwater is a crucial source of water supply for agriculture, domestic and industrial uses in the ALZLB. The water supply for villages and towns are predominately rely on groundwater sources and also more than 25% of water demand for irrigation has been directly abstracted from aquifers in the basin (Halcrow, 2009; JICA, 2012). Groundwater may be manifested as springs, streams, and wetlands. The perennial streams would not have permanent flow without groundwater contribution as baseflow (Kresic & Mikszewski, 2013). Besides this, it has a great role in sustaining water resources in the basin. For instance, groundwater is believed to have a connection with the chain of lakes located in the rift floor of the basin. The highlands and plateau areas are mainly considered as the potential recharge areas.

On the contrary, the rift floor is the region where groundwater found at shallow depth and discharge zone in the basin. Baseflow is considered as groundwater discharged to the streams and a simple baseflow separation method shows that baseflow contributes to Ketar and Mike rivers flows. There is a continuously increasing demand of groundwater development that may lead to overexploitation of groundwater resources and growing impacts of human actives on aquifers, such as a decline in hydraulic head and degrade groundwater quality.

This resource has been extracted without adequate knowledge about its inherent nature (Ayenew, 2007) and this may lead to water resources degradation in the basin. So far, a few studies on a standalone numerical groundwater model have been carried out with the objective mainly focusing on its potential(Birhanu, 2011; Kumo, 2006) and groundwater interaction with the lakes (Ayenew, 1998). Yet, no work has been done on water resources management perspectives. Its function is to make quantitative study or evaluation on the groundwater system.

5.1.1. Using Models to solve groundwater problems

A model is an entity built to reproduce some aspect of the behavior of a natural system. Groundwater model is supposed to reproduce groundwater variables (head and discharge) and solute transport (concentration, solute fluxes, etc.), and so forth. It is rely on the basic principle Darcy's law and the law of conservation of mass (Konikow & Mercer, 1988). The mathematical model is prepared by converting a conceptual model in the form of governing equations with related to boundaries and initial conditions (Anderson & Woessner, 1992; Karamouz et al., 2011).

As described in (Kresic & Mikszewski, 2013) One of the utmost extensively practiced mathematical models is a numerical model that describes the whole flow field of concern at the same time, giving solutions for the extend defined by the user. Numerical models use estimates of either finite differences or finite elements to resolve the differential equations explaining groundwater flow or solute transport. It requires that the model domain and time be discretized. The geology/hydrogeology of the model domain is represented as a discrete block. The discretization process involves the representation by inter-connected grid cells or elements; and the time step used during simulation. Hence, the Finite difference and finite-element approaches are two popular numerical approaches that are widely practiced in solving s the groundwater flow equation provided that model parameters, and initial and boundary conditions are properly defined.

Finite difference and finite-element methods are two popular numerical methods that are widely practiced in solving the groundwater flow equation while other model variables properly implemented (Fig. 5.1). The Finite elements grid typed is widely used to express irregular model boundary and geological faults. However, the finite difference models are simpler to program, needs less data and ease for data entry, and display better mass conservation than finite-element options. The output of the model is hydraulic heads as the discretization grid cell specified. Models are widely used to enhance the understanding the nature of groundwater systems (Mercer & Faust, 1980).

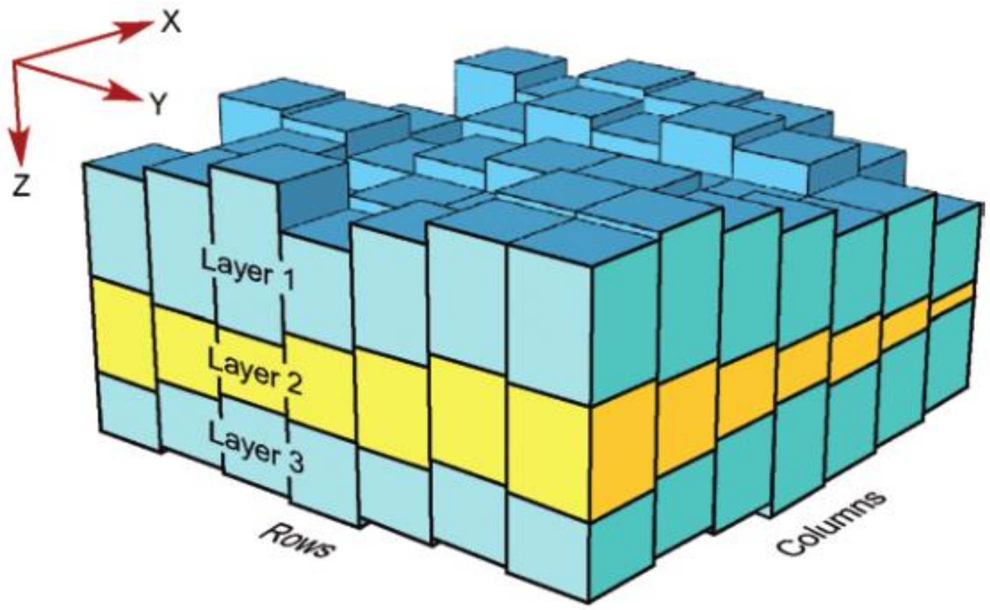

Fig. 5.1 Three-dimensional model domain in MODFLOW divided into layers and cells after (Adopted from Kresic & Mikszewski, 2013)

Generally, numerical groundwater flow model offer an approach to integrate available hydrogeological information into an inherently coherent mathematical illustration of a actual world or process and, thus, supportive investigating conceptual models or hypotheses of groundwater-flow systems (Konikow & Reilly, 1999). A three-dimensional groundwater-flow model was prepared for the groundwater flow system in the ALZLB based on the USGS computer program code MODFLOW–2000 (Harbaugh and others, 2000).

Therefore, the groundwater flow numerical model is essential to quantify its potential and understand the response of the groundwater system to anthropogenic activities and natural changes (stresses) and is a tool to support groundwater management. The purposes of this numerical model were to (1) simulate the of groundwater flow system in the ALZLB, (2) better understand the interaction between surface water systems, and (3) assess potential effects of groundwater development; irrigation expansion, and future projected climate change impact on water resources when linked to the WEAP model.

5.1.2. Numerical groundwater flow development process

The following Fig. 5.2 shows the recommended steps to follow in developing a groundwater flow model:

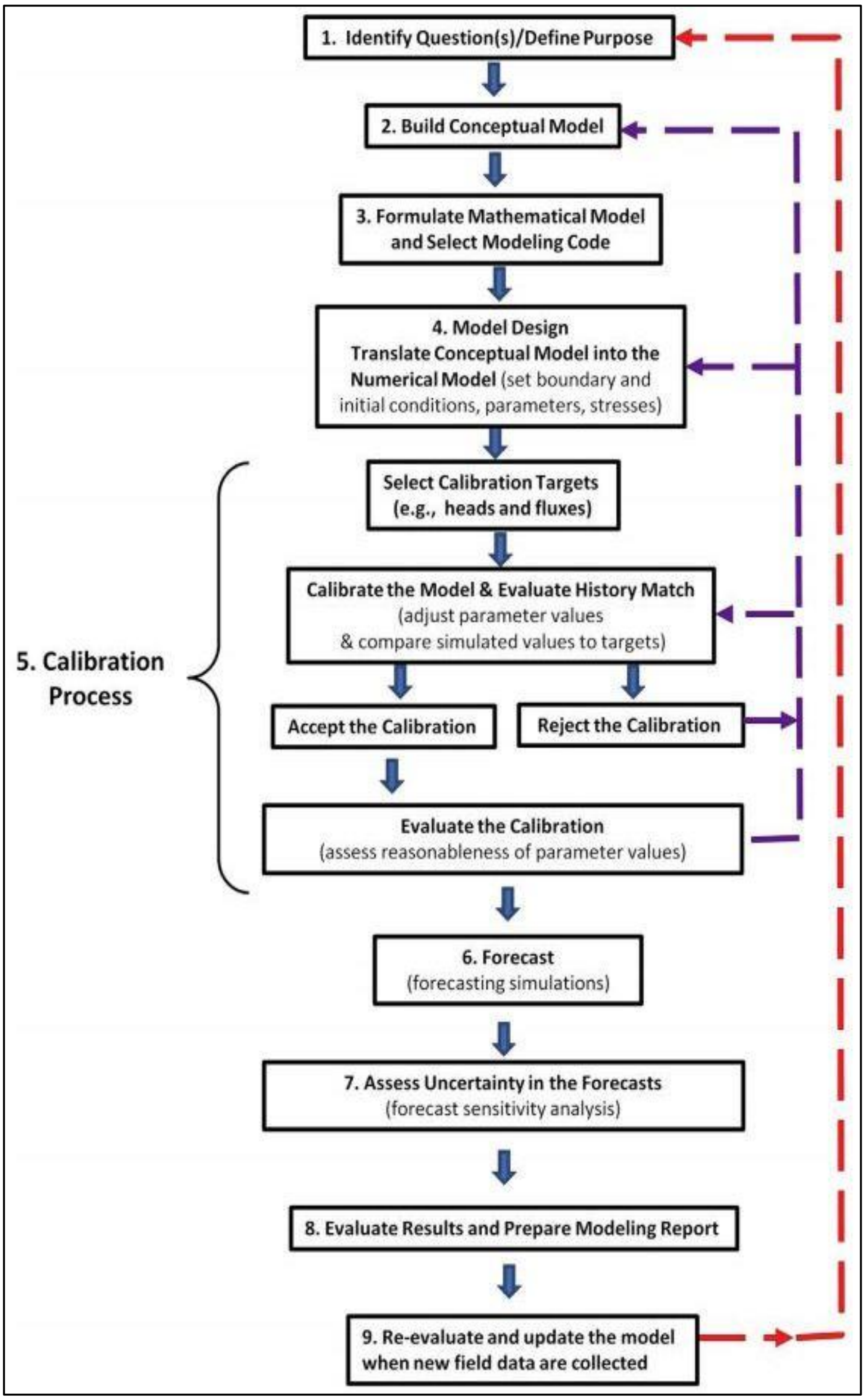

Fig. 5.2 General flow chart showing development process (after Anderson et al., 2015)

5.2. Building MODFLOW Model

5.2.1. Development of Conceptual Model

The first steps in building the Mudflow model begin with creating a conceptual model of the basin. A hydrogeological conceptual model is a qualitative illustration of multiple natural and human elements that control and provide to the dynamics of groundwater in the subsurface. It is address questions associated to the origin, potential, and dynamics of groundwater, hydrogeological properties of geological units, groundwater system behavior under various stresses both natural and anthropogenic (Kresic & Mikszewski, 2013).

Setting a modeling concept is the most crucial step of every modeling exercise. The proper familiarity with hydrogeology, hydrology, and groundwater movement in and around the area of interest is required. It is aimed to create a simplified model of the system to be simulated, by simplifying a system to an level that a logical model methods with suitable model procedures (Anderson & Woessner, 1992; Anderson et al., 2015; Kresic, 2007; Kresic & Mikszewski, 2013).

Developing a conceptual model for the groundwater-flow system in the ALZLB Basin requires the definition of the hydrogeologic framework: the identification of hydrogeologic units within the lacustrine and alluvial deposits and volcanic units that can be characterized as aquifers or as unconfining /confining units and grouped into aquifer systems. An additional part in this conceptual model is the geological structures. The presences of faults, especially in the escarpment of the basin, affect groundwater flow.

The second part of the conceptual model consists of the hydrologic behavior of the regional flow system in terms of shallow and deep flow, and regional divides.

The flow system is also characterized by sources of water (recharge, movement of water from surface water to groundwater, release of water from storage) and sinks (discharge to surface waters, pumping centers, addition of water to storage). The recharges in the highlands may emerge as springs at lithological contacts and faulted zones. There are varying amounts of sources and sinks in the case of lakes that may have a large influence on water levels and water movement. The third part of the conceptual model element is the connection of groundwater and surface water (Fig. 5.3). The pumping of groundwater can appreciably alter the natural pattern of local and regional discharge to the lakes in the region. This in turn, affects the levels of lake water.

The aquifers properties organized into the model was obtained from hydrologic data and geological studies. The top layer is considered as an unconfined aquifer whereas the bottom layer is considered a confined aquifer system. Finally, the calibration of the was carried out against the observed borehole data the manual method through the trial-and-error method.

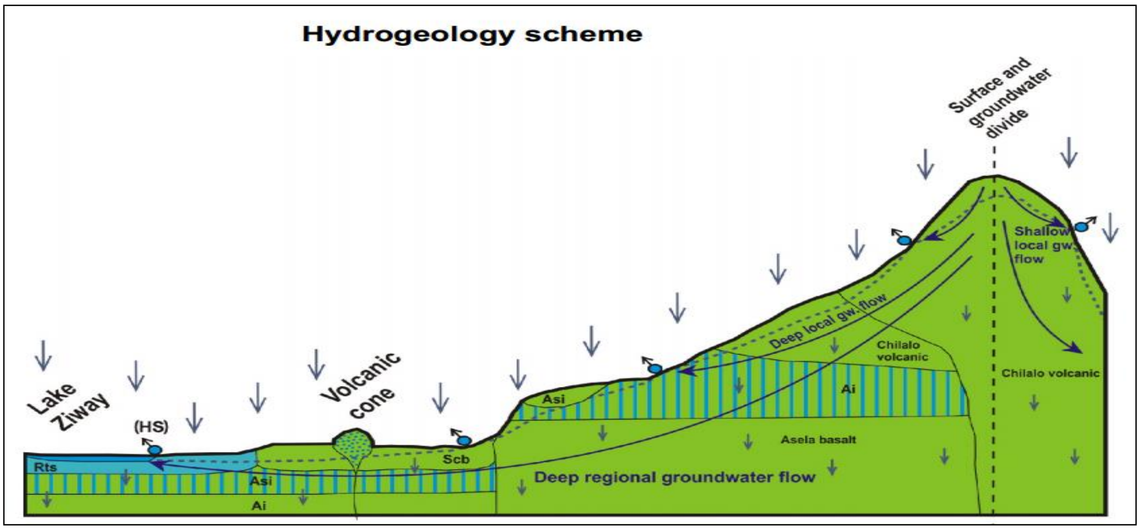

Fig. 5.3 Schematic Conceptual model for groundwater flow condition

5.2.2. General assumptions

The following assumptions were made based on the above schematic conceptual model:

1. The source water (groundwater, spring and rivers) in the basin is from precipitation in the both sides of the escarpments and plateau.

2. From the conceptual model the groundwater flow direction is directed towards the lakes. However, as it approaches the lakes the flow directed to the south to Lake Shalla.

3. There are assumption made that the occurrence of groundwater in western and eastern escarpment is because of the hydrological and hydrogeological properties within various geomorphological units and lakes.

- The groundwater recharge zone is considered western and eastern mountains and flow towards the lakes' region.
- Butajira Crescent is assume to be the recharged from runoff coming from the escarpment, and direct rainfall on the plain.

- Lake Ziway receives water form groundwater, surface water, and direct rainfall on the Lake Surface and outflows groundwater at its south-eastern sides and through Bulbula River.
- Lake Langano gain water from groundwater, surface water, and direct rainfall on the Lake Surface and outputs through Horakelo River and groundwater.

4. The main persistent rivers are Ketar and Meki are believed to have link to groundwater.

5.2.3. Governing flow Equations

Governing flow equations are a physically based mathematical models originated from Darcy's law and the law of conservation of mass (Konikow & Mercer, 1988). The equation assumes that a flow system that permits both horizontal and vertical flows via the aquifers system in three-dimensional outlines (Anderson & Woessner, 1992). The governing partial differential equation executed by the MODFLOW to designate the groundwater flow for a Steady-state condition, there is no change in the head with time, therefore, change in storage became zero, whereas for the transient condition when a change in storage with time exists.

Therefore, steady-state and transient flow equations are given in (5.1) and (5.2) respectively.

$$\frac{\partial}{\partial x}\left(K_{xx}\frac{\partial h}{\partial x}\right)+\frac{\partial}{\partial y}\left(K_{yy}\frac{\partial h}{\partial y}\right)+\frac{\partial}{\partial z}\left(K_{zz}\frac{\partial h}{\partial z}\right)-W=0 \qquad (5.1)$$

And for the transient model the equation became:

$$\frac{\partial}{\partial x}\left(K_{xx}\frac{\partial h}{\partial x}\right) + \frac{\partial}{\partial y}\left(K_{yy}\frac{\partial h}{\partial y}\right) + \frac{\partial}{\partial z}\left(K_{zz}\frac{\partial h}{\partial z}\right) - W = S_s\frac{\partial h}{\partial t} \qquad (5.2)$$

Where:

K_{xx}, K_{yy}, and K_{zz} are values of hydraulic conductivity in the x, y and z directions. Hydraulic conductivity (LT^{-1}), *h* is the hydraulic head (L), *W* is a volumetric flux per unit volume and represents Sinks and/or sources (T^{-1}), S_s is the specific storage of the porous material (L^{-1}), and *T* is time (T).

5.2.3. Model Design (Model domain and Specification)

In order to put the conceptual model in to suitable form of numerical model, model designing step is mandatory. This step in comprises the layout of the grid cells, simulation time steps, boundary and initial conditions, and preliminary selection of values of aquifer parameters and hydrologic stresses. The Finite-Difference grid model consisted of two layers made up of 90 rows-oriented East to West and 95 columns-oriented North to South with equal 1500m grid-cell dimension. The thicknesses of the aquifers vary from 150m to 200m, and 250m to 300m in the rift floor to the highland for the top layer and bottom layer respectively.

5.2.3.1. Boundary conditions

The model boundary conditions delineated by defined hydraulic heads, flux and head dependents flux. It determines the flux of water enter and leave the model domain. Similarly, in the study basin, the groundwater flow system is mainly controlled by geologic and hydrologic boundaries. Hence No-flow boundary is used to determine the geographic extent of the groundwater flow system and inflows and outflows along the model boundary and the general head boundary is used to represent the groundwater outflow and inflow depending on the head at the boundary in the southern part of the model domain.

In general, there are three types groundwater model boundary domain (Anderson et al., 2015).

- Specified (constant) head boundaries (which are examples of Dirichlet or first-type boundary conditions). A specified head boundary is implemented by fixing head values at the nodes along the boundary; hence, specified boundary heads do not change in response to hydrologic stresses.

  $$H = h_{(t)} \qquad (5.3)$$

  Example: Direct surface water-groundwater connection, lakes

- Specified flux boundaries (which are examples of Neumann or second-type boundary conditions)

  $$q = q_{(t)} \qquad (5.4)$$

  Example: impermeable bodies (No flow); wells; recharge

- Mixed or Head-dependent flux boundaries (which are examples of Cauchy or Type-three boundary conditions)

  $$q = C(h_0 - h_i) \qquad (5.5)$$

Indirect connection (e.g., river/lake, leaky aquifers, drains, distant boundary), C= hydraulic conductance of the boundaries, h=heads, q=discharge or recharge flux and ho and hi = hydraulic head outside and inside the model boundary respectively.

River Leakage:

Discharge to streams was simulated using the Modflow River packages (Harbaugh, 2005). Perennial streams were represented with the River package. The River package simulates the connection between surface water and groundwater. The hydraulic conductance between the streambed and aquifer (streambed conductance) is defined as the hydraulic conductivity of the riverbed material times the cross-sectional area of the stream reach divided by the streambed thickness (McDonald & Harbaugh, 1988). River cells can remove water from or add water to the aquifer depending on the direction of the gradient between river stage and aquifer hydraulic head. Initially, a cell representing perennial stream depending on the order of rivers streambed hydraulic conductance given ranging from 8.0m/s to 0.43m^2/s was assigned.

The mathematical expression for the river package is given as follows:

$$Q_{RIV} = C_{RIV} * (H_{RIV} - h) \qquad h > R_{BOT} \qquad (5.6)$$

$$Q_{RIV} = C_{RIV} * (H_{RIV} - R_{BOT}) \qquad h \leq R_{BOT} \qquad (5.7)$$

$$C_{RIV} = \frac{(K * L * W)}{M} \qquad (5.8)$$

Where,

$Q_{RIV} -$ $Rate\ of\ leakage\ between\ the\ river\ and\ the\ aquifer, (L^3T^{-1})$

$C_{RIV} - \ Hydraulic\ conductance\ of\ the\ river\ bed, (L^2T^{-1})$

$H_{RIV} - Head\ in\ the\ river, (L)$

$h - \ Hydraulic\ head\ in\ cell, (L)$

$R_{BOT} - \ Elevation\ of\ the\ bottom\ the\ riverbed\ (L)$

$K - \ Hydraulic\ conductivity\ of\ the\ riverbed\ material, (LT^{-1})$

$L - Length\ of\ the\ river\ within\ a\ cell, (L)$

$W - \ Width\ of\ the\ river, (L)$ and,

$M - \ Thickness\ of\ the\ riverbed, (L)$

The outside of the model sub-basin was considered as a special type of Specified flux boundaries (which are examples of Neumann or second-type boundary conditions). It is specified as an inactive boundary cell (no flow boundary) except in a few extents in the southern part where the groundwater outflow is evident (Ayenew, 1998) and treated as the general head boundary (Fig. 5.4). For the initial model input purpose, river properties (depth, width, and hydraulic conductivity) were estimated as shown in Table 5.1. However, these values are subjected to be modified during model calibration process.

Table 5.1 Estimated stream properties

Elevation(m)	Depth (m)	Width(m)	Kc	
>2500	1	3	Similar to the underlain aquifers	
2500-2000	2	5	“	
<2000	3	10	“	

General Head Boundary

The head-dependent boundary was simulated using Modflow packages of the General Head Boundary (GHB) Package (Harbaugh, 2005). It simulates a source of water outside the model area that removes water from or adds water to adjacent cells depending on the hydraulic-head difference between the source and the model cell (McDonald & Harbaugh, 1988). In the study area, groundwater outflow in the southern part from the model boundary shown in (Fig. 5.4) and general head boundary condition is implemented to estimate the amount of outflow.

The rate of flow water between the model cell and the outside source or sink is given by equation (5.9)

$$Q = C(HB - h) \quad (5.9)$$

Where, Q is the rate of flow into or out of the model cell [L^3/T], HB is the head assigned to the external source or sink [L], h is the hydraulic head within the model cell [L] values of C. (Where, C=KL), where K is the hydraulic conductivity between the model cell & the boundary head [L/T], and L is the length of the general head boundary within a cell. For initial the value of C is 9.5m^2/day for the top layer and 6m^2/day for the bottom layer.

5.2.4. Model parameter

5.2.4.1. Hydraulic properties

During groundwater modeling, it is a very challenging activity to obtain realistic hydraulic conductivity values at appropriate spatial distribution in the field, preferably by pumping tests. So that, hydraulic conductivity is often the most important and variable modeling parameter (Kresic, 2007). The initial horizontal hydraulic conductivity of the basin is compiled from different literature (Ayenew, 1998; Dereje, 2011; Kumo, 2006). Based on the above sources the horizontal hydraulic conductivity values were shown in the (Fig. 5.5). The highest hydraulic value is assigned to the ignimbrite unit at the eastern escarpment and followed by and the rift floor alluvial-lacustrine deposits where primary porosity plays a significant role in groundwater storage and transmission.

The least value was given to balchi with insignificant areal coverage. The vast Oligocene-Early Pliocene Volcanites and Late Miocene-Pliocene Volcanites groups of rocks located at the highlands in both sides (at Eastern and western) have been assigned value of 5-10 and 0.1-1m/day at initial stage and later will be changed through calibration processes. However, there are locally higher or lower hydraulic conductivity values than the hydraulic conductivity zones shown in the (Fig. 5.5).

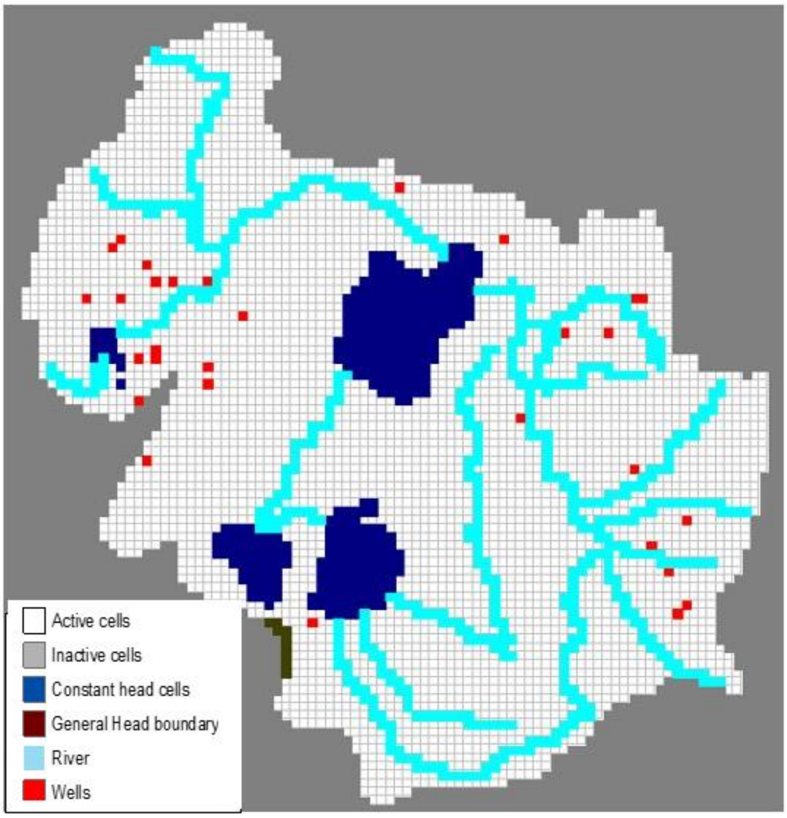

Fig. 5.4 Boundary conditions of the model domain

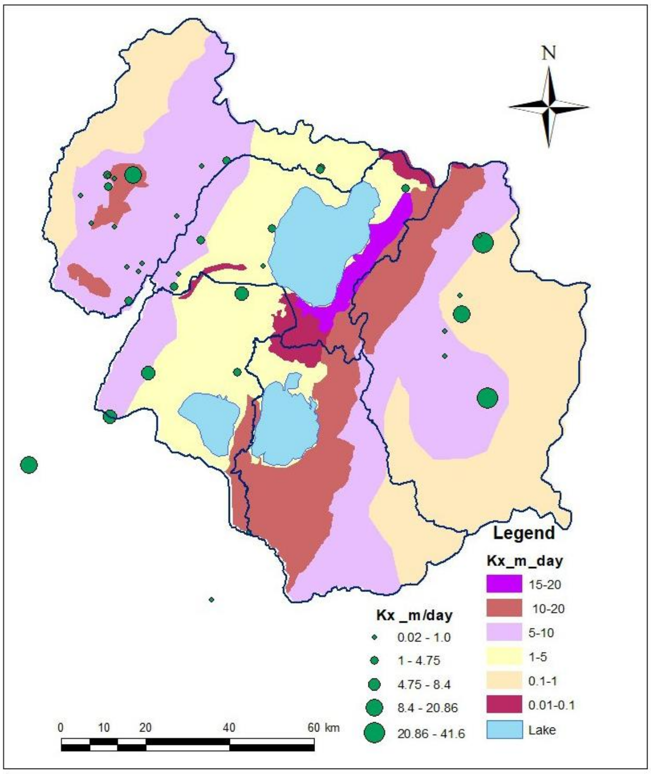

Fig. 5.5 hydraulic conductivity map of the study basin

5.2.4.2. Groundwater Recharge Zones

Groundwater recharge rate is one of the most variable and yet the most important parameter in groundwater modeling, despite its difficulty to accurately measure and estimate it because it occurs in a wide spatio-temporal dimension. In the case of the study basin, the major source of recharge to the aquifer comes from precipitation and river channel losses.

As the main recharge mechanism, direct or diffuse recharge is supposed to take place in almost areas of the basin with exception to where low permeable lacustrine soil (diatomite) exists in the rift floor, around Lake Ziway (OWWDSE, 2016). According to Ayenew(2003) the mean annual recharge estimated using catchment soil-water balance mode with 50mm soil moisture-holding capacity is about 10% and 13% of precipitation for Ketar and Meki subbasins respectively. In another study by (EWTC, 2008) the average annual recharge assessed using the chloride mass balance method at Butajira (Meki subbasin) and Ziway area were about 10% and 0.068% of the precipitation respectively). According EWTC (2008) recharge estimates from different methods were summarized as Table 5.2.

Table 5.2 Summary recharge estimates using different methods

Subbasin	WEAP model	Simple water balance method	Bucket model	Chloride method	Average
Ketar	4.6	-	1	-	3%
Meki	10%	13%	13%	10%	12%
Rift floor	-	-	-	0.68%	

Existing studies on groundwater recharge estimated about 5% and 1% of rainfall at the highlands and lowlands area (Legesse et al., 2003) respectively. Hence for this study groundwater recharge was estimated using topographic regions that were higher than 2000m above sea level (asl), 1750-2000m asl and lower than 1750m asl their rates of recharge were estimated as 5%, 3%, and 1%, respectively. In this study the initial recharge has been allocated in the model ranges from 3.86×10^{-5} to 3.1×10^{-4} m/day based on the topographic zones (Fig. 5.6). The least recharge is in areas where less permeable clay and lacustrine soils exist. Much of the watershed highland plateaus and the permeable volcanic areas get the maximum recharge.

5.2.4.3. Initial and Prescribed Hydraulic Heads

For this model, the initial hydraulic head was generated using interpolation of static groundwater elevation from observations to characterize the initially prescribed head and it is used as the initial condition in the system at the beginning of the simulation (Fig. 5.7).

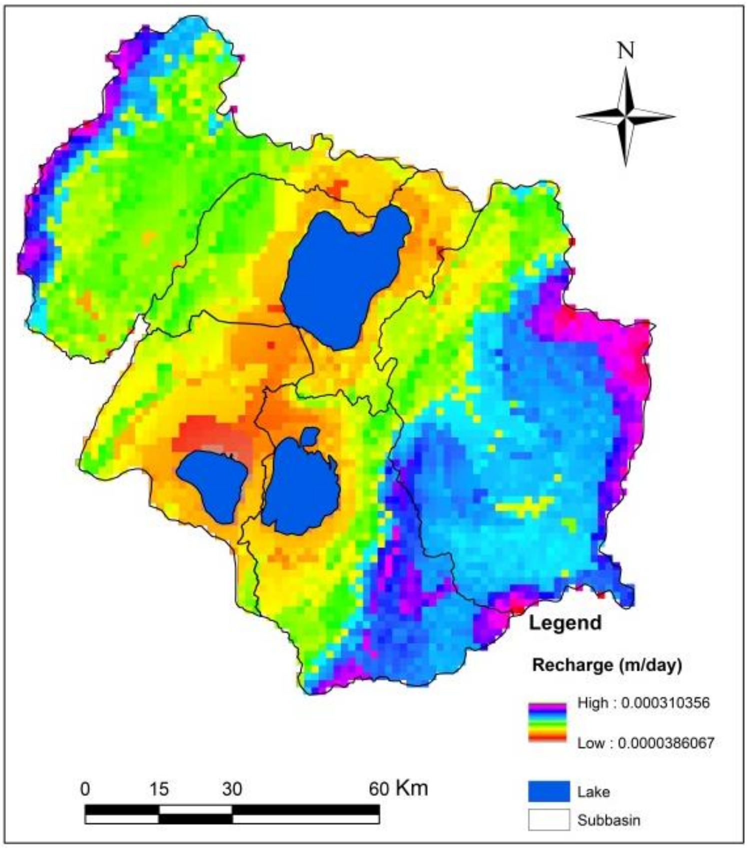

Fig. 5.6 Recharge estimation map

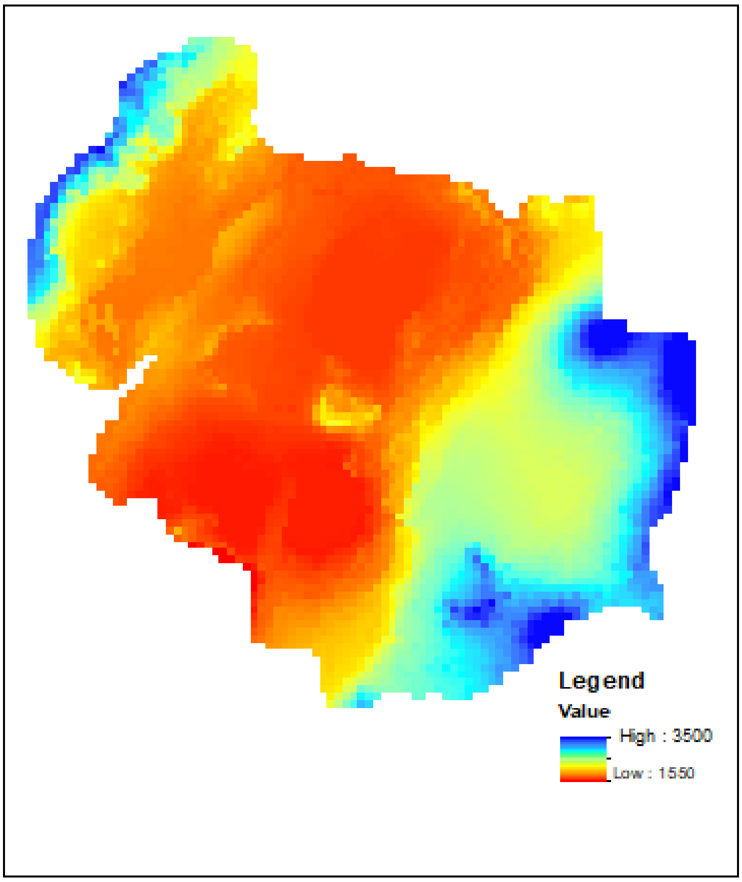

Fig. 5.7 Initial hydraulic head of the basin

5.2.5. Model calibration

The study basin groundwater flow model was calibrated using the trial-and-error technique by altering initial estimates of aquifer properties hydraulic conductivities, recharge, and discharge to become the best fit among simulated hydraulic heads and observed water levels. It was calibrated under steady-state condition.

The overall mean variance between simulated and observed heads was expressed, as given in (Anderson & Woessner, 1992) using statistical comparison. These are commonly used statistical comparison criteria: Mean Error (ME), Absolute Mean Error (AME), Root Mean Squared Error (RMSE), Nash-Sutcliff coefficient (NSE), and Coefficient of Determination (R^2).

1. **The mean error (ME)** is the mean differences between measured heads (h_m) and simulated heads (h_s)

$$ME = \frac{1}{n}\sum_{i=1}^{n}(h_i{}^m - h_i{}^s) \qquad (5.8)$$

Where $\boldsymbol{h_m}$ is measured head, $\boldsymbol{h_s}$ is calculated head and $\boldsymbol{n}$ is number of head measurements.

2. **The mean absolute error (MAE)** is the mean of the absolute value of the differences in measured and simulated heads.

$$MAE = \frac{1}{n}\sum_{i=1}^{n}|h_i{}^m - h_i{}^s| \qquad (5.9)$$

3. **The root mean square (RMS)** error or the standard deviation is the mean of the squared differences in measured and simulated heads and can be calculated using the equation.

$$RMSE = \sqrt{\frac{1}{n}\sum_{i=1}^{n}({h_i}^{m} - {h_i}^{s})^2} \qquad (5.10)$$

Since RMS is a measure of differences between the observed and simulated data, lower number reflects a better model fit.

Normalized RMSE

$$RMSE = \frac{\sqrt{\frac{1}{n}\sum_{i=1}^{n}({h_i}^{m} - {h_i}^{s})^2}}{{\bar{\mathrm{h}}_i}^{m}} \times 100\% \qquad (5.10)$$

Where $\boldsymbol{h_i^m}$ is measured hydraulic head; $\boldsymbol{\bar{h}_i^m}$ is obseved average hydraulic head; $\boldsymbol{h_i^s}$ is simulated hydraulic head; $\boldsymbol{\overline{h}_i^s}$ is average simulated hydraulic head at i and $\boldsymbol{n}$ is number of head measurements.

5.3. Result and Discussion

5.3.1. Model calibration

The objective of model calibration is to obtain parameter values that minimize the difference between calculated and field measured variables by changing model input values in an effort to match simulated and actual conditions within an acceptable range. Model calibration is usually an iterative process that attempts. The major parameters to be adjusted or modified during model calibration were the hydraulic conductivity and groundwater recharge flux inputs. Finally, the simulated hydraulic conductivity and recharge flux were presented in (Fig. 5.8) and (Fig. 5.9).

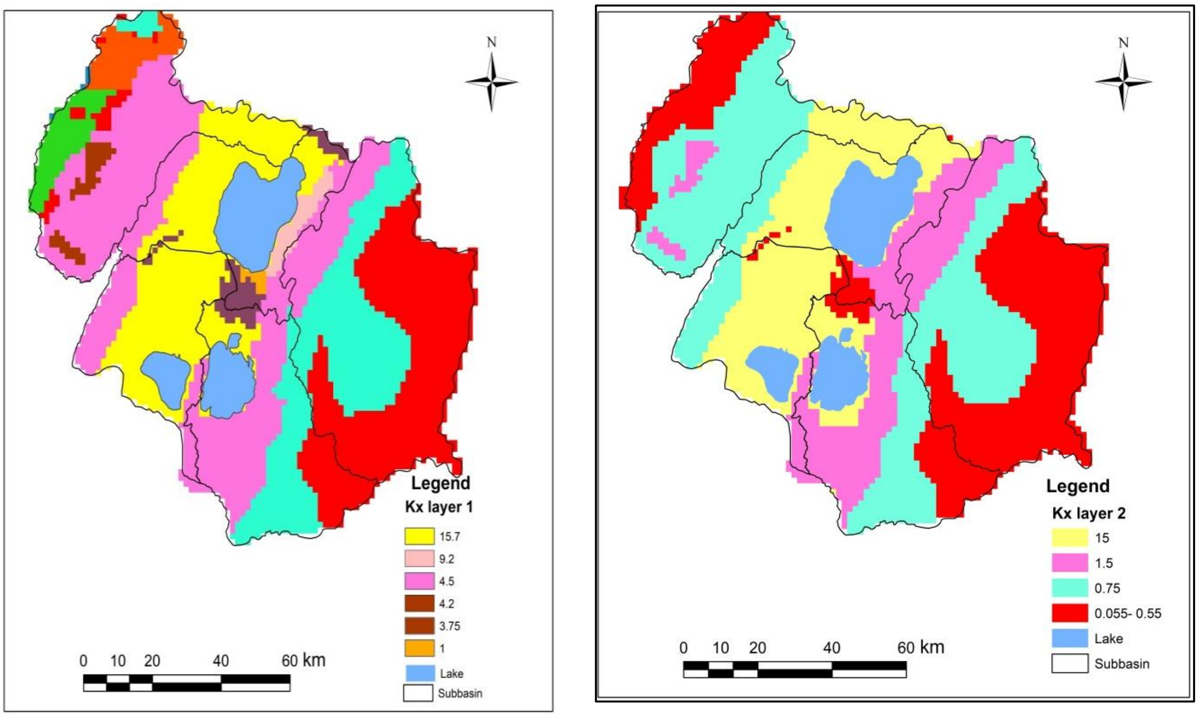

Fig. 5.8 Simulated hydraulic conductivity of layer 1 and layer 2

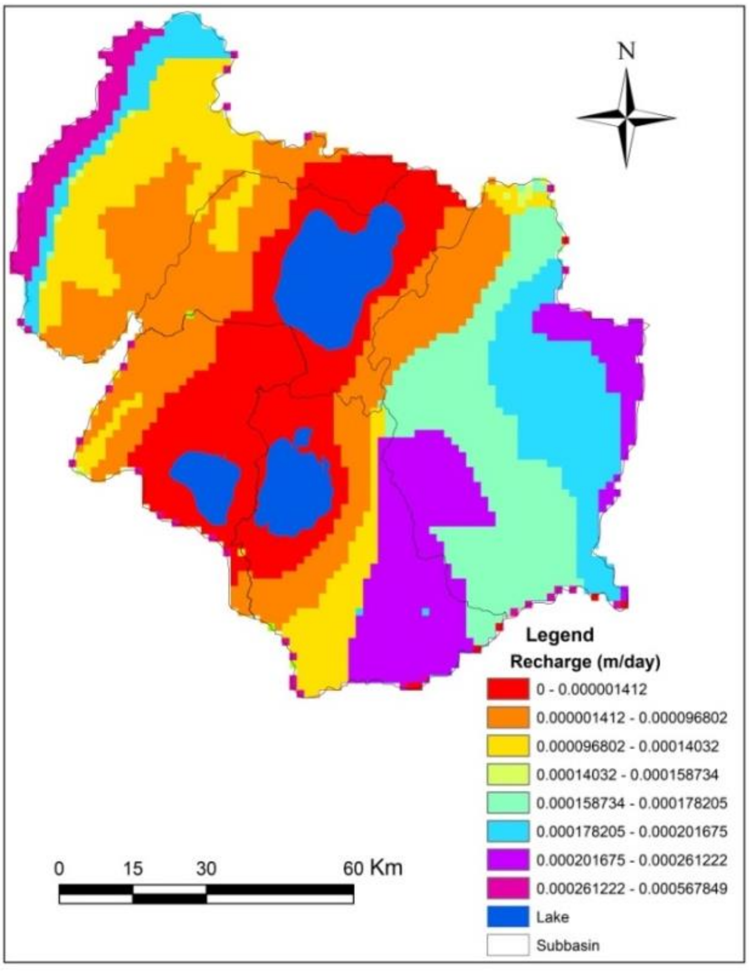

Fig. 5.9 Simulated recharge flux

5.3.1.1. Steady-state model simulation

The model performance was assessed by (1) model performance statistics (2) comparison of groundwater hydraulic heads of simulated and observed data as scatter plot or spatial distribution (3) histogram of residuals estimated. The calibrated result indicated that the performance statistics between the simulated groundwater head and observed head of 163 observations were presented in Table 5.3 and (Fig. 5.10). These, model performance statistics showed that a good-fit between simulated and measured heads. The simulated hydraulic head distribution for layer 1 and layer 2 are presented in (Fig. 5.12). The groundwater flow contours gradient showed groundwater flow direction in the aquifers and subdued replica of the basin topographic configuration. The comparison of simulated and observed groundwater heads were presented in Fig. 5.13. The result of histogram residual error was shown in (Fig. 5.11). The histogram residual of simulated and observed hydraulic heads revealed that 65% and 82% of wells were found to be bounded within $\pm$20m and $\pm$30m error, respectively.

Table 5.3 Model performance statistics

Model performance Statistic	Unit	Value
R^2	-	0.98
NSE	-	0.97
ME	meter	-8.3
MAE	meter	17.5
RMSE	meter	21.9
NRMSE	%	1.28%

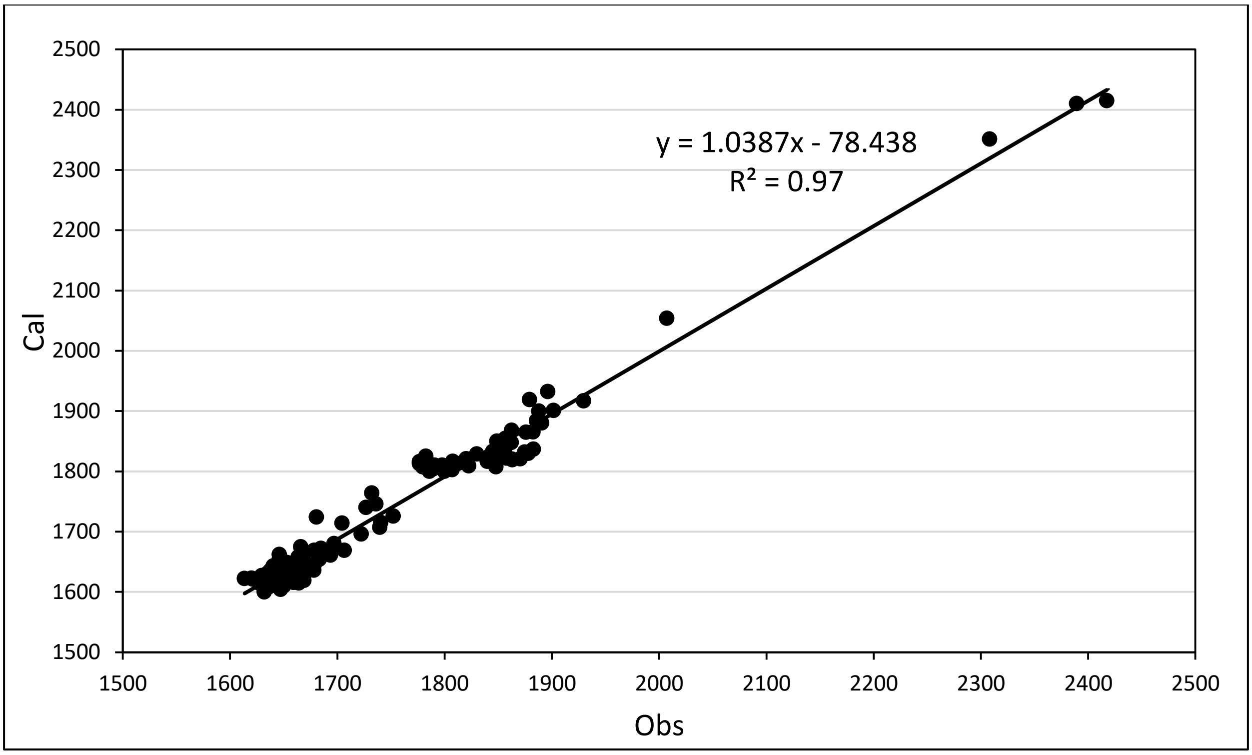

Fig. 5.10 Linear regression of observed and simulated heads

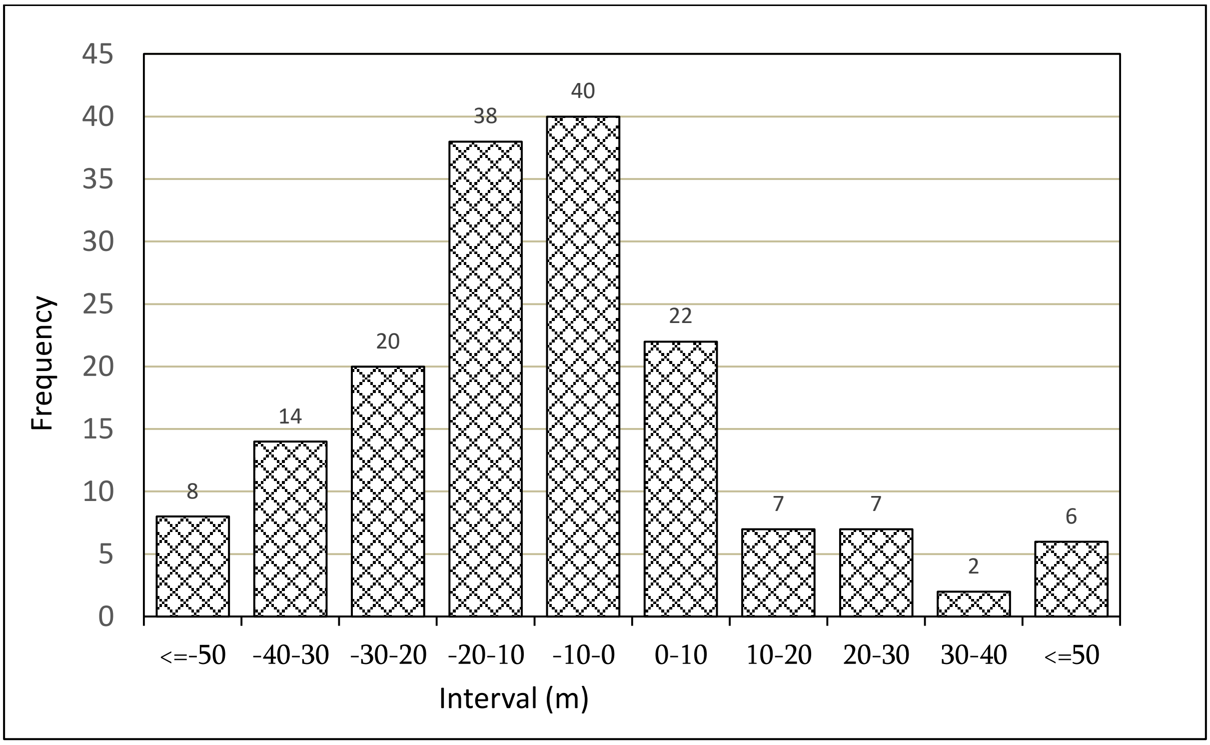

Fig. 5.11 Histogram of residuals of estimated

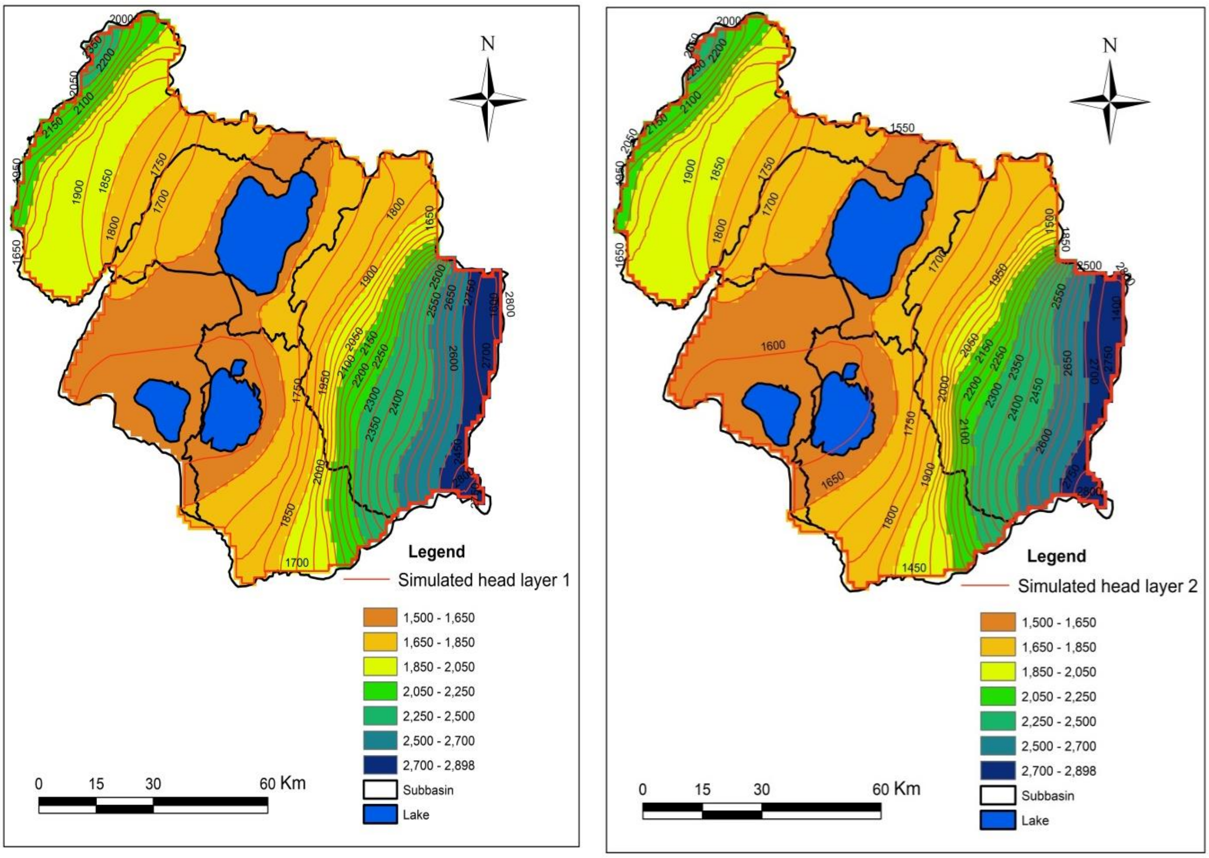

Fig. 5.12 Simulated hydraulic head distribution of steady state for layer 1 and layer 2

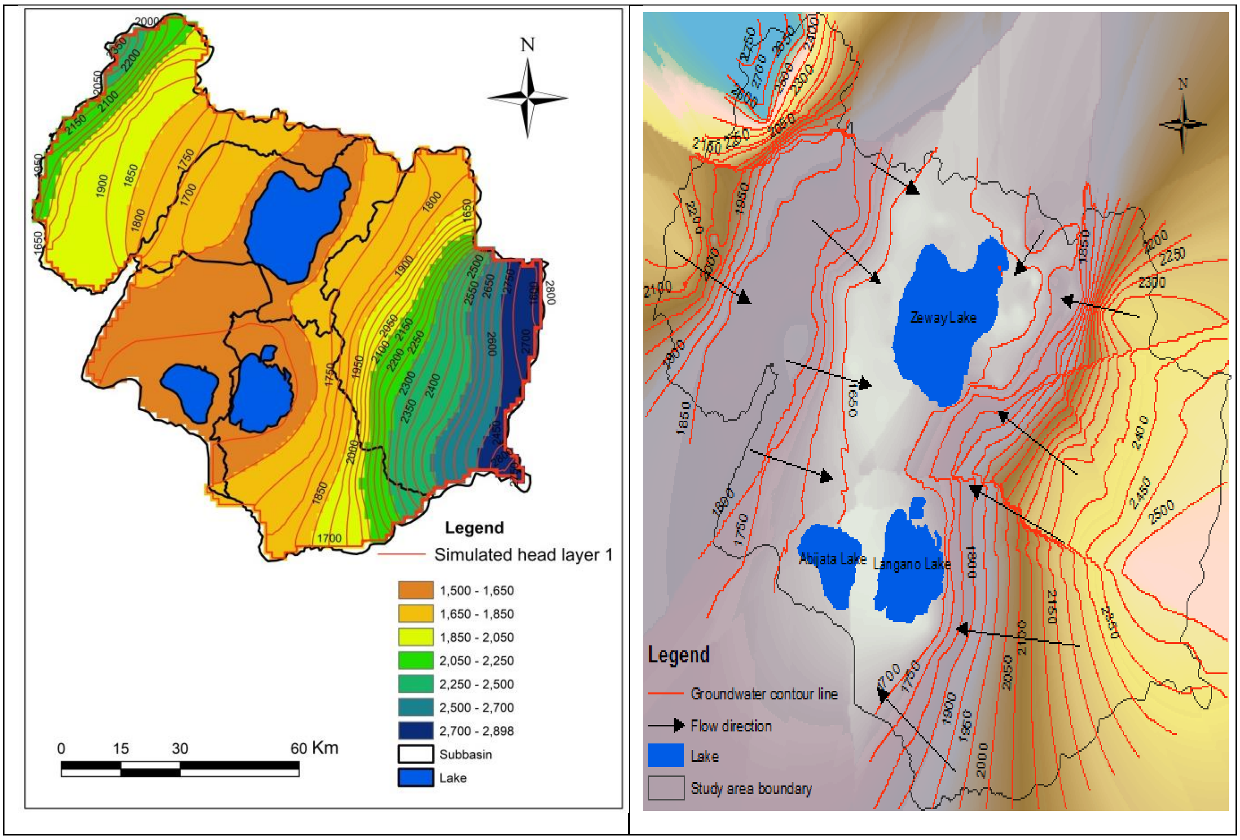

Fig. 5.13 Simulated and observed groundwater head

5.3.2. Model sensitivity Analysis

After model calibration attained optimum level, sensitivity analysis is carried out to measure the uncertainties in model that arise from input variables, stress, and boundary conditions (Anderson & Woessner, 1992). A sensitivity analysis is used to evaluate the response of the calibrated model to a range of values for different input parameters. It helps to identify model parameters that have the highest effect on the model result. The findings of the study can be used to direct future data collection activities aimed at reducing model errors.

It is achieved by changing one input parameter's value while holding the others constant. Sensitivity is the difference in the relative rate of a selected output as a result of a unit change in the input. The model is more responsive to the input that causes the most change in output. The model responses to the input variables are also governed by the model setup. For example, a model with high permeability is more sensitive to recharge than its corresponding low permeability. A sensitivity analysis of a groundwater model on aquifer parameters may help to better understand the overall efficiency of the model. During model calibration, sensitivity analyses are helpful in defining initial estimates of input parameters. When the model is more responsive to an input parameter, additional data on that parameter can enhance the model calibration statistics. In this study to assess model sensitivity, an increase or a decrease of a certain percent of horizontal hydraulic conductivity and groundwater recharge rate were used. And the corresponding outputs of hydraulic heads were compared against the observed hydraulic heads and model performance metrics to assess model sensitivity for each parameter.

The sensitivity analysis result indicated that a slight change in either the hydraulic conductivity values of the aquifers or in recharge impacts significantly the groundwater head distribution in the basin. The model is responsive for increase or decrease in both hydraulic conductivity and recharge input parameters. However, the model is more responsive to an increase in recharge flux than the same magnitude increases in hydraulic conductivity (Fig. 5.14).

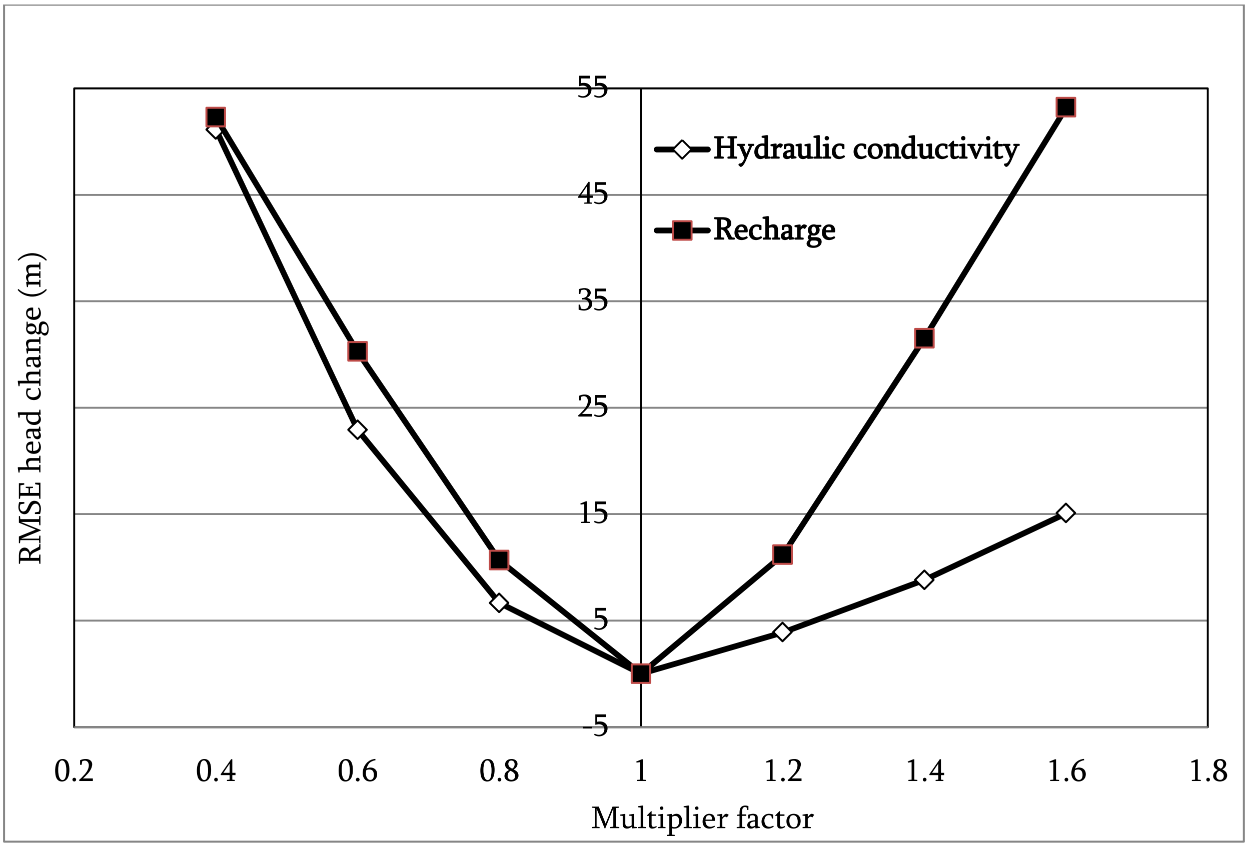

Fig. 5.14 Sensitivity analyses of hydraulic conductivity and recharge

5.3.3. Groundwater balance

The model computes the water budget between the sum of inflows and outflows through the aquifer system of the entire model domain. It is an indirect way of checking the model capability by computing the water budget of each flow term in comparison with the total simulated inflows and outflows of the entire model domain. The inflow term comprises constant head, general head boundary, and river leakage whereas, the outflow term contains constant head, general head boundary, river leakage and wells (abstraction) under natural conditions. The model result showed that both inflow and outflow components were consistent with the steady-state modeling condition at a discrepancy of -0.75 (Table 5.4). The water budget of the layer -1 and Layer-2 are shown in table.5.5 and Table 5.6.

Table 5.4 Water budget of the entire study basin

WATER BUDGET OF THE WHOLE MODEL DOMAIN:

FLOW TERM	IN	OUT	IN-OUT
STORAGE	0.0000000E+00	0.0000000E+00	0.0000000E+00
CONSTANT HEAD	2.4593317E+05	1.4222762E+06	-1.1763431E+06
WELLS	0.0000000E+00	1.6293270E+04	-1.6293271E+04
DRAINS	0.0000000E+00	0.0000000E+00	0.0000000E+00
RECHARGE	1.2205944E+06	0.0000000E+00	1.2205944E+06
ET	0.0000000E+00	0.0000000E+00	0.0000000E+00
RIVER LEAKAGE	8.8733083E+02	1.9116510E+04	-1.8229180E+04
HEAD DEP BOUNDS	0.0000000E+00	2.0778653E+04	-2.0778652E+04
STREAM LEAKAGE	0.0000000E+00	0.0000000E+00	0.0000000E+00
INTERBED STORAGE	0.0000000E+00	0.0000000E+00	0.0000000E+00
RESERV. LEAKAGE	0.0000000E+00	0.0000000E+00	0.0000000E+00
SUM	1.4674149E+06	1.4784646E+06	-1.1049750E+04
DISCREPANCY [%]	-0.75		

Table 5.5 Water budget of layer-1

WATER BUDGET OF LAYER 1

FLOW TERM	IN	OUT	IN-OUT
STORAGE	0.0000000E+00	0.0000000E+00	0.0000000E+00
CONSTANT HEAD	1.0203565E+05	1.2808739E+06	-1.1788382E+06
HORIZ. EXCHANGE	0.0000000E+00	0.0000000E+00	0.0000000E+00
EXCHANGE (UPPER)	0.0000000E+00	0.0000000E+00	0.0000000E+00
EXCHANGE (LOWER)	6.2322428E+05	6.3750075E+05	-1.4276472E+04
WELLS	0.0000000E+00	1.6293270E+04	-1.6293271E+04
DRAINS	0.0000000E+00	0.0000000E+00	0.0000000E+00
RECHARGE	1.2256769E+06	0.0000000E+00	1.2256769E+06
ET	0.0000000E+00	0.0000000E+00	0.0000000E+00
RIVER LEAKAGE	8.8441306E+02	2.1701840E+04	-2.0817428E+04
HEAD DEP BOUNDS	0.0000000E+00	6.5097116E+03	-6.5097114E+03
STREAM LEAKAGE	0.0000000E+00	0.0000000E+00	0.0000000E+00
INTERBED STORAGE	0.0000000E+00	0.0000000E+00	0.0000000E+00
RESERV. LEAKAGE	0.0000000E+00	0.0000000E+00	0.0000000E+00
SUM OF THE LAYER	1.9518212E+06	1.9628795E+06	-1.1058250E+04
DISCREPANCY [%]	-0.56		

Table 5.6 Water budget of layer-2

WATER BUDGET OF LAYER 2

FLOW TERM	IN	OUT	IN-OUT
STORAGE	0.0000000E+00	0.0000000E+00	0.0000000E+00
CONSTANT HEAD	0.0000000E+00	0.0000000E+00	0.0000000E+00
HORIZ. EXCHANGE	0.0000000E+00	0.0000000E+00	0.0000000E+00
EXCHANGE (UPPER)	6.3750075E+05	6.2322428E+05	1.4276472E+04
EXCHANGE (LOWER)	0.0000000E+00	0.0000000E+00	0.0000000E+00
WELLS	0.0000000E+00	0.0000000E+00	0.0000000E+00
DRAINS	0.0000000E+00	0.0000000E+00	0.0000000E+00
RECHARGE	0.0000000E+00	0.0000000E+00	0.0000000E+00
ET	0.0000000E+00	0.0000000E+00	0.0000000E+00
RIVER LEAKAGE	0.0000000E+00	0.0000000E+00	0.0000000E+00
HEAD DEP BOUNDS	0.0000000E+00	1.4276435E+04	-1.4276436E+04
STREAM LEAKAGE	0.0000000E+00	0.0000000E+00	0.0000000E+00
INTERBED STORAGE	0.0000000E+00	0.0000000E+00	0.0000000E+00
RESERV. LEAKAGE	0.0000000E+00	0.0000000E+00	0.0000000E+00
SUM OF THE LAYER	6.3750075E+05	6.3750069E+05	6.2500000E-02
DISCREPANCY [%]	0.00		

The calibrated result of steady-state water balance revealed that simulated groundwater recharge was about 445MCM. Whereas, the initially, estimated groundwater recharge was 555MCM. The major inflows into groundwater components were groundwater recharge and constant head boundary and they account for 445MCM/year and 90MCM/year, respectively. On the other hand, the major groundwater outflow (discharge) was a constant head boundary and simulated to be 519MCM/year.

5.4. Model limitations

The study basin is made up of volcano-sedimentary rock groups highly modified /impacted/ by volcano-tectonic events since its formation to now. This creates variable hydrogeological and hydrological parameters. Besides, these information limitations, the numerical groundwater model is a device intended to approximate the field scale conditions of groundwater with a reasonable limit. It may not reproduce the complexity of nature as a whole. Hence, the following limitations may apparently exist:

- The hydrogeological properties of the basin are mainly inherited from its geologic nature which leads to high variable hydraulic conductivities (the geometry) and structurally controlled systems.
- Variable recharge rate because of hydraulic property of the aquifers and recharge mechanisms, despite receiving a similar amount of rainfall.
- Boundary conditions (pertinent to hydrogeological properties and fractures).
- Recharge rate (recharge mechanisms and aquifer properties, climate, soil, geomorphic and landuse characteristics).

- Conceptual model, since numerical groundwater flow model is a simplified form of the reality to approximate groundwater flow conditions.
- Spatial discretization (1500m*1500m) de-emphasizes detailed variability of the aquifers. In addition, the practice of using hydraulic heads measured at site-specific to compare with simulated heads which average the cell size of flows and heads during calibration of the model.
- Simultaneous calibration of fluxes and conductivities may bring uncertainties.

6. Linking Surface Water and Groundwater Models

6.1 Introduction

Integrated water resource management always plays a significant role in garnering maximum benefit sought from available water resources in environmental and socio-economic aspects. The demand for freshwater is increasing at an alarming rate globally (Davies & Simonovic, 2011). The situation in the ALZLB is not different from the global context and it has been experiencing a steady increase in demand for freshwater that arises from growing population and socio-economic activities in the basin. Moreover, it is accompanied by global climate change and dynamics of landuse and land cover conditions. These could impose impact/stress/ on available water unless proper water resources management is implemented.

While studying water resources management, isolating surface water and subsurface water systems may not yield a wanted result. Because both surface water and subsurface water systems interact together in the earth's hydrologic system despite the modeling inadequacy in dealing as a comprehensive system. Hence, to implement integrated water resources management approach, some sort of coupling/ linking between surface water and groundwater model is often required to address issues related to water resources management holistically. However, there is no similar study was performed in the ALZLB.

WEAP embedded groundwater modeling has limited capabilities, WEAP simulates the aquifer as "water reservoir" (lumped), overlooking the interaction of surface and groundwater interactions (Ahmadi et al,.2018; Dehghanipour et al,.2019). MODFLOW model is needed to simulate these interactions. MODFLOW is used to model groundwater systems because of its high capability, numerous modules, and its ability to capture the interaction between river flow and underlying aquifers. The coupling of WEAP-MODFLOW has the advantage of simulating complex cases (Sieber & Purkey, 2015). The dynamic link of the WEAP-MODFLOW models gave a configuration to investigate the interaction between groundwater and surface water management, and conjunctive use management scenarios that may have policy implication on demand and supply management that would impact the water resources (Ahmadi et al,.2018).

Therefore, this study involves the development of Water Evaluation and Planning System (WEAP) models for surface water and the numerical groundwater flow model (MODFLOW) for subsurface water simulation. The Linking processes were carried out after calibrating the standalone models. The linking has to address that the correct assignment of the outputs of the WEAP model to the corresponding MODFLOW grid cells as well as the outputs of the MODFLOW model to WEAP objects and has been carried out using LinkKitchen software (BGR, 2013; Huber, 2013) for exploring and implementing scenario analysis. Such linking of WEAP-MODFLOW had been practiced in the Arab countries in Syria, Morocco (Droubi et al., 2008) and found a proven method for water resources management. A similar study (Berehanu, 2017) was carried out in the Awash basin, Ethiopia and to address the water supply-demand challenge in Addis Ababa City and found viable results by implementing integrated supply and demand management with different population growth and climate change scenarios.

Finally, the linked WEAP-MODFLOW model was used for Water Resources System Simulation (WRSS) modelling that supports to examine the connection between available water resources and the demand various scenarios. Since Modelling water resources are a prerequisite and an integral part of water resource management scenario analysis for which various basic software system can be used depending on the specific objectives at hand (Ahmadi et al., 2018).

6.2. WEAP-MODFLOW Simulation

This approach includes steps through which linkages between WEAP and MODFLOW model are implemented to examine interacting components. A schematic illustration of WEAP-MODFLOW model is presented in (Fig.6.1). Interacting components: the topsoil layer, the aquifers, rivers, and reservoirs are spatially discretized to calculate water balance in the coupled model.

The preparation of linkage shapefile and filling with necessary parameters requires advanced GIS skills and very time-consuming activity. However, without the prerequisite for further use of GIS and spreadsheet software, the interface between WEAP and MODFLOW was supported using LinkKitchen Software, which was originated and was funded by the Federal Institute for Geosciences and Natural Resources (BGR) in Hanover, German, (www.bgr.bund.de).

According to Dehghanipour et al., 2019; Droubi et al., 2008; MaBmann et al., 2010; Maßmann et al., 2012, implementation of the GW flow model in MODFLOW involves preparation of various input files, one for each MODFLOW “package”. The GW flow grid

(Fig. 2) is implemented via the Basic and Discretization packages, spatially variable aquifer parameters and properties are specified via the Block-Centered flow package, and interactions with the other model components are implemented using Recharge, Well, River and Drain packages. Lateral GW flow through the aquifer boundaries was specified using computed flows.

The coupling of MODFLOW and WEAP is achieved via a GIS shape file that maps MODFLOW grid cells to WEAP spatial elements, i.e. catchment and GW nodes in each subbasin and river elements. The shape file's attribute table has a record for each active MODFLOW grid cell that contains cell row, cell column, and identifiers for the relevant WEAP elements.

The WEAP and MODFLOW coupling is accomplished through a GIS shapefile, which draws MODFLOW grid cells to WEAP spatial elements, i.e., catchment and groundwater nodes, and river elements. Thus, WEAP does not recognize any spatial relationship contrary to MODFLOW. For each active MODFLOW grid cell, the attribute table of the shapefile has a record containing cell row, cell column, and identifiers for respective WEAP elements. This shapefile linkage enables the dynamic transfer of data between WEAP and MODFLOW. The coupling precisely consists of the following steps: (1) the groundwater recharge, pumping rates, and river water levels determined by WEAP are sent as inputs to MODFLOW, (2) MODFLOW input files are modified and the model executes for a single stress duration, and (3) MODFLOW simulated output is provided to WEAP as input for groundwater heads, lateral groundwater flows, and river aquifer interactions. This feedback is executed for each month between WEAP and MODFLOW, and this process continues until the simulation period ends.

The WEAP model estimates the total value of each catchment's groundwater recharge and uniformly applies that value to all active MODFLOW grid cells within a catchment. Applying the Linked Kitchen tool, the following linkage files preview were created as an interface between WEAP and MODFLOW models (Fig.6.2), (Fig.6.3), (Fig.6.4), and the WEAP link to groundwater model (Appendix.4).

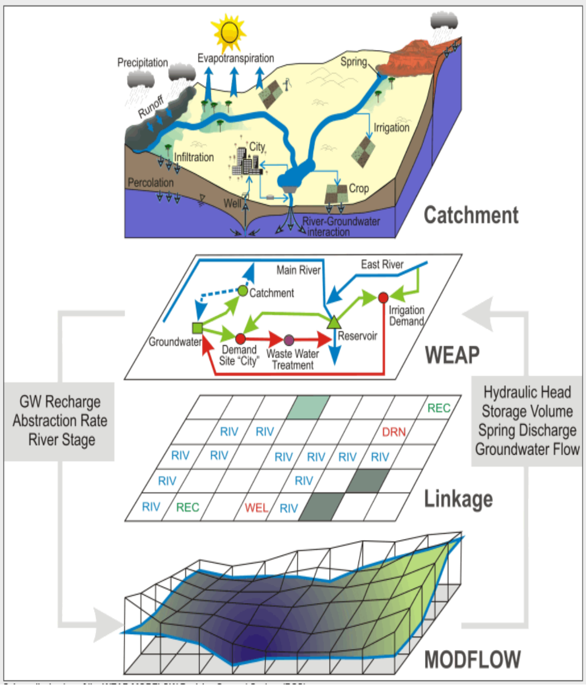

Fig. 6.1 Schematic setup of the WEAP-MODFLOW Model

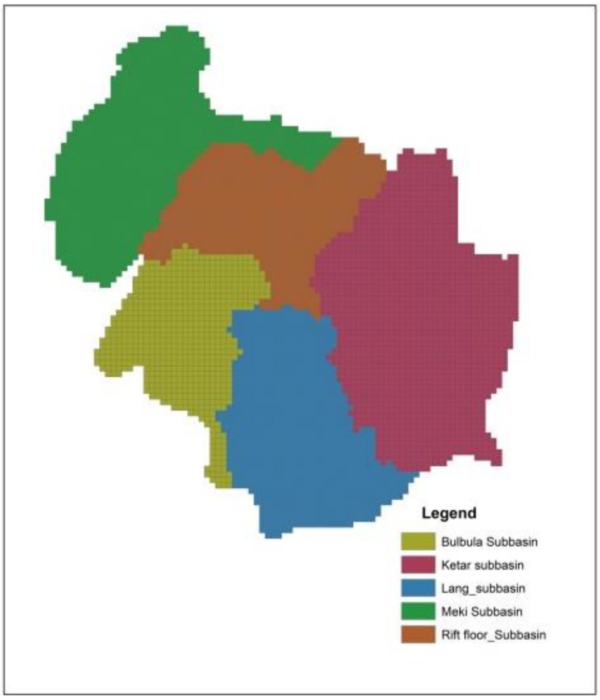

Fig. 6.2 Linkage files preview for each sub-basin in the ALZLB

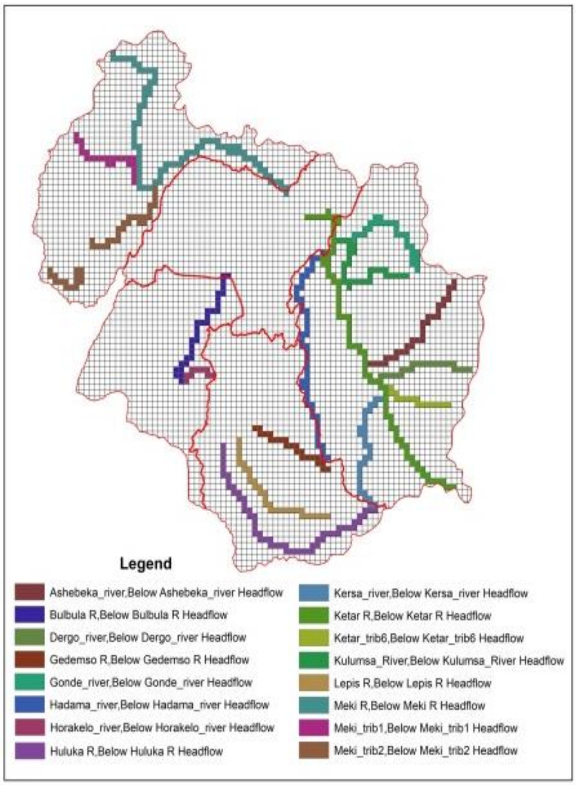

Fig. 6.3 Linkage files preview for river reach in the ALZLB of Ethiopia

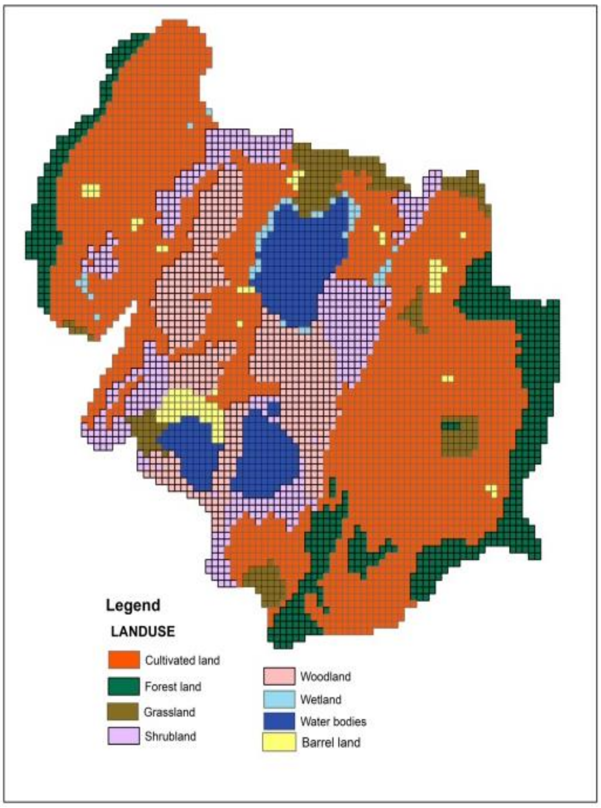

Fig. 6.4 Linkage files preview for landuse in the ALZLB of Ethiopia

6.3. Result and Discussion

6.3.1. WEAP-MODFLOW Model Calibration

The linked WEAP-MODFLOW model performance was assessed by using model performance statistics and a scatter plot graph between measured and simulated flows at gauging stations for Ketar and Meki subbasins. The calibration results of monthly and monthly average flows were presented in Table 6.1 and (Fig. 6.5-Fig. 6.6). The simulated groundwater hydraulic head was presented in (Fig. 6.7). Its result showed a concise match with the observed head. Hence, these results indicated a good fit between the observed and simulated flows at both subbasins and hydraulic heads across the basin. Therefore, the linked WEAP-MODFLOW model can simulate the basin's surface and groundwater characteristics at a reasonably acceptable limit. It could be used for impact evaluation either on supply-side and demand sites and adaptation strategies in the basin.

Table 6.1 Model performance statistics

Subbasin		R^2	NSE	IA	RMSE	NRMSE	RSR
Ketar	Monthly	0.81	0.95	0.95	7.1	0.59	0.44
	Monthly average	0.99	0.98	0.99	1.98	0.16	0.13
Meki	Monthly	0.75	0.74	0.93	7.2	0.67	0.5
	Monthly average	0.96	0.96	0.99	2.2	0.2	0.2

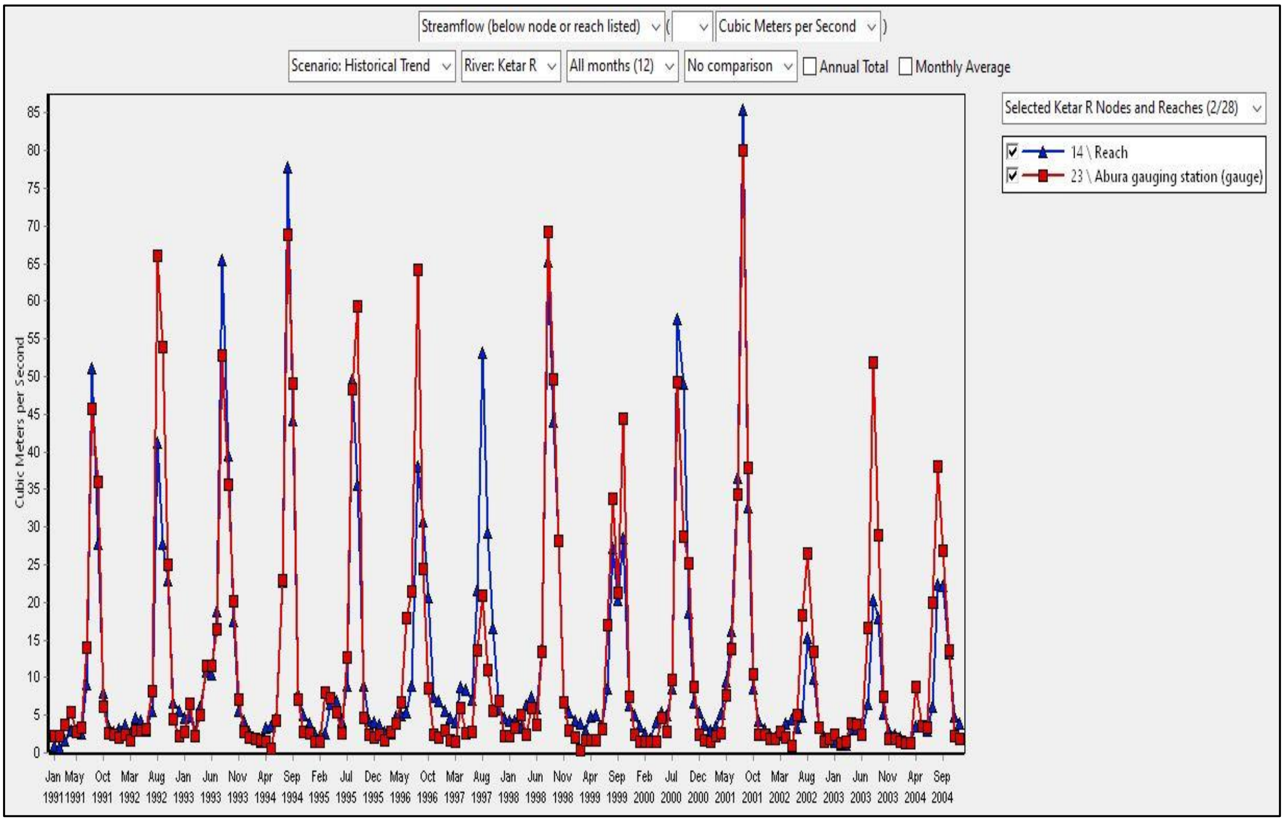

Fig. 6.5 Monthly hydrograph of measured and simulated flows of Ketar River at Abura outlet

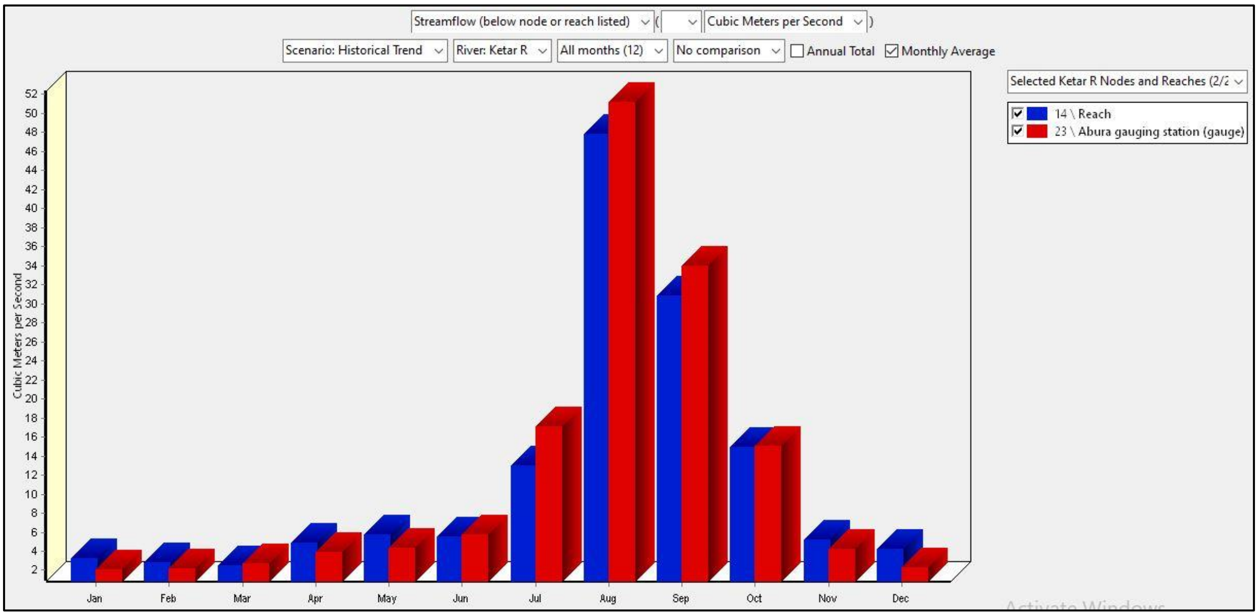

Fig. 6.6 Monthly average measured and simulated flows of Ketar River at Abura outlet

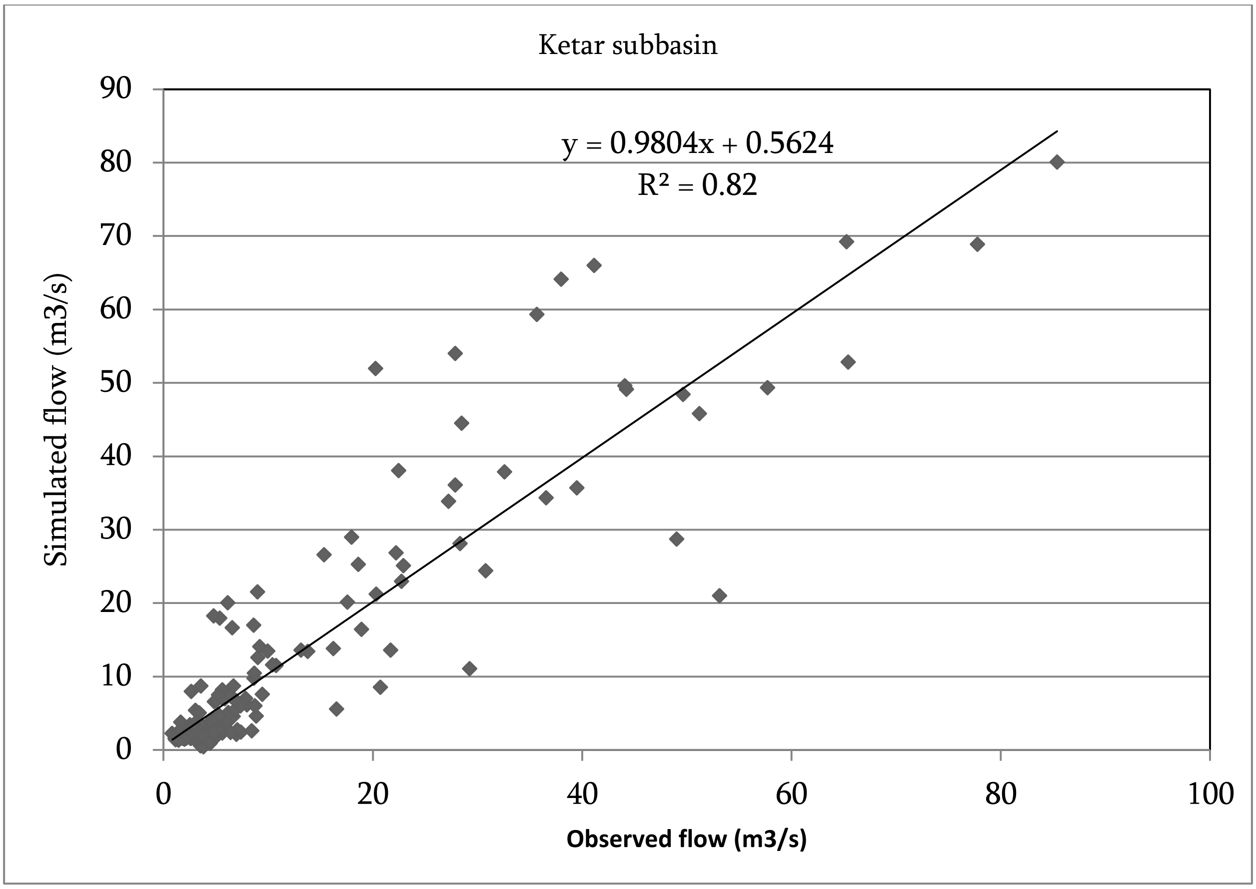

Fig. 6.7 Scatter plot of between monthly observed and simulated flows in Ketar River

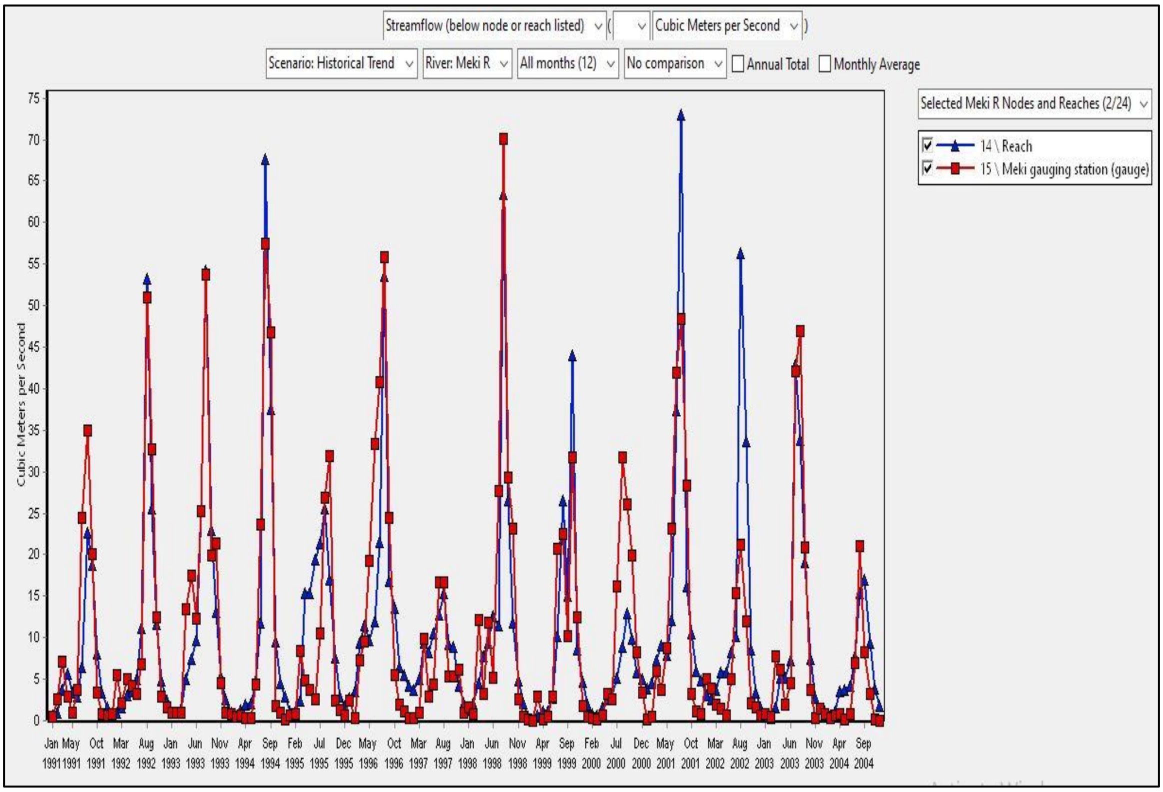

Fig. 6.8 Monthly hydrograph of measured and simulated streamflow of Meki River

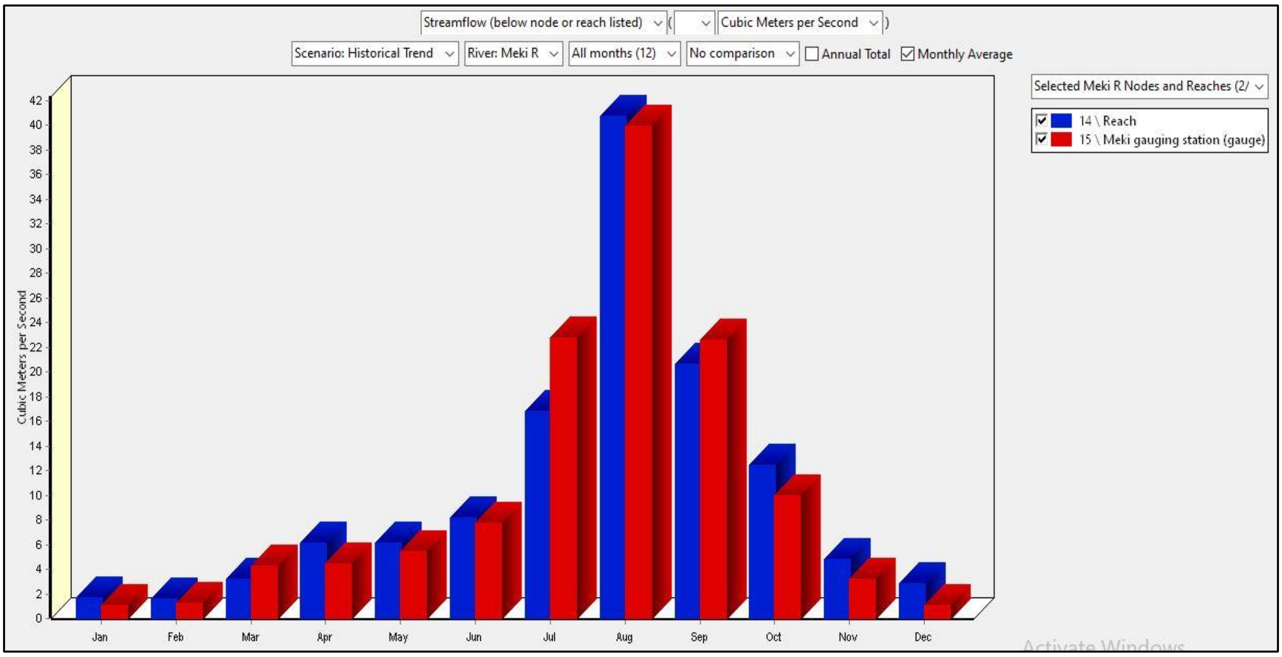

Fig. 6.5 Monthly average measured and simulated flows of Meki River at the outlet

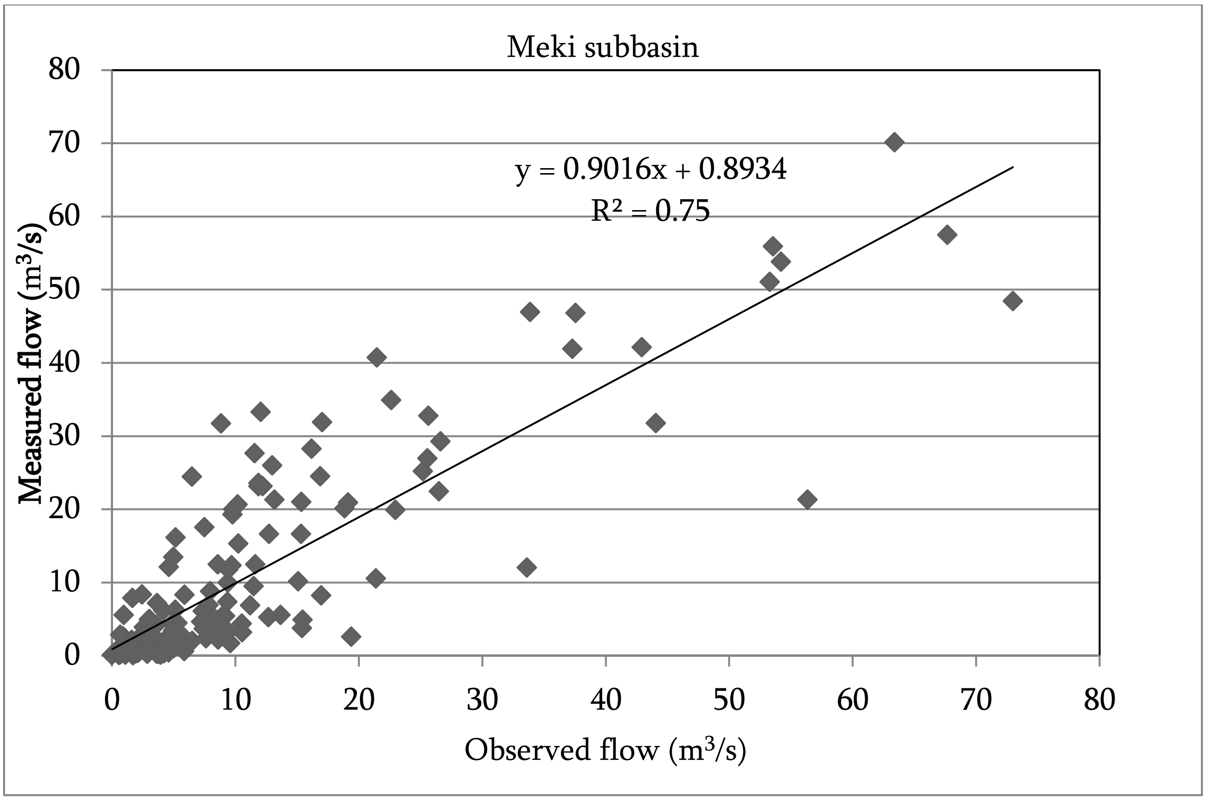

Fig. 6.6 Scatter plot of between monthly observed and simulated flows of Meki River

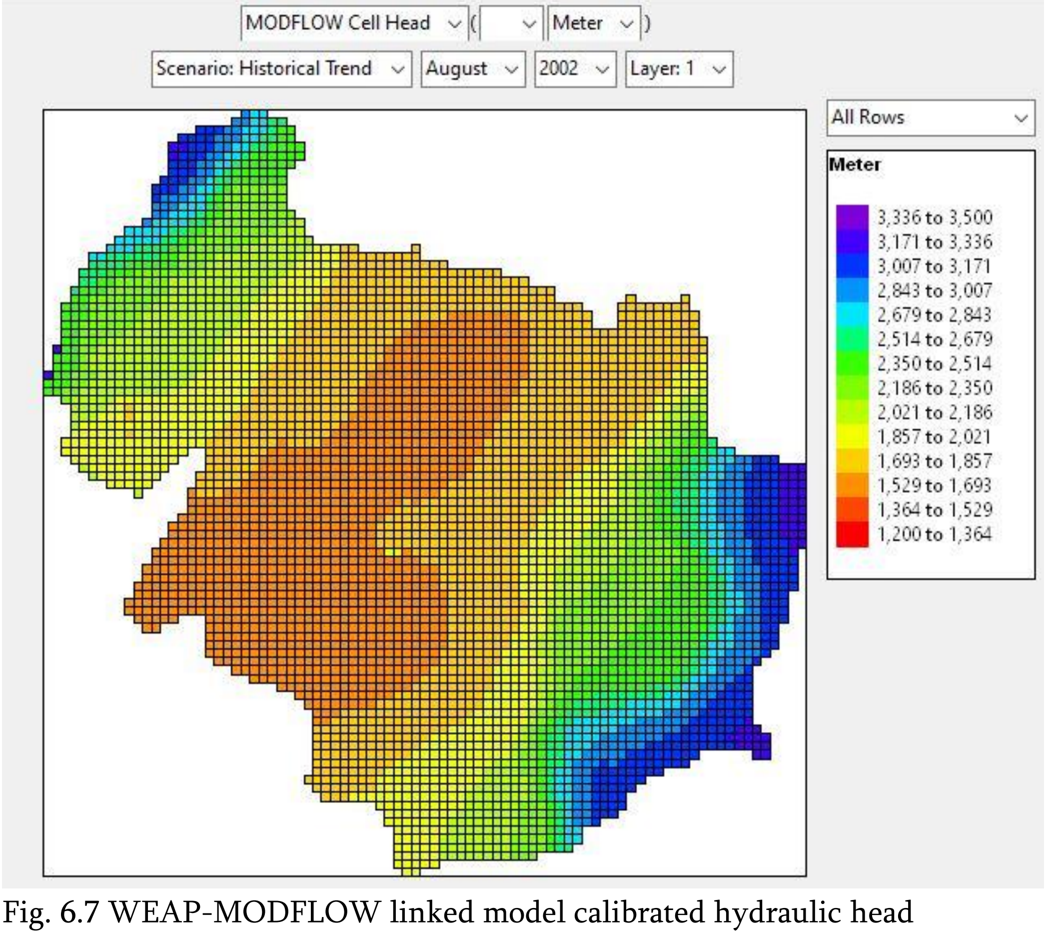

Fig. 6.7 WEAP-MODFLOW linked model calibrated hydraulic head

7. Modeling Climate Change Impacts on Water Resources

7.1. Introduction

Our world is currently facing the global climate warming phenomena with mixed perceptions and readiness on its existence to adaptation strategies. The Intergovernmental Panel for Climate Change (IPCC) in 2014 forecasts that global warming is steadily increasing across the world. Owing to the soaring human-induced greenhouse gases concentrations in the atmosphere in the present century with comparison to the pre-industrial period. This affects the capability of the atmosphere to capture and recycle energy emitted by the earth's surface which is very crucial for maintaining a stable climate. Consequently, higher temperatures arise from intensified greenhouse gas emissions will have a destabilizing effect on global weather conditions and long-term climate patterns. The main deriving factors considered are growing population, economic activity, energy use, land use pattern, technology, and climate policy in determining the greenhouse gases concentration worldwide.

Though, future climate change types and the level of severity of its impacts may vary from geographic region to region. It is very tough to precisely forecast the coming global greenhouse gases concentration in the atmosphere in the spatio-temporal dimensions and associated with its intrinsic unpredictability and uncertainties. Thus, the IPCC sets four scenarios that are based on the accumulation of greenhouse gases projection in the atmosphere which is denoted as "Representative Concentration Pathways" (RCPs) projection. The RCPs scenarios are consistent with extended possible changes in future greenhouse gases emission to reduce uncertainties upon concluding of the twenty-one century (Van Vuuren et al., 2011).

The RCPs include RCP2.6 (a rigorous mitigation scenario) that aimed to retain global temperature progress below 2^0C compared to earlier to the industrial revolution (Van Vuuren et al., 2011), and the two intermediate scenarios are (RCP 4.5 and RCP 6.0) and the one with very high greenhouse gases level is (RCP8.5) scenario and corresponds likely to warming of 3.8-5.7^0C above the pre-industrial level until upon completion 2100. As stated by (IPCC, 2014) the radiative forcing capacities of global warming gases in the atmosphere are projected to reach 2.6, 4.5, 6.0, and 8.5W/M2 for scenarios RCP2.6, RCP4.5, RCP6.0, and RCP8.5, respectively. According to the IPCC assessment report, the global mean temperature will climb between 1.4 and 5.8°C and precipitation would vary up to ±20% by 2100 as compared to the 1990 level. Currently, Global Climate Models (GCMs) are enhanced and numerical-based coupled models to understand global systems like the atmosphere, the oceans, and the ice, and they are helpful in projecting climate and studying the future changes in the climate (Mahmood & Jia, 2017). The available GCMs data have a coarser spatial resolution, and downscaling is required to capture a specific geographic extent. With sets of scenarios, the (RCPs) or emission levels are aimed at predicting the upcoming climate parameters. The models' outcomes could be used for examining the effects of climate variables on the hydrologic processes or water resources.

7.1.1. Future Climate change Projection in Ethiopia or Local scale

Regarding Ethiopia, the future climate projections were assessed by several authors using various downscaled Global Circulation Model (GCM) models. The mean temperature has been increasing by 0.37°C/decade for the past 40years, which is somewhat lesser than the mean global temperature increment and also the majority of the temperature increment was measured during the second half of the 1990s in Ethiopia (EEA, 2008).

In Ethiopia, future climate projections were assessed by several authors using various downscaled GCM models (e.g. Abraham, Woldemicheala, Muluneha, & Abateb, 2018; Biniyam & Kemal, 2017; Serur & Sarma, 2017; Setegn, Rayner, Melesse, Dargahi, & Srinivasan, 2011; Wagesho, Jain, & Goel, 2013; Zeray, Roehrig, Alamirew, & Dilnesaw, 2007) using GCM data sources on different catchments. Particularly, over the Rift Valley basin of Ethiopia, future climate projections have been assessed (Abraham et al., 2018; Biniyam & Kemal, 2017; Wagesho et al., 2013; Zeray et al., 2007).

Prior studies by (Aich et al., 2014) analyzed ensembles of GCM acquired from Coupled Model Intercomparison Project Phase 5 archive (CMIP5) Earth System Models (ESMs) for (RCP8.5) and (RCP2.6) during 1950-2099. The study focused on the four representative basins in Africa to assess climate parameters. The outputs of the models, for the Upper Blue Nile Basin (Ethiopia), more than 80% of the model outputs indicate a positive precipitation trend. Similarly, the corresponding temperatures are estimated to climb between 4 to 6°C across all the modeling years over the African continent. Later, the outcomes from models were used by the hydrologic model to assess the effects of altering climate on stream discharge. A 25% surge in precipitation will cause an intensification of 50% in discharge. In contrast, a 25% reduction in annual precipitation will bring about a 25% discharge decline.

Other similar work in the Ethiopian Blue Nile Basin (Beyene et al,.2010) investigated predicting future climate variables after downscaling and making bias corrections on eleven GCMs data under multiple emission scenarios. The result revealed that there is an ascending trend in precipitation during early (2010-2039) and an ascending trend in precipitation during mid-term (2040-2069) and late (2070-2099) across all the models.

Previous studies by (Serur & Sarma, 2017) examine the future of climate effect on the Weyib River Subbasin in Ethiopia under RCP2.6, RCP4.5, and RCP8.5 conditions. They obtained GCM models (GFDL- ESM2M, CanESM2, and GFDL-ESM2G) from CMIP5 and the statistical downscaling method and bias correction methods were deployed to forecast the future climate parameters. The outputs of the three-model revealed that, when compared to the baseline (1981-2005), there is a generally upward trending for the yearly average of temperature and rainfall for the three scenarios during the period of 2020s, 2050s, and 2080s. However, there is variation among the models' outputs for both the average precipitation and temperature trends. For instance, the increment in projected precipitations varies between 13.68-33.69%, 6.68-26.69%, and 6.68-26.69% among the formerly mentioned three models in a row over the 21st century, respectively.

In the recent study by (Bekele et al.,2018) twenty GCMs were being downscaled employing the Statistical Downscaling Method (SDSM) and assessed with the respect to intermediate(RCP4.5) and high emission (RCP8.5) scenarios for mid-and the end-of-century in the Keleta watershed, Awash basin, Ethiopian. The outcomes of the models indicated that the mid-century minimum temperature will continue to soar from 1.8 to 1.6^{0}C for RCP4.5 and 2.6 to 2.1^{0}C for RCP8.5, respectively. While, the maximum temperature is projected to surge with a magnitude ranging from 2.4 to 2.0^{0}C for RCP4.5 and 4.6 to 3.7^{0}C for RCP8.5, respectively. Moreover, the average precipitation is estimated to escalate by about 15.2 and 17.2% under the RCP4.5 scenario for mid and end-of-century, respectively. On the contrary, the prediction of average precipitation hike varies substantially from 19.9 and 34.4% under RCP8.5 for the middle and ending of the century, respectively. Similar studies by (Zeray et al., 2007) also indicate that both precipitation and temperature show a rising tendency in the Central Rift Valley Basin over the 21st century. The findings showed an increment of 9.4-29%, and 29% in precipitation on monthly and yearly basis, respectively.

In contrast, the monthly and annual temperatures are anticipated to climb by 3.6 to 1.95^{0}C and 4.2 to 2.0^{0}C upon the termination of 2100, respectively. In the Awash Basin, a rising trend both in rainfall and temperature was observed under low, intermediate, and high emission scenarios (Gebrechorkos et al., 2019). On the other hand, a similar study was conducted on the Awash basin (Gebrechorkos et al., 2020) using the SDSM of GCMs to predict future climate variables. The output revealed that the precipitation has no trend (high variability) under the four RCP scenarios over the 21st century. The future temperatures show an increasing trend under all RCP scenarios.

An earlier study (Abraham, Woldemicheala, et al., 2018) examined the future of climate variables in the Central Rift Valley Basin under (RCP4.5) and (RCP8.5) emission scenarios using bias-corrected HadGEM2-ES, CCSM4, and CSIRO-MK-3-6-0 Models across the 21st century. The result showed a general widening trend for maximum temperature for both emission scenarios for the CCSM4 model. The outputs of the HadGEM2-ES, and CSIRO-MK-3-6-0 models indicated that an increasing trend for maximum temperature under both emission scenarios with exception to September and March.

However, the forecasted trend in precipitation is unclear both ups and downs were observed based on the RCP scenarios and GCM model applied. There is a moderate growth tendency in annual rainfall amounts for RCP8.5 throughout the current century, respectively. However, a continuous slight decline under RCP4.5 during the middle and ending of the present century, respectively.

In general, authors predicted the increase of the temperature across the 21 century and irrespective of the model used, despite the difference in the magnitudes. However, until 20115 published papers across the basin were reviewed with climate change perspectives, and the outputs for future precipitation trends are highly variable and this is a huge challenge for the basin water resources (Taye et al., 2015).

Subsequently, many authors have assessed the consequences of changing climate on water resources. Attempts by Biniyam & Kemal (2017) to evaluate the climate change-induced effects on precipitation and flood frequency in the Hare watershed, the Southern portion of the Rift Valley Basin of Ethiopia. Accordingly, there is a rising trend in precipitation in magnitude under both scenarios (RCP4.5), and (RCP8.5) over the 21st century. Additionally, the investigation by Wagesho et al.(2013) on the consequence of the change in climate on runoff levels in the same Basin. This paper predicts the extent of precipitation generally shows an increasing trend from (1990-1999). Therefore, the results studies indicated that high variability in precipitation both declining or rising trends were projected based on the model chosen, emission scenario, and duration under consideration. However, the temperature is likely to uptrend over the whole study period.

Globally, Water resources are under threat as an outcome of future changing climate (Arnell & Gosling, 2013). However, the effect of climate change on Ethiopian hydrology in general, and the watershed under investigation in particular, is still uncertain. As a result of the different climate change forecast outputs utilized in simulating hydrological responses, the model outputs were inconsistent among authors.

For instance, a decline in runoff and streamflow was reported (Abraham, Woldemicheala, et al., 2018; Mechal, Wagner, & Birk, 2015; A. L. Zeray et al., 2007). Oppositely, an scaling up in runoff was published (Bekele et al., 2018; Gebrechorkos et al., 2019; Gebrechorkos et al., 2020; Lemann et al., 2016). The variable result, Both rising and falling trends of runoff was found (Biniyam & Kemal, 2017; Wagesho et al., 2013).

Moreover, several existing studies are mainly available on the likely effect of climate parameters on surface water systems employing the application of various hydrological models. Yet, the WEAP-MODFLOW model has not been applied, and little is known about groundwater recharge rate variability in association with climate variation in the Ethiopian Rift Valley Basin. The underlying processes in the WEAP hydrologic model are the relative change in soil water storage for given land use described as effective precipitation divided into evapotranspiration, over land flow, interflow, and baseflow components of the watershed.

Therefore, this investigation is primarily aimed at understanding the likely effects of future situations on the hydrologic water balance, particularly, on the recharge rate in the ALZLB using the WEAP-MODFLOW model. Moreover, Previous studies revealed that the Soil Moisture Method of the WEAP model is a more sophisticated and effective method for estimating groundwater recharge (Ingol-Blanco & McKinney, 2013). The direct diffused recharge is considered the main recharge mechanism in the area. Hence, the projected climate variables are then used to enforce the WEAP model, a climate-driven hydrologic model. Then, the result was evaluated by comparing various hydrological components against the baseline conditions. This approach aimed to examine the general behavior of the hydrological response and, with great emphasis on groundwater recharge change to possible changes in climatic variables (i.e., precipitation and temperature) inputs.

7.2. Methodology

7.2.1. General approach

The basis of this work was the development of a modeling framework that incorporates projected climate data, as well as hydrologic processes. The WEAP-MODFLOW model was calibrated against monthly flow data and applied to estimate hydrologic processes for a historical period (1991-2005) and groundwater head. Multiple climate change scenarios have been established to model the influences of climate variation on watershed hydrology and groundwater recharge (Fig. 7.1).

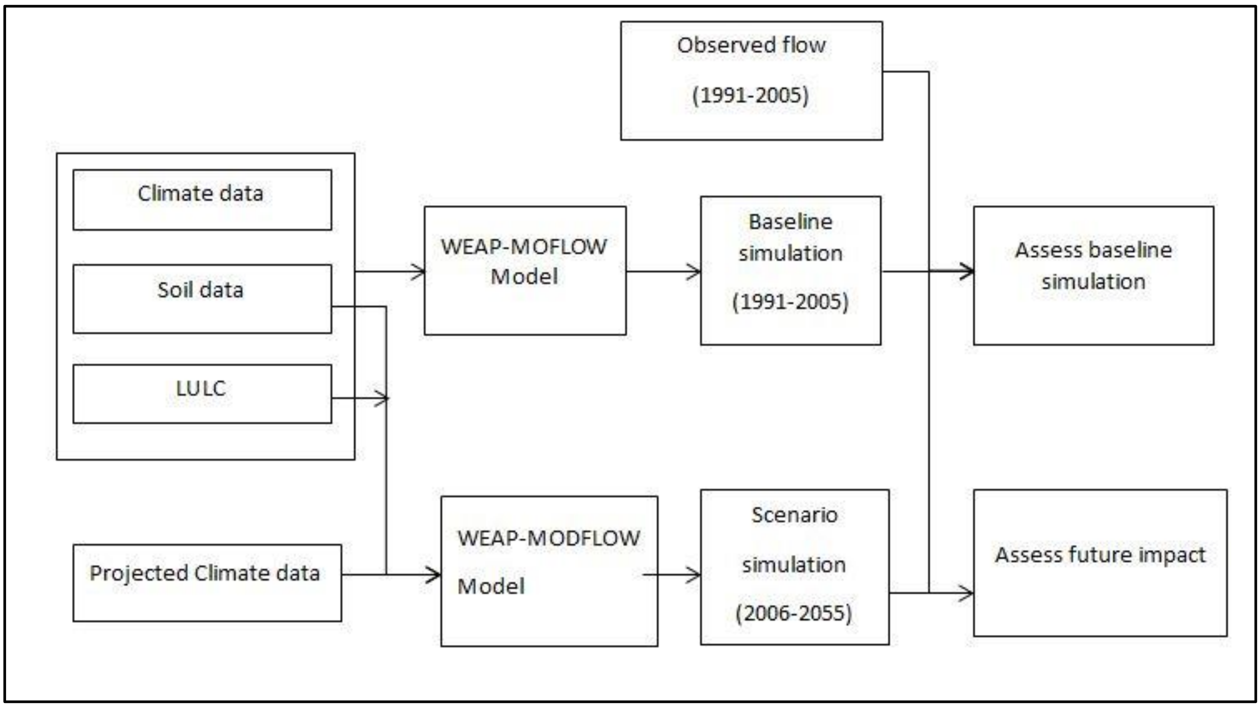

Fig. 7.1 The schematic diagram for WEAP-MODFLOW model procedure

7.2.2. Projected climate scenario /Climate Models/

Future climate impact assessments were carried out by manipulating the variables of the climate data (precipitation and temperature) against the baseline using Coupled WEAP-MODFLOW model. For the present study, the bias corrected and downscaled RCM models for predicting the future climate were acquired from Coordinated Regional Climate Downscaling Experiment (CORDEX) with the supports of the World Climate Research Program (WCRP) on https://dataservices.gfz-potsdam.de. The WCRP has been engaged to downscale different RCM models to produce an collective of high-resolution past and future climate forecasts for the Continent of Africa (Giorgi et al., 2009; Taylor et al., 2012).

This dataset delivers bias-corrected daily precipitation and temperature covering the Ethiopian landmass for historical (1970-2001) and is projected over the 21st century for RCP 4.5 and RCP 8.5 and is subjected to dynamic downscaling at spatial resolution 0.44^0 x 0.44^0 and a linear bias-correction method (Liersch et al., 2018). Hence, the CanESM2, CNRM-CMS, and NorESM1-M RCM models were acquired in Net CDF file (.nc) format and analyzed using ArcGIS software to a specified location or basin. During analysis, the data were banded with time intervals of 2020-2040, 2040-2060, 2060-2080, and 2080-2099 on the monthly average basis for future climate variables (Rainfall and temperature) for the study basin (Table 7.1).

Table 7.1 Description of the CORDEX-AFRICA regional climate model (RCA4) simulation

Institution	Name	country	GCM resolution
Canadian Centre for Climate Modelling and Analysis	CanESM2	Canada	2.8^0*2.8^0
Centre National de Recherches Meteorolo-Giques/Centre Europeen de Recherche et Formation Avanceesencalcul scientifique	CNRM-CM5	France	1.4^0*1.4^0
Norwegian Climate Centre	NorESM1-M	Norway	1.9^0*2.5^0

The output of re-analysis of the CanESM2, CNRM-CMS, and NorESM1-M GCM RCM models of the future climate trends have been assessed and presented in (Fig.7.2 and Fig.7.3). The average annual rainfall and temperature values vary across the models and scenarios used in the basin of Ethiopia compared to the baseline years. The CNRM-CMS model projected the lowest percent change in average precipitation with -5.1%, -5.0% (RCP4.5) and 3%, 3% (RCP8.5) in 2020-2040, and 2040-2060, respectively. The CanESM2 projected the average annual precipitation increase by 20.7, 47.5% (RCP4.5) and 41, 53.4% (RCP8.5) in 2020-2040, and 2040-2060, respectively. While the NorESM1-M model estimated the future average annual precipitation increase by 37.6, 74.4% (RCP4.5) and 53.6, 40.3% (RCP8.5) in the time spans of 2020-2040, and 2040-2060, respectively.

Regarding the temperature conditions, the NorESM1-M model estimated the modest average annual temperature increase by 1.1^{0}C, 1.46^{0}C (RCP4.5) and 1.1^{0}C, 1.75^{0}C (RCP8.5) in the time spans of 2020-2040, and 2040-2060, respectively. The CanESM2 projected the average annual temperature increase by 1.47^{0}C, 2.1^{0}C (RCP4.5) and 1.4^{0}C, 2.53^{0}C (RCP8.5) in the 2020-2040, and 2040-2060, respectively. Whereas, in the 2020-2040 and 2040-2060 time periods, the CNRM-CMS model predicted average temperatures to rise by 1.0°C, 1.57°C (RCP4.5), and 1.06°C, 2.5°C (RCP8.5), respectively.

The GCM models, the predicted average annual precipitation showed an increase of about 25%. However, in case of adverse conditions, considering the minimum of the three GCMs revealed that a decrease of about 25% as compared to the historical time over the study interval. Nevertheless, the average temperatures showed rising trend prevail over the century, despite the variation in amount among the GCM models and RCP scenarios considered.

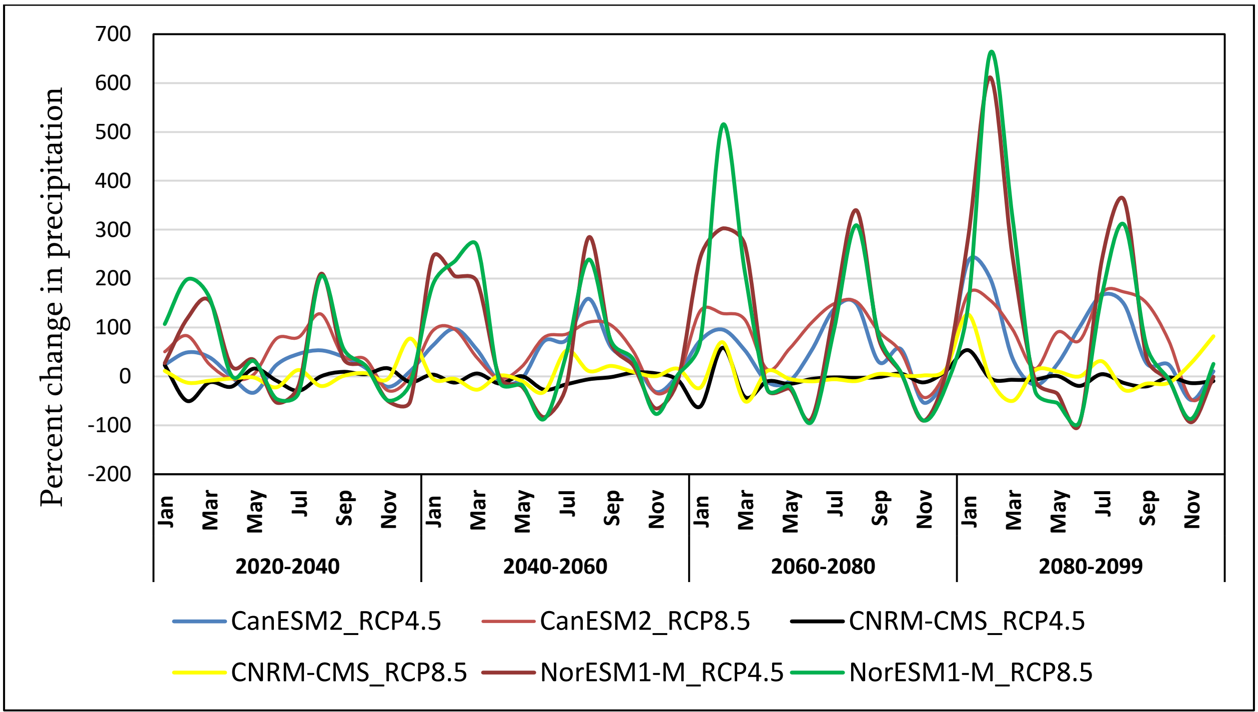

Fig.7.2 Percent change in average monthly between historical and projected precipitation under RCP4.5 and RCP8.5 scenarios

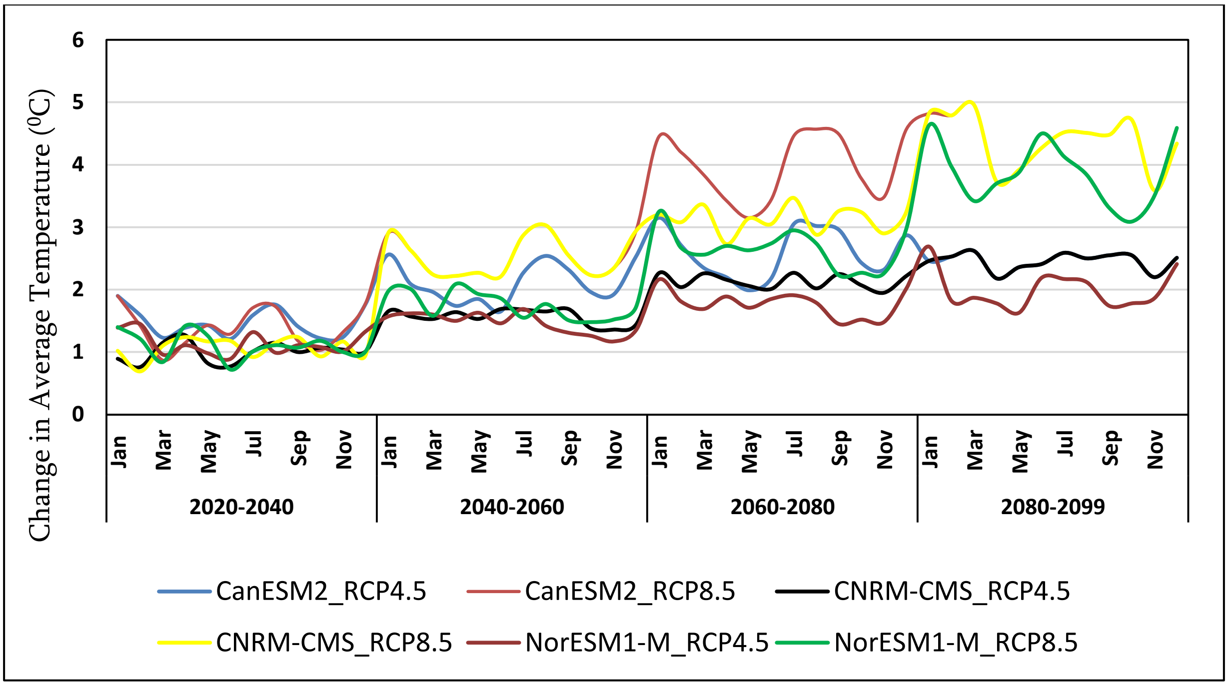

Fig.7.3 *Change in average monthly temperature for the three models under RCP4.5 and RCP8.5 scenarios over the 21century*

Nevertheless, numerous studies are already available on future climate projection, with no agreement upon the direction and amount of change on the future climate variables among the authors. Because, the results of models are influenced largely by the choice of GCM model type, RCPs scenarios, and downscaling method applied to assess these variables (Meixner et al., 2016; Taylor et al., 2012).

Consequently, a range of scenarios will help in understanding how a complex system could evolve in the upcoming decades. The scenarios are an image of the future or alternative situations. The scenarios are not predictions or forecasts. Instead, every scenario is a different view of how the future could evolve. The scenario assists in the evaluation of possible changes of dynamic systems that are inherently unpredictable or have significant scientific uncertainties (IPCC, 2007). Moreover, hypothetical scenarios were formulated purposively to reduce uncertainty and comprehend the anomalies (Zhang et al., 2016). The range of magnitude is, however, based on the results of climate projections of various studies over Ethiopia, within the next 100 years. The projected climate change in Ethiopia is generally a growing trend in temperature and evaporation compared to the current climate. The projected warming across all simulations within the ranges of high and low emission scenarios indicates temperature climbs by about 1 to 4°C upon the completion of the century.

By contrast, intensity and overall variability of rainfall patterns are expected. The outputs of GCM models estimated that a strengthening in precipitation is expected (Bekele et al., 2018; Beyene et al., 2010; Biniyam & Kemal, 2017; Wagesho et al., 2013; Zeray et al., 2007). Nevertheless, numerous authors predict the variable conditions of rainfall (Abraham et al., 2018; Aich et al., 2014; Taye et al., 2015). The estimated increment in rainfall, however, varies seasonally and does not display a regularly growing or lowering pattern throughout the year over Ethiopia (McSweeney et al., 2008). Nonetheless, the forecast studies suggest that general growth in annual rainfall amounts up to 20 percent, even more in some areas. As a result of variation in the model prediction results, scenarios were opted to applied to investigate the impacts of climate change on water resources in the basin under consideration.

Therefore, framing plausible scenarios is imperative to explore the impacts imposed by climate on hydrologic components of the study Basin over the coming three decades (until the 2050s). Taking these uncertainties into consideration and for a better insight of the climate effects on the water resources, accordingly, eight scenarios were adapted to comprehend a range of climate variables applicable in assessing hydrological processes of the watershed. In this study, the scenarios were set to include a continuous upward trend in monthly temperature of 0.025^0C and 0.04^0C/year (2.5 and 4^0C at the last decade of the 21^{st} century). And also, a potential change in monthly precipitations of ($\pm$20%) and the combinations of these scenarios were incorporated (described in Table 7.2). Other climate parameters like wind speed relative humidity, cloud cover, and solar radiation are subjected to change.

Table 7.2 Adapted climate change scenarios used to simulate the hydrologic components of the water balance of the subbasins

Scenario	Scenario description
Base case	The baseline (1991-2005)
Scenario:1 (S1)	Increase in temperature by 0.025^{0}C/year (2.5^{0}C by 2100)
Scenario: 2 (S2)	Increase in temperature by 0.04^{0}C/year (4^{0}C by 2100)
Scenario: 3 (S3)	Increase in precipitation by 20% on a year-round basis
Scenario: 4 (S4)	decrease in precipitation by 20% on a year-round basis
Scenario: 5 (S5)	Combination of Scenario 1 and Scenario 3
Scenario: 6 (S6)	Combination of Scenario 1 and Scenario 4
Scenario: 7 (S7)	Combination of Scenario 2 and Scenario 3
Scenario: 8 (S8)	Combination of Scenario 2 and Scenario 4

7.3. Results and Discussions

7.3.1. Effects of Climate Change Scenarios on water balance components

The result of the model has presented the mean annual water balance component of the basin for adapted scenarios compared against the baseline (1991-2005). The output of the WEAP model showed that both scaling up and reduction results across the scenarios over the study period of 2005-2050 and the detailed result are presented (Table 7.3). The mean annual surface runoff (SR) will be diminished by about 3%, and 5% (S1) and (S2) for scenarios involving steady advances in temperatures for the basin, respectively. Conversely, the average annual potential evapotranspiration (PET) shows a small rise by 4%, and 5% (S1) and 5%, (S2), respectively.

While, a 20% increase in average annual precipitation (S3) will produce an increment of 71%, 12%, and 27% of mean annual SR, evapotranspiration (ET), and recharge to groundwater (R) as compared to the baseline, respectively. In contrast to this, an adverse scenario with a 20% decline in annual mean precipitation (S4) is expected to bring a decrease by 42, 15, and 37% mean annual SR, ET, and R with the respect to the baseline condition in the basin, respectively. Moreover, an increase of 20% in annual mean precipitation and with the corresponding growing up in temperatures of 2.5^{0}C and 4^{0}C (S5 and S7) will boost the mean annual SR by 65%, and 61% under (S5) and (S7), respectively. This is accompanied by rising of mean groundwater recharge by 24%, and 22% for (S5) and (S7) scenarios, respectively.

Conversely, considering an adverse scenario in precipitation that may occur as a recurrent drought, a 20% decline in the amount of annual rainfall and respective rising of 2.5^{0}C and

4^0C in temperatures (S6 and S8) will decline by 44% and 45% of the mean annual SR, and 40%, and 42% groundwater recharge, respectively. In addition to this, the mean annual of ET shows a decline by 15% for the basin over the study period. However, the mean annual PET showed a mild increment of 4% to 5% under all scenarios involving a change in temperature and precipitation. This is because of rising in temperature is the dominant factor to enhance the potential evapotranspiration (Luo et al.,2021).

Table 7.3 Percent change in hydrologic components compared to the baseline year in the basin

Scenario	PET	ET	Recharge	Surface runoff
Scenario: 1	4	1	-5	-3
Scenario: 2	5	2	-7	-5
Scenario: 3	1	12	27	71
Scenario: 4	1	-15	-37	-42
Scenario: 5	4	13	24	67
Scenario: 6	4	-15	-40	-44
Scenario: 7	5	14	22	61
Scenario: 8	5	-15	-42	-45

7.3.2. Effects of Climate Change projection scenarios on Streamflow

One of the ways impacts of climate change on the water system is manifested as streamflow amount change. The results of climate change scenarios on the Ketar and Meki streams were investigated against the baseline. The result indicated that a 20% annual precipitation upsurge along with warming in temperature (S5) and (S7), streamflow is likely to be amplified by 76% and 70% in the Ketar flows; and 75%, 70% in Meki flow at their outlets as compared to the baseline, respectively. On the other hand, with a 20% annual precipitation shrinking with a corresponding increment in temperature (S6) and (S8), the streamflow is expected to deplete by 59% and 61% (Ketar streamflow), 65%, 67% (Meki streamflow), respectively.

Some other similar study employed the CORDEX-Africa dataset derived climate parameters to enforce SWAT model for Ketar and Meki watershed and found an increase of 62% and 26.3% streamflow for (RCP 4.5), and 74.2% and ,51.4% (RCP 8.5) at the end of present century respectively (Musie et al., 2020). Moreover, (Lemann et al., 2016) showed that a 50% increment in annual streamflow as compared to the baseline with a 24% surge in annual precipitation. In the Awash basin, a 34-50.5% rise in annual average streamflow over the 21 century was reported (Gebrechorkos et al., 2020) for annual average increase in precipitation by 10-1.4%. In similar studies in the Awash basin about 65.5-75.4% increase of streamflow was reported for different RCP scenarios (Gebrechorkos et al., 2019) in the 2050s'. Other studies on the at the Mara River basin (2081-2100) (Dessu & Melesse, 2013) also indicate that a 50% boost in rainfall will have a doubling effect on the runoff during the wet interval.

Hence, an improvement in precipitation causes a disproportionally high relative change in the surface runoff than the same magnitude of reduction in precipitation. Because a continuing of more rain falling on saturated soils will enhance surface runoff (Jha et al., 2004) and rainfall is the dominant factor that influences the hydrologic systems of the Watershed. Concerning the surface runoff, the Ketar river hydrograph shows high discharge during the wet period. Since the trends of precipitation govern the trend of surface runoff and similar findings were noted by another study (Huang & Zhang, 2004).

7.3.3. Impacts of climate change on Reservoir/Lake Ziway

Climate change alters inflow from upstream to the reservoir and thereby affects the reservoir storage amount and outflow from the reservoir. The inflow into Lake Ziway under climate scenarios is shown in Fig. 7.4. Thus, the model output showed that the inflows to the reservoirs would likely decrease ranging from 5.7-13.5% (SC1), 7-19% (SC2) as compared to the baseline over the year 2015-2055. While, a 20% annual precipitation increase along with warming in temperature (S5) and (S7), inflow to Lake Ziway is likely to be amplified by 76% and 71% with the respect to the baseline, respectively. On the other hand, with a 20% annual precipitation shrinking with a corresponding increment in temperature (S6) and (S8, the surface runoff is expected to deplete by 44% and 45%, respectively.

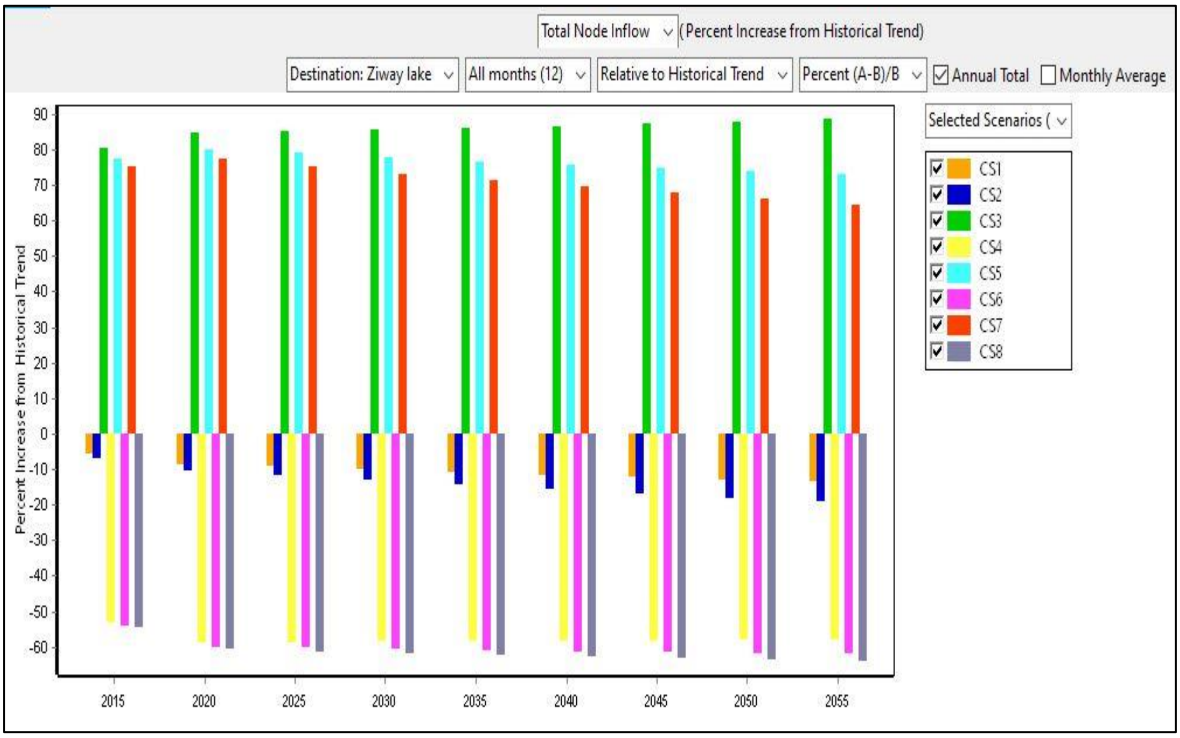

Fig. 7.4 Percent change in surface water inflow to Lake Ziway under climate scenarios

7.3.4. Impacts of climate change prediction scenarios on groundwater head

The implications of potential climate change on the groundwater recharge rate are mainly influenced by the amount of rainfall and by local recharge mechanisms of unconfined aquifers. The result of coupled WEAP-MODFLOW model revealed that there would be a likely change by about -5m to +5m in groundwater level for ±20% annual precipitation at the Row and Column number (R=42, C=38) in the Rift floor subbasin. The same climate scenario will cause a change of about -41m to +39m, and -13 to +12m in the Ketar subbasin (R=43; C=57) and Meki subbasin (R=20; R=24) in the groundwater head, respectively. It is noticeable that the difference in groundwater levels (minimum and maximum values) is shown in the figures (Fig. 7.5-Fig. 7.7). The groundwater head exceedance of climate scenarios was shown at different subbasins in the figures (Fig. 7.8-Fig. 7.11). Hence, the outputs of the coupled model can simulate the impact of climate scenarios on groundwater levels in the basin.

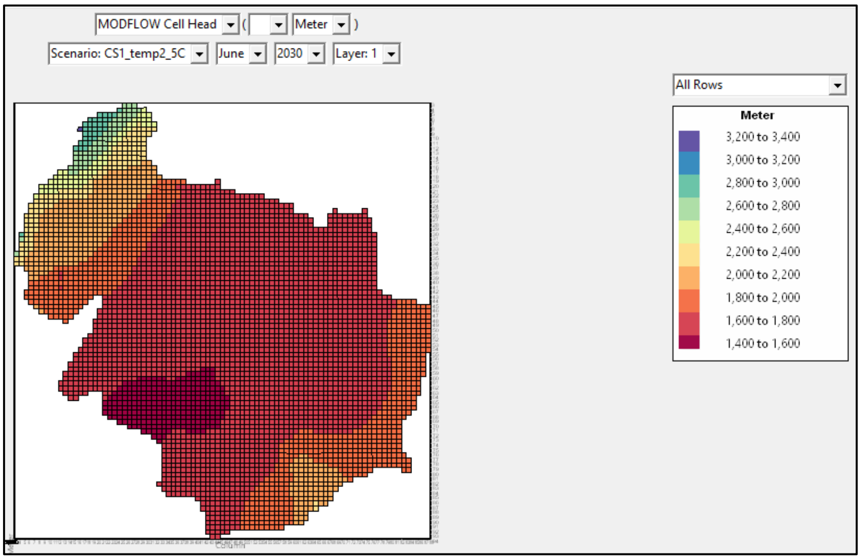

Fig. 7.5 Shows groundwater level no change in precipitation (baseline)

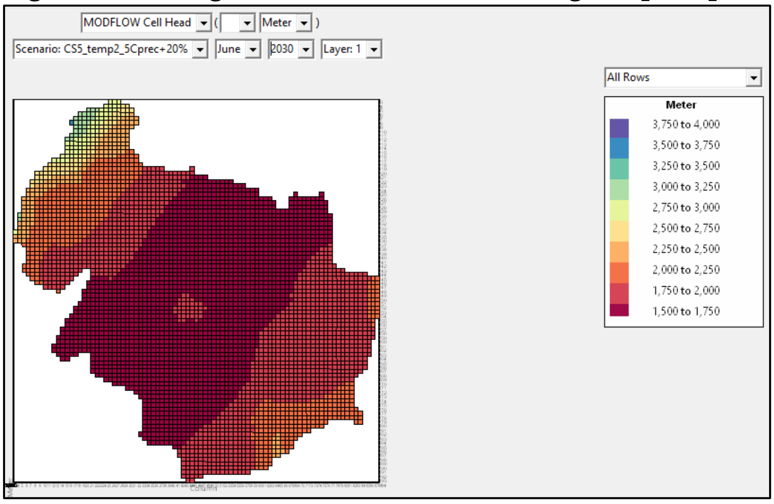

Fig. 7.6 Depicts groundwater level under +20% precipitation change as compared to the baseline

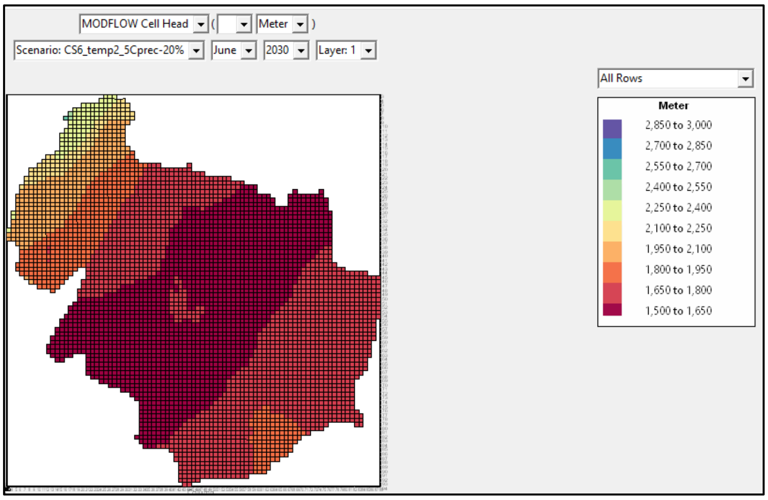

Fig. 7.7 Shows groundwater level under -20% precipitation change compared to the baseline

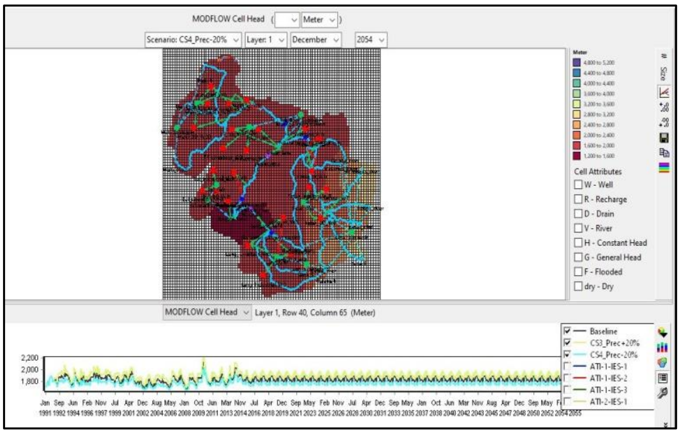

Fig. 7.8 Groundwater head trends under climate scenarios (Baseline, CS3, and CS4)

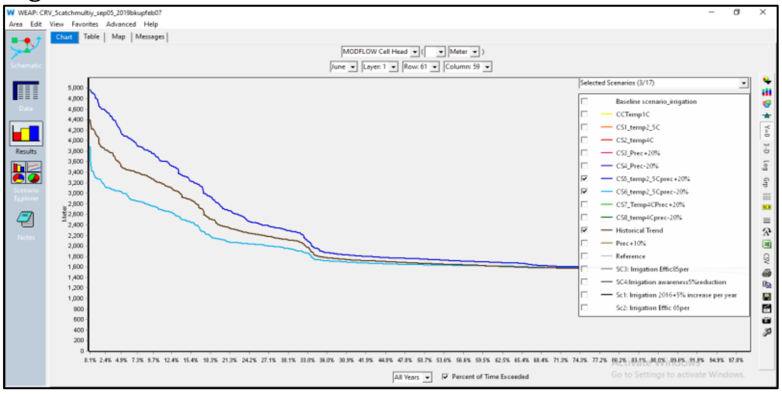

Fig. 7.9 Groundwater head exceedance Row=61, column=59 at middle Ketar watershed

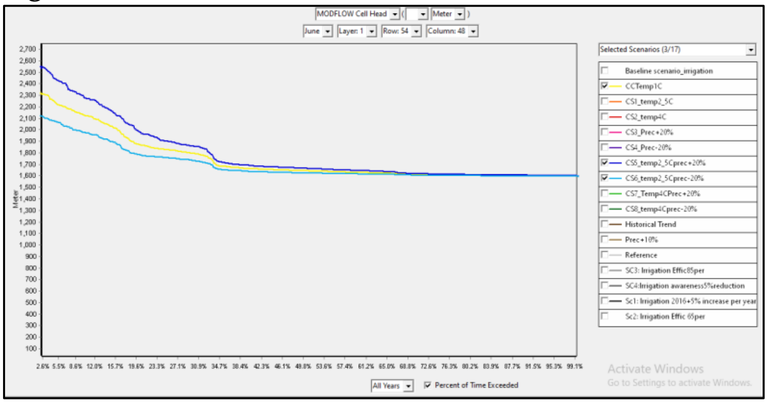

Fig. 7.10 Groundwater head exceedance Row=54, column=48 at rift floor (central part of the rift basin)

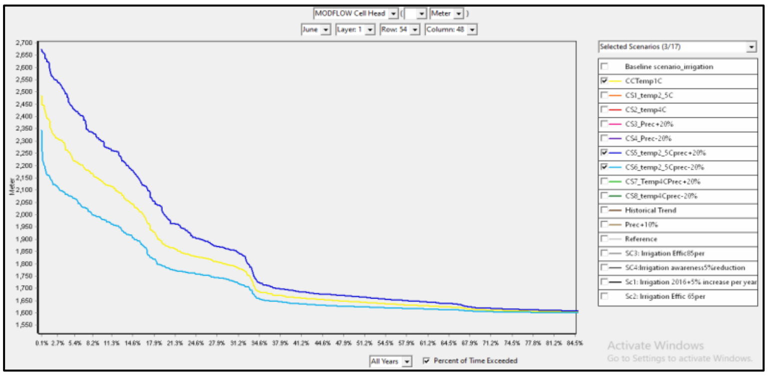

Fig. 7.11 Groundwater head exceedance Row=54, column=48 at rift floor (central part of the rift valley basin)

8. Water Availability, Demand and Adaptation Strategies under Irrigation Expansion Scenarios

8.1. Introduction

The agricultural sector in Ethiopia contributes for approximately 45-50% of the gross domestic product (GDP) of the country (Worqlul et al.,2015). However, It is usually subsistence-based and rain-fed, which sustains a recurrent rainfall failure (Seleshi & Camberlin, 2006). Rainfall variability hinders crop productivity. For instance, 70-90% of annual rainfall is concentrated in a short rainfall season, mainly in the summer season. Besides, nearly 90-95% of the total annual crop production is produced during the summer season (Mario, James, & Prisca, 2010). Dependence on rain-fed agriculture systems leads to sustained food insecurity across the country. To come out of the food insecurity situation, transforming rain-fed-based agriculture into irrigated farms using available water resources has been the key strategy of the government of Ethiopia in recent decades. Therefore, irrigation is the regulated use of water in a timely manner to increase or sustain crop production. It is essential to ensure food security because irrigated crops contribute to 40% of worldwide food production (Siebert & Döll, 2010).

However, one of the biggest problems facing our planet is achieving sustainable water use while ensuring a high level of food security. The impacts of irrigation are likely to rise with the increasing population and demand for food across the world (Tilman et al., 2011). And also, a rising climate warming will expected to escalate the demand for irrigation water (Hanasaki et al., 2013; Leng et al., 2015; Wada et al., 2013). On the other hand, of around 70% freshwater extracted, 90% are used for irrigation purposes (Döll, 2009).

Consequently, this huge water drain of water from rivers, reservoirs, dams, lakes, and aquifers has the potential to alter the earth's water and energy cycles directly and substantially (Famiglietti et al., 2011; Leng, Huang, Tang, Gao, & Leung, 2014; Sorooshian, Li, Hsu, & Gao, 2012; Wada et al., 2010; Zeng et al., 2016). Some of these impacts can be perceived as direct environmental impacts of irrigation as a decrease in water flow downstream and groundwater storage depending on the sources; an increase in groundwater level in irrigated areas and an increase of evaporation in irrigated areas.

Irrigated lands increase water lost via evaporation, this may resulted in instability in the atmosphere and rise the rainfall downwind of the irrigation(Lawton et al., 2017; Lawston et al., 2015). In water segment, irrigation water management will necessitate an enhanced awareness of water resources' feedback to human interference, including local water management(Ferguson & Maxwell, 2012). Unless properly implemented, irrigation could bring ecological degradation, waterlogging effect and soil salinity, in the long-term these, in turn, ends up with unanticipated productivity loss and socioeconomic problems(Pascual-Ferrer et al., 2014).

Currently, the policy of the government of Ethiopian strongly supports export focused on irrigated horticulture and floriculture as a way of improving foreign currency incomes and job creation prospects. Besides, efforts to satisfy the ever-growing food demand in Ethiopia. The ALZLB basin is one of the potential areas in Ethiopia where these policies have led to large investments in floriculture and fast-growing irrigation schemes for smallholder farmers. The ALZLB is characterized by high population growth rate and increasing water demand for irrigation to ensure food availability. Over the last three decades, the rate of growth of irrigated areas has been expanding considerably in a row, and it is believed that irrigation has contributed significantly to the agricultural production of the region, though there is no detailed information available on the contribution of irrigation in the ALZLB.

Even though, irrigation is the major water user in the basin and is primarily extracted from surface water and followed by groundwater (OWWDSE, 2016) and considerably imbalance sustainable water resources use. However, the major driver for smallholders to exploit water resources is poverty and have other option rather than irrigated forming; in addition, there is no regulatory framework for proper management of water abstraction in the ALZLB.

These led to tight competition for access to water for irrigation which could cause over-exploitation of limited water resources in the ALZLB (Pascual-ferrer et al., 2014). On the other hand, luck of awareness of water among users and it is linked to rainfall variability rather than upstream irrigation water users along Ketar and Mike subbasins (Vilalta, 2010). It is well known that the basin has high temporal water variability associated with the rainfall pattern of the basin. Water resources are threatened by the degradation from overexploitation owing to irrigation expansion in the study basin. In recognition of these challenges, achieving sustainable water use while maintaining ever-increasing irrigation water demand is the key challenge facing in the ALZLB.

Therefore, understanding the role of irrigation is important for the adaptive planning of water resources and assessing irrigation impacts on water availability in the basin under study. To address these problems WEAP-MODFLOW model was implemented to analyze scenario-based supply-demand and management strategies. This study aimed at evaluating the potential impacts/effects of irrigation on water resources, and adaptive management on irrigation water supply in the ALZLB.

8.1.1. Irrigation expansion trends in the basin

Over the past 25 years (1990-2015), the basin has experienced rapid development in irrigation expansion, and the growth rate of irrigation development also varies by sub-catchments (Table 8.1). Accordingly, Rift floor, Meki, and Ketar subbasins have undergone a high rate of growth compared to Langano and Bulbula subbasins. The availability of suitable arable land for irrigation is the determining factor for the rate of irrigation expansion.

Study in the Ziway-Shalla basin (GIRDC, 2021) the irrigation suitability class (highly, and moderately) has been estimated to more than 395,880ha and marginally suitable land which demands extra investment cost to bring to either highly suitable or moderately suitable status estimated to 288,989ha and the more detailed can be seen Table 8.2 In general, the irrigated area has increased rapidly from time to time. Large-scale private investors and smallholder farmers can practice irrigated agriculture to improve their income. They have started the production of vegetables, fruits, vegetables, and flowers on irrigated farms.

Table 8.1 Irrigation expansion trend over the past 25 years

Sub-basin	Source of Water	1991/2	2006/7	2015/16
Bulbula (ha)	Surface	733	2316	5136
Ketar (ha)	Surface	939	2340	22,012
Meki (ha)	Surface	286	1290	31,511
Rift floor (ha)	Surface (lake)	2306	3712* (2005)	13,080
Rift floor (ha)	Groundwater	No data	No data	13,908
Langano (ha)	Surface	492	645	1588
Total irrigated land (ha)		**4,756**	**10,303**	**87,235**

Sources: (Dribsa, 2006; Halcrow, 2009; D Legesse et al., 2004; OWWDSE, 2016)

Table 8.2 land suitability class in the Ziway-Shalla basin

Suitability class	**Area (ha)**	
Highly suitability (S1)	287,674	
Moderately suitable (S2)	108,208	
Marginally suitable (S3)	288,989	
Currently not suitable (N1)	194,170	
Permanently not suitable (N2)	155,621	
Other land use/land cover not recommended for cultivation	295,179	
Total Area (Ha)	**1,329,841**	

Source:(GIRDC, 2021)

8.1.2. Irrigation Application Methods and Water use Efficiencies

Based on the irrigated farming system, irrigation systems in the basin can be classified into the surface and pressurized irrigation systems.

Surface irrigation: It is most widely practiced method of irrigation type. Flooding, furrow and basin irrigation are among the widely used surface irrigation method. Despite its low cost, they are not efficient and desirable system, and not recommended where there is scarcity of water exists and water abstraction affects downstream water bodies (lakes). Since the basin has extensive land potential but relatively limited water resources, and as downstream impacts on lakes need to be minimized, these types of irrigation application techniques need to be gradually converted to more water-use efficient methods, certainly for new developments, and also through rehabilitation and extension of existing schemes. Surface irrigation methods dominate existing and many proposed community schemes. Hence with some upgrading, these surface irrigation systems could potentially be improved to achieve overall efficiencies as high as 55% - 65%.

Pressurized irrigation: These include sprinkler and drip irrigation systems which are efficient in water application, but are relatively expensive. There are also current encouraging trends in manufacturing drip systems in the country. A few farms use this method and the promotion of household drip systems has started in some woredas. In addition, there has been a plan for large-scale irrigation development of more than 15,000ha of land to be developed around Lake Ziway, which is intended to use drip and sprinkler systems decades ago. However, according to (OWWDSE, 2016) report, the current irrigation efficiencies in the five subbasins are 43, 45, 55, 55, and 45% in the Ketar, Meki, Rift floor, Bulbula, and Langano, respectively. It meant that a large percentage (57-45%) of water extracted to supply the irrigated farm was lost because of the inefficiency of irrigation systems. This led to elevated water demand to irrigate a hectare of the plot. The recently, aggregated irrigation water requirement estimated by (Halcrow, 2009; OWWDSE, 2016) is shown in Table 8.3.

Table 8.3 Irrigation water requirement

Subbasin	Irrigation water requirement (M3/ha/year)
Ketar	5255
Meki	6331
Rift Floor	6197
Langano	5255
Bulbula	6197

However, based on the analysis of the Meki and Ketar rivers, about 4.7 Mm^3/year and 9.8 Mm^3/year are diverted to irrigate 388 ha and 856 ha of land, respectively. Direct pumping from Ziway Lake is estimated at 25.4Mm^3/year to irrigate about 2000 ha of land. Water pumped from the Bulbula River is estimated at 13.9 Mm^3/year to irrigate 1095 ha. Tributary rivers of Langano Lake are diverted to irrigate 830 ha amounting to 10.5Mm^3/year. From these data, the required water allocation amount has been estimated for each subbasin as shown in Table 8.4. The volume of water abstracted varies based on the cropping season, which is given as monthly water use variation (Table 8.5).

Table 8.4 Existing irrigated land and water demand

No	Irrigated land (ha)	Total area in (ha)	Required water (l/s/ha)	Required water allocation (m^3/ha)	Total water required (Mm^3)
1	Meki	856	0.25	12,087	4.7
2	Ketar	388	0.18	11,487	10
3	Ziway	2000	0.25	12,691	25.4
4	Langano	830	0.25	12,691	10.5
5	Bulbula	1095	0.25	12,691	13.9
6	Sher Ethiopia	500	0.25	14,600	7.5
	Total	**5,669**			**71.9**

Table 8.5 Monthly water use variation (%)

Sub-basin	Jan	Feb	Mar	Apr	May	Jun	Jul	Aug	Sep	Oct	Nov	Dec
Ketar	17.7	6.9	9.9	13.3	12.6	2.5	0.1	0.1	1.1	3.8	12.8	19.1
Meki	15.0	6.7	9.6	11.9	11.3	6.5	1.5	1.3	1.1	6.0	13.1	15.9
Rift floor	16.6	4.5	7.3	10.2	10.6	5.7	1.1	0.8	0.5	7.6	16.4	18.7
Bulbula	16.6	4.5	7.3	10.2	10.6	5.7	1.1	0.8	0.5	7.6	16.4	18.7
Langano	17.7	6.9	9.9	13.3	12.6	2.5	0.1	0.1	1.1	3.8	12.8	19.1

(Source: OWWDSE, 2015/16)

8.2. Method/Future Irrigation Water Demand Analysis/

The hydrological characterization of sub-basins was done using WEAP-MODFLOW model-based hydrological model that employs the Rainfall-Runoff (Soil moisture Method). The model uses meteorological records, discharge of streams at their outlet, and land and soil properties of the respective sub-basin to calibrate and validate the model outputs (the details can be seen in Chapter 4). The water supply-demand analysis was done using dynamically linked WEAP-MODFLOW model to predict/forecast future water demand along with adaptation strategies under various scenarios.

Irrigation water requirement (IWR) is estimated based on rainfall amount, evapotranspiration, crop coefficients, and water use efficiency of the irrigation site (Omran, Negm, & Practices, 2020). In turn, the Crop Water Requirement (CWR) comprises evapotranspiration and crop coefficient (Allen, et al., 1998; Jensen, 1968). The monthly crop coefficients are required, which is changing according to the types of crops, intensity, and cropping pattern. Owing to the absence of such data for a particular irrigation site, generalized crop coefficients were used within the WEAP models that relate a typical crop and cropping pattern to the agro-ecological conditions of the site.

In the Ethiopian rift valley basin, (Halcrow, 2009) crop water requirement was estimated using the WEAP model and applying simplified agro-ecological zones (i.e., altitude zones) based on the altitude of the irrigation site (Table 8.6) based on the FAO-56 model(Allen, Pereira, Raes, Smith, et al., 1998). However, irrigation water demand considers the irrigation system efficiency that may slightly vary with subbasins in addition to crop water requirement (ET_c), and the amount of water demand is getting higher for lower irrigation water use efficiency.

$$\textbf{Net Irrigation Water Requirement (NIWR)} = \boldsymbol{ET_c + W_{rs} - P_e} \qquad (8.1)$$

$$\mathbf{ET}_c = \mathbf{K_c} * \mathbf{ET_o} \qquad (8.2)$$

$$\textbf{Reqiured Water allocation} = \frac{\boldsymbol{NIWR}}{\boldsymbol{IWUE}} \qquad (8.3)$$

Where, NIWR: Net Irrigation Water Requirement; ET_c: crop evapotranspiration; W_{rs}: is a total amount of water for land preparation, and seepage loss from the irrigated field; Pe: effective precipitation; K_c: Crop coefficient; ET_o: potential evapotranspiration; and IWUE: Irrigation Water use efficiency –loss attributed to application loss, and conveyance loss. Summary of Monthly Irrigation Water Requirements for Diversified cropping (m3/day/ha) was shown in Table 8.6 for the basin under study.

Table 8.6 Irrigation water demand

No	Subbasin	Irrigation water use efficiency	Required water (l/s/ha)	Irrigation water requirement (M^3/ha/year)	Required water allocation (m^3/ha/year)
	Ketar	43	0.18	4939	11,487
1	Meki	45	0.25	5439	12,087
2	Ziway	55	0.25	6980	12,691
3	Langano	45	0.25	5711	12,691
4	Bulbula	55	0.25	6980	12,691

(Source: Halcrow, 2009)

8.2.1. Irrigation water use and management scenario development

One part of water resources management drivers is the demand-side analysis that irrigation abstraction, domestic, livestock, and industrial water uses. In the study basin, irrigation is the main water consumer as compared to other uses, and also only the unmet demand will be analyzed for irrigation water use, the remaining water use will be given priority. Three irrigation expansion amounts and each with different irrigation schemes efficiency scenarios were adapted to evaluate the effects on water resources compared against baseline scenarios.

With the assumptions of continuous irrigation expansion and there will be an investment in agricultural technology that progressively improves irrigation efficiency over the study periods. Three irrigation expansion rates were considered to comprehend the low, middle, and high rates of irrigation expansion in the coming decades as depicted in Fig. 8.1. The scenarios for irrigation water demands were framed as follows:

Baseline scenario: was developed assuming the condition of the current account (1991) that kept water allocation for irrigation unchanged and other demands were projected over the study period. Since priority is given to non-irrigation demands.

Irrigation Expansion Scenario -1 (IES-1): The current trend of irrigation intensification from rain-fed-based to irrigated cultivation assumed a modest increase of 75% at the end of 2055 compared to 2015 with the current irrigation efficiency.

Irrigation Expansion Scenario -2 (IES-2): The current trend of irrigation intensification from rain-fed-based to irrigated cultivation and assumed to be doubled at the end of 2055 compared to 2015 with the current irrigation efficiency.

Irrigation Expansion Scenario -3 (IES-3): The current trend of irrigation intensification from rain-fed-based to irrigated cultivation and projected to be increased by 150% at the end of 2055 compared to 2015 with the current irrigation efficiency.

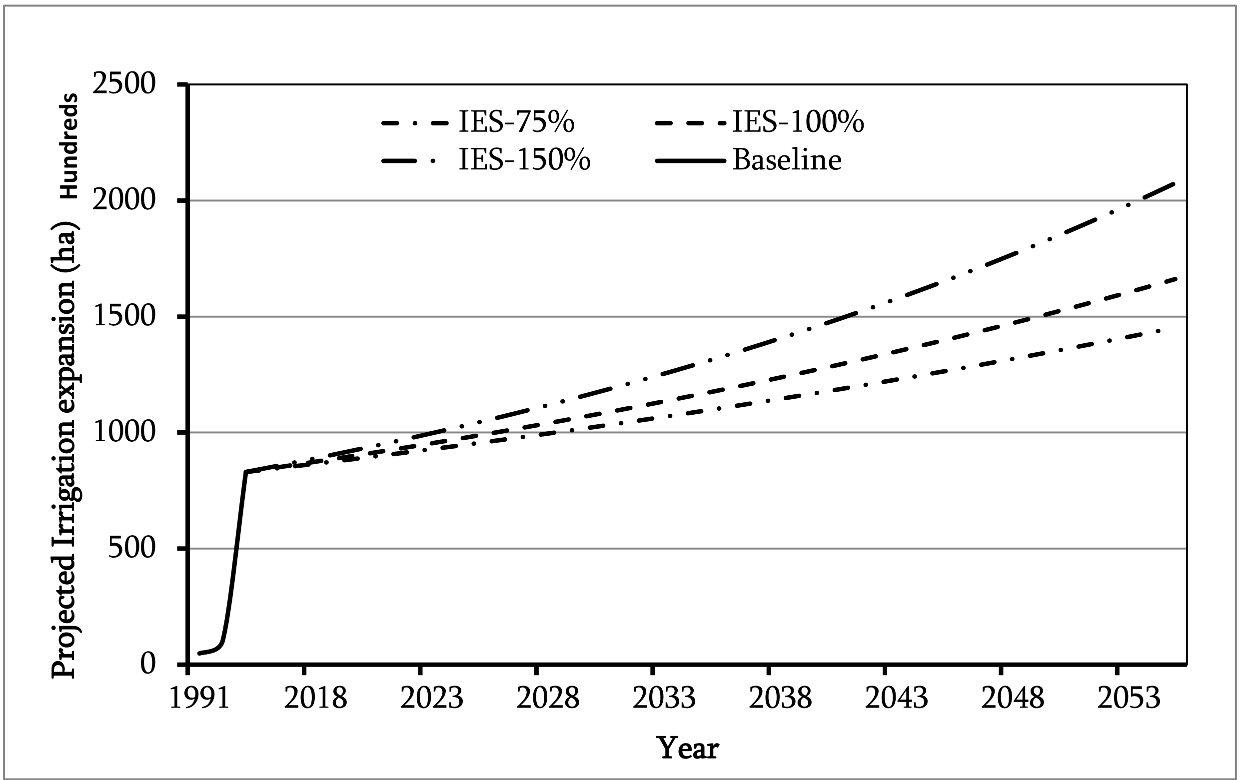

Fig. 8.1 Projected irrigation expansion scenarios in the basin

If there are any unmet demands for all scenarios, adaptation strategies have to be devised. To reduce the unmet demands, there are combinations of irrigation expansion scenarios with adaptation strategies to cope up with alarmingly increasing water requirements for irrigation expansion. These adaptation strategies involve agricultural technology improvement (ATI) to enhance irrigation schemes' water use efficiencies. These scenarios assume progressive enhancement in irrigation efficiency over the study period as shown in Fig. 8.2. Hence, it requires attitude change, skill development, policies and allocation of resources to achieve the assumed efficiency. These scenarios were adapted as shown in (Table 8.7).

Table 8.7 Demand-side management scenarios-Agricultural Technology Improvement (ATI)

	Definition of Agricultural Technology Improvement (ATI) Scenarios
ATI -1	Investment in agricultural technology to enhance the current weighted irrigation efficiency to 65% at the end of 2055 with a similar rate of growth of IES-1.
ATI -2	Investment in agricultural technology to enhance the current weighted irrigation efficiency to 85% at the end of 2055 with a similar rate of growth of IES-1.
ATI -1	Investment in agricultural technology to enhance the current weighted irrigation efficiency to 65% at the end of 2055 with a similar rate of growth of IES-2.
ATI -2	Investment in agricultural technology to enhance the current weighted irrigation efficiency to 85% at the end of 2055 with a similar rate of growth of IES-2.
ATI -1	Investment in agricultural technology to enhance the current weighted irrigation efficiency to 65% at the end of 2055 with a similar rate of growth of IES-3.
ATI -2	Investment in agricultural technology to enhance the current weighted irrigation efficiency to 85% at the end of 2055 with a similar rate of growth of IES-3.

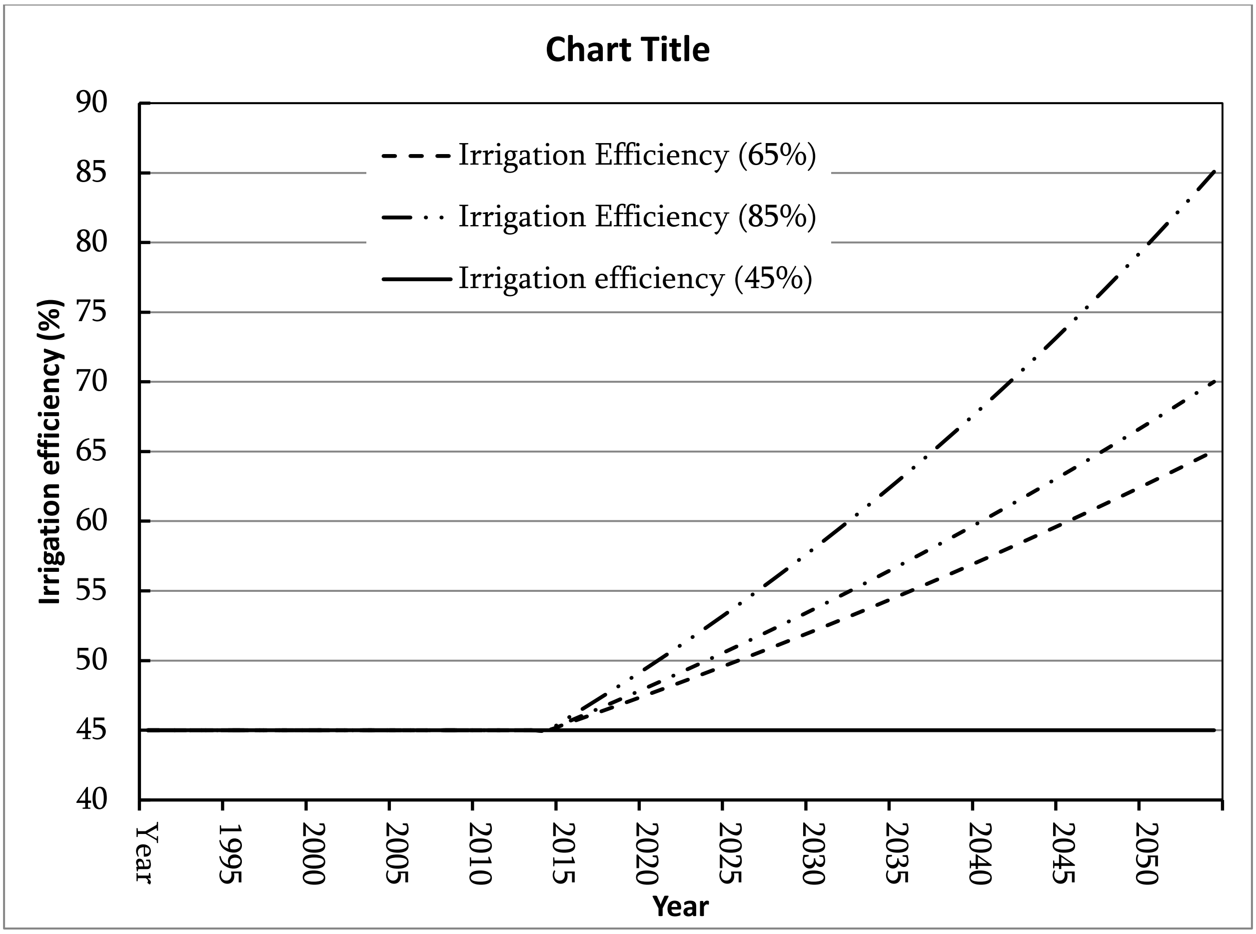

Fig. 8.2 projected Irrigation efficiency scenarios

8.3. Results and Discussions

8.3.1. Water demand Projections

The sustainability of water resources highly relies on the equilibrium between supply and demand. The availability of water in the basin had already suffered climbing irrigation water demand over the years. Hence, adaptation strategies are required to sustain water resources and crop production. Prediction of irrigation extent and irrigation water source preference and method of irrigation and its efficiency are crucial factors in irrigation development and demonstrating its impacts on the water resources. Table 8.8 shows that irrigation is the largest water consumer that computed to about 95.5% and followed by 2.3%, 1.8% of domestic and livestock water demand as compared to total demand in 2015.

In the future also irrigation water demand will be projected to continue increasing over the study period. Irrigation water demand is expected to grow over 75% (IES-1), 100%, (IES-2), and 150% (IES-3) in 2055 as compared to 2015 under the current irrigation efficiency. Similarly, domestic water demand is expected to hit 227% in 2055 as compared to 2015 considering the 3% population growth rate in the country/region. The livestock water demand doesn't show change which is attributed to the number of livestock, its number does not significantly rise.

Table 8.8 Water demand for the year (2015-2055) in MCM

Scenario	Water demand sector	2015	2025	2035	2045	2055
Baseline	Irrigation water demand	1093	1093	1093	1093	1093
	Domestic water demand	26	35	47	63	85
	Livestock water demand	21	21	21	21	21
	Industrial water demand	1.3	1.3	1.3	1.3	1.3
	Sum	**1141**	**1141**	**1141**	**1141**	**1141**
IES-1	Irrigation water demand	1093	1258	1446	1664	1913
	Domestic water demand	26	35	47	63	85
	Livestock water demand	21	21	21	21	21
	Industrial water demand	1.3	1.75	2.3	3	4
	Sum	**1141**	**1316**	**1516**	**1751**	**2023**
IES-2	Irrigation water demand	1093	1300	1547	1840	2188
	Domestic water demand	26	35	47	63	85
	Livestock water demand	21	21	21	21	21
	Industrial water demand	1.3	1.7	2.3	3	4
	Sum	**1141**	**1358**	**1617**	**1927**	**2298**
IES-3	Irrigation water demand	1093	1360	1693	2103	2611
	Domestic water demand	26	35	47	63	85
	Livestock water demand	21	21	21	21	21
	Industrial water demand	1.3	1.7	2.3	3	4
	Sum	**1,141**	**1418**	**1763**	**2190**	**2720**

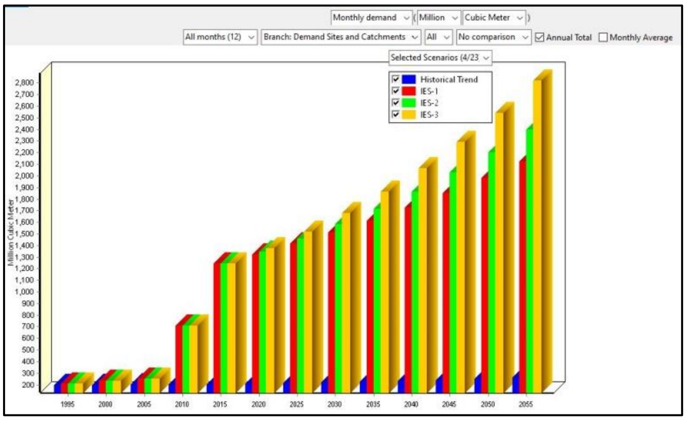

Fig. 8.3 Projected water demand of all sectors (1995-2055)

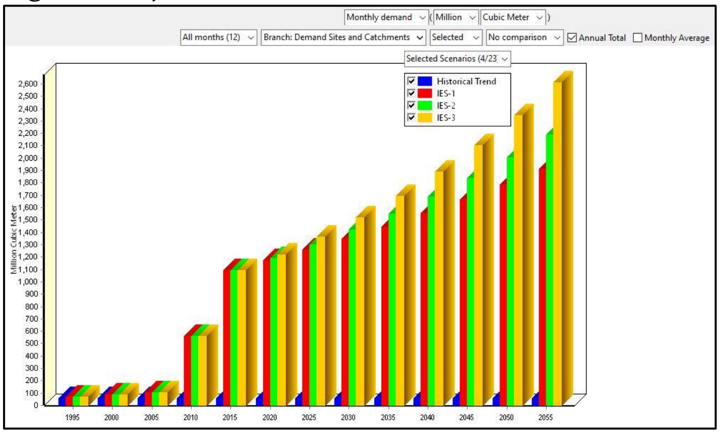

Fig. 8.4 Projected irrigation water demand under IES-1, IES-2, IES-3 and Baseline scenario

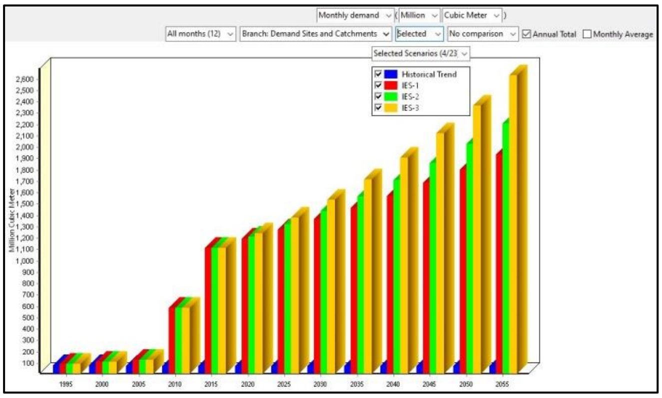

Fig. 8.5 Projected agricultural water demands (Irrigation and livestock sector) (1995-2055)

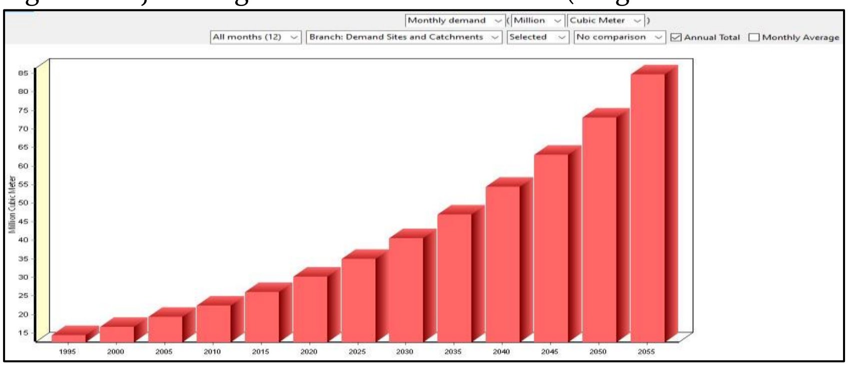

Fig. 8.6 Projected domestic water demand (1995-2055)

8.3.2. Change in streamflow under irrigation projection scenarios

Streamflow is the key element of the water resource, which directly affects water resources management. Modifications in the long-term discharge of streamflow can be caused by climate change, and man-made practices such as building water reservoirs, land use pattern basin, and, abstraction of water for irrigation. The irrigation water demand decreases stream flows by the amount delivered or to be delivered to the demand sites. The outputs of the model result revealed that because of irrigation water demand the total streamflow (Ketar and Meki rivers) to the Lake Ziway has been expected to shrink by 12% as compared to the baseline scenario under irrigation scenarios. The expected amount of water that can be delivered to the demand sites has to be much higher than the model outcome, which is about 12% of the annual streamflows.

This is explained by the variation of temporal water availability in the streams and monthly irrigation water demand. Since streams are characterized by high discharge during the main rainy season (80-92%). Whereas, the irrigation water demand is almost null (rainfall based) these months. Conversely, the basin has experienced high irrigation water demand and thus, causes huge unmet demands during dry months. The temporal imbalance of supply-and-demand has posed a huge challenge for sustainable water resources management in the Ketar and Meki subbasins.

8.3.3. Change in groundwater depth under irrigation projection scenarios

When the groundwater extraction rate surpasses the recharge rate for the specified aquifer, is a potential signal of water scarcity (Richey et al., 2015; Triana et al., 2020). In this case, the main driver of water strain is groundwater withdrawal for irrigation use which lead to the depletion of aquifer (Bartolino & Cunningham, 2003). The outputs of the coupled WEAP-MODFLOW model showed that there will be a significant change in the groundwater table as a result of water extraction from aquifers. For instance, on Column and Row number (C=38, R=43) in the aquifer of the Rift floor subbasin in the month of May (10.6% of monthly variation in a year). The comparison of groundwater heads under IES-1 showed that groundwater level will be likely changed by -7m (2020), -11.9m (2030), -14.9m (2040), and -21m (2055) with the respect the baseline scenario. While, ISE-2 showed that groundwater level will be likely change -7.3m (2020), -12.8m (2030), -16.9m (2040), and -27.9m (2055) with the respect the baseline scenario. Similarly, -7.6m (2020), -14.5m (2030), -21.1m (2040), and -39.1m (2055) decline of groundwater head under IES-3 as compared to baseline and the pictorially shown in (Fig. 8.7 and Fig. 8.8).

For the Meki subbasin, on Column and Row number (C=24, R=30) in the aquifer of the Meki subbasin in the month of Nov (13.2% of monthly variation in a year). The impacts of irrigation expansion scenarios are shown in (Fig. 8.9 and Fig. 8.10). The comparison of groundwater heads under IES-1 showed that groundwater levels will likely change -11.2m (2020), -16.5m (2030), -32.7m (2040), and -70m (2055) with the respect to the baseline scenario. While, ISE-2 showed that groundwater levels will likely change -12.3m (2020), -20.3m (2030), -41.6m (2040), and -90.1m (2055) with the respect to the baseline scenario. Similarly, -14.4 (2020), -27.6m (2030), -65m (2040), and -119m (2055) decline of groundwater head under IES-3 as compared to baseline.

For the Ketar subbasin, on Column and Row number (C=57, R=43), the comparison of groundwater head under IES-1 showed that groundwater level will likely change -5.2m (2020), -7m (2030), -8.3m (2040), and -10.9m (2055) with the respect the baseline scenario. While, ISE-2 showed that groundwater levels will likely change -5.4m (2020), -7.4m (2030), -9.3m (2040), and -14.9m (2055) with the respect to the baseline scenario. Similarly, -5.6m (2020), -8.3m (2030), -11.2m (2040), and -21.7m (2055) decline of groundwater head under IES-3 as compared to baseline and it is shown in (Fig. 8.11 and Fig. 8.12).

Consequently, the smallholder farmers have access to groundwater using shallow dug wells (10 to 50m). If pumping from groundwater sources continues as projected irrigation water demand, the smallholder farmers will have faced difficulties as a result of lowering the groundwater table. This would in turn threatens the region's food security as in many part of the world (Jain et al., 2021).

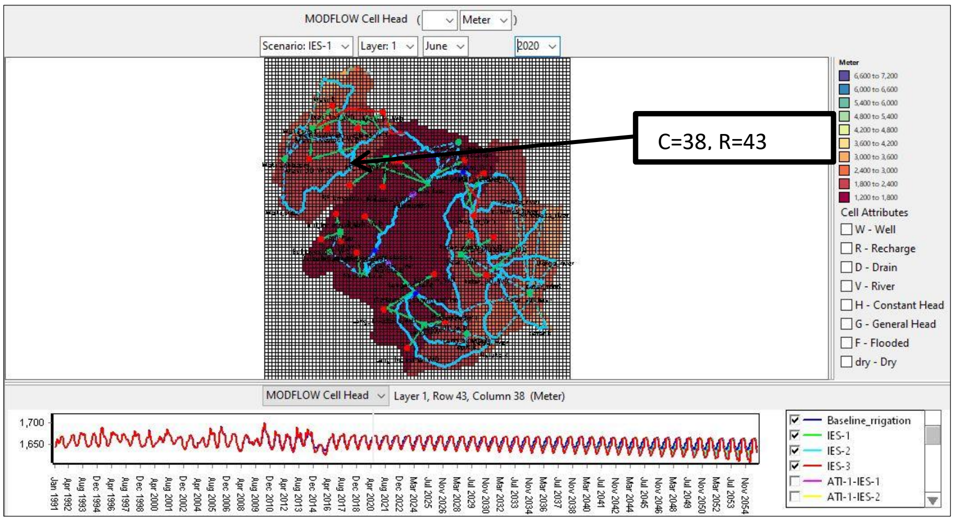

Fig. 8.7 Trend groundwater head at (C=38, R=43) under scenarios (IES-1, IES-2, and IES-3)

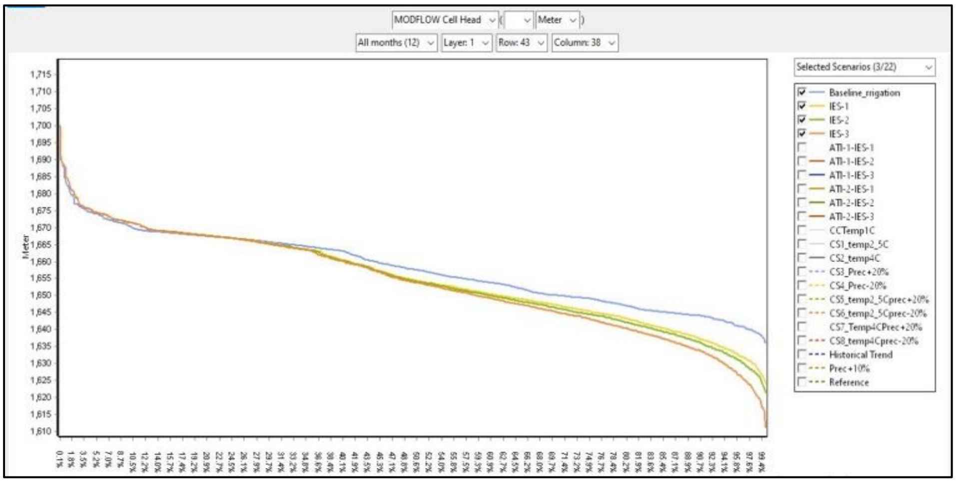

Fig. 8.8 Percent exceedance of groundwater head at (C=38, R=43) under scenarios (IES-1, IES-2, and IES-3

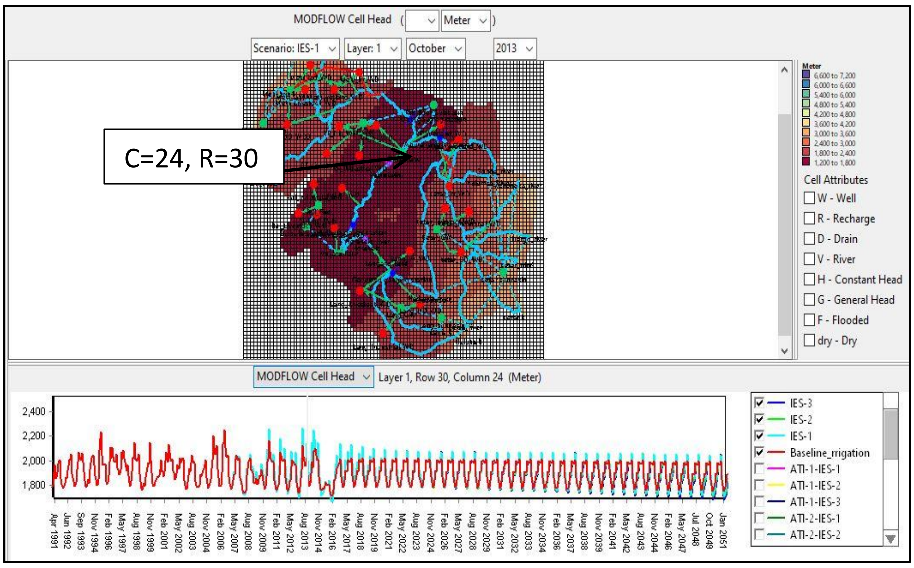

Fig. 8.9 Trend groundwater head at (C=24, R=30) under scenarios (IES-1, IES-2, and IES-3)

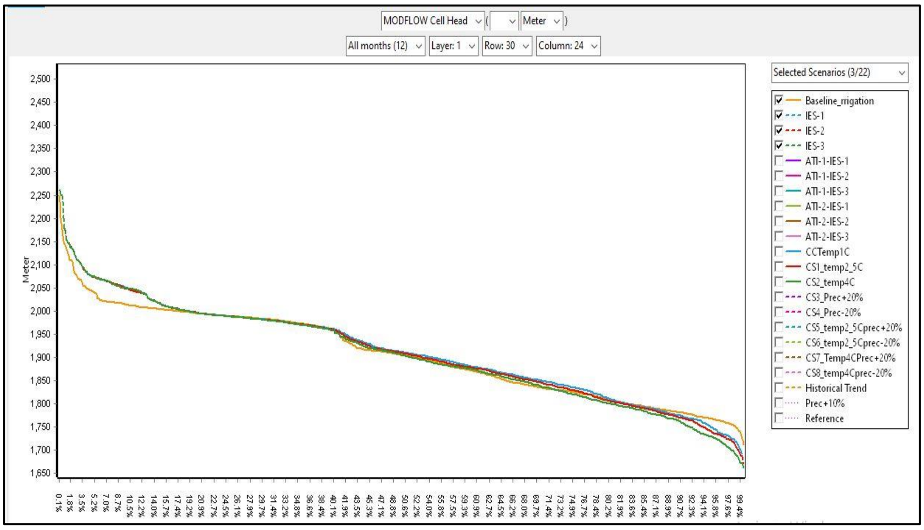

Fig. 8.10 Percent exceedance of groundwater head at (C=24, R=30) under scenarios (IES-1, IES-2, and IES-3)

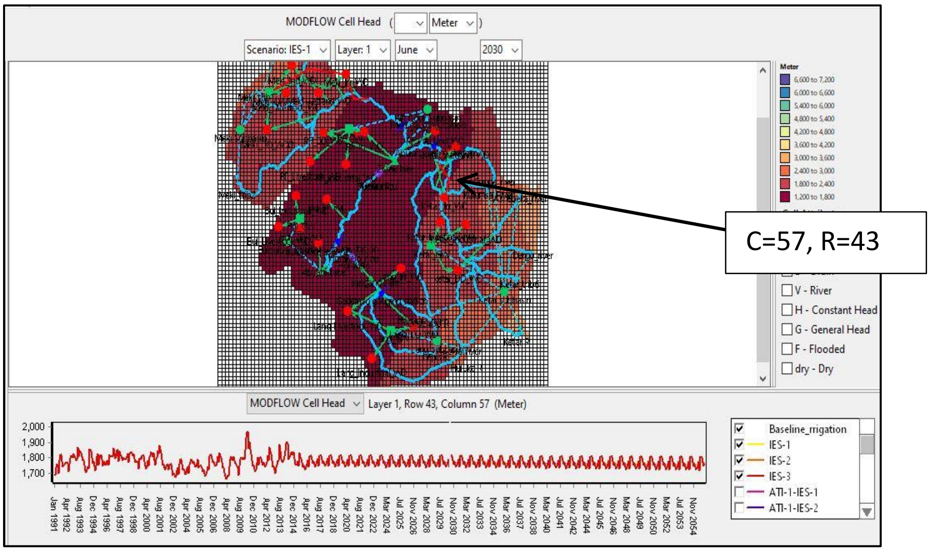

Fig. 8.11 Trend groundwater head at (C=57, R=43) under scenarios (IES-1, IES-2, and IES-3)

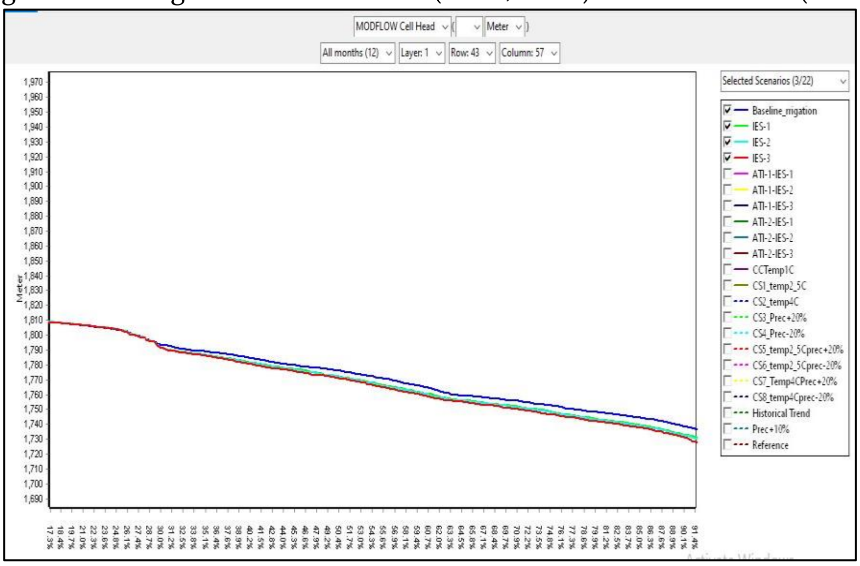

Fig. 8.12 Percent exceedance of groundwater head at (C=57, R=43) under scenarios (IES-1, IES-2, and IES-3)

8.3.4. Unmet demand

In the basin, water shortages occurred during the dry periods of the year in the case of IES-1, IES-2, and IES-3 scenarios as illustrated in Fig. 8.13. It is clear that throughout the rainy season (July to October), no water shortages existed. Peak water shortage is observed in the dry season (December to April) and moderate in (May, June, and November). The greatest shortfall is related with the highest rate of irrigation expansion scenario (IES-3) followed by (IES-2) and the least corresponds to IES-1.

This shows that the basin has high temporal water variability that aggravates water scarcity at these months of the year. The annual unmet demand is steadily increasing across all irrigation expansion scenarios as shown in Fig. 8.14 and Table 8.9. The annual unmet demand will be 429MCM, 506MCM, and 636MCM for IES-1, IES-2, and IES-3 at the end of 2055, respectively. The increasing unmet demand needs water resource management strategies to reduce its impacts.

Table 8.9 Annual unmet water demand (in MCM)

Irrigation expansion scenario	2015	2020	2025	2030	2035	2040	2045	2050	*2055*
IES-1	184	208	248	272	298	325	355	391	*429*
IES-2	184	213	259	289	323	360	406	456	*506*
IES-3	184	219	273	314	357	413	475	549	*636*

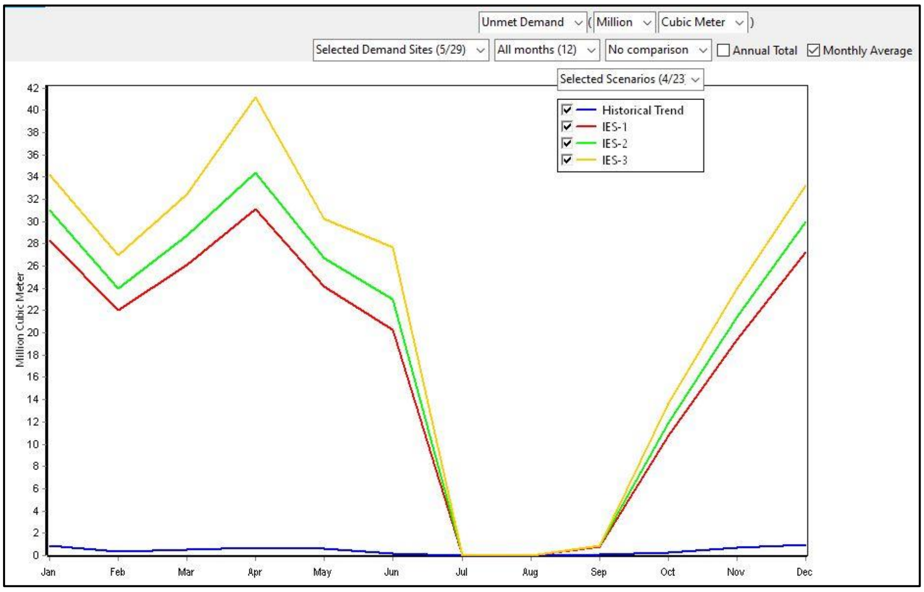

Fig. 8.13 Monthly average unmet demand

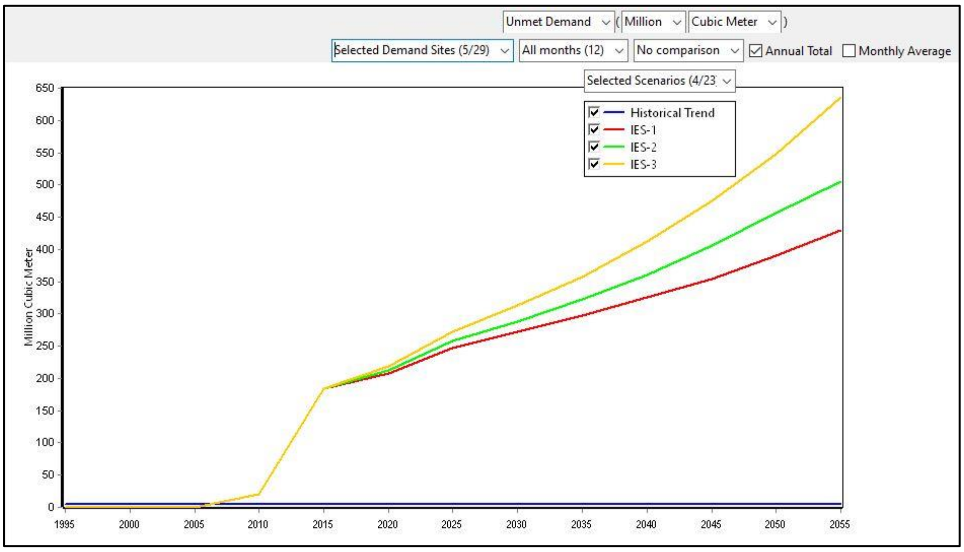

Fig. 8.14 Annual unmet demand under three scenarios

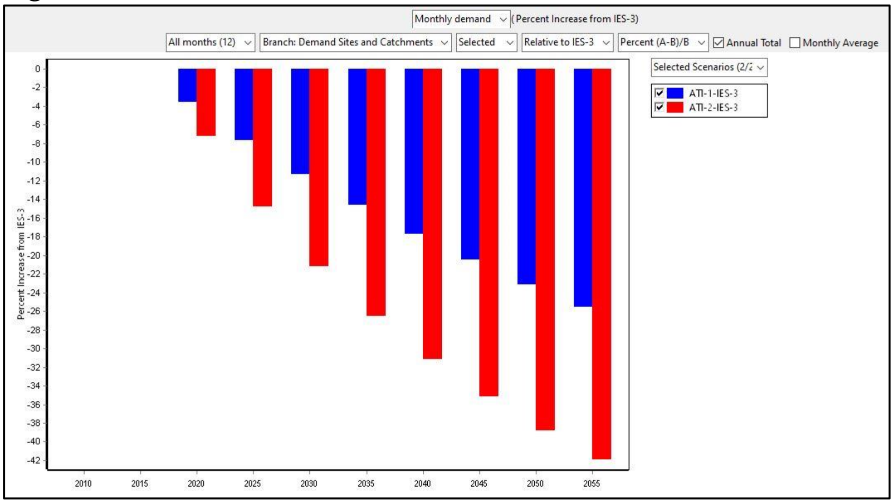

Fig. 8.15 The Percentage change ATI-1 and ATI-2 compared to IES-3

8.3.5. Adaptation or management strategies

The expansion of irrigated land had continued to increase disproportionately compared to the available water in the basin. Now, the irrigation water demand surpassed/exceeded the basin water supply. There is increasing stress from irrigation water demand and environmental sustainability concerns to reduce the depletion rate of water resources while maintaining the rising demand for irrigation in the semi-arid part of the basin. One of the strategic mechanisms to minimize this unmet demand is to optimize irrigation water use. The main approach used to optimize irrigation water use is improving irrigation water use efficiency (Reba et al., 2017; Wichelns, 2014). Therefore, understanding farming practices and their corresponding water use plays a significant role in optimizing irrigation water use. The effects of management scenarios on irrigation water demand were shown in Fig. 8.15.

Water resources use management scenarios, for instance, scenarios will cut progressively required water for irrigation demand ranging from 4% to 26% (under ATI-1) and 7% to 42% (under ATI-2) for (IES-1, IES-2, and IES-3) as compared to its corresponding scenario without adaptation strategies over the study period. Moreover, the unmet irrigation water demand will be predicted to decrease by 4% (2020), 15% (2035), and 26% (2055) under ATI-1 scenario. Similarly, ATI-2 will lower progressively required irrigation water demand by 7% (2020), 24% (2035), and 42% (2055) over the simulation period for (IES-1, IES-2), and IES-3) as compared to its corresponding scenario without irrigation demand management.

The extraction of groundwater resources is expected to increase than it was before, because of irrigation expansion, population and, and climate change. To cope up with this situation, better viable management measures that can minimize the decreasing conditions of groundwater heads have to be realized. The simulation result showed that enhancing efficiency will reverse the plunge experienced by the aquifer at the Rift floor (C=38, R=43) With the respect to IES-1, the rate of decline will be reversed by 0.3m (2020), 1.1m (2030), 2.5m (2040) and 5.5m (2055) under the ATI-1-IRS-1.

Moreover, under ATI-2-IES-1 the rate of decline will be reduced by 0.3m (2020), 1.7m (2030), 3.9m (2040), and 8.7m (2055), and the trend was shown in Fig. 8.16. ATI-1-IES-2 will reduce the groundwater decline by 0.3m (2020), 1.1m (2030), 2.4m (2040), and 7.9m (2055) with the respect to IES-2. With the scenario ATI-2-IES-2, the groundwater table improved the lowering of the water table by 0.4m (2020), 1.9m (2030), 3.9m (2040), and 11.1m (2055) with the respect to IES-2 and it was shown in Fig. 8.17. As compared to IES-3, shown in Fig. 8.18, the model revealed that will reverse the slump in the water table by 0.3m (2020), 1.3m (2030), 3.5m (2040), and 9.6m (2055) under the ATI-1-IES-3. ATI-2-IES-3 the rate of decline will be reduced by 0.6m (2020), 2.2m (2030), 5.3m (2040), and 15.7m (2055).

In line with this, one of the most effective practices to reduce groundwater abstractions is by implementing shifting to more efficient irrigation technologies (Shah et al., 2000). The increased water demand for irrigation could affect farm productivity, soil salinity conditions, water quality, water protection, aquatic ecosystems, and continual use of this resources in the basin (Gautam, Paudel, & Guidry, 2020). Therefore, irrigation schemes' water use efficiency enhancement is the key concern in the agriculture sector and it is directly associated with sustainable water resource utilization.

These management and irrigation expansion scenarios may be further influenced by climate change. Hence, **the best case scenario** that composed of IES-1 and ATI-2 or ATI-2-IES-1 and 20% increase in precipitation. A 20% increase in precipitation could slight reduce by 1.6-2.2% across the subbasins on irrigation water allocation.

On the contrary, **the adverse case scenario** that composed of ATI-1-IES-3 along with a 20% decline in precipitation will likely increase by 1.6-2.1% in the subbasins in irrigation water allocation. However, these decrease or increase in precipitation may be largely influences in negatively or positively water affects water available in the rivers, lakes and groundwater storage, besides modifying irrigation water requirement of the basin.

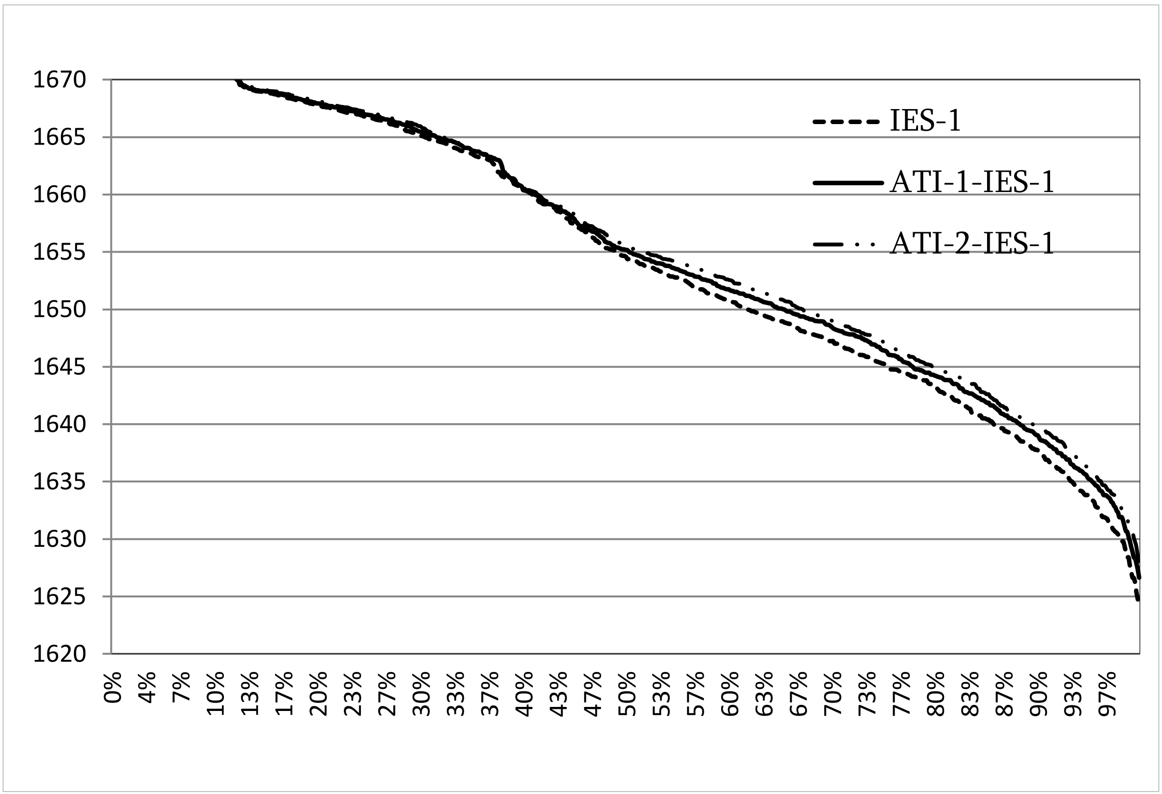

Fig. 8.16 Percent exceedance of groundwater head under IES-1 and adaption scenarios (ATI-1 and ATI-2)

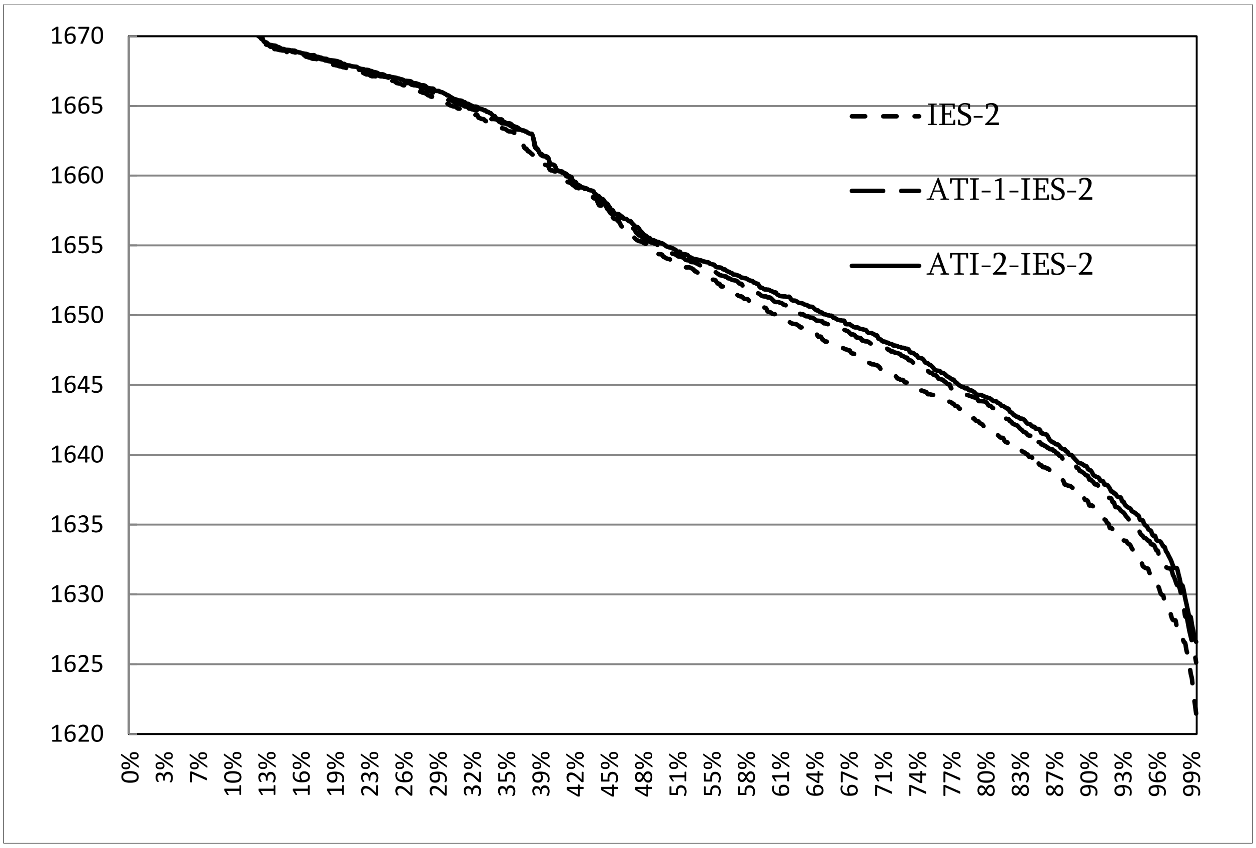

Fig. 8.17 Percent exceedance of groundwater head under IES-2 and adaption scenarios (ATI-1 and ATI-2)

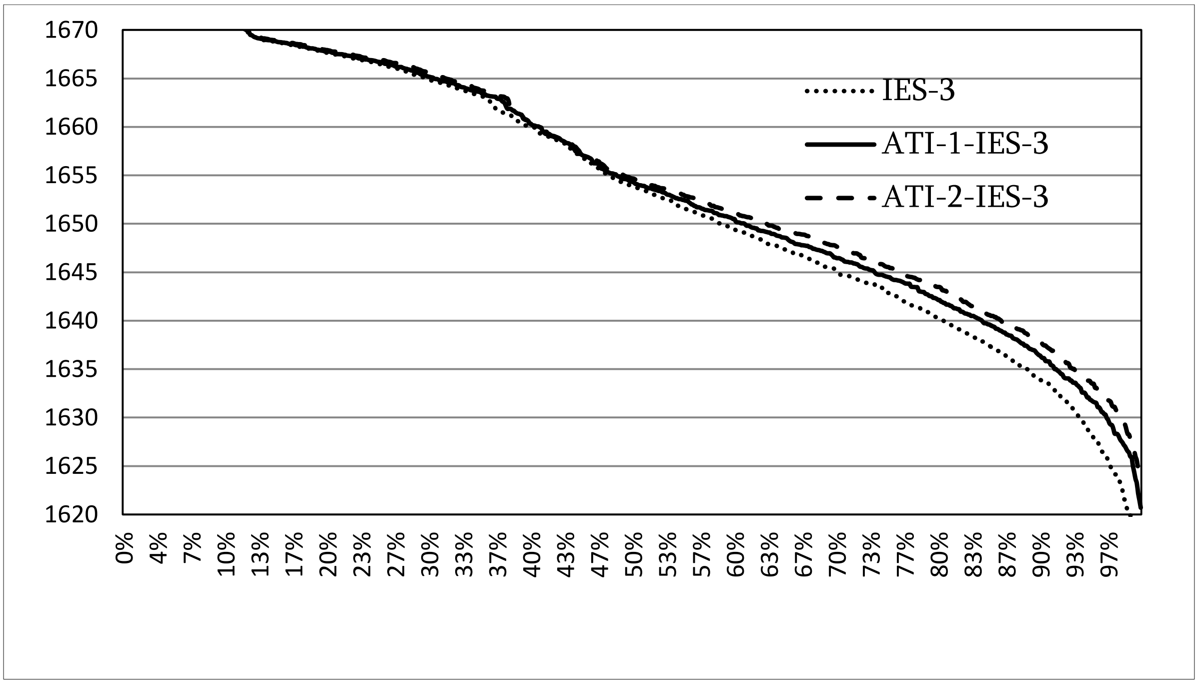

Fig. 8.18 Percent exceedance Groundwater head under IES-3 and adaption scenarios (ATI-1 and ATI-2)

9. Conclusions and Recommendations

9.1. Conclusions

The Abijata-Langano-Ziway Lakes Basin (ALZLB) is located in the Central Section of the Central Main Ethiopian Rift valley, which encompasses part of Oromia and Southern Nations and Nationalities and Peoples' Administrative Regions. It is a part of the Ethiopian Rift Valley Basin and it is bounded by geographic coordinates of 414500-545180mE longitude and 797930- 93592mN latitude.

Unsustainable utilization of water for growing irrigation has posed a challenge to water resources management along with climate changes. Particularly, the central part of the rift basin is highly endowed with water resources (surface and groundwater) and became a center for irrigation development. The study aimed to understand and provide the scientific basis for the response of water resources to various stress.

The geology and hydrogeological setting of the area control the availability and distribution of water in the region. The basin is described by humid to sub-humid in the plateaus and arid and semi-arid in the rift floor. Besides, there is high rainfall variability in spatio-temporal distribution exists in the basin that seems to be controlled by topographic variation (1550-4184masl). The climate of the basin is humid to sub-humid in the highlands and semi-arid on the rift floor.

The WEAP-based hydrological model integrity assessment records showed a very good consistency among monthly observed and simulated streamflow at the outlets for both the Ketar and Meki subbasins for calibration. While for validation period their output were rated as very good and good for Ketar and Meki subbasin, respectively. Generally, the model was able to preserve a very good in reproducing of the overall streamflow characteristics of the subbasin. The WEAP model outcomes revealed that evapotranspiration and lake water evaporation are the largest water consumers in the basin. The annual stream discharge is mainly composed of interflow that contributes a major part of flow during the wet season and is followed by the baseflow that is critical to sustaining the streamflow during the dry season.

While considering water availability in a temporal context, more than 80% of the annual total discharge is clustered in July-October and the remaining months are largely dependent on the baseflow contribution to the streamflow. This is because of the seasonality of rainfall in the catchment. However, in recent years, water requirement for irrigation, in particular, is increasing in the dry periods as a result of little precipitation in these months.

Therefore, the sustainable water availability of the Ketar and Meki streams are dependent on the baseflow throughout the year and anything that alters the hydrologic behavior of the catchment may bring an impact on the precipitation, Evapotranspiration/ evaporation, baseflow, and Surface runoff amount and could affect the sustainability of streamflow. Later, it may affect sequentially the downstream water users and water level of Ziway Lake and lastly Lake Abijata.

Whereas, to understand the groundwater system, the numerical groundwater flow model using MODFLOW was investigated. Based on the calibrated outputs of the numerical groundwater flow model results showed that the model can reproduce the aquifers' properties and produce a good fit model. This result revealed that concisely matches with the adapted conceptual model and assumption articulated.

The dynamic link of surface-groundwater model was done with the help of the Linked kitchen tool. The coupled WEAP-MODFLOW showed a good-fit among measured and simulated flows and the hydraulic heads. The calibrated coupled surface-groundwater (WEAP-MODFLOW) model was used to evaluate the water resource availability of the basin and can be applied for impact evaluation. The calibrated WEAP-MODFLOW model offers the capability to examine, equate and evaluate several options for water supply, water demand, and management scenarios. Upcoming restraints such as a change in demographic, climate, irrigation expansion, and irrigation efficiency can be taken into consideration. The output results can be seen as maps, graphs and table depicting the impacts of the given scenario on the supply-demand of the basin.

The balance between the supply and demand sides determines the basin’s water availability conditions. The major factor that governs the supply side is climate change. On the other hand, the demand side is mainly influenced by the basin irrigation water demand.

Water resources are inevitably connected climate variables, so the projected change in climate may consequences for water availability. The reanalysis of RCM data revealed an increase of 25% rainfall in mid-century and 2.5^{0}C to 4^{0}C in temperature at the end of 21th

century. However, $\pm$ 20% change in annual precipitation and 2.5^{0}C and 4^{0}C scenarios were used to avoid uncertainty to evaluate its impacts on water resources in the basin.

The change in rainfall and temperature would bring significant changes in the hydrologic components and, thereby, the streamflow and groundwater table of the subbasin. The susceptibility of mean annual recharge to changes in rainfall or temperature is found to be variable over the simulation period. The annual surface runoff, groundwater recharge, and streamflow are expected to surge by 61-71%, 22-27%, and 70-76% with a 20% rainfall increment and corresponding warming in temperature, respectively. On the contrary, considering adverse scenarios that may occur as a recurrent drought, a 20% rainfall reduction and respective warming in temperature will have resulted in a decline of annual surface runoff, groundwater recharge, and streamflow by 42-45% and 37-42%, and 59-67% over the coming three decades compared with the baseline period, respectively.

Though, the basin has endowed with a high potential of water, and water is the vital resource for developments. There has high irregularity in spatial and temporal distribution marker water an extremely scarce resource in some part of the basin and certain times of the year. The simulated result also indicates that the recharge is highly correlated to the annual rainfall and follows a reduced duplication of the rainfall pattern of the watershed. The study results will have connections and insights on groundwater recharge and its susceptibility to climate change at the subbasin level, and water resources (lakes) in the low-lying rift floor region. Since the highlands or plateaus of the Ketar

River watershed is considered a potential recharge zone and the origin of many streams and it contributes a significant amount of water to streamflow in the form of base flow. Besides, groundwater contributes to the lakes and low-lying rift floor region of the basin. The hydrology of the watershed is more responsive to precipitation than temperature change in general. A little change in evapotranspiration, recharge, and interflow was shown for scenarios that only consider the temperatures change in the Ketar watershed. The simulated outputs showed that the changing climate could have both favorable and adverse effects on the hydrologic components of the basin.

Irrigation use is the biggest water consumer sector in the basin and is also expected to continue rising with different magnitudes (IES-1, IES-2, and IES-3) over the study period, despite its poor irrigation water use efficiency that ranges from 43-55%. The basin has high variability in space-time dimension water availability, as a result, there is unmet demand in dry months (October to June), though there is high water resource potential in the basin on the annual basis.

The projected irrigation expansion scenarios will exert more pressure on stream flows, inflow to reservoirs, and groundwater head. Eventually, these could impact water quality (salinity), and cause environmental problems (ecosystem, ecology of the basin). Moreover, tighten the competition to get access to water resources and thereby trigger conflicts on the water resources. Increase the cost to access groundwater due to depletion of the water table and possess difficulties for smallholder farmers. At last, it may adversely affect soil fertility status and reduce yield and endanger the food security of the region.

To reduce these challenges, proper demand-side management has paramount importance to reconcile the difference among the demand and supply sides. Hence, the study assessed different adaption strategies /management strategies/scenarios that focus on improving irrigation technology were investigated. Implementing ATI-1 and ATI-2 could significantly reduce irrigation water scarcity at the end of the study period.

9.2. Recommendations

The WEAP-based hydrological model could be applied for future effect valuation and evaluation (climate change) and management option setting plausible scenarios. The calibrated WEAP model can be implemented as the water allocation model since it represents the demand sites as a node, the supply preference can be determined and supply sources can be one or more at a time. Thorough monitoring of groundwater wells, rivers and lakes is suggested to understand the temporal-based change in groundwater heads and enhance the model accuracy.

Coupled WEAP-MODFLOW model is a viable water management model that integrates the surface and groundwater system in a holistic manner, and is used for impact evaluation on both systems due to alteration of natural and anthropogenic activities. Uncertainty in a model either surface water or groundwater is unenviable because of the errors on the dataset or intrinsic parameter properties, assumptions, and simplification made to simplify the complex natural systems. It is tolerable if it is in the acceptable range. The projected climate may impact water resources since basin water resource is more susceptible to changes in precipitation. However, a temperature change will be bringing a very modest change to the water resources system. Besides, there is huge uncertainty in GCM models to predict future climate conditions and thereby estimate the optimal water potential of the basin.

Climate change adaptation mechanisms have to be encouraged in the basin i.e., watershed management activities. Water storage schemes are required for optimum use in water in the basin, a large amount of water available in a few months (wet season). On the contrary, dry months are water-scarce (uneven temporal distribution).

The temporal availability of water and demand are at opposite time, or conjunctive use of surface and groundwater could play a significant role in easing the challenge of growing water demands in the basin. Hence, water resources use and development strategies in the basin should be focused not only on the potential of water development but also on improving its temporal-spatial distribution.

Implementing adaption strategies could significantly reduce water scarcity in the basin and will sustain the farming practices that help to ensure the food security of the area. Over-exploitation of water resources for extended periods could degrade the water quality (Salinity and Sodicity, alkalinity). So, it is essential to implement proper water allocation regulations guidelines (e.g., water pricing, licensing).

10. Reference

Abbate, E., & Sagri, M. (1980). *Volcanites of the Ethiopian and Somali plateaux and major tectonic lines:In: Geodynamic Evolution of the Afro-Arabic Rift System, Accad. Naz. Lincei, Roma, Atti Convegni, 47, pp. 219–227.*

Abebe, T., Balestrieri, M. L., & Bigazzi, G. (2010). The Central Main Ethiopian Rift is younger than 8 Ma: Confirmation through apatite fission-track thermochronology. *Terra Nova*, *22*(6), 470–476. https://doi.org/10.1111/j.1365-3121.2010.00968.x

Abraham, T., Abate, B., Woldemicheal, A., & Muluneh, A. (2018). Impacts of Climate Change Under CMIP5 RCP Scenarios on the Hydrology of Lake Ziway Catchment , Central Rift Valley of. *Journal of Environment and Earth Science*, *8*(7), 81–90.

Abraham, T., Woldemicheala, A., Muluneha, A., & Abateb, B. (2018). Hydrological Responses of Climate Change on Lake Ziway Catchment , Central Rift Valley of Ethiopia. *Earth Science & Climatic Change*, *9*(6). https://doi.org/10.4172/2157-7617.1000474

Abtew, W., & Melesse, A. (2013). *Evaporation and Evapotranspiration: Measurements and Estimations*. https://doi.org/10.1007/978-94-007-4737-1

Ahmadi, A., Ohab-Yazdi, S. A., Zadehvakili, N., & Safavi, H. R. (2018). A dynamic model of water resources management using the scenario analysis technique in downstream of the Zayandehroud basin. *International Journal of River Basin Management*, *0*(0), 1–13. https://doi.org/10.1080/15715124.2018.1505734

Aich, V., Liersch, S., Vetter, T., Huang, S., Tecklenburg, J., Hoffmann, P., … Hattermann, F. F. (2014). Comparing impacts of climate change on streamflow in four large African river basins. *Hydrology and Earth System Sciences*, *18*(4), 1305–1321. https://doi.org/10.5194/hess-18-1305-2014

Alemayehu, T., Ayenew, T., & Kebede, S. (2006). Hydrogeochemical and lake level changes in the Ethiopian Rift. *Journal of Hydrology*, *316*(1–4), 290–300. https://doi.org/10.1016/j.jhydrol.2005.04.024

Alizadeh, H., & Mousavi, S. J. (2013). Coupled stochastic soil moisture simulation-optimi- zation model of deficit irrigation. Res. 49, 4100–4113. *Water Resour.*, *49*, 4100–4113.

https://doi.org/10.1002/wrcr.20282.

Allen, R. G., Pereira, L. S., Raes, D., & Smith, M. (1998). FAO Irrigation and Drainage Paper Crop by. In *Irrigation and Drainage* (Vol. 300).

Allen, R. G., Pereira, L. S., Raes, D., Smith, M., & Ab, W. (1998). *Crop evapotranspiration - Guidelines for computing crop water requirements - FAO Irrigation and drainage paper 56 By* (pp. 1–15). pp. 1–15.

Anderson, M. P., & Woessner, W. W. (1992). *Applied Groundwater Modeling Simulation of Flow and Advective Transport*. Academic Press.

Anderson, M. P., Woessner, W. W., & Hunt, R. J. (2015). *Applied Modelling Simulation of Flow and Advective Transport Second Edition*. Academic Press.

Arno, V., Di paola, G. M., & Berhe, S. M. (1993). The Kella Horst; its origin and significance in crustal attenuation and magmatic processes in the Ethiopian rift valley Arno,. *In: Geology and Mineral Resources of Somalia and Surrounding Regions*, (113 a), 323–338. Firenze: Instituto Arronomico L'oltremar.

Arnold, J. ., Srinivasan, R., Muttiah, R. ., & Williams, J. . (1998). Large area hydrologic modeling and assessment part I: Model development. *Am. Water Resour. Assoc*, *34*.

Asghar, A., Iqbal, J., Amin, A., & Ribbe, L. (2019). Integrated hydrological modeling for assessment of water demand and supply under socio-economic and IPCC climate change scenarios using WEAP in Central Indus Basin. *Journal of Water Supply: Research and Technology - AQUA*, *68*(2), 136–148. https://doi.org/10.2166/aqua.2019.106

Ayenew, T. (1998). *The hydrogeology of the lake district basin. Published PhD thesis.* Free university of Amsterdam. The Netherlands.

Ayenew, T. (2003). Evapotranspiration estimation using thematic mapper spectral satellite data in the Ethiopian rift and adjacent highlands. *Journal of Hydrology*, *279*(1–4), 83–93. https://doi.org/10.1016/S0022-1694(03)00173-2

Ayenew, T. (2004). Environmental implications of changes in the levels of lakes in the Ethiopian Rift since 1970. *Regional Environmental Change*, *4*(4), 192–204.

https://doi.org/10.1007/s10113-004-0083-x

Ayenew, T. (2007). Water management problems in the Ethiopian rift: Challenges for development. *Journal of African Earth Sciences*, *48*(2–3), 222–236. https://doi.org/10.1016/j.jafrearsci.2006.05.010

Bakker, M., & Bartholomeus, R. P. (2013). "Groundwater recharge: processes and quantififcation." *Hydrol.Earth Syst.Sci*, *116*(4), 2653–2655. https://doi.org/10.1029/2011JG001693

Balek J., Simmers, I. (1987). *Estimation of Natural Groundwater Recharge NATO ASI Series*.

Barbaro, B. J. R., & Zarriello, P. J. (2006). *A Precipitation-Runoff Model for the Blackstone River Basin , Massachusetts and Rhode Island: U.S. Geological Survey Scientific Investigations Report 2006–5213, 95 p.*

Bartolino, J. R., & Cunningham, W. L. (2003). Ground-Water Depletion Across the Nation. *U.S Geological Survey Fact Sheet 103-03*, (November), 103–03. Retrieved from http://pubs.usgs.gov/fs/fs-103-03/#pdf

Bates, B. C., Kundzewicz, Z. W., Wu, S., & J.P. Palutikof, E. (2008). Climate Change and Water. Technical Paper of the Intergovernmental Panel on Climate Change, IPCC Secretariat, Geneva, 210 pp. In *IPCC*. https://doi.org/10.1007/978-3-319-41372-3_12

Bekele, D., Alamirew, T., Kebede, A., Zeleke, G., & Melesse, A. M. (2018). Modeling Climate Change Impact on the Hydrology of Keleta Watershed in the Awash River Basin , Ethiopia. *Environmental Modeling & Assessment*, *24*, 95–107.

Benvenuti, M., Carnicelli, S., Belluomini, G., Dainelli, N., Di Grazia, S., Ferrari, G. A., … Kebede, S. (2002). The Ziway-Shala lake basin (main Ethiopian rift, Ethiopia): A revision of basin evolution with special reference to the Late Quaternary. *Journal of African Earth Sciences*, *35*(2), 247–269. https://doi.org/10.1016/S0899-5362(02)00036-2

Berehanu, B. (2017). *Evaluation of the Water Supply Systems of Addis Ababa and its Environs Using WEAP and MODFLOW Coupled with LinkKitchen*.

Berhe, M. S. (1986). Geologic and geochronologic constraints on the evolution of the Red Sea-Gulf of Aden and Afar depression. *Journal of African Earth Sciences*, *5*(2), 101–117.

https://doi.org/10.1016/0899-5362(86)90001-1

Beyene, T., Lettenmaier, D. P., & Kabat, P. (2010). Hydrologic impacts of climate change on the Nile River Basin: Implications of the 2007 IPCC scenarios. *Climatic Change*, *100*(3), 433–461. https://doi.org/10.1007/s10584-009-9693-0

BGR. (2013). *LinkKitchen*. Retrieved from www.brg.bund.de

Bigazzi, G., Bonadonna, F., Paola, G., & Giuliani, O. (1993). K-Ar and fission track ages of the last volcano tectonic phase in the Ethiopian Rift Valley (Tullu Moye' Area). *In: Geology and Mineral Resources of Somalia and Surrounding Regions.*, (113 a), 311–322. Firenze: Instituto Agronomico L'Oltremar.

Biniyam, Y., & Kemal, A. (2017). The Impacts of Climate Change on Rainfall and Flood Frequency: The Case of Hare Watershed, Southern Rift Valley of Ethiopia. *Earth Science & Climatic Change*, *8*(1), 1–5. https://doi.org/10.4172/2157-7617.1000383

Chernet, Tadiwos, Hart, W. K., Aronson, J. L., & Walter, R. C. (1998). New age constraints on the timing of volcanism and tectonism in the northern Main Ethiopian Rift - southern Afar transition zone (Ethiopia). *Journal of Volcanology and Geothermal Research*, *80*(3–4), 267–280. https://doi.org/10.1016/S0377-0273(97)00035-8

Chernet, Tesfaye. (1982). *Hydrogeology of the Lakes Region, Ethiopia*.

Chernet, Tesfaye, Travi, Y., & Valles, V. (2001). Mechanism of degradation of the quality of natural water in the lakes region of the Ethiopian Rift Valley. *Water Research*, *35*(12), 2819–2832. https://doi.org/10.1016/S0043-1354(01)00002-1

Chu, D., & Gordon, R. G. (1998). Current plate motions across the Red Sea. *Geophysical Journal International*, *135*(2), 313–328. https://doi.org/10.1046/j.1365-246X.1998.00658.x

Dainelli, N., Benvenuti, M., & Sagri, M. (2001). *Geological Map of the Ziway-Shala Lakes Basin (Ethiopia),1:250,000 scale,European commission Project*.

Davies, E. G. R., & Simonovic, S. P. (2011). Advances in Water Resources Global water resources modeling with an integrated model of the social – economic – environmental system. *Advances in Water Resources*, *34*(6), 684–700.

https://doi.org/10.1016/j.advwatres.2011.02.010

Dehghanipour, A. H., Zahabiyoun, B., Schoups, G., & Babazadeh, H. (2019). A WEAP-MODFLOW surface water-groundwater model for the irrigated Miyandoab plain, Urmia lake basin, Iran: Multi-objective calibration and quantification of historical drought impacts. *Agricultural Water Management*, *223* (February), 105704. https://doi.org/10.1016/j.agwat.2019.105704

Delfs, J. O., Wang, W., Kalbacher, T., Singh, A. K., & Kolditz, O. (2013). A coupled surface/subsurface flow model accounting for air entrapment and air pressure counterflow. *Environmental Earth Sciences*, *69*(2), 395–414. https://doi.org/10.1007/s12665-013-2420-1

Dereje Birhanu, M. (2011). *Numerical Groundwater Flow Modeling of the Meki River Catchment , Central Ethiopia. Unpublishe M.sc thesis, Addis Ababa University*. Addis Ababa.

Dessu, S. B., & Melesse, A. M. (2013). *Impact and uncertainties of climate change on the hydrology of the Mara River basin , Kenya / Tanzania*. *2986*(June 2012), 2973–2986. https://doi.org/10.1002/hyp.9434

Desta, H., & Lemma, B. (2017). Journal of Hydrology : Regional Studies SWAT based hydrological assessment and characterization of Lake. *Journal of Hydrology: Regional Studies*, *13*(August), 122–137. https://doi.org/10.1016/j.ejrh.2017.08.002

Di Paola, G. M. (1972). The Ethiopian Rift Valley (between 7° 00′ and 8° 40′ lat. north). *Bulletin Volcanologique*, *36*(4), 517–560. https://doi.org/10.1007/BF02599823

Doherty, J. (2010). *PEST-Model-Independent Parameter Estimation -User Manual (5th ed.). Watermark Numerical Computing. Brisbane,AUS*. Brisbane, Australia.

Döll, P. (2009). Vulnerability to the impact of climate change on renewable groundwater resources: A global-scale assessment. *Environmental Research Letters*, *4*(3). https://doi.org/10.1088/1748-9326/4/3/035006

Dougherty, M., Dymond, R. L., Grizzard, T. J., Godrej, A. N., Zipper, C. E., & Randolph, J. (2007). Quantifying long-term hydrologic response in an urbanizing basin. *Journal of Hydrologic Engineering*, *12*(1), 33–41. https://doi.org/10.1061/(ASCE)1084-0699(2007)12:1(33)

Dribsa, A. (2006). Groundwater–Surface water Interaction and Analysis of Recent Change Hydrologic Environment of Lake Ziway Catchment. Addis Ababa University, Ethiopia.

Droubi, A., Al-Sibai, M., Abdallah, A., Wolfer, J., Huber, M., Hennings, V., … Dechiech, M. (2008). *Development and Application of a Decision Support System (DSS) for Water Resources Management in Zabadani bassin, Syria and Berrechid Basin, Morocco*. (July), 116.

Droubi, A., Al-Sibai, M., Abdallah, A., Zahra, S., Obeissi, M., Wolfer, J., … Schelkes, K. (2008). A Decision Support System (DSS) for Water Resources Management, – Design and Results from a Pilot Study in Syria. *Climatic Changes and Water Resources in the Middle East and North Africa*, 199–225. https://doi.org/10.1007/978-3-540-85047-2_16

Duncan, H. P. (2019). Baseflow separation – A practical approach. *Journal of Hydrology*, *575*(May), 308–313. https://doi.org/10.1016/j.jhydrol.2019.05.040

Dutta, D., Rahman, A., Paul, S. K., & Kundu, A. (2019). Changing pattern of urban landscape and its effect on land surface temperature in and around Delhi. *Environmental Monitoring and Assessment*, *191*(9). https://doi.org/10.1007/s10661-019-7645-3

Ebinger, C. J. (1989). Cynthia J. Ebinger 1. *Tectonics*, *8*(1), 117–133.

Eckhardt, K. (2008). A comparison of baseflow indices, which were calculated with seven different baseflow separation methods. *Journal of Hydrology*, *352*(1–2), 168–173. https://doi.org/10.1016/j.jhydrol.2008.01.005

EWTC. (2008). *Ministry of water resources butajira – ziway areas development study hydrogeology and growndwater*.

Famiglietti, J. S., Lo, M., Ho, S. L., Bethune, J., Anderson, K. J., Syed, T. H., … Rodell, M. (2011). Satellites measure recent rates of groundwater depletion in California's Central Valley. *Geophysical Research Letters*, *38*(3), 2–5. https://doi.org/10.1029/2010GL046442

Fang, W., Huang, S., Ren, K., Huang, Q., Huang, G., Cheng, G., & Li, K. (2019). Examining the applicability of different sampling techniques in the development of decomposition-based streamflow forecasting models. *Hydrol*, (568), 534–550.

Ferguson, I. M., & Maxwell, R. M. (2012). Human impacts on terrestrial hydrology: Climate change versus pumping and irrigation. *Environmental Research Letters*, *7*(4). https://doi.org/10.1088/1748-9326/7/4/044022

Freeze, A., & Cherry, J. (1979). *Groundwater*. Prentice Hall.

Gautam, T. k, Paudel, K. p, & Guidry, K. M. (2020). *water An Evaluation of Irrigation Water Use E ffi ciency in*. 1–14.

Gebrechorkos, S. H., Bernhofer, C., & Hülsmann, S. (2019). Impacts of projected change in climate on water balance in basins of East Africa. *Science of the Total Environment*, *682*, 160–170. https://doi.org/10.1016/j.scitotenv.2019.05.053

Gebrechorkos, S. H., Bernhofer, C., & Hülsmann, S. (2020). Climate change impact assessment on the hydrology of a large river basin in Ethiopia using a local-scale climate modelling approach. *Science of the Total Environment*, *742*, 140504. https://doi.org/10.1016/j.scitotenv.2020.140504

Gebrechorkos, S. H., Hülsmann, S., & Bernhofer, C. (2019). Regional climate projections for impact assessment studies in East Africa. *Environmental Research Letters*.

Gianelli, G., & Teklemariam, M. (1993). Water-rock interaction processes in the Aluto-Langano geothermal field (Ethiopia). *Journal of Volcanology and Geothermal Research*, *56*(4), 429–445. https://doi.org/10.1016/0377-0273(93)90007-E

Giorgi, F., Jones, C., & Asrar, G. (2009). *Addressing Climate Information Needs at the Regional Level: the CORDEX Framework*.

GIRDC. (2021). *Generation Integrated Rural Development Consultantant (GIRDC): EFDR, Basin Development Authority (BDA), Rift Valley Lakes Basin Development Office (RVLBDO) and IDH: Water Resources Potential and Demand study of Ziway Shalla Sub-basin (Final Report)*.

Hailu, B. T., & Girma, S. (2019). *Spatio Temporal Lake Level Change of Lake Abijata , Ethiopia : A Remote Sensing Approach*. https://doi.org/10.31031/EAES.2019.06.000627

Halcrow. (2009). *Halcrow Group Limited and Generation Integrated Rural Development (GIRD) Consultants .The Federal Democratic Republic of Ethiopia Ministry of Water Resources: Rift*

Valley Lakes Basin Integrated Resources Development Master Plan Study Project. Addis Ababa, Ethiopia.

Hamlat, A., Errih, M., & Guidoum, A. (2013). Simulation of water resources management scenarios in western Algeria watersheds using WEAP model. *Arabian Journal of Geosciences*, *6*(7), 2225–2236. https://doi.org/10.1007/s12517-012-0539-0

Han, D. (2010). *Concise Hydrology* (1st ed.). Brestol, German: Dawei Han & bookboon.coms.

Hanasaki, N., Fujimori, S., Yamamoto, T., Yoshikawa, S., Masaki, Y., Hijioka, Y., … Kanae, S. (2013). A global water scarcity assessment under Shared Socio-economic Pathways - Part 2: Water availability and scarcity. *Hydrology and Earth System Sciences*, *17*(7), 2393–2413. https://doi.org/10.5194/hess-17-2393-2013

Harbaugh, A. W. (2005). *MODFLOW-2005 , The U . S . Geological Survey Modular Ground-Water Model — the Ground-Water Flow Process MODFLOW-2005 , The U . S . Geological Survey Modular Ground-Water Model — the Ground-Water Flow Process*.

Harmel, R. D., & Smith, P. K. (2007). Consideration of measurement uncertainty in the evaluation of goodness-of-fit in hydrologic and water quality modeling. *Journal of Hydrology*, *337*(3–4), 326–336. https://doi.org/10.1016/j.jhydrol.2007.01.043

Höllermann, B., Giertz, S., & Diekkrüger, B. (2010). Benin 2025-Balancing Future Water Availability and Demand Using the WEAP "Water Evaluation and Planning" System. *Water Resources Management*, *24*(13), 3591–3613. https://doi.org/10.1007/s11269-010-9622-z

Holman, I. P., Allen, D. M., Cuthbert, M. O., & Goderniaux, P. (2012). Towards best practice for assessing the impacts of climate change on groundwater. *Hydrogeology Journal*, *20*(1), 1–4. https://doi.org/10.1007/s10040-011-0805-3

Huang, M., & Zhang, L. (2004). *Hydrological responses to conservation practices in a catchment of the Loess Plateau , China*. *1898*(November 2002), 1885–1898. https://doi.org/10.1002/hyp.1454

Huber, M. (2013). *LinkKitchen: User manual* (Vol. 1). Retrieved from www.bgr.bund.de

Ingol-Blanco, E., & McKinney, D. C. (2013). Development of a Hydrological Model for the Rio

Conchos Basin. *Journal of Hydrologic Engineering*, *18*(3), 340–351. https://doi.org/10.1061/(asce)he.1943-5584.0000607

IPCC. (2007). *Climate Change 2007: Impacts, Adaptation and Vulnerability,Contribution of Working Group II to the Fourth Assessment Report of the Intergovernmental Panel on Climate Change* (L. Parry et al (eds), Ed.). https://doi.org/10.1007/s13163-011-0090-7

IPCC. (2014). Climate Change 2014 Synthesis Report Summary Chapter for Policymakers. In *Ipcc*. https://doi.org/10.1017/CBO9781107415324

Jain, M., Fishman, R., Mondal, P., Galford, G. L., Bhattarai, N., Naeem, S., … DeFries, R. S. (2021). Groundwater depletion will reduce cropping intensity in India. *Science Advances*, *7*(9), 1–10. https://doi.org/10.1126/sciadv.abd2849

Jansen, H., Hengsdijk, H., Dagnachew, L., Tenalem, A., Hellegers, P., & Spliethoff, P. (2007). *Land and water resources assessment in the Ethiopian Central Rift Valley*. 81.

Jensen, M. E. (1968). Water consumption by Agricultural plants. In K. T.T. (Ed.), *Water Deficits in plant Growth,Vol.2* (pp. 1–22). Academic Press,New York.

Jestin., F., Huchon, P., & Aulier, J. . (1994). The Somalia plate and the East African Rift System: present-day kinematics. *Geophysical Journal International*, *116*(3), 637–654. https://doi.org/10.1111/j.1365-246X.1994.tb03286.x

Jha, M., Pan, Z., Takle, E. S., & Gu, R. (2004). *Impacts of climate change on streamflow in the Upper Mississippi River Basin : A regional climate model perspective*. *109*(January), 1–12. https://doi.org/10.1029/2003JD003686

JICA. (2012). *The Study on Groundwater Resources Assessment in the Rift Valley Lakes Basin in Ethiopia*.

Joyce, B., Vicuña, S., Dale, L., Dracup, J., Hanemann, M., Purkey, D., & Yates, D. (2006). *Climate Change Impacts on Water for Agriculture in California: A Case Study in the Sacramento Valley.* (March 2006), 85.

Karamouz, M., Ahmadi, A., & Akhbari, M. (2011). *Groundwater Hydrology Groundwater: Engineering,Planning, and Management*. CRC Press - Taylor & Francis Group.

Kazmin, V., Seife, M. B., Nicoletti, M., & Petrucciani, C. (1980). Evolution of the northern part of the Ethiopian Rift. In: Geodynamic Evolution of the Afro-Arabian Rift System. *Accademia Nazionale Dei Lincei, International Meeting April 1979, Atti Dei Convegni Lincei 47*, 275–292.

Kebede, S. (2013). Groundwater in Ethiopia. In *Groundwater in Ethiopia*. https://doi.org/10.1007/978-3-642-30391-3

Kebede, S., Travi, Y., Alemayehu, T., & Ayenew, T. (2005). Groundwater recharge, circulation and geochemical evolution in the source region of the Blue Nile River, Ethiopia. *Applied Geochemistry*, *20*(9), 1658–1676. https://doi.org/10.1016/j.apgeochem.2005.04.016

Kebede, S., Travi, Y., Asrat, A., Alemayehu, T., Ayenew, T., & Tessema, Z. (2007). Groundwater origin and flow along selected transects in Ethiopian rift volcanic aquifers. *Hydrogeology Journal*, *16*(1), 55–73. https://doi.org/10.1007/s10040-007-0210-0

Konikow, L. ., & Mercer, J. . (1988). Groundwater Flow and Transport Modeling. *Hydrology*, *100*, 379–409.

Konikow, L. ., & Reilly, T. . (1999). Groundwater modeling. In J. W. Delleur (Ed.), *The handbook of groundwater engineering:Boca Raton,* (p. 940). CRC Press.

Krause, P., Boyle, D. P., & Bäse, F. (2005). Comparison of different efficiency criteria for hydrological model assessment. *Advances in Geosciences*, *5*, 89–97. https://doi.org/10.5194/adgeo-5-89-2005

Kresic, N. (2007). Hydrogeology and groundwater modeling. In *CRC press* (2nd ed.). CRC Press Taylor&Francis Group.

Kresic, N. (2009). *Groundwater Resources: Sustainability, Management, and Restoration*. The McGraw-Hill Companies,Inc.

Kresic, N., & Mikszewski, A. (2013). *Hydrogeological Conceptual Site Models: Data Analysis and Visualization*. CRC Press Taylor&Francis Group.

Kumo. (2006). *Numerical Groundwater flow modeling of ketar River catchmet , Central Ethiopia*. Addis Ababa University.

Laury, R. L., & Albritton, C. C. (1975). Geology of Middle Stone Age archaeological sites in the main Ethiopian Rift Valley. *Bulletin of the Geological Society of America*, *86*(7), 999–1011. https://doi.org/10.1130/0016-7606(1975)86<999:GOMSAA>2.0.CO;2

Lawston, P. M., Santanello, J. A., & Kumar, S. V. (2017). Irrigation Signals Detected From SMAP Soil Moisture Retrievals. *Geophysical Research Letters*, *44*(23), 11,860-11,867. https://doi.org/10.1002/2017GL075733

Lawston, P. M., Santanello, J. A., Zaitchik, B. F., & Rodell, M. (2015). Impact of irrigation methods on land surface model spinup and initialization of WRF forecasts. *Journal of Hydrometeorology*, *16*(3), 1135–1154. https://doi.org/10.1175/JHM-D-14-0203.1

Le Turdu, C., Tiercelin, J. J., Gibert, E., Travi, Y., Lezzar, K. E., Richert, J. P., … Taieb, M. (1999). The Ziway-Shala lake basin system, Main Ethiopian Rift: Influence of volcanism, tectonics, and climatic forcing on basin formation and sedimentation. *Palaeogeography, Palaeoclimatology, Palaeoecology*, *150*(3–4), 135–177. https://doi.org/10.1016/S0031-0182(98)00220-X

Legesse, D, Abiye, T. A., Vallet-Coulomb, C., & Abate, H. (2010). Streamflow sensitivity to climate and land cover changes: Meki River, Ethiopia. *Hydrology and Earth System Sciences*, *14*(11), 2277–2287. https://doi.org/10.5194/hess-14-2277-2010

Legesse, D, Vallet-Coulomb, C., & Gasse, F. (2003). Hydrological response of a catchment to climate and land use changes in Tropical Africa: Case study south central Ethiopia. *Journal of Hydrology*, *275*(1–2), 67–85. https://doi.org/10.1016/S0022-1694(03)00019-2

Legesse, D, Vallet-Coulomb, C., & Gasse, F. (2004). Analysis of the hydrological response of a tropical terminal lake, Lake Abiyata (main Ethiopian rift valley) to changes in climate and human activities. *Hydrological Processes*, *18*(3), 487–504. https://doi.org/10.1002/hyp.1334

Legesse, Dagnachew, & Ayenew, T. (2006). Effect of improper water and land resource utilization on the central Main Ethiopian Rift lakes. *Quaternary International*, *148*(1), 8–18. https://doi.org/10.1016/j.quaint.2005.11.003

Lemann, T., Roth, V., & Zeleke, G. (2016). *Impact of precipitation and temperature changes on hydrological responses of small-scale catchments in the Ethiopian Highlands*. *6667*(August).

https://doi.org/10.1080/02626667.2016.1217415

Leng, G., Huang, M., Tang, Q., Gao, H., & Leung, L. R. (2014). Modeling the effects of groundwater-fed irrigation on terrestrial hydrology over the conterminous United States. *Journal of Hydrometeorology*, *15*(3), 957–972. https://doi.org/10.1175/JHM-D-13-049.1

Leng, G., Huang, M., Tang, Q., & Leung, L. . (2015). A modeling study of irrigation effects on global surface water and groundwater resources under a changing climate. *Journal of Advances in Modeling Earth Systems*, 1285–1304. https://doi.org/10.1002/2015MS000437.Received

Lerner, D. N. (2002). Identifying and quantifying urban recharge: A review. *Hydrogeology Journal*, *10*(1), 143–152. https://doi.org/10.1007/s10040-001-0177-1

Li, Z., Deng, X., Wu, F., & Hasan, S. S. (2015). Scenario analysis for water resources in response to land use change in the middle and upper reaches of the heihe river Basin. *Sustainability (Switzerland)*, *7*(3), 3086–3108. https://doi.org/10.3390/su7033086

Liersch, S., Tecklenburg, J., Rust, H., Dobler, A., Fischer, M., Kruschke, T., … Hattermann, F. F. (2018). Are we using the right fuel to drive hydrological models? A climate impact study in the Upper Blue Nile. *Hydrology and Earth System Sciences*, *22*(4), 2163–2185. https://doi.org/10.5194/hess-22-2163-2018b

Lorenz, D. L., & Ziegeweid, J. R. (2015). Methods to estimate historical daily streamflow for ungaged stream locations in Minnesota. *U.S. Geological Survey Scientific Investigations Report*, (2015–5181), 18. Retrieved from http://pubs.usgs.gov/sir/2015/5181/sir20155181.pdf

Luo, Y., Gao, P., & Mu, X. (2021). Influence of Meteorological Factors on the Potential Evapotranspiration in Yanhe River Basin, China. *MDPI*, *13*(9), 1222. https://doi.org/10.3390/w13091222

MaBmann, J., Wolfer, J., Huber, M., Schelkes, K., Hennings, V., Droubi, A., & Al-Sibai, M. (2010). WEAP-MODFLOW as s Decision Support System (DSS) for Integrated water resources management: Design of the coupled model and results from a pilot study in Syria. In A. Zuber, J. Kania, & E. Kmiecik (Eds.), *Groundwater Quality Sustainability,XXXVIII IAH Congress* (pp. 887–893). Krakow, Poland.

Mahmood, R., & Jia, S. (2017). An extended linear scaling method for downscaling temperature and its implication in the Jhelum River basin, Pakistan, and India, using CMIP5 GCMs. *Theoretical and Applied Climatology*, *130*(3–4), 725–734. https://doi.org/10.1007/s00704-016-1918-3

Mario, Z., James, B., & Prisca, K. (2010). Special report: FAO/WFP crop and food security assessment mission to Ethiopia. Rome: Publication of Food and Agriculture Organization of the United Nations, and World Food Programme. In *Assessment*.

Maßmann, J., Wolfer, J., Huber, M., Schelkes, K., Hennings, V., Droubi, A., & Al-Sibai, M. (2012). WEAP-MODFLOW as a decision support system (DSS) for integrated water resources management: Design of the coupled model and results from a pilot study in Syria. *Groundwater Quality Sustainability*, 173–188.

Mccabe, G. J., & Legates, D. R. (1999). Evaluating the use of "goodness-of-fit" measures in hydrologic and hydroclimatic model validation. *Water Resources Research*, *35*(1), 233–241.

McDonald, M. ., & Harbaugh, A. . (1988). *A modular three-dimensional finite-difference groundwater flow model: U.S. Geological Survey Techniques of Water-Resources Investigations*.

Mcsweeney, C., New, M., & Lizcano, G. (2008). *UNDP Climate Change Country Profiles: Ethiopia*. Retrieved from http://country-profiles.geog.ox.ac.uk

Mechal, A., Wagner, T., & Birk, S. (2015). Recharge variability and sensitivity to climate : The example of Gidabo River Basin , Main Ethiopian Rift. *Journal of Hydrology : Regional Studies*, *4*, 644–660.

Mehta, V. K., Haden, V. R., Joyce, B. A., Purkey, D. R., & Jackson, L. E. (2013a). Irrigation demand and supply, given projections of climate and land-use change, in Yolo County, California. *Agricultural Water Management*, *117*, 70–82. https://doi.org/10.1016/j.agwat.2012.10.021

Mehta, V. K., Haden, V. R., Joyce, B. A., Purkey, D. R., & Jackson, L. E. (2013b). Irrigation demand and supply , given projections of climate and land-use change , in Yolo County , California. *Agricultural Water Management*, *117*, 70–82.

https://doi.org/10.1016/j.agwat.2012.10.021

Meixner, T., Manning, A. H., Stonestrom, D. A., Allen, D. M., Ajami, H., Blasch, K. W., … Walvoord, M. A. (2016). Implications of projected climate change for groundwater recharge in the western United States. *Journal of Hydrology*, *534*, 124–138. https://doi.org/10.1016/j.jhydrol.2015.12.027

Melesse, A. M., Abtew, W., & Dessalegne, T. (2009). *Evaporation Estimation of Rift Valley Lakes: Comparison of Models*. (2009). https://doi.org/10.3390/s91209603

Mercer, J. W., & Faust, C. R. (1980). Ground-water Modeling: An overview. *Ground Water*, *18*, 108–115.

Merla, G., Abbate, E., Azzaroli, A., Bruni, P., Canuti, P., Fazzuoli, M., … Tacconi, P. (1975). A Geological Map of Ethiopia and Somalia (1973) 1:2,000,000 and Comment with a map of Major Landforms. *CNR, Firenze*.

Meshesha, D. T., Tsunekawa, A., & Tsubo, M. (2012). Continuing land degradation: Cause-effect in Ethiopia's Central Rift Valley. *Land Degradation and Development*, *23*(2), 130–143. https://doi.org/10.1002/ldr.1061

Mohammadi, B., Ahmadi, F., Mehdizadeh, S., & Guan, Y. (2020). Developing Novel Robust Models to Improve the Accuracy of Daily Streamflow Modeling. *Water Resources Management*.

Mohammadi, B., Guan, Y., Moazenzadeh, R., Jafar, M., & Safari, S. (2020). Catena Implementation of hybrid particle swarm optimization-differential evolution algorithms coupled with multi-layer perceptron for suspended sediment load estimation. *Catena*, (October), 105024. https://doi.org/10.1016/j.catena.2020.105024

Mohammadi, B., Mehdizadeh, S., Ahmadi, F., Thi, N., Lien, T., Thi, N., & Linh, T. (2020). Developing hybrid time series and artificial intelligence models for estimating air temperatures. *Stochastic Environmental Research and Risk Assessment*, *7*. https://doi.org/10.1007/s00477-020-01898-7

Mohr, P. A. (1967). *Major volcano-tectonic lineament in the Ethiopian Rift System*. *213*(5077), 664–665. https://doi.org/10.1038/213664a0

Mohr, P., Mitchell, J. G., & Raynolds, R. G. H. (1980). Quaternary volcanism and faulting at O'A caldera, central ethiopian rift. *Bulletin Volcanologique*, *43*(1), 173–189. https://doi.org/10.1007/BF02597619

Mohr, Paul. (1987). Patterns of faulting in the Ethiopian rift valley. *Tectonophysics*, *143*(1–3), 169–179. https://doi.org/10.1016/0040-1951(87)90086-2

Moriasi, D. N., Arnold, J. G., Liew, M. W. Van, Bingner, R. L., Harmel, R. D., & Veith, T. L. (2007). model evaluation guidelines for systematic quantification of accuracy in watershed simulations. *American Society of Agricultural and Biological Engineers ISSN*, *50*(3), 885–900.

MOWR. (2007). *Rift Valley Lakes basin integrated resources development master plan study project. Draft phase 1 report. Ministry of water resources. The Federal Democratic Republic of Ethiopia. Addis Ababa: Halcrow Group Limited and Generation Integral Rural Develop*.

Musie, M., Sen, S., & Srivastava, P. (2020). Application of CORDEX-AFRICA and NEX-GDDP datasets for hydrologic projections under climate change in Lake Ziway sub- basin, Ethiopia. *Journal of Hydrology: Regional Studies*, *31*(August), 100721. https://doi.org/10.1016/j.ejrh.2020.100721

Nash, J., & Sutcliff, J. (1970). Riverflow forecasting through conceptual models, part I—a discussion of principles. *Hydrol*, *10*, 282–290. https://doi.org/10.1080/00750770109555783

Niu, G. Y., Paniconi, C., Troch, P. A., Scott, R. L., Durcik, M., Zeng, X., … Goodrich, D. C. (2014). An integrated modelling framework of catchment-scale ecohydrological processes: 1. Model description and tests over an energy-limited watershed. *Ecohydrology*, *7*(2), 427–439. https://doi.org/10.1002/eco.1362

Notter, B., Hurni, H., Wiesmann, U., & Abbaspour, K. C. (2012). Modelling water provision as an ecosystem service in a large East African river basin. *Hydrology and Earth System Sciences*, *16*(1), 69–86. https://doi.org/10.5194/hess-16-69-2012

Omran, E. E., Negm, A. M., & Practices, B. M. (2020). *Technological and Modern Irrigation Environment in Egypt*.

OWWDSE. (2016). *Impact Assessment of Water Resources Exploitation on Lake Ziway*.

Pacheco, F. A. L. (2015). Regional groundwater flow in hard rocks. *Sci. Total Environ.*, (506–507), 182–195.

Pascual-ferrer, J., & Candela, L. (2015). *Water Balance on the Central Rift Valley Water Balance on the Central Rift Valley* (GDEE (eds), Ed.). Retrieved from Global Dimension in Engineering Education website: https://upcommons.upc.edu/handle/2117/89152

Pascual-ferrer, J., Candela, L., & Pérez-foguet, A. (2013). Ethiopian Central Rift Valley basin hydrologic modelling using HEC-HMS and ArcSWAT. *Geophysical Research Abstracts*, *15*(1), 10563.

Pascual-ferrer, J., Pérez-foguet, A., Codony, J., & Raventós, E. (2014). Assessment of water resources management in the Ethiopian Central Rift Valley : environmental conservation and poverty reduction. *International Journal of Water Resources Sevelopment*, *0627*. https://doi.org/10.1080/07900627.2013.843410

Pulido-Velazquez, M., Peña-Haro, S., García-Prats, A., Mocholi-Almudever, A. F., Henriquez-Dole, L., Macian-Sorribes, H., & Lopez-Nicolas, A. (2015). Integrated assessment of the impact of climate and land use changes on groundwater quantity and quality in the Mancha Oriental system (Spain). *Hydrology and Earth System Sciences*, *19*(4), 1677–1693. https://doi.org/10.5194/hess-19-1677-2015

Purkey, D. R., Joyce, B., Vicuna, S., Hanemann, M. W., Dale, L. L., Yates, D., & Dracup, J. A. (2008). *Robust analysis of future climate change impacts on water for agriculture and other sectors : a case study in the Sacramento Valley*. *87*. https://doi.org/10.1007/s10584-007-9375-8

Reba, M. L., Massey, J. H., Adviento-Borbe, M. A., Leslie, D., Yaeger, M. A., Anders, M., & Farris, J. (2017). Aquifer Depletion in the Lower Mississippi River Basin: Challenges and Solutions. *Journal of Contemporary Water Research & Education*, *162*(1), 128–139. https://doi.org/10.1111/j.1936-704x.2017.03264.x

Richey, A. S., Thomas, B. F., Lo, M. H., Reager, J. T., Famiglietti, J. S., Voss, K., … Rodell, M. (2015). Quantifying renewable groundwater stress with GRACE. *Water Resources Research*, *51*(7), 5217–5237. https://doi.org/10.1002/2015WR017349

Santhi, C., Arnold, J. G., Williams, J. R., Dugas, W. A., Srinivasan, R., & Hauck, L. M. (2001). Validation of the SWAT model on a large river basin with point and nonpoint sources. *Journal of the American Water Resources Association*, *37*(5), 1169–1188. https://doi.org/10.1111/j.1752-1688.2001.tb03630.x

Santos, R. M. B., Sanches Fernandes, L. F., Moura, J. P., Pereira, M. G., & Pacheco, F. A. L. (2014). The impact of climate change, human interference, scale and modeling uncertainties on the estimation of aquifer properties and river flow components. *Hydrol.*, (519), 1297–1314.

Scanlon, B. ., Keese, K. ., Flint, A. ., Flint, L. ., Gaye, C. ., Edmunds, M. ., & Simmers, I. (2007). Global synthesis of groundwater recharge in semiarid and arid regions. *Hydrological Processes*, *20*, 3335–3370. https://doi.org/10.1002/hyp

SEI. (2007). Water evaluation and planning system, WEAP. In *Boston*.

Seiber, J., & Purkey, D. (2015). *Water Evaluation and planning System (WEAP) user Giude.*

Seleshi, Y., & Camberlin, P. (2006). Recent changes in dry spell and extreme rainfall events in Ethiopia. *Theoretical and Applied Climatology*, *83*(1–4), 181–191. https://doi.org/10.1007/s00704-005-0134-3

Sen, Z. (2015). *Practical and applied Hydrogeology*. Elsevier.

Serur, A. B., & Sarma, A. K. (2017a). Climate change impacts analysis on hydrological processes in the Weyib River basin in Ethiopia. *Theoretical and Applied Climatology*, *134*(3–4), 1301–1314. https://doi.org/10.1007/s00704-017-2348-6

Serur, A. B., & Sarma, A. K. (2017b). *Statistical Downscaling of Daily Temperatures and Precipitation Data from Coupled Model Inter-comparison Project 5 (CMIP5)-RCPs Experiment: In Weyib River Basin, Southeastern Ethiopia*. *5*, 47–70. https://doi.org/10.1007/978-981-10-5714-4_5

Setegn, S. G., Rayner, D., Melesse, A. M., Dargahi, B., & Srinivasan, R. (2011). Impact of climate change on the hydroclimatology of Lake Tana Basin, Ethiopia. *Water Resources Research*, *47*(4), 1–13. https://doi.org/10.1029/2010WR009248

Shah, T., Molden, D., Sakthivadivel, R., & Seckler, D. (2000). The global groundwater situation:

overview of opportunities and challenges. *The Global Groundwater Situation: Overview of Opportunities and Challenges.* https://doi.org/10.5337/2011.0051

Shaw, E. M., Beven, K. J., Chappell, N. A., & Lamb, R. (2011). Hydrology in practice. In *Hydrology in Practice, Fourth Edition* (4th ed.). Spon Press.

Shimelis, S. (2008). *Environmental problems of Central Rift Valley of Ethiopia.Unpublished . Intermo ́n Oxfam.*

Sieber, J., & Purkey, D. (2015). Water Evaluation And Planning System: User Guide. *Stockholm Environment Institute, U.S. Center*, p. 400. Retrieved from http://www.weap21.org/WebHelp/index.html

Siebert, S., & Döll, P. (2010). Quantifying blue and green virtual water contents in global crop production as well as potential production losses without irrigation. *Journal of Hydrology*, *384*(3–4), 198–217. https://doi.org/10.1016/j.jhydrol.2009.07.031

Singh, J., Knapp, H., & Demissie, M. (2005). Hydrologic modeling of the Iroquois River watershed using HSPF and SWAT. ISWS CR 2004-08. *Journal of American Water Resources Association (JAWRA)*, *2*, 343–360. Retrieved from http://scholar.google.com/scholar?hl=en&btnG=Search&q=intitle:Hydrologic+Modeling+of+the+Iroquois+River+Watershed+Using+HSPF+and+SWAT#3

Sorooshian, S., Li, J., Hsu, K. L., & Gao, X. (2012). Influence of irrigation schemes used in regional climate models on evapotranspiration estimation: Results and comparative studies from California's Central Valley agricultural regions. *Journal of Geophysical Research Atmospheres*, *117*(6), 1–8. https://doi.org/10.1029/2011JD016978

Taye, M. T., Dyer, E., Hirpa, F. A., & Chales, K. (2018). *Climate Change Impact on Water Resources in the Awash Basin, Ethiopia*. 1–16. https://doi.org/10.3390/w10111560

Taye, M. T., Willems, P., & Block, P. (2015). Implications of climate change on hydrological extremes in the Blue Nile basin: A review. *Journal of Hydrology: Regional Studies*, *4*, 280–293. https://doi.org/10.1016/j.ejrh.2015.07.001

Taylor, K., Stouffer, R., & Meehl, G. (2012). An overview of CMIP5 and the experiment design. *Bull. Am. Meteorol.Soc*, *4*(94), 485–498. Retrieved from http://dx.doi.org/10.1175/BAMS-D-

11-00094

Taylor, R. G., Scanlon, B., Doll, P., Rodell, M., Beek, R. Van, Wada, Y., … Chen, J. (2012). Ground water and climate change. *Nature Climate Change*, *3*(April). https://doi.org/10.1038/NCLIMATE1744

Tilman, D., Balzer, C., Hill, J., & Befort, B. L. (2011). Global food demand and the sustainable intensification of agriculture. *Proceedings of the National Academy of Sciences of the United States of America*, *108*(50), 20260–20264. https://doi.org/10.1073/pnas.1116437108

Triana, J. S. A., Chu, M. L., Guzman, J. A., Moriasi, D. N., & Steiner, J. L. (2020). Evaluating the risks of groundwater extraction in an agricultural landscape under different climate projections. *Water (Switzerland)*, *12*(2). https://doi.org/10.3390/w12020400

Vallet-coulomb, C., Legesse, D., Gasse, F., Travi, Y., & Chernet, T. (2001). Lake evaporation estimates in tropical Africa. *Journal of Hydrology*, *245*, 1–18.

Van Liew, M. W., Veith, T. L., Bosch, D. D., & Arnold, J. G. (2007). Suitability of SWAT for the conservation effects assessment project: Comparison on USDA agricultural research service watersheds. *Journal of Hydrologic Engineering*, *12*(2), 173–189. https://doi.org/10.1061/(ASCE)1084-0699(2007)12:2(173)

Van Vuuren, D. ., Edmonds, J., Kainuma, M., Riahi, K., Thomson, A., Hibbard, K., … N., Smith, S., Rose, S. (2011). The representative concentration pathways: an overview. *Clim. Change*, *5*(109).

Vilalta, E. R. (2010). *Water Resorces Management in the Central Rift Valley of Ethiopia*. UNIVERSITAT POLITECNICA DE CATALUNYA.

Wada, Y., Van Beek, L. P. H., Van Kempen, C. M., Reckman, J. W. T. M., Vasak, S., & Bierkens, M. F. P. (2010). Global depletion of groundwater resources. *Geophysical Research Letters*, *37*(20), 1–5. https://doi.org/10.1029/2010GL044571

Wada, Y., Wisser, D., Eisner, S., Flörke, M., Gerten, D., Haddeland, I., … Schewe, J. (2013). Multimodel projections and uncertainties of irrigation water demand under climate change. *Geophysical Research Letters*, *40*(17), 4626–4632. https://doi.org/10.1002/grl.50686

Wagesho, N., Jain, M. K., & Goel, N. K. (2013). *Effect of Climate Change on Runoff Generation : Application to Rift Valley Lakes Basin of Ethiopia*. (August), 1048–1063. https://doi.org/10.1061/(ASCE)HE.1943-5584.0000647.

Wakgari Furi, K. (2010). *Hydrogeology of complex volcanic systems in continental rifted zone. Integrated geochemical, geophysical and hydrodynamic approach. Middle Awash basin, Main Ethiopian Rift, Ethiopia.*

Wang, S., Huang, G., Baetz, B., & Huang, W. (2016). Probabilistic inference coupled with possibilistic reasoning for robust estimation of hydrologic parameters and piecewise characterization of interactive uncertainties. *Hydrometeorol*, *17*(4), 1243–1260.

Wheater, H. S., Mathias, S. A., & Li., X. (2010). *Groundwater modelling in Arid & Semi-Arid Areas*. Cambridge University Press.

Wichelns, D. (2014). Do estimates of water productivity enhance understanding of farm-level water management? *Water (Switzerland)*, *6*(4), 778–795. https://doi.org/10.3390/w6040778

Williams, F. M., Williams, M. A. J., & Aumento, F. (2004). Tensional fissures and crustal extension rates in the northern part of the Main Ethiopian Rift. *Journal of African Earth Sciences*, *38*(2), 183–197. https://doi.org/10.1016/j.jafrearsci.2003.10.007

Willmott, C. J. (1981). On the validation of models. *Physical Geography*, *2*(2), 184–194. https://doi.org/10.1080/02723646.1981.10642213

Wittenberg, H., & Sivapalan, M. (1999). Watershed groundwater balance estimation using streamflow recession analysis and baseflow separation. *Journal of Hydrology*, *219*(1–2), 20–33. https://doi.org/10.1016/S0022-1694(99)00040-2

Woldegabriel, G., Aronson, J. L., & Walter, R. C. (1990). *Geological Society of America Bulletin Main Ethiopia Rift Geology, geochronology, and rift basin development in the central sector of the*. *102*, 439–458. https://doi.org/10.1130/0016-7606(1990)102<0439:GGARBD>2.3.CO;2

Worqlul, A. W., Collick, A. S., Rossiter, D. G., Langan, S., & Steenhuis, T. S. (2015). Assessment of surface water irrigation potential in the Ethiopian highlands: The Lake Tana Basin. *Catena*, *129*, 76–85. https://doi.org/10.1016/j.catena.2015.02.020

Yates, D., Sieber, J., Purkey, D., & Huber-Lee, A. (2005). WEAP21 - A Demand-, Priority-, and Preference-Driven Water Planning Model. Part 1: Model Characteristics. *Water International*, *30*(4), 487–500.

Yates, David, Purkey, D., Sieber, J., Huber-Lee, A., & Galbraith, H. (2005). WEAP21 - A demand-, priority-, and preference-driven water planning model. Part 2: Aiding freshwater ecosystem service evaluation. *Water International*, *30*(4), 501–512. https://doi.org/10.1080/02508060508691894

Zeng, Y., Xie, Z., Yu, Y., Liu, S., Wang, L., Zou, J., … Jia, B. (2016). Effects of anthropogenic water regulation and groundwater lateral flow on land procecesses. *Journal of Advances in Modeling Earth Systems*, *8*, 1289–1309. https://doi.org/10.1002/2013MS000282.Received

Zeray, A. L., Roehrig, J., Alamirew, C., & Dilnesaw. (2007). Climate Change Impact on Lake Ziway Watershed Water Availability, Ethiopia. *In:Paper Presented at the Conference on International Agriculture Research for Development.University of Bonn.*, PP.1-25.

Zhang, L., Nan, Z., Xu, Y., & Li, S. (2016). Hydrological impacts of land use change and climate variability in the headwater region of the Heihe River Basin, northwest China. *PLoS ONE*, *11*(6), 1–25. https://doi.org/10.1371/journal.pone.0158394

Mohr, P. (1983). *Volcanotectonic aspects of Ethiopian Rift evolution. In: Popoff, M., Tiercelin, J.-J. (Eds.), Ancient Rifts and Troughs, Symposium of the French National Centre of Scientific Research (CNRS), Marseilles, Nov. 30–Dec. 2, 1982, pp. 175–189.* 320.

Appendix

Appendix 1: Percentage weight of Thiessen polygon

Station	Ketar Upstream	Meki Upstream	Rift floor	Langano	Bulbul
Adamitulu	-	-	39.77	3.11	19.71
Arsi Negele	-	-	-	6.66	2.12
Asella	13.7	-	3.68	-	-
Bekoji	35.73	-	-	0.23	-
Bui	-	32.7	-	-	-
Bulbula	-	-	-	11.76	34.38
Butajira	-	37.23	0.95	-	-
Degaga	4.41	-	-	41.45	-
Ketar genet	34.63	-	2.49	1.85	-
Kulumsa	11.5	-	6.35	-	-
Langano	-	-	-	16.42	16.99
Meki	-	12.69	40.23	-	-
Sire	-	-	-	18.53	-
Tora	-	17.38	5.97	-	26.8
Sum	100	100	100	100	100

Appendix 2: Livestock data by zones in the subbasin

Name of Woreda	Cattle	Sheep	Goats	Poultry	Donkeys	Horse	Mule
Degelu-Tijo	242537	133547	10593	83028	33923	43676	3021
LimuBilbilo	150457	168834	16611	48475	25386	32684	2261
Tiyo	106349	93764	17064	73462	37435	10623	660
Hitosa	35197	11239	10252	28024	3673	13885	201
Alaba	160487	202495	177551	121648	22993	2321	336
Lanfero	73172	41229	36594	78567	22350	363	509
Mareko	61785	16593	16078	86645	6420	1230	145
Meskane	114893	51103	30985	137996	16971	2358	0
SedenSodo	6560	5287	699	3743	532	1039	8
Silti	134729	59346	36240	132313	24372	400	561
Welberg	108617	49259	68404	82581	17478	432	462
Sodo	80663	23586	28235	134292	17210	4104	1979
Dugda	149728	38946	39784	130156	13431	2049	1241
ZiwayDugda	168221	48191	54109	67076	20786	1861	1114
Munessa	239718	147963	7928	82669	17057	27057	1014

Kore	88968	74546	1561	27230	3542	21793	437
Arsi Negele	272353	55892	61036	160067	28015	14126	1456
ATJK*	155928	35326	90166	142421	27487	3019	1410
Dalocha	176846	87843	80639	340078	23353	0	0
Total	2527208	1344989	784529	1960471	362414	183020	16815

* Adami tulu gido Kombolcha

Appendix: 3 The schematic diagram for WEAP Hydrologic Model procedure

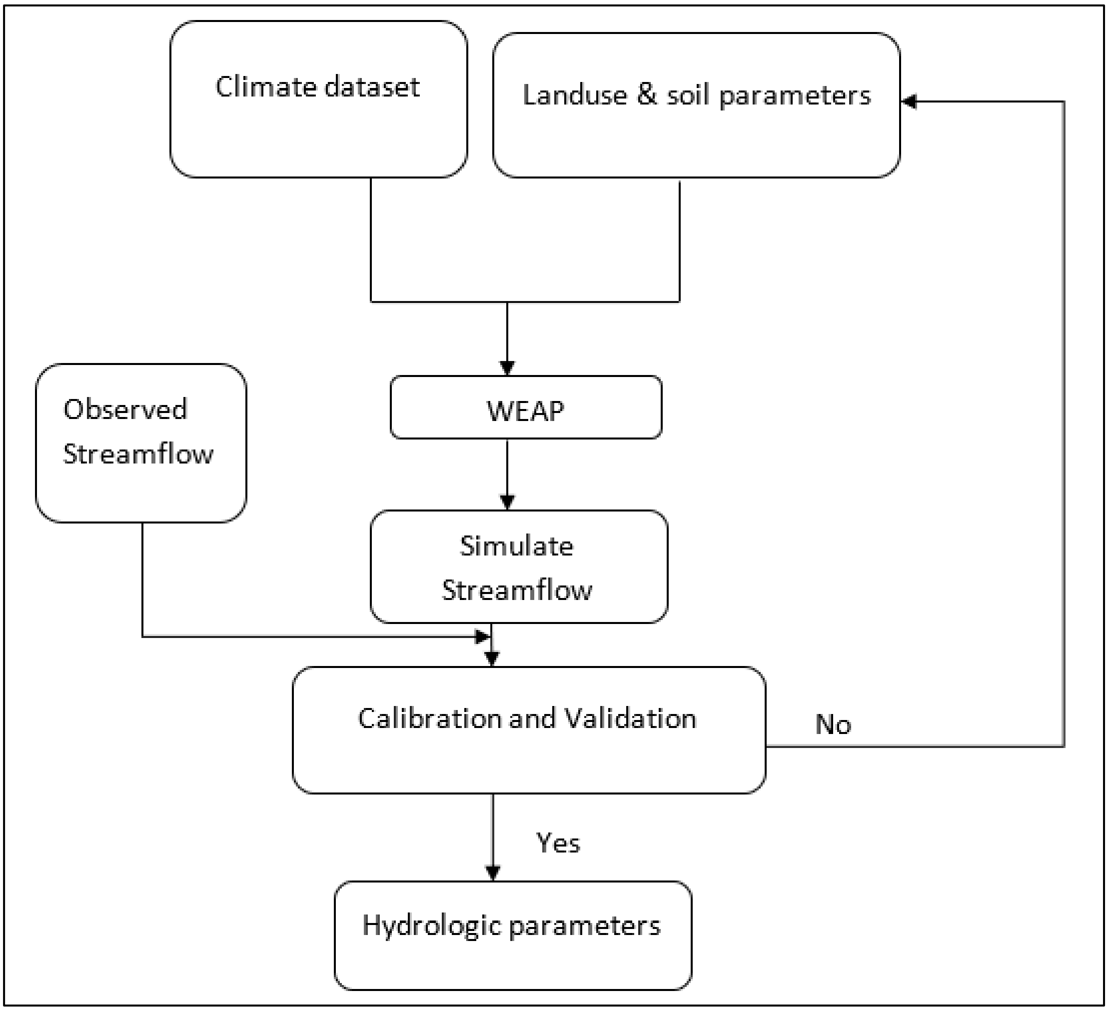

Appendix: 4 Landuse/land cover of the subbasin

LULC of 2003	Subbasin									
	Ketar		Meki		Rift floor		Langano		Bulbula	
	Ha	%age	Ha	%age	Ha	%age	Ha	%age	Ha	%age
Cultivated	210692	64.4	151799	67.1	59729	34.7	88554	44	36025	26.5
Grassland	22901	7	15101	6.68	6368	3.7	7446	3.7	5675	4.0
Forestland	55617	17	27580	12.2	-	-	33408	16.6	-	-
Shrubland	30741	9.4	25385	11.23	56803	33	28981	14.4	16993	12.5
Woodland	-	-	-	-	-	-	17429	8.66	50164	36.9
Barren	6732	2.1	4560	2.0	5508	3.2	3018	1.5	11066	8.14
Water bodies	100	0.1	146	0.1	42688	24.8	23373	11.6	15497	11.4
Wetland	554	0.2	2701	0.5	1202	0.7	136	0.1	81	0.1
Area (ha)	327161	100	226070	100	172132	100	201259	100	135946	100

Appendix: 5 WEAP-MODFLOW Model link